

**Synthesis and Evaluation of Pharmaceutical
and Fine Chemicals Processes for
Intensification and Sustainability Benefits**

by

Ruili Feng

*Thesis submitted for the degree of Doctor of Philosophy
in the Faculty of Science, Agriculture and Engineering of
the Newcastle University*

School of Chemical Engineering and Advanced Materials

Newcastle University

Newcastle upon Tyne, U.K.

September 2017

Acknowledgements

I am especially grateful to Dr. Kamelia Boodhoo for the opportunity to pursue a PhD degree in ICES and thankful for the support, care and encouragement she has given me in these four years. The frequent meetings for discussion of results and interpretation are extremely appreciated.

I also wish to express my gratitude to Dr Teoh Soo Khean and Prof. Paul Sharratt, my ICES co-supervisors, for their guidance throughout this project and providing support when needed. I appreciate the constructive feedback on my work and have learned valuable lessons from those interactive.

I am also grateful to my Newcastle University co-supervisors, Dr. Li Chunzhao and Dr. Cindy Lee for their enthusiasm and encouragement throughout this project. I appreciate their care and understanding during stressful times.

I also like to thank Dr. Ming Tham for his timely and valuable advice on my progress.

I thank Dr. Guo Liang Feng for the BTEM curve resolution and multiple linear regressions which enabled the study of in-situ IR measurement for ortho-lithiation reaction.

I thank Dr. Lee Huai-Chin Jim for the rheometry analysis of the amidation solid-liquid suspension which enabled good understanding of the physical characteristics of the suspension.

I thank my group mates in ICES who have been extremely helpful in the result analysis, setting up of equipment and troubleshooting when needed. It would not have been possible to obtain so much result in such a short time frame without their timely help. I duly acknowledge Dr. Song Wei Benjamin Tan, Mr. Sushil Ramchandani, Mr. Salih Noorulameen, Ms. Eleen Lim Xiu Yan, Dr. Romain Frederic Cadou and Dr. Huang Huancong for their help. The assistance provided by all the staff at ICES INCOME Team is sincerely appreciated.

Special thanks to Mr. Rob Dixon for his kind assistance during my time in Newcastle University.

I am thankful to GSK-EDB Singapore for the financial assistance through my scholarship and project funding enabling the completion of this work.

I highly appreciate the company of the post graduate students at ICES, thanks to Margarete, Elmira, Parviz, Poovizhi, Thomas, Nana, Ulrike, Oslessya and Roman.

The list is not complete without mentioning my husband, Mr. Lim Rui De who has been giving me his fullest support over the course of my PhD, even when the times were tough.

I am forever grateful to my parents, Mr. Feng Zhigang and Mrs. Li Manping for their resolute belief in me. Their unwavering support and encouragement has helped me regain my confidence during the low points.

Abstract

In the face of global competition and tighter safety and environmental regulations, the pharmaceutical industry is exploring new areas and technologies that could potentially bring about step change in process performance. Process intensification has the potential to improve early development by introducing new process options, which are capable of achieving green and sustainable benefits in production.

In this thesis, the objective is to demonstrate the synthesis and evaluation of pharmaceutical processes for intensification and sustainability benefits. This is illustrated with two main processes – the amidation process and the ortho-lithiation process. Based on the experiences gained at the end of the case studies, a general framework that summarizes the approach to Process Intensification (PI) for pharmaceutical processes is developed.

Firstly, the amidation process has been successfully intensified with the implementation of a number of PI options, which are proven feasible in lab-scale experiments. These options are represented in terms of three intensified cases - the intensified batch case, the continuous reaction case and the continuous process case, are compared to the batch base case. To compare their sustainability performance, the respective plants are designed at a hypothetical throughput of 3 tons per year. Overall, the intensified batch case provided the most benefits, with cost savings of up to 40%, and more than 70% improvements in total material efficiency and E-factor compared to the batch base case. This also indicates that batch mode operation in this particular process is more suitable than continuous mode.

The second case study on the ortho-lithiation process consists of three parts. The first part investigates ortho-lithiation reaction in continuous flow reactors at ambient temperature. The findings demonstrated that the highest reaction yield of 99% was obtained in a T-reactor as a result of short residence time and good mixing. The Spinning Disc Reactor (SDR) also showed distinct advantage in handling this reaction with mild solid precipitation. The second part focuses on the comparison of the T-reactor, the SDR and the Stirred Tank Reactor (STR) based on the sustainability metrics. The results showed that the T-reactor process achieved 66% and 11% reduction in energy consumption and operating expenditure respectively as compared to the STR process. The last part of the ortho-lithiation process focuses on the study of the whole process including workup. To avoid dealing with inefficient separation process, consecutive reaction has been attempted by avoiding the isolation of ortho-lithiation crude product and directly transferring it into the next reactor for subsequent reaction. This is experimentally proven feasible and resulted in a greener process.

Table of Contents

Chapter 1.	Introduction	1
1.1	Research Motivations	1
1.2	Aims and Objectives	3
1.3	Thesis Layout	4
Chapter 2.	Literature Review	6
2.1	Background: Manufacturing of Pharmaceuticals	6
2.2	Process Intensification (PI)	7
2.3	Conventional and PI equipment in Pharmaceutical Industry	9
2.3.1	Microreactors	9
2.3.2	Spinning Tube in Tube Reactor	10
2.3.3	Gas-Liquid-Solid Trickle Flow Reactor	11
2.3.4	Catalytic Foam Stirrer Reactors	11
2.3.5	Heat Exchanger (HEX) Reactors	12
2.3.6	Static Mixer and Static Mixer Reactor	12
2.3.7	Oscillatory Baffled Reactor (OBR).....	13
2.3.8	Thin-film Spinning Disc Reactor	14
2.3.9	Rotor-Stator Spinning Disc Reactor	15
2.3.10	Hydrodynamic Cavitation Reactor.....	16
2.3.11	Taylor-Couette Reactor.....	16
2.3.12	Monolithic Reactor	17
2.3.13	Impinging Jets Reactor.....	18
2.3.14	Rotating Packed Bed.....	18
2.3.15	Reactive Distillation.....	19
2.3.16	Simulated Moving Bed (SMB)	20
2.3.17	Rotating Annular Chromatographic Reactor	20
2.3.18	Centrifugal Extractor.....	21
2.3.19	Agitated Columns	22

2.3.20	Nutsche Filters	23
2.3.21	Centrifugal Filters	24
2.3.22	Rotary Vacuum Drum Filter	25
2.3.23	Conventional Pharmaceutical Dryers	26
2.3.24	Wiped Film Evaporator (WFE)	27
2.3.25	Agitated Thin Film Dryer	28
2.3.26	Spray Dryer	29
2.3.27	Microwave Drying.....	30
2.4	Pharmaceutical Plant-wide Process Intensification – Batch to continuous	34
2.4.1	Economics	34
2.4.2	Quality	34
2.4.3	Safety	34
2.4.4	Environmental	35
2.5	PI of ortho-Lithiation	36
2.6	Review of PI Methodology.....	36
2.6.1	Phenomena Approach.....	37
2.6.2	Framework for Choice of Intensified Equipment.....	37
2.6.3	Local and Global Process Intensification Approach	38
2.6.4	Thermodynamics Approach	39
2.6.5	Modularisation Approach.....	39
2.6.6	Decomposition Based Solution Approach.....	39
2.6.7	Elementary Process Function Approach.....	40
2.6.8	Optimisation and Integration for Reactive Separation	41
2.6.9	Framework for Batch to Continuous	41
2.6.10	PI Equipment Database Focused Approach	42
Chapter 3.	Amidation Process – Synthesis and Evaluation for Intensification and Sustainability Benefits.....	44
3.1	Introduction.....	44

3.2	Aims and Objectives	44
3.3	Experimental Apparatus and Procedures	45
3.3.1	Batch base case experiment/RC1 Experiment	45
3.3.2	Amidation mixing study in toluene solvent system	46
3.3.3	Amidation kinetic study in toluene solvent system	46
3.3.4	Intensified Batch Case Experiment in Toluene-Water Solvent System ...	47
3.3.5	Continuous Reaction in Static Mixer	47
3.3.6	Continuous Extraction using Centrifugal Extractor	49
3.3.7	Wiped Film Evaporator	50
3.3.8	Feasibility Study of Consecutive reactions from amidation to ortho-lithiation: THF drying study	51
3.4	Reaction Understanding	52
3.5	Investigation of process intensification options	56
3.5.1	Reduce Number and Amount of Reagents Used	57
3.5.2	Reduce Toluene Usage	57
3.5.3	Reduce Wash Medium in Separation Process	58
3.5.4	Consecutive Reaction from Amidation to ortho-Lithiation	59
3.5.5	Continuous reaction	59
3.5.6	Continuous whole process	60
3.5.7	Summary of PI options	61
3.6	Design of batch base case, intensified batch case, continuous reaction case and continuous whole process case for 3 tons per year production (amide 1)	63
3.7	Comparisons of sustainability performance	65
3.8	Conclusion	68
Chapter 4.	Ortho-Lithiation process – Part 1: Process Understanding	69
4.1	Introduction	69
4.2	Reaction System	70
4.3	Experimental Apparatus and Procedures	71

4.3.1	Microreactors.....	71
4.3.2	Stainless Steel Reactor	73
4.3.3	PTFE T-reactor	73
4.3.4	Spinning Disc Reactor (SDR).....	74
4.4	Feasibility Study of Flow Process	75
4.4.1	Microreactors (Microchip 1 and 2) Results and Discussions.....	75
4.4.2	Stainless Steel Reactor Results and Discussions.....	76
4.5	Development of T-reactor (PTFE) Flow Process	79
4.5.1	Effect of DMF Addition Mode.....	80
4.5.2	Effect of Bath Temperature in step 1	80
4.5.3	Effect of Residence Time in Step 1	81
4.5.4	CFD Simulation of Mixing in T-mixer.....	82
4.6	Development of Spinning Disc Reactor (SDR) Flow Process	85
4.6.1	Mode of DMF Addition.....	85
4.6.2	Position of n-BuLi Feed	85
4.6.3	Effect of SDR Coolant Temperature	86
4.6.4	Effect of Total Flow Rate	86
4.6.5	Effect of Disc Speed	87
4.6.6	Visual Observations.....	89
4.7	Summary	90
Chapter 5.	Ortho-lithiation Process – Part 2: Assessment of Sustainability Benefits for Reaction	92
5.1	Design of STR Reaction System for 3 tons per year Production.....	92
5.2	Design of T-reactor and SDR Reaction Systems for 3 tons per year Production	93
5.3	Comparisons of Sustainability Performance.....	96
5.4	Summary	100

Chapter 6.	Ortho-lithiation to Reduction Process – Part 3: Assessment of Sustainability Benefits for Whole Process Featuring Consecutive Reaction from ortho-Lithiation to Reduction	101
6.1	Introduction	101
6.2	Experimental Apparatus and Procedures	102
6.2.1	Method of analysis in ortho-lithiation and reduction workup.....	102
6.2.2	Ortho-lithiation laboratory-scale workup according to literature procedure	103
6.2.3	Modified safe and scalable ortho-lithiation workup	103
6.2.4	Reduction experiments (in-situ IR).....	103
6.2.5	Reduction laboratory-scale workup	104
6.3	Bottlenecks in ortho-lithiation Batch Base Case Separation Process.....	105
6.4	Feasibility of performing consecutive reactions from ortho-lithiation to reduction in batch mode	106
6.4.1	Solvent compatibility	106
6.4.2	Feasibility of workup after the consecutive reactions in batch mode	109
6.5	Design of combined batch base case and continuous consecutive reaction processes for 3 ton per year production.....	110
6.6	Comparison of process performance between combined base case and continuous consecutive reaction.....	112
6.7	Conclusion.....	114
Chapter 7.	General Framework	115
7.1	Lab-scale Batch Experiments	116
7.2	Safe and Scalable Batch Base Case.....	119
7.3	Generation of PI Options.....	119
7.4	Synthesis of Intensified Cases (Whole Process)	125
7.5	Comparison of Sustainability Metrics	125
Chapter 8.	Conclusions and Recommendations	127
8.1	Conclusions	127

8.2	Recommendations for Future Work	128
References	131	
Appendices	143	
Appendix A. Amidation Process - Synthesis and Evaluation for Intensification and Sustainability Benefits 143		
A.1	Rheometer study.....	143
A.2	Amidation kinetic study (Batch base case)	146
A.3	Analytical methods.....	149
A.4	Amidation in toluene-water solvent system (Intensified batch case).....	151
A.5	THF drying study	152
A.6	Sustainability performance.....	154
A.7	Sustainability metrics	158
Appendix B. Ortho-Lithiation Process – Part 1: Process Understanding		
B.1	In-situ IR monitoring of ortho-lithiation in STR.....	166
B.2	Analytical methods, n-BuLi titration, stability of aldehyde 1	170
B.3	Differential scanning calorimetry (DSC): Amide 1 and Aldehyde 1	171
B.4	Stirred tank reactor (STR): Experiment procedure and results	172
Appendix C. Ortho-Lithiation Process – Part 2: Assessment of Sustainability Benefits for Reaction.....		
C.1	Stirred tank reactor	176
C.2	T-reactor	178
C.3	Spinning disc reactor	180
Appendix D. Ortho-Lithiation to Reduction Process – Part 3: Assessment of Sustainability Benefits for Whole Process Featuring Consecutive Reaction from Ortho-Lithiation to Reduction		
D.1	IR and GC calibration	184
D.2	Ortho-lithiation workup results and discussion.....	185
D.3	Reaction mechanism for reduction reaction using aqueous base NaBH ₄ . 187	
D.4	Derivation of combined batch base case	189

D.5	Schematic of the continuous consecutive reaction process	195
E.	Presentations and Publication.....	196

List of Figures

Figure 2-1 Frequency of unit operations used in pharmaceutical syntheses. Derived from GlaxoSmithKline's phase III and new product portfolio (Jiménez-González et al., 2011).....	7
Figure 2-2 Process intensification concept (Stankiewicz and Moulijn, 2000).....	9
Figure 2-3 Example of microchip reactor (Sigma-Aldrich, 2017).....	10
Figure 2-4 Spinning Tube in a Tube, HOLL-Reactor® (Costello, 2017).....	11
Figure 2-5 Example of trickle bed reactor (Mederos et al., 2009).....	11
Figure 2-6 Example of rotating foam reactor (Visscher et al., 2013).....	12
Figure 2-7 Example of a HEX reactor (Murphy et al., 2014).....	12
Figure 2-8 Example of SMX Sulzer static mixer (Sulzer, 2017a).....	13
Figure 2-9 Schematic of oscillatory baffled reactor (University, 2017).....	14
Figure 2-10 Thin film SDR with (a) a grooved disc surface (Boodhoo, 2013); (b) underneath the disc surface (NewcastleUniversity, 2017).....	14
Figure 2-11 Schematic of SpinPro R300 (Flowid, 2015).....	16
Figure 2-12 (a) Schematic of hydrodynamic cavitation (Parthasarathy et al., 2013); (b) emulsion formation using cavitation (Zhang et al., 2016).....	16
Figure 2-13 Example of Taylor-Couette reactor (Tran et al., 2016).....	17
Figure 2-14 Example of monoliths (Rouhi, 2003).....	17
Figure 2-15 CFD simulation of an impinging jet reactor (Gavi et al., 2007).....	18
Figure 2-16 Schematic of the rotating packed bed reactor (Visscher et al., 2013).....	19
Figure 2-17 Schematic of reactive distillation (Cárdenas-Guerra et al., 2010).....	19
Figure 2-18 Schematic of simulated moving bed (SMB) (KNAUER, 2017).....	20
Figure 2-19 Schematic of rotating annular chromatographic reactor (Visscher et al., 2013) ..	21
Figure 2-20 Example of two CINC CE in series (ColeParmer, 2017).....	21
Figure 2-21 (a) Scheibel column (KMPS, 2017c); (b) asymmetric rotating disc contactor (Separationprocesses, 2017); (c) Karr column (KMPS, 2017a).....	23
Figure 2-22 Schematic of Nutsche filtration and drying process (Systems, 2017b).....	24
Figure 2-23 Schematic of centrifugal filter (Heinkel, 2017a).....	25
Figure 2-24 Schematic of rotary drum vacuum filter (Komline-Sanderson, 2017).....	26
Figure 2-25 (a) Example of tray dryer (PRISMpharma, 2017); (b) Schematic of fluid bed dryer (Deviatkin, 2013); (c) Example of a conveyor dryer (Alibaba, 2017b); (d) Schematic of double drum type drum dryer (Katsuragi, 2017).....	27
Figure 2-26 Schematic of the WFE (a) Scrapper spreading a thin film on the walls; (b) Direction of liquid flow (FoodProcessingTechnologies, 2017).....	28
Figure 2-27 Schematic of agitated thin film dryer (Aquacare, 2017).....	29

Figure 2-28 Example of spray drying technology (Sonarome, 2017).....	29
Figure 3-1 Base case amidation reaction in a 500 mL RC 1 reactor.	46
Figure 3-2 Amidation kinetic study in a 150 mL stirred tank reactor.....	47
Figure 3-3 Schematic of the continuous static mixer setup.	48
Figure 3-4 Continuous amidation reaction in static mixer setup (Static mixers not visible)...	49
Figure 3-5 A single Noritake static mixer (Source: Noritake (2017a))	49
Figure 3-6 (a) Schematic of CINC V02 centrifugal extractor (Source: CINC (2017)); (b) Actual setup used in experiment.....	50
Figure 3-7 POPE Wiped Film Evaporator used in actual experiments.....	51
Figure 3-8 Schematic of cavern formation (Paul et al., 2004).....	53
Figure 3-9 a) Mixing dependency of the amidation experiments; b) Temperature profile of the experiments	54
Figure 3-10 Microscope photography of the final reaction mixture slurry at 6 w/w%	54
Figure 3-11 Schematics of cavern observed in mixed tanks, where grey areas indicate regions that are well mixed and white indicates unmixed areas. (Kresta et al., 2015).....	55
Figure 3-12 Crystalline solid amide 1 obtained after workup under anhydrous condition.....	56
Figure 3-13 Photo of large biphasic slugs of toluene and water phases in the bare PTFE tubing section. Large liquid-liquid slugs observed in red circle	60
Figure 3-14 Breakdown of OPEX for all 4 cases.....	67
Figure 4-1 (a) Setup of the entire microreactor system; (b) Schematic of glass microchip 1 with two inlets in use.....	72
Figure 4-2 Schematic of glass microchip 2 with three inlets	72
Figure 4-3 (a) Setup of the stainless steel reactor; (b) Reagents delivered into stainless steel reactor via syringe pumps, submerged in circulated silicon oil bath.	73
Figure 4-4 PTFE T-reactor setup	74
Figure 4-5 (a) Schematic of the SDR (10 cm diameter) set-up; (b) view of disc surface; (c) picture of the set-up.....	75
Figure 4-6 Microchip 1 – (a) Clogging in premixing region; (b) clogging in entire microchip	75
Figure 4-7 (a) Smooth run; (b) particle accumulation in Microchip 2 channel	76
Figure 4-8 (a) Stainless steel reactor setup; (b) Schematic of stainless steel reactor setup	77
Figure 4-9 Temperature profile on the surface of the T-mixer and surface of inlet of R1 tube for (a) 0.12 mL/s and (b) 1.18 mL/s respectively (Bath temperature was at 17 °C).....	78
Figure 4-10 Effect of circulation bath temperature on step 1 under constant residence time (0.4 s) and combined flow speed.....	81

Figure 4-11 (a) Aldehyde 1 yield; (b) Overall conversion against residence time (Step 1) using T-reactor for different Re numbers of 1219 and 2437.....	81
Figure 4-12 Schematic picture of T-mixer used in step 1 in T-reactor	82
Figure 4-13 Simulation result of scenarios 1 to 3 showing particle traces and contour plots of volume fraction. (Red: THF stream; Blue: Hexane stream).....	83
Figure 4-14 (a) Aldehyde 1 yield; (b) overall conversion; (c) Aldehyde 1 selectivity against Re (Step 1) using T-reactor under constant residence times of 0.4 s and 0.8 s	84
Figure 4-15 Effect of circulated bath temperature under constant residence time (0.4 s), total flow rate (1.2 mL/s) and disc speed (1,400 rpm).	86
Figure 4-16 Effect of total flow rate (step 1) under constant disc speed of 1400 rpm.	86
Figure 4-17 Estimated residence time (Boodhoo and Al-Hengari, 2012) of Step 1 on the disc at different flow rates and disc speeds. Data within the pink area represents the corresponding residence times at 1400 rpm	87
Figure 4-18 (a) Aldehyde 1 yield; (b) overall conversion against disc speeds of 400 to 2400 rpm at different flow rates.....	88
Figure 4-19 Estimated film thickness (Boodhoo, 2013) at different disc speed at constant total flow rates.	88
Figure 4-20 (a) SDR disc before experiment; (b) SDR after 2 hours of usage; (c) SDR disc after 6 hours of usage.....	89
Figure 4-21 (a) T-reactor under constant residence time (0.4 s) and total flow rate (1.3 mL/s); (b) SDR under constant total flow rate (1.2 mL/s) and disc speed (1,400 rpm). (Circulated bath at 17 °C).....	89
Figure 5-1 Schematic process diagram for batch process	93
Figure 5-2 Schematic process diagram for T-reactor flow process.....	94
Figure 5-3 Schematic process diagram for SDR flow process.....	95
Figure 5-4 Breakdown of the energy consumption	98
Figure 5-5 Cost breakdown of the OPEX.....	99
Figure 5-6 Cost breakdown of the CAPEX.....	100
Figure 6-1 Summary of major process steps in (a) continuous consecutive reaction. Blue boxes indicate ortho-lithiation related steps; yellow boxes indicate reduction related steps; (b) combined base case process;	102
Figure 6-2 (a) 150 mL stirred tank reactor (STR) used for performing batch IR experiments; (b) STR connected to IR computer via IR probe	104

Figure 6-3 Aldehyde 1 concentration profiles tracked by in-situ IR measurement for two different forms of NaBH ₄ used.....	107
Figure 7-1 Stepwise framework for intensification	115
Figure 7-2 Thought process for the generation of PI options	119

List of Tables

Table 2-1 List of PI and conventional equipment for pharmaceutical applications.....	31
Table 3-1 Four amidation cases to be evaluated.....	44
Table 3-2 Initial AC and DIPA concentrations used for amidation kinetic study.....	47
Table 3-3 Kinetic parameters of amidation reaction	55
Table 3-4 Cost comparison of amine reagents	57
Table 3-5 Summary of the improvement actions taken to minimise amount of wash medium used.....	58
Table 3-6 Summary of reaction and separation information in literature, base case and intensified batch case, continuous reaction and continuous process	62
Table 3-7 Comparisons of sustainability metrics between batch base case, intensified case, continuous reaction, continuous whole process at design scale of about 3 ton amide 1 per year.	65
Table 4-1 Microchip 2 result at 20 °C	76
Table 4-2 Effect of flow rate at constant residence time and temperature for stainless steel reactor	77
Table 4-3 Reaction profile at different temperatures.....	78
Table 4-4 Experiments using different quantities of DMF carried out under constant step 1 residence time of 0.4 s and bath temperature set at 17 °C	80
Table 4-5 Simulated flow conditions in T-reactor using three different flow speeds	82
Table 4-6 Effect of position of n-BuLi feed on reaction profile	85
Table 4-7 Highest yield obtained in the different reactors and their respective operating conditions	91
Table 5-1 Specifications of the raw materials	96
Table 5-2 Comparisons of sustainability metrics between STR, T-reactor and SDR process at design scale of about 3 tons per year aldehyde 1	96
Table 6-1 Lab-scale batch reduction reaction conditions using different forms of NaBH ₄ ...	103
Table 6-2 Summary of ortho-lithiation safe and scalable base case operations.....	105
Table 6-3 Effect of amount of side product on purification	106
Table 6-4 Comparison of reduction rate between solid and liquid form NaBH ₄ used.....	107
Table 6-5 Summary of the advantages and disadvantages of different reduction cases	108
Table 6-6 Material cost comparison between options 1 and 2	109
Table 6-7 Composition of reaction mixtures from STR and T-reactor after ortho-lithiation reaction and two water washes.	109
Table 6-8 Reduction laboratory scale experiments and observations	110

Table 6-9 Summary of small-scale continuous consecutive reaction operations	111
Table 6-10 Performance metrics of combined ortho-lithiation and reduction base case at design scale of about 3 tons per year alcohol 1	112
Table 7-1 Initial evaluation of characteristics of lab-scale batch chemical systems	117
Table 7-2 Potential benefits and barriers to PI options for amidation process	121
Table 7-3 Potential benefits and barriers to PI options for ortho-lithiation process	123
Table 7-4 Sustainability metrics	126

Nomenclature

D	Diameter of vessel [m]
E_a	Activation energy [kJ mol ⁻¹]
k	Rate constant [L mol ⁻¹ s ⁻¹] (overall second order)
k_0	Frequency factor [s ⁻¹]
M	Concentration [mol L ⁻¹]
N_p	Power number
Q	Volumetric flow rate [m ³ s ⁻¹]
r	Radial position from disc center [m]
Re	Reynolds number
τ_{res}	Residence time [s]
t	Time [s]

Greek alphabets

ε	Power dissipation [W kg ⁻¹]
ρ	Density [g L ⁻¹]
δ	Film thickness [m]
ω	Rotational speed [rad s ⁻¹]
ν	Kinematic viscosity [m ² s ⁻¹]

Subscripts

<i>i</i>	Inner radius of the disc
<i>o</i>	Outer radius of the disc

Acronyms

API	Active Pharmaceutical Ingredient
CAPEX	Capital Expenditure
CE	Centrifugal Extractor
CFD	Computational Fluid Dynamics
CSTR	Continuous Stirred Tank Reactor
DSC	Differential Scanning Calorimetry
GC	Gas Chromatography

OPEX	Operational Expenditure
PI	Process Intensification
PTFE	Polytetrafluoroethylene
RC 1	Reaction Calorimeter
SDR	Spinning Disc Reactor
STR	Stirred Tank Reactor
WFE	Wiped Film Evaporator

Symbols

AC	4-chlorobenzoyl chloride
Alcohol 1	4-chloro-N,N-diisopropyl-2-(hydroxymethyl)benzamide
Aldehyde 1	4-chloro-N,N-diisopropyl-2-formylbenzamide
Amide 1	4-chloro-N,N-diisopropylbenzamide
DIPA	Diisopropylamine
DIPA.HCl	Diisopropylamine hydrochloride
DMF	Dimethylformamide
mol eqv	Mole equivalent with respect to starting material (AC/Alcohol 1/Aldehyde 1/Amide 1)
SP1/SP2	Side products 1 or 2
TEA	Triethylamine
TEA.HCl	Triethylamine hydrochloride
THF	Tetrahydrofuran
i.d.	Internal diameter
o.d.	Outer diameter

Chapter 1. Introduction

The pharmaceutical industry is one of the most innovative sectors when it comes to inventing and developing new chemical lead structures and finding new therapeutic approaches. For the last decades this industry has developed blockbuster drugs for a wide range of illnesses, although a number of diseases are still presenting significant challenges to find effective cures. The drivers for large pharmaceutical companies to invest in improved production methods have been weak. Only recently, the issues on sustainability of the development, production and application of medicines have gained public attention. Regulatory authorities such as the United States Food and Drug Administration (FDA) have begun to provide guidance for industry to develop more sustainable manufacturing. In order to create and maintain sustainable businesses in the face of global competition and tighter safety and environmental regulations, the pharmaceutical industry is exploring new areas and technologies that could potentially bring about significant improvements in process performance.

Process intensification (PI) has the potential to improve early development or to retrofit existing processes by creating new process options, which are required to achieve green and sustainable benefits in production. Reported works on PI are mostly case specific, that is, applying particular PI equipment (e.g. Spinning Disc Reactor) or method (e.g. Reactive Distillation) to improve a specific process. The main barrier to adopting PI generally includes the investment required, the uncertainty associated with implementation of such technologies and lack of experience in their operation. One reason for this is the lack of simple systematic identification of PI option for any given process. This includes the method of deciding in the early stage where and how the process should be intensified for improvements in product quality, productivity and process sustainability. Although there are substantial methodologies documented in the literature, a practical methodology which analyses the whole process flow from reaction to work-up for a range of reactions with different characteristics is still unavailable.

1.1 Research Motivations

In contrast to processes that are encountered in large, continuous processing plants, batch pharmaceutical processes often have chemistries that are substantially more complex. The amount of resources required to evaluate the kinetics and physical parameters to the accuracy required to apply 'standard' chemical engineering design methods (e.g. define reaction time by integrating the rate equation) would be immense.

Simulation is a tool that has been described useful by many methodologies reported in the literature in earlier chapter. It can be used to model and predict physical properties, as well as to optimize yield based on mathematical model. However, these published methodologies are seldom used in practical situations and fail in real life application. In the event of inaccurately extrapolated data, the resulting impact is more serious in PI technologies/continuous process than batch process. The common problems faced when using modelling based methodologies include:

- Inaccurate and missing chemical, physical and process data due to insufficient time and resources to obtain them
- Uncertainty in suitability of new/PI equipment due to insufficient PI equipment data or knowledge and lack of standardized characterization test for benchmarking
- Time taken to familiarize with the chemical transformation and new/PI equipment is too long

However despite the poor quality of information, the decision on which production technologies to use is usually made at the early stage of process development. The risk of failure is therefore quite high if the wrong decision is made. The decision is further complicated by a number of decision criteria – cheap, safe, environmental-friendly and fast time to market.

The availability of wide range of technology is not necessarily a good measure of development capability as there may be potential mismatch of technologies. There may also be other forms of intensification options besides the application of new technology (e.g. reduce solvent and reagent usage, recycle, etc.). The vast options to intensify a process made decisions difficult for the typical project technical team (of non-process intensification experts) to identify the best option within the time constraints of a project. As pointed out by some of the big pharmaceutical companies, the industry requires practical methodologies to evaluate the processes and swiftly identify feasible options for greener and more sustainable manufacturing (Jiménez-González et al., 2011).

Another weak link is the pharmaceutical workup process, in contrast to bulk chemical production, there has been little focus on separation steps which have been reported to be the major contributors of the overall processing energy and costs of a synthesis (i.e. distillation and drying steps often consume more than 50% of the energy requirements) (Poechlauer et al., 2012).

1.2 Aims and Objectives

The primary focus of this project is to showcase the evaluation of pharmaceutical processes (reaction and workup) for intensification and sustainability benefits. The current research may be categorized into the following sections:

1. Amidation process – Synthesis and evaluation for intensification and sustainability benefits
2. Ortho-lithiation process – Part 1: Process understanding
3. Ortho-lithiation process – Part 2: Assessment of sustainability benefits for reaction
4. Ortho-lithiation to reduction process – Part 3: Assessment of sustainability benefits for whole process featuring consecutive reaction from ortho-lithiation to reduction
5. General framework

The objective of the amidation process case study is to evaluate the sustainability benefits of intensification of a conventional batch amidation process. PI options, proven feasible in lab-scale experiments are adopted and represented in terms of three intensified cases - the intensified batch case, the continuous reaction case and the continuous whole process case, which are compared to the batch base case. To compare their sustainability performance, the respective plants are designed at the same basis of about 3 ton per year throughput. The sustainability metrics used in this study are volume efficiency, maximum processing inventory at any point of time, material efficiency, E-factor, energy efficiency, capital and operational expenditure.

The ortho-lithiation process consists of three parts. The objective of the first part of this work is to demonstrate the technical feasibility of performing ortho-lithiation reaction in continuous flow reactors (the microreactor, the stainless steel reactor, the T-reactor and the SDR) at ambient temperature to obtain high purity product. For example, it is known that clogging tends to occur in microreactor during ortho-lithiation. It is envisioned that the use of the SDR which allows a free surface film flowing over the disc surface instead of through an enclosed channel would overcome this potential limitation.

Based on the experimental performance of the intensified continuous flow reactors, the most promising two have been selected – the T-reactor and the SDR for further theoretical evaluation. The objective of the second part of the ortho-lithiation process focuses on theoretical evaluation of the sustainability benefits of operating the reaction in the T-reactor and the SDR as compared to the conventional stirred tank reactor (STR). This chapter only studies the reaction step at a hypothetical design scale of 3 tons per year, excluding workup. The potential

benefits that could be achieved are higher reaction selectivity, higher material efficiency, lower energy consumption, improved safety and economic savings.

As a continuation, the last part of the ortho-lithiation process would study the sustainability performance of the whole process including workup for the batch (STR) and flow (T-reactor) processes. With the understanding that T-reactor is able to obtain higher reaction yield than the STR, it would be ideal to investigate the impact of reaction yield on downstream processes. The primary objective of this study is aimed at intensifying the workup steps by avoiding the isolation of aldehyde 1 and directly transferring it into the next reactor for subsequent reaction. The potential benefits that could be achieved from consecutive reactions are significant savings from wash solvents, lower energy consumption, higher material efficiency and reduction in loss of product. A detailed study of the selected reduction reaction is thus performed to assess its compatibility and limitations in performing the consecutive reactions. Upon validating the feasibility of the consecutive reactions, the batch process and the continuous consecutive reaction process would be conceptually synthesized at a hypothetical design scale of 3 tons per year and compared based on their sustainability metrics.

Based on the experience gained from the different processes, this thesis presents a general framework which summarizes the approach to PI for pharmaceutical processes. This framework aims to facilitate the early stage of process development by offering the initial estimation of benefits versus costs and generates possible intensification options through an experimental approach.

1.3 Thesis Layout

Chapter 1 introduces the research motivations and the aims and objectives of the work. The next chapter, Chapter 2, provides an overview to the background of pharmaceutical manufacturing, followed by a summary of the list of PI techniques and conventional equipment relevant to the pharmaceutical industry. A critical review of the existing PI methodologies is also provided.

Chapter 3 presents the sustainability benefits of intensification of a conventional batch amidation process. This includes experimental validation of the potential PI options and comparison between different intensified cases and the batch base case.

The ortho-lithiation continuous flow experiments performed in various PI reactors are presented and discussed in Chapter 4. The T-reactor and the SDR are selected to compare with the conventional batch stirred tank reactor based on the sustainability metrics at a hypothetical production scale of 3 tons per year in Chapter 5. Intensification of workup is included in Chapter

6 where the evaluation of sustainability benefit of performing consecutive reaction from ortho-lithiation to the subsequent reaction (reduction) is investigated.

Chapter 7 presents the general framework which summarizes the approach to PI for the two main chemical transformations discussed in Chapter 3 and 4. This chapter serves as a reflection of the learning points gathered from the case studies.

Finally, the conclusions and recommendations for future investigations are presented in Chapter 8.

Chapter 2. Literature Review

2.1 Background: Manufacturing of Pharmaceuticals

Currently pharmaceutical manufacture is mostly dominated by batch processing (Sharratt, 1997). This is an industry characterized as traditionally operating in flexible multipurpose batch plants. One key feature of pharmaceutical batch process is the tendency to use the same piece of equipment for multiple operations – usually a stirred tank manufactured in a corrosion-resistant material. The stirred tank might be used for blending reagents, warming them to reaction temperature, cooling, perform liquid-liquid extraction, solvent evaporation and crystallise the product. Other than the stirred tank, common batch process equipment includes filters and dryers. Often, solid handling is involved with a significant manual effort.

The design and operation of batch processes for the manufacture of active pharmaceutical ingredients (API) is very different from those for the manufacture of bulk chemicals by continuous process. The process chemistry tends to be more complex and less well understood than those in a continuous process. Often, reactions are carried out in the liquid phases, in the presence of a solvent at moderate temperatures and atmospheric pressure. The products are often solids which necessitate operations like good mixing and filtration. The conventional typical batch manufacturing process is to react the starting material, followed by workup (e.g. evaporation, solvent swap, filtration, etc.) and purification (e.g. crystallisation). Although the reaction is often the focus of the process, it usually takes only a portion of the time, energy and material consumption. The frequency of common unit operations in pharmaceutical syntheses is shown in Figure 2-1. Majority of the unit operations is in separations, for example, extractions, distillation, drying, filtration, etc. Separations are usually performed in batch or semi-batch manner, where intensified methods are uncommon. In terms of mass efficiency, the separation steps usually contribute about 40-90% of the mass intensity of a pharmaceutical synthesis process. In terms of energy consumption, the distillation and drying steps often accounts for more than 50% of the energy consumed and are usually the bottleneck operations due to their long cycle time (Jiménez-González *et al.*, 2011). Consequently, the amount of time and energy required for separation are often much higher than for the reaction which results in increased equipment size, higher energy usage and higher capital and operating costs.

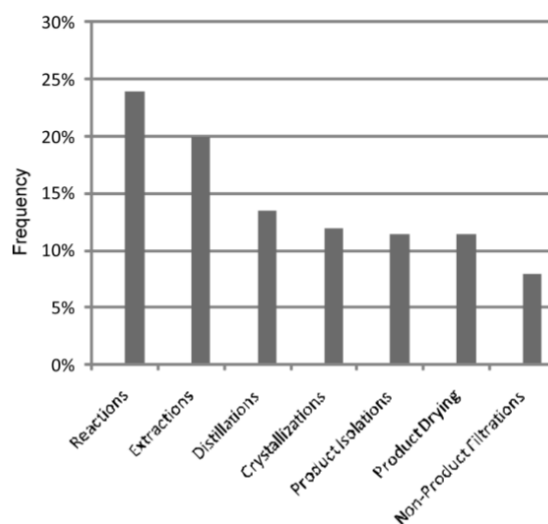


Figure 2-1 Frequency of unit operations used in pharmaceutical syntheses. Derived from GlaxoSmithKline's phase III and new product portfolio (Jiménez-González et al., 2011)

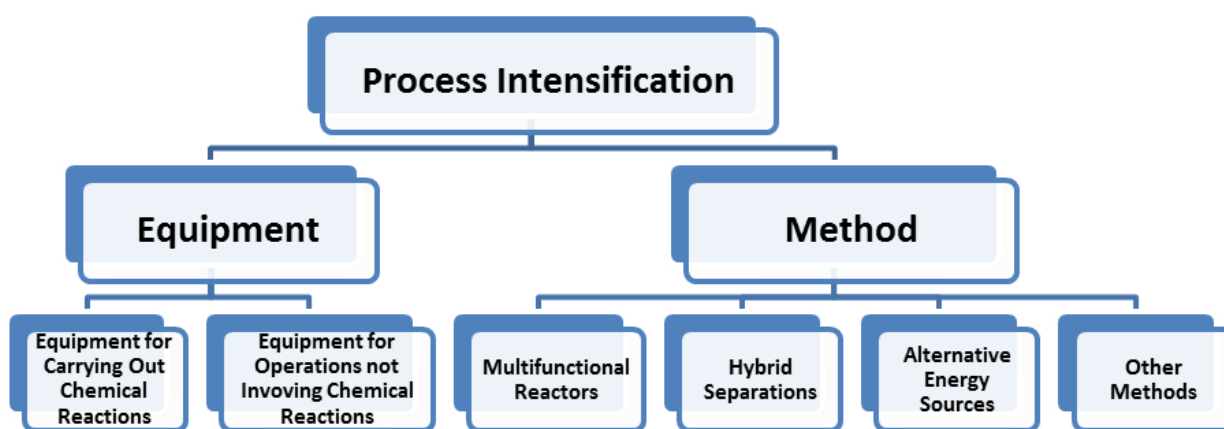
The widespread use of stirred tanks and other 'generic' equipment has led to the standardization of mechanical engineering design within batch processing companies. For example, it is convenient to buy glass-lined steel tank reactors, ready-fitted with agitator and motor, in a wide range of sizes. The commonly used heat exchangers (e.g. plate) also come in fixed sizes. It is common to have oversized vessels but the time-saving benefit of using these standardised equipment outweighs the benefit of customising the vessel to the exact size for the duty.

2.2 Process Intensification (PI)

Process Intensification (PI) has emerged to become one of the most promising trends in process engineering during the past thirty years. The concept of PI has evolved over time, from technologies aiming at volume reduction as proposed in 1980s by Colin Ramshaw to PI as an integrated approach for overall process improvement (Ramshaw, 1999). PI is defined as "*any chemical engineering development that leads to a substantially smaller, cleaner and more energy efficient technology*" which ultimately result in cheaper, safer environmental-friendlier and sustainable technologies (Stankiewicz and Moulijn, 2000). To achieve PI, van Gerven and Stankiewicz (Van Gerven and Stankiewicz, 2009) defined four explicit goals of PI: (1) maximize the effectiveness of intra- and intermolecular events; (2) optimize the driving forces at every scale and maximize the specific surface area to which these forces apply; (3) maximize synergistic effects, and (4) give each molecule the same processing experience. Lutze, Gani and Woodley (Lutze *et al.*, 2010) define four principles for PI, which are (a) integration of unit operations, (b) integration of functions, (c) integration of phenomena and (d) targeted enhancements of phenomena in a given operation. In the pharmaceutical and fine chemical

context, for example, instead of slowing down a reaction to fit into the limited capabilities of a batch multipurpose reactor, the reaction environment is optimized for the respective requirements of the reaction. Therefore, costly and environmentally unfriendly tasks like dilution and operation at very low temperature would be rendered unnecessary. As the energy and material efficiencies of an intensified process are better than those of non-intensified process, so the aim of sustainable manufacturing will require intensification of selected process steps.

Within process intensification two broad categories of technology can be distinguished: novel equipment and new processing methods as shown in Figure 2-2. A few of the PI equipment and methods, for example, reactive distillation (Harmsen, 2007b), rotating packed beds (Rao *et al.*, 2004) and microreactors (Kockmann *et al.*, 2011) have been commercialised and operated at industrial scale, while others are still in the research phase and require more technical information. One point to note is that many pharmaceutical processes require solid handling and intensification of processes involving solids tends to be more challenging. Recently, a review focusing on PI applied to solid handling has been published (Wang *et al.*, 2017).



Examples						
Spinning Reactor	Disc Static Mixers	Reverse-Flow Heat Reactors	Membrane Absorption	Centrifugal Fields	Supercritical Fluids	
Static Reactor	Mixer Exchangers	Reactive Heat Distillation	Membrane Distillation	Ultrasound	Dynamic Reactor Operation	
Static Catalysts (KATAPAKs)	Microchannel Mixing Exchangers	Reactive Rotor/Stator Mixers	Adsorptive Distillation	Solar Energy	Microwaves	
Monolithic Reactors	Rotating Beds	Packed Reactive Crystallization		Electric Fields	Plasma Technology	
Microreactors	Centrifugal Adsorber	Chromatographic Reactors				
Heat Exchange (HEX) Reactors		Periodic Separating Reactors				

Supersonic	Membrane
Gas/Liquid	Reactors
Reactor	Reactive Extrusion
Jet-Impingement	Reactive
Reactor	Comminution
Rotating Pack-Bed	
Reactor	

Figure 2-2 Process intensification concept (Stankiewicz and Moulijn, 2000)

2.3 Conventional and PI equipment in Pharmaceutical Industry

This review summarises some of the PI and conventional equipment that can be used in the pharmaceutical process. They are classified broadly under different unit operations – reaction, liquid-liquid extraction, filtration, purification and drying. To date, the majority of the PI equipment discussed in this chapter have been successfully applied in the pharmaceutical industry and commercialised as summarised in Table 2-1.

One of the most important aspect of pharmaceutical processing is mixing/agitation. Mixing is involved in various tasks such as blending of reagents, suspension of solids, dispersion of two immiscible liquid phase, enhancing heat and mass transfer rates, etc. Depending on the production scale, mixing times can be of the orders of minutes or longer in batch stirred tank. Inefficiency mixing can affect process efficiency which is most noticeable upon scale-up from laboratory scale. It is important to identify and address any potentially mixing-sensitive operations with suitable mixing equipment to achieve appropriate mixing performance on the production scale. Superior mixing can be achieved by using various PI equipment (Visscher *et al.*, 2013), such as the microreactor, spinning disc reactor, static mixer reactor, spinning-tube-in-tube reactor, Taylor-Couette reactor, oscillatory baffled reactor, HEX reactor, impinging jet reactor and rotating packed bed reactor. For reaction involving catalysts, the gas-liquid-solid trickle flow reactor, the catalytic foam stirrer reactor and monolithic reactor are applicable.

2.3.1 Microreactors

Microreactors (Figure 2-3) are chemical reactors of extremely small dimensions and usually have a sandwich-like structure, consisting of a number of layers constituted by micromachined channels whose diameter may range between 20-500 μm (Hartman *et al.*, 2011). Microreactors allow very high heat transfer rates that are not achievable in other equipment. This makes isothermal operation of highly exothermic process possible. Very low reaction-volume-to-surface-area ratios make microreactors attractive for reactions involving poisonous or explosive reactants (Nagaki *et al.*, 2014b). Compared to traditional reactors, heat dissipation

in microreactors is significantly enhanced by passing the reaction fluid through very small channels, realized in high thermally conductive metal blocks which, depending on the endothermic or exothermic nature of the reactions, are heated or cooled, respectively. The major advantage of microreactors is the excellent control of reaction temperature. The main drawbacks, instead, are high pressure drops, relevant clogging tendency and high unit cost. Microreactors may be successfully exploited in both fine chemistry and pharma (Yoshida et al., 2008; Kockmann and Roberge, 2011; Dencic and Hessel, 2013; Schwolow et al., 2016).

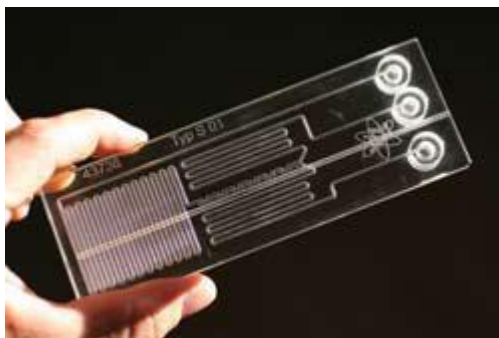


Figure 2-3 Example of microchip reactor (Sigma-Aldrich, 2017)

2.3.2 *Spinning Tube in Tube Reactor*

The spinning tube in tube reactor (Figure 2-4) is a reactor with tubular geometry. It consists of a rotating tube (rotor) inside a stationary tube (stator), which are mounted at a concentric radial spacing between 0.25×10^{-3} and 0.44×10^{-3} m (Visscher et al., 2013). The gap between the inner diameter of the rotor and the outer diameter of the stator is filled with reactants, where typical volume varies from 1×10^{-5} to 1×10^{-3} m³. Typical rotational speed for the rotor is between 3000 and 12,200 rpm. As a result of the small distance between the cylindrical rotor and stator, the reactants inside the annual volume are exposed to high shear rates in the range of $30,000 \text{ s}^{-1}$ to $70,000 \text{ s}^{-1}$. Excellent heat transfer rates, mass transfer rates and phase interactions are expected due to the high shear rates and low reactor volume, thus making the reactor suitable for highly exothermic reactions that require only a small amount of catalyst.

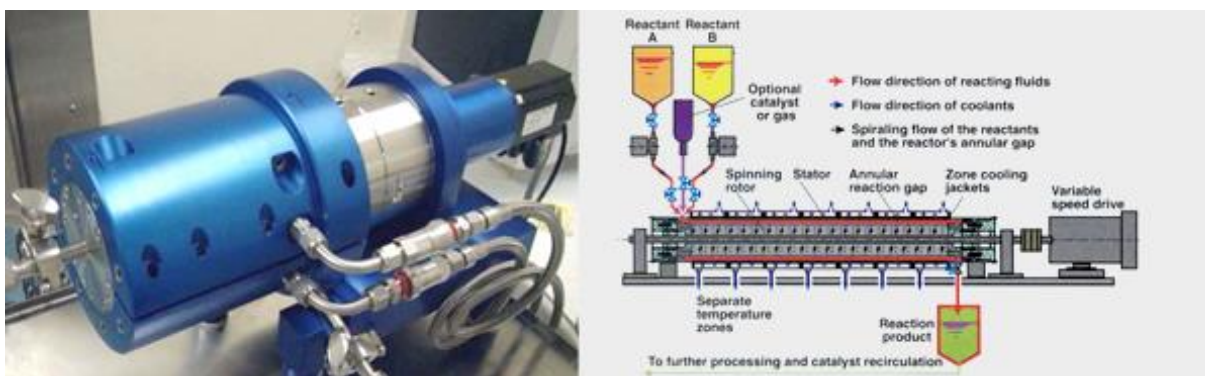


Figure 2-4 Spinning Tube in a Tube, HOLL-Reactor® (Costello, 2017)

2.3.3 Gas-Liquid-Solid Trickle Flow Reactor

In a gas-liquid-solid trickle flow reactor (Figure 2-5), fine adsorbent trickles through the fixed bed of catalyst, which selectively removes in-situ one or more of the products from the reaction zone. An example is methanol synthesis, which involves feeding CO and H₂ are fed to a gas-solid-solid trickle flow reactor consisting of three tubular reactor sections with cooling sections in between. Silica-alumina powder was used as adsorbent and complete conversion was achieved (Kuczynski et al., 1987).

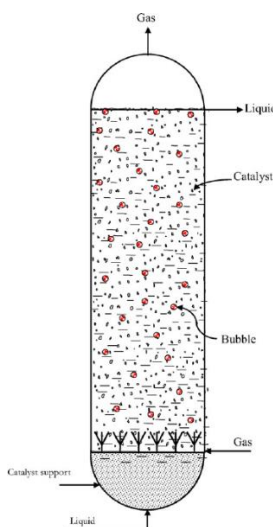


Figure 2-5 Example of trickle bed reactor (Mederos et al., 2009)

2.3.4 Catalytic Foam Stirrer Reactors

Catalytic foam reactors (Figure 2-6) use a solid foam as stirrer blades and as support for deposition of catalyst for reactions of liquid and/or gas phase reactants (Tschentscher et al., 2010a; Tschentscher et al., 2010b; Leon et al., 2011; Leon et al., 2012; Leon et al., 2013). One of the advantages of such a foam stirrer is easy catalyst handling. This approach greatly enhances mass transfer since foam has high surface area for deposition of the catalytic material and has potential to lower pressure drop, leading to lower energy consumption. This technology

is still in the early stage of development. Research shows that foam reactor is 10 times more energy efficient as compared to conventional packed bed reactors (Stemmet et al., 2006).

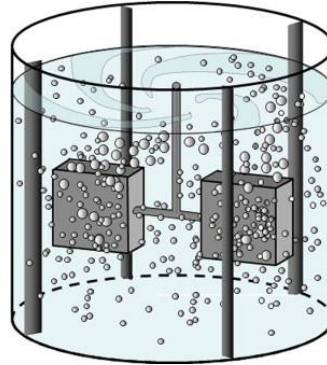


Figure 2-6 Example of rotating foam reactor (Visscher et al., 2013)

2.3.5 Heat Exchanger (HEX) Reactors

In a HEX reactor (Figure 2-7), reactions take place adjacent to a heat exchange surface. The design of a HEX reactor is largely based on compact heat exchangers geometries, where metallic foams, fins, etc. can be inserted to improve reactions conditions such as mixing and residence time, etc (Anxionnaz et al., 2008). The main advantage of a HEX reactor is that heat generated in the reaction can be easily removed (or supplied in the case of endothermic reactions). There are different designs of HEX reactors, e.g. Marbond (Phillips and Symonds, 2007), plate heat exchanger reactors, ProxHeatex (Delsman et al., 2004), microstructure heat reactor (Rebrov *et al.*, 2001), counter-current heat exchanger reactor (Friedle and Vesper, 1999), printed circuit heat exchanger (Johnston et al., 2001). HEX reactors have large potential for fast reactions with a high heat of reaction.

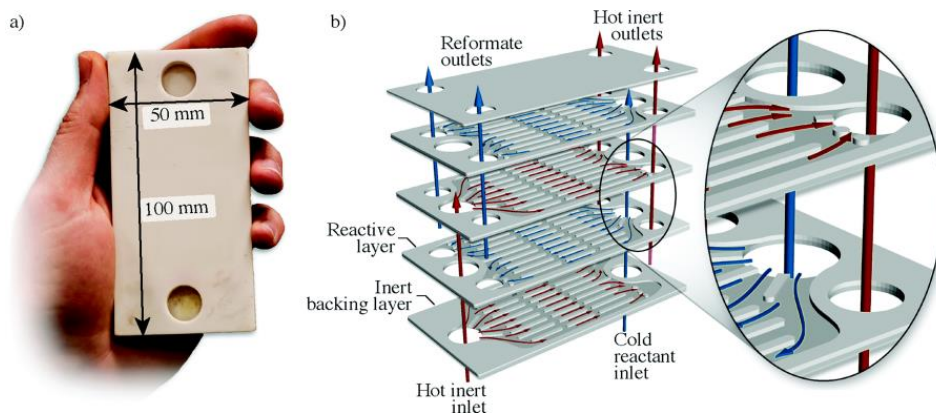


Figure 2-7 Example of a HEX reactor (Murphy et al., 2014)

2.3.6 Static Mixer and Static Mixer Reactor

Stirring technology has greatly advanced during the last 30 years not only by through improvements in conventional mechanical mixer, but also significant process made in of static

mixers that are increasingly favoured. Static mixers (Figure 2-8) are pipe inserts which generate radial mixing, and for multiphase systems, provide interfacial surface area in the form of fine bubbles or droplets (Lobry et al. 2011). The fluids to be mixed can be liquid streams, gas streams, disperse gas into liquid, or immiscible liquids. The energy for mixing is extracted from the loss in pressure of the fluids as they flow through the static mixer and as such extra pumping duty is required. Static mixers are particularly useful for the continuous processing of chemicals and are also incorporated as part of a batch system in pump around loop. Compared to conventional mixing systems, static mixers have higher energy dissipation rate. The main disadvantage of static mixer is their relatively high sensitivity to clogging by solid.

Static mixer reactor provides a combination of intensive mixing, heat and mass transfer. For instance, Sulzer (2017a) has mixing element made of heat-transfer tubes. The mixing and mass transfer is provided by the insertion of mixing elements in the reactor tubes while the heat transfer is achieved via the shells or jackets. The potential advantages of such system are compactness of unit, high selectivity and high thermal efficiency. In general, static mixers are suitable for relatively fast reactions with short residence time.



Figure 2-8 Example of SMX Sulzer static mixer (Sulzer, 2017a)

2.3.7 *Oscillatory Baffled Reactor (OBR)*

The OBR (Figure 2-9) generally consists of a cylindrical column or tube containing equally spaced orifice baffles and superimposing with fluid oscillation (Vilar *et al.*, 2008). Eddies are generated when fluid flow passes through the baffles, enabling significant radial motions where events at the wall are of the same magnitude as these at the centre. The generations and cessation of eddies creates uniform mixing in each baffled cell, collectively along the column or tube. This allows nearly plug-flow conditions even at low flow rate, thus inducing enhanced mass and heat transfers as compared to conventional stirred tank reactor. The degree of mixing is independent of the net flow, thus much longer residence time is achievable compared to other tubular device. The main advantages of OBR are significant energy/utility savings, higher yields and less side product. In addition, capital cost savings are achieved through much more compact designs. This technology is applicable to industrial production involving solid, liquid and gas phases. The main barriers are dealing with high

viscous or high density liquids, high gas production in reaction, high concentration of solid, and reactions with long intrinsic reaction times.

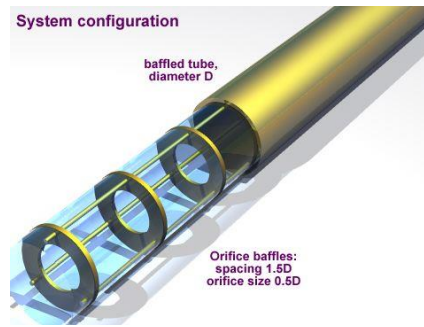


Figure 2-9 Schematic of oscillatory baffled reactor (University, 2017)

2.3.8 *Thin-film Spinning Disc Reactor*

The objective of the Spinning Disc Reactor (SDR) (Figure 2-10) is to generate a highly sheared liquid film (typically 50 to 500 μm) when a liquid is supplied to the unit at or near the centre (Boodhoo, 2013). The film is instantly accelerated tangentially by the shear stresses established at the disc/liquid interface and breaks down into an array of spiral ripples. The detail form of the film depends on various factors including the viscosity of the fluid, the speed of rotation, the geometry of the disc, etc. The liquid film is intrinsically unstable and allows for high rates of mass transfer and heat transfer.

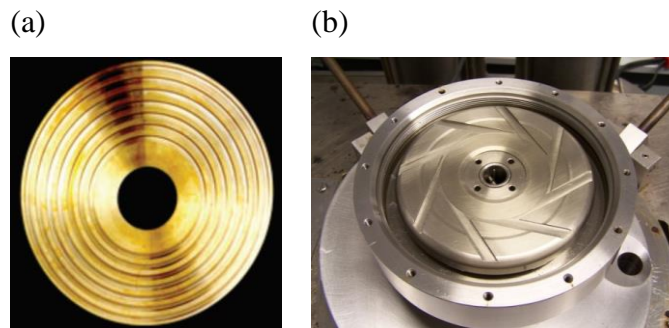


Figure 2-10 Thin film SDR with (a) a grooved disc surface (Boodhoo, 2013); (b) underneath the disc surface (NewcastleUniversity, 2017)

A SDR generally has a working disc with a diameter between 10 cm and 1 m. Discs are made of various metals, often with a base of copper and thin chrome plating for chemical resistance. The disc can be smooth, grooved or meshed depending on the application and the throughput requirement. The rotational speeds of the disc can vary from 100 to 6000 rpm (typically ~ 1000 rpm). The characteristic of SDR make it particularly attractive for applications in fast, highly exothermic reactions, also involving highly viscous liquids.

Expressions for various SDR parameters, such as film thickness and residence time have been developed (Boodhoo, 2013) as presented below:

$$t_{res} = \left(\frac{81\pi^2 v}{16\omega^2 Q^2} \right)^{\frac{1}{3}} (r_o^{\frac{4}{3}} - r_i^{\frac{4}{3}}) \quad 2-1$$

$$\delta = \left(\frac{3}{2\pi} \frac{vQ}{\omega^2 r^2} \right)^{\frac{1}{3}} \quad 2-2$$

Where, v : kinematic viscosity ($\frac{\mu}{\rho}$) [m^2/s]

ω : rotational speed ($\frac{2\pi N}{60}$) [rad/s]

Q =volumetric flowrate [m^3/s]

t_{res} =mean residence time [s]

δ =film thickness [m]

r_i : radial distance across disc surface [m]

r_o : radius at exit [m]

The above simplified representation of the hydrodynamics of thin films on a rotating surface are based on the Nusselt model for a fully developed laminar flow, which neglects the effect of surface instabilities and inertia on flow regimes.

2.3.9 Rotor-Stator Spinning Disc Reactor

The rotor-stator spinning disc reactor (Figure 2-11) is a multiple phase rotating reactor that is developed as an improvement of the thin-film spinning disc reactor. This reactor consists of a spinning disc (rotor) located between two stationary discs (stators) (Meeuwse et al., 2011). The axial distance between the rotor and the stator is typically in the range of 1 mm. The rotational disc speed typically around 1000 rpm but rotational speed of up to 4500 rpm is also reported. High velocity gradient is present in the gap between the rotor and the stator, which acts as a shear force which breaks gas bubbles, leading to a high gas-liquid interfacial area. Small turbulent eddies are formed due to the rotation of the disc, which increase the gas-liquid and liquid-solid mass transfer coefficients. Scale up can be achieved by stacking single stage rotor-stator units in series.

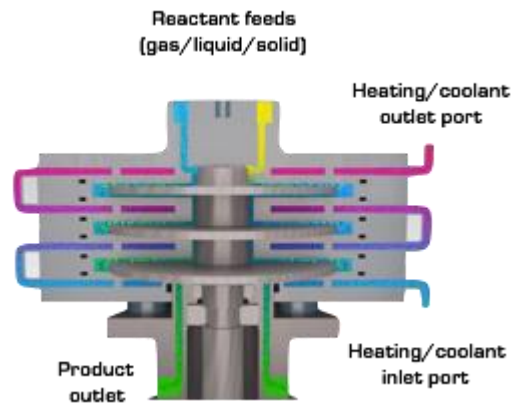


Figure 2-11 Schematic of SpinPro R300 (Flowid, 2015)

2.3.10 Hydrodynamic Cavitation Reactor

In a hydrodynamics cavitation reactor (Figure 2-12), the energy of the liquid flow, instead of exposing to ultrasound (see supersonic reactors), can be utilized to create cavitation. Possible applications would be found in all fields of chemical as well mechanical processing of fluids streams. Possible fields of application include mixing (gas-liquid, liquid-liquid or liquid-solid), extraction, disintegration of particles and colloidal suspensions, homogenisation, and increase of chemical reactions and synthesis (e.g. oxidation, formulation of metal catalysts, etc.).

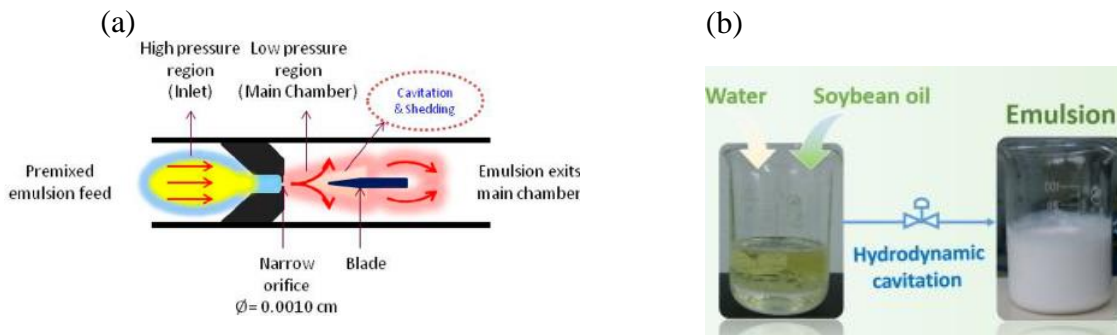


Figure 2-12 (a) Schematic of hydrodynamic cavitation (Parthasarathy et al., 2013); (b) emulsion formation using cavitation (Zhang et al., 2016)

2.3.11 Taylor-Couette Reactor

A Taylor-Couette type of flow (Figure 2-13) is observed in reactors in which only the inner or both inner and the outer cylinders are rotating. The advantages are short residence times, low processing volume, centrifugally accelerated settling and flexible phase ratios (Visscher et al., 2013; Wang et al., 2017). The residence time distribution for such a reactor is close to plug flow behaviour for Taylor number (ratio of centrifugal to the viscous forces) above 60 (Pudjiono and Tavare, 1993).

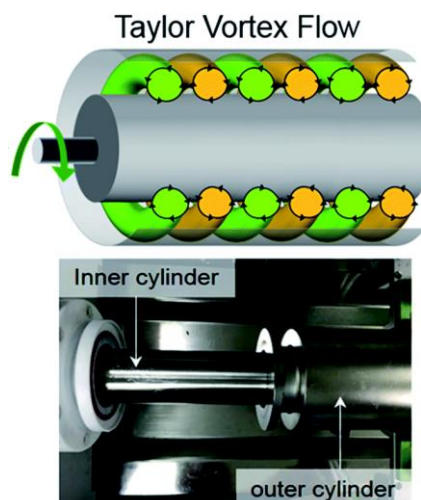


Figure 2-13 Example of Taylor-Couette reactor (Tran et al., 2016)

2.3.12 Monolithic Reactor

In a monolithic reactor (Figure 2-14), the catalyst is prepared in the form of a structured material, the “monolith”, consisting of a regular or irregular network of channels (Porta et al., 2016). Characteristics of monolithic reactors are high specific geometric areas, low mass transfer resistances and very low pressure drop. The main advantage of a monolithic reactor compared to a pack-bed is that the packing is more homogeneous and a consistent fluid dynamics can be expected. Limitation is poor radial heat transfer due to the absence of the radial mixing and thus poor heat removal. This technology is generally used in gas-phase catalytic processes, e.g. gas-phase cleaning of off-gas, de-NO_x-ing. Commercial-scale applications in gas-liquid chemical processes have also been realized. Pilot-scale study using monolithic catalysts as more efficient three-phase reactors was given by Nijhuis et al. (Nijhuis et al., 2001) where they obtained higher productivity for a monolithic reactor compared to a trickle-bed reactor for solid catalysed gas-liquid reaction that is mass transfer limited in the gas-phase reactant.



Figure 2-14 Example of monoliths (Rouhi, 2003)

2.3.13 Impinging Jets Reactor

Impinging jets reactor (Figure 2-15) is a high-intensity reactor for liquid-liquid reactions. In this reactor, after introducing the reactants in a suitable way, the combined flows are commingled and made to flow through a series of baffles having inlet and outlet ports. The mixed flow forms into a series of jets, which are in turn directed against another baffles, or in some cases against each other. High intensity shear regions are formed in the reactor, resulting in excellent conditions for mixing, heat and mass transfer. Potential benefits are energy savings, cost saving, narrower product quality. Fundamental research is required to understand characteristics of impinging jet reactors (Siddiqui et al., 2009).

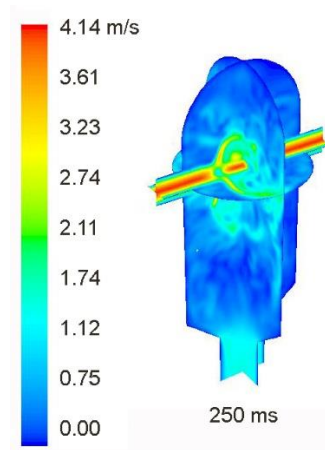


Figure 2-15 CFD simulation of an impinging jet reactor (Gavi et al., 2007)

2.3.14 Rotating Packed Bed

Original known as HIGEE technology (Figure 2-16), rotating packed beds greatly intensify mass transfer processes by applying high centrifugal forces. It is usually applied to gas-liquid system, and has potential application to other phase combinations, such as liquid-liquid, and gas-liquid-solid. In a rotating packed bed, heavy phase enters the eye of rotor, being distributed on the rotor packing, and the light phase enters the stationary housing and passes through the rotor from outside to inside. Not only mass transfer, but also heat transfer and momentum transfer can be intensified. Rotating packed bed can not only be applied in different separation processes include absorption, stripping, liquid-liquid extraction, crystallization, etc, but also reacting systems especially when mass transfer is a limitation (Liu et al., 1996). Potential benefits are smaller processing volumes and better product quality.

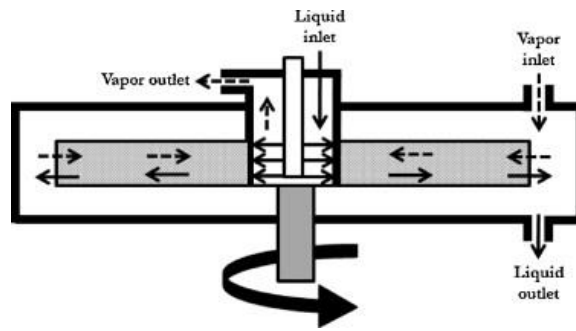


Figure 2-16 Schematic of the rotating packed bed reactor (Visscher et al., 2013)

2.3.15 Reactive Distillation

Reactive distillation (Figure 2-17), also known as catalytic distillation, is a technology combines chemical reaction and distillation in one apparatus. The process take place in a conventional distillation column where chemicals are reacted and the products are continuously separated by fractionation. Chemical reaction equilibrium can be shifted to favour generation of products so that high conversion can be reached. Advantages include lower energy requirements, increased yields and selectivity, simpler process and lower capital investments.

Major commercial technology providers are CDTECH and Sulzer Chemtech. Up to 2006, CDTECH has licensed up to over 200 commercial scale processes include production of ethers (MTBE, TAME, ETBE), hydrogenation of aromatics and light sulphur, dydrodesulfurisation, isobutylene production from C4 stream, and ethyl benzene production. A review of commercial applications, research, scale-up, design and operation for reactive distillation can be found in reference (Harmsen, 2007a). Issues include catalyst development and lack of expertise in fine chemistry and pharma.

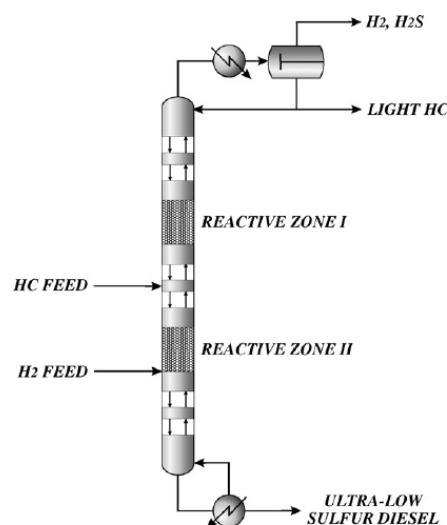


Figure 2-17 Schematic of reactive distillation (Cárdenas-Guerra et al., 2010)

2.3.16 Simulated Moving Bed (SMB)

A simulated moving bed (SMB) (Figure 2-18) is used to separate one chemical compound or one class of chemical compounds from one or more other chemical compounds to provide significant quantities of the purified or enriched material at a lower cost than could be obtained using batch chromatography. The technology can be applied to processes where chromatography separation is a necessary step, but cannot provide any separation or purification that cannot be done by a simple column chromatography. Simulated moving bed reactor (SMBR) combines continuous countercurrent chromatographic separation and reactions (Lode et al., 2001). This is a hybrid process, not energy-intensive and is competitive with traditional processes in which reaction and separation are carried out in different devices. Higher yields and better conversion can be achieved by separating products from the reagents to shift chemical equilibrium. SMBR can be applied to large scale processes, but it is more realistic to smaller scale processes in fine chemicals and pharmaceuticals. Examples of applications are esterifications, transesterifications, etherifications, acetylations, some isomerisations, hydrogenations, some enzyme reactions (Migliorinia et al., 1999).

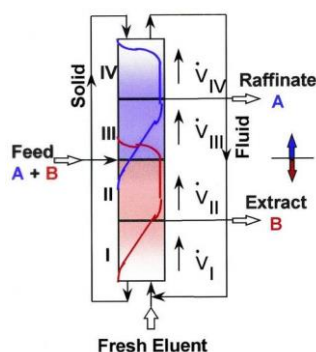


Figure 2-18 Schematic of simulated moving bed (SMB) (KNAUER, 2017)

2.3.17 Rotating Annular Chromatographic Reactor

Similar to the simulated moving bed reactor (Figure 2-19), in rotating annular chromatographic reactor the chemical and biochemical reactions are carried out together with a chromatographic separation. The difference is rotating annular chromatographic reactor works in the co-current mode, where different reagents are selectively adsorbed and as a result of the rotation of the reactor, take different helical path through the bed and be continuously collected at fixed location. The advantage of a RACR is similar to that of a SMBR. A comparison is given by Molga et al. (Molga et al., 2009).

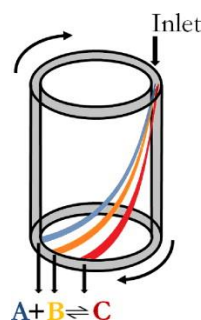


Figure 2-19 Schematic of rotating annular chromatographic reactor (Visscher et al., 2013)

Liquid-liquid extraction has been a successful separation technique applied in the pharmaceutical industry because of its inherent flexibility and its suitability for processing heat-sensitive products. Comparing the extraction applications with most other industries, very dilute solutions are usually used in pharmaceutical process (Goldberg, 2012) and multiple stages/units are involved. Technical improvements have been made and many of the extractors that are developed for pharmaceutical applications are still in use today. Examples include the centrifugal extractor, the Scheibel column, the Kuhni column, the asymmetric rotating disc contactor and the Karr column.

2.3.18 Centrifugal Extractor

The centrifugal extractor uses the rotation of the rotor inside a centrifuge to mix two immiscible liquid outside the rotor and to separate the liquids based on their density difference inside the rotor. It can obtain continuous extraction from one phase into another liquid phase. The CE is able to handle liquids with small density difference and requires short contact time due to its efficient mixing and separation. Furthermore, it has a smaller equipment volume compared to traditional tanks, mixer settlers and extraction columns. However, the centrifugal extractors are expensive and it has mechanical parts that require frequent maintenance. It has low number of contact stages, so for multi-stage extractions, several CEs are required to operate in series (CINC, 2017).



Figure 2-20 Example of two CINC CE in series (ColeParmer, 2017)

2.3.19 Agitated Columns

The Scheibel column (Figure 2-21 (a)) was the first agitated column extractor developed for pharmaceutical applications. The column is vertically divided, by baffles, into several mixing and settling zones. Each mixing zone has an agitator (between inner baffles), once mixed, the fluids are directed to the outer region (outer baffles) to allow phase separation before entering the next mixing zone. It is a compact extractor with multiple stages incorporated which is suitable for difficult extractions. However, one operating problem with this column is the emulsification of fluids which might require additional processing in another extractor. Kuhn columns differ from Scheibel columns with its mixing compartments separated by perforated plates which are attached to the impeller. The design of the perforated plates (area and holes) is important to the efficiency of this column. The rotating disc contactor uses disc rotating inside the mixing compartment, followed by settling compartments to provide separate mixing and settling zones. The asymmetrical rotating disc contactor (Figure 2-21 (b)) is similar to the original rotating disc contactor but its rotating discs have been moved off the axial centre of the extractor. This is to create a side of agitated region within the column and form a series of mixing stages divided by adjacent horizontal stators. Karr columns (Figure 2-21 (c)) have reciprocating plates (180° out of phase with one another) with holes for dispersion of liquids. Although the capacity and efficiency of the counter-motion plate columns is improved, the columns are mechanically more complex and require greater maintenance. Karr column have frequently been used in pharmaceutical separations and have several advantages over other columns. One major advantage is the nature of the reciprocating plates to minimise emulsification. It is suitable for extraction process where residence time requirements are not so critical as to require a centrifugal extractor. This is particularly the case for difficult extraction where many stages are required (Goldberg, 2012).

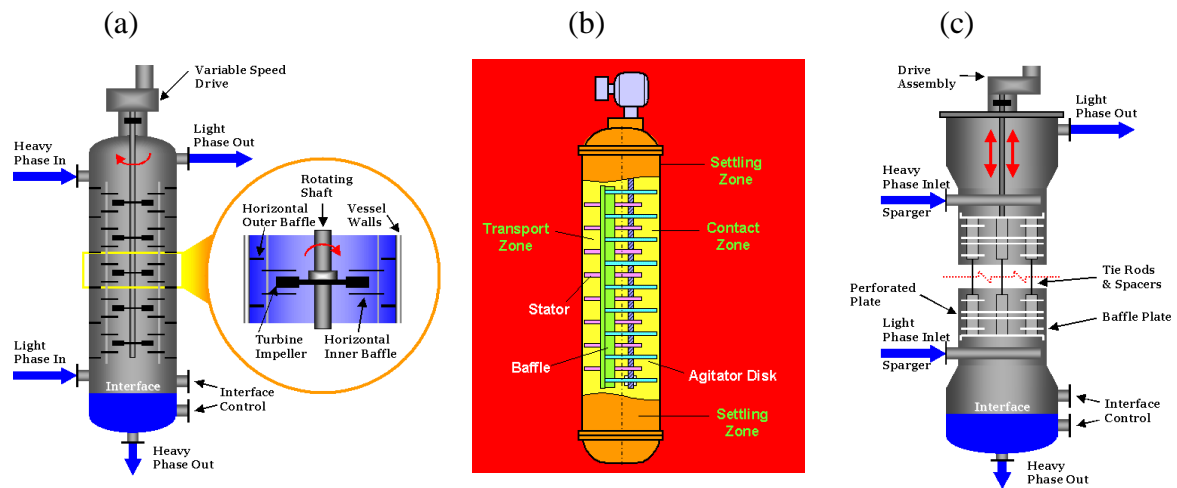


Figure 2-21 (a) Scheibel column (KMPS, 2017c); (b) asymmetric rotating disc contactor (Separationprocesses, 2017); (c) Karr column (KMPS, 2017a)

Another important aspect of pharmaceutical process is the handling of solids in crystallisation, filtration and drying. Batch filtration involves the separation of suspended solids from a slurry containing liquid. The type of filter to be used and the suitability of filter medium must be considered. The problem of equipment selection is made difficult by the enormous number of options available. This review contains a list of some of the filtration equipment used in separations. Guidelines to obtain the ‘best’ solution to the equipment selection have been published (Wakeman, 1995). However, very often the best solution does not mean an optimum filter selection, as it would still require a large amount of effort and time to optimise with a wide range of variables. The guidelines prevent the purchase of a completely unsuitable system and avoid severe process difficulties. Examples of three common filters are discussed in this review – nutsche filter, centrifugal filter and rotary vacuum drum filter.

2.3.20 Nutsche Filters

Nutsche filters (Figure 2-22) are particularly application in pharmaceutical industry where rigorous cake washing is required. The batch vessel unit can be multi-function – crystallisation/precipitation, extraction, filtration, dryer (vacuum/convection). Agitators are designed to provide agitation for slurry, smoothing and discharge of filter cake (Sharratt, 1997).

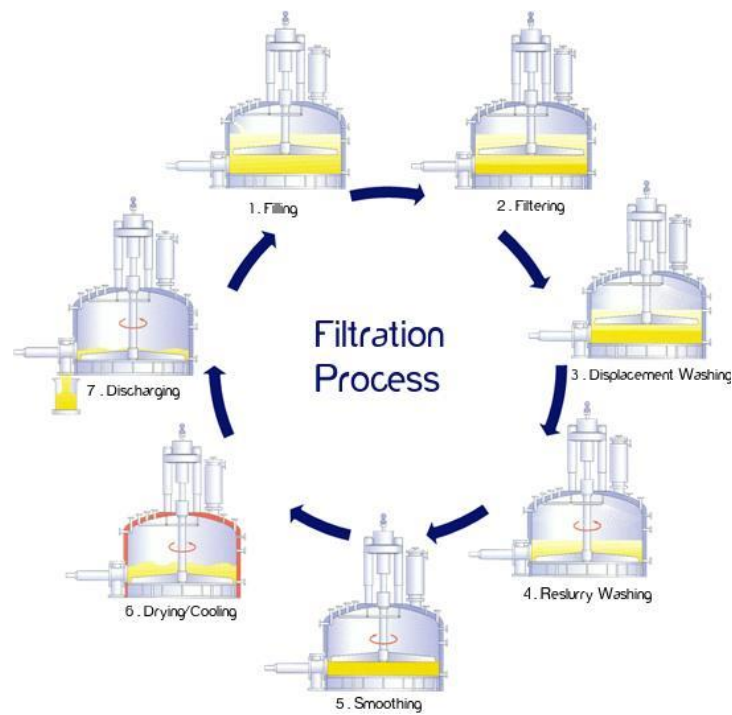


Figure 2-22 Schematic of Nutsche filtration and drying process (Systems, 2017b)

2.3.21 Centrifugal Filters

The separation principle is similar to that of sedimentation, where the driving force is resulting from the difference in density between the solid particles and the liquid (Majekodunmi, 2015). Centrifugal force generates a pressure which forces the liquid through the filter cake, filter medium and basket perforations (Figure 2-23). The filter cloth retains the solid particles inside the rotating basket. Washing can be introduced and controlled in the same manner as the slurry. The separated solids are discharged by inverting the filter cloth through axial movement of the shaft while the bowl rotates slowly. The inverting centrifugal filter is equipped with pressure (Anlauf, 2007). The features of this system are full automatic solid discharge, compact and homogeneous cake structure (Heinkel, 2017b). The only consideration is the time taken for acceleration and deceleration of the drum consists a significant fraction of the cycle time (Sharratt, 1997).

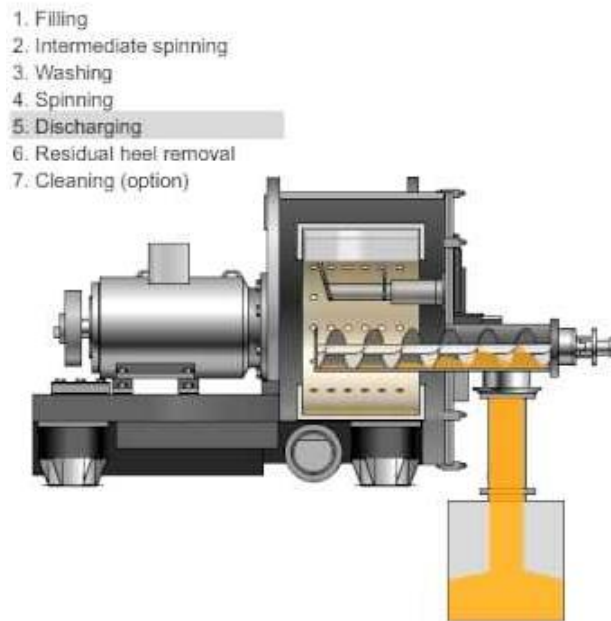


Figure 2-23 Schematic of centrifugal filter (Heinkel, 2017a)

2.3.22 Rotary Vacuum Drum Filter

Rotary vacuum filter drum (Figure 2-24) consists of a drum rotating in a suspension to be filtered. The drum is pre coated with a filter aid which acts like a sieve and rotates through the suspension. The vacuum “sucks” liquid and solids onto the drum pre-coat surface, the filtrate is transported through the filter media to the central duct and pumped away. The solids adhere to the outside of the drum, which then passes under a knife, where the filter cake is cut. It is a continuous operation, commonly used in pharmaceutical industry, handling suspensions with solid loading up to 30 w/w%. The advantages include low labour cost as its operation is mainly automatic and continuous and the process can be modified by controlling the speed of drum rotation. The disadvantages include high energy consumption by the vacuum pump, it is relatively expensive and the filter aid may be clogging if the solids form sticky cake. This continuous filtration system is commonly used in the pharmaceutical industry.

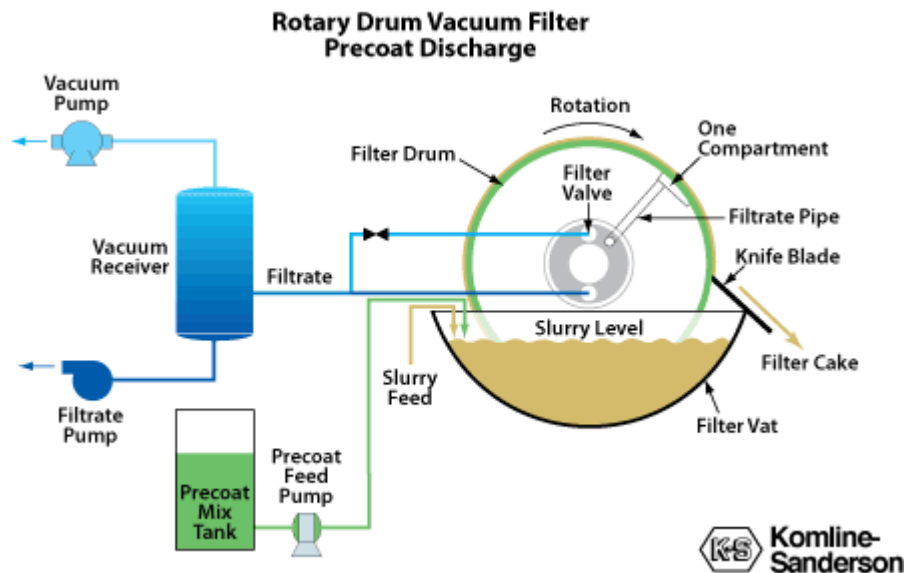


Figure 2-24 Schematic of rotary drum vacuum filter (Komline-Sanderson, 2017)

Drying of product can be carried out in a range of driers. Tray driers, fluidized bed driers, belt driers and rotary drum driers are all currently used in the pharmaceutical industry. The types of drier chosen will depend on factors such as the properties of the solids, mode of operation, extent of drying required and the cost of equipment. Recently, several PI equipment have shown potential to achieve more efficient drying – wiped film evaporator, agitated thin film dryer, spray dryer and microwave drying.

2.3.23 Conventional Pharmaceutical Dryers

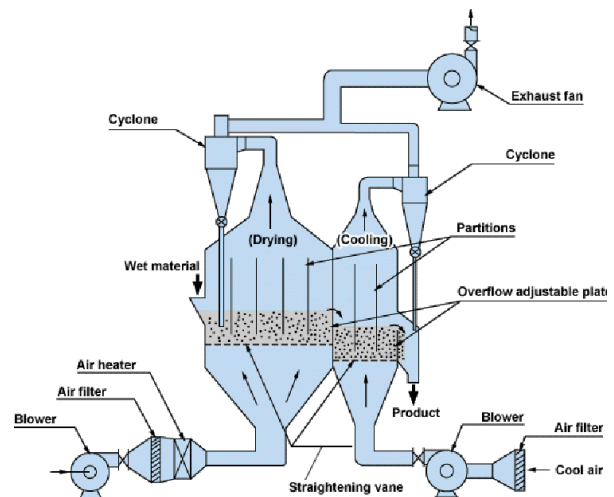
The tray dryer (Figure 2-25 (a)) consists of multiple trays of wet solids placed on top of each other in a drying oven. Heat is provided by circulation of hot air by electric heaters or steam in radiator coils. The system is designed so that heating is uniform within the oven. The tray dryer can be equipped with vacuum which is mainly used for drying high grade, hygroscopic and temperature sensitive products. It is usually used in small batch production operations. However, it is labour intensive to operate and has a long cycle time (Faure et al., 2001). The fluid bed dryer (Figure 2-25 (b)) is suitable for drying granular crystalline material in pharmaceuticals but inappropriate for sticky paste-like material. Fluidization produces agitation of solid particles as each particle is in direct contact with hot air introduced from the base of the product container (Faure et al., 2001). Due to the high heat transfer rate, drying at relatively low temperature and short residence time is often sufficient. Unlike tray dryer, fluid bed dryer occupy less floor space and less labour intensive. Belt dryer (Figure 2-25 (c)) is continuous drying equipment that can handle pasted material like the filter cake after shaped through granulator. The wet material is first distributed on the conveyor belt through crusher or granulator. The conveyor passes through the heating unit where hot air passes from above and

below the wet material (Vaxelaire and Puiggali, 2002). The drum dryer (Figure 2-25 (d)) consists of a heated hollow metal drum which rotates on its longitudinal axis and dips in the solution. As the dipping process completed, the solution forms a liquid film on the surface of the heated dryer. Upon evaporation of the solution, a layer of solid forms on the surface of the metal drum and a scraper/knife is present to off the dried solid close to the surface of the drum. In general, the drum dryer allows rapid drying to take place due to good heat and mass transfer and it has a small equipment volume. However, its maintenance cost is high and skilled operators are needed to control the thickness of the film. It is not suitable for suspension with the presence of solid. Drum dryer can be used to dry thermos sensitive APIs (Mujumdar and Menon, 1995).

(a)



(b)



(c)



(d)

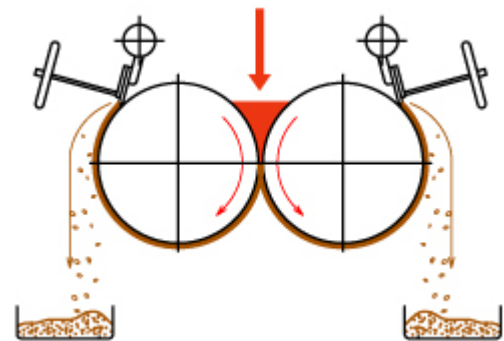


Figure 2-25 (a) Example of tray dryer (PRISMpharma, 2017); (b) Schematic of fluid bed dryer (Deviatkin, 2013); (c) Example of a conveyor dryer (Alibaba, 2017b); (d) Schematic of double drum type drum dryer (Katsuragi, 2017)

2.3.24 Wiped Film Evaporator (WFE)

The wiped film evaporator (Figure 2-26) separate volatile from less volatile components with a gentle process utilizing the thin-film wiping action of feed liquid through a heated cylindrical vacuum chamber with high vacuum. The unique features of the WFE include short

residence time of the feed liquid, lowered temperature due to vacuum capability and efficiency in mass and heat transfer due to thin liquid film. It is mainly applied in the pharmaceutical industry where heat-sensitivity is a determining factor. A major disadvantage of WFE is cost which is high compared to other evaporators. Furthermore, it has rotating parts which can result in higher maintenance cost and its application is considered rather limited compared to agitated thin film dryer.

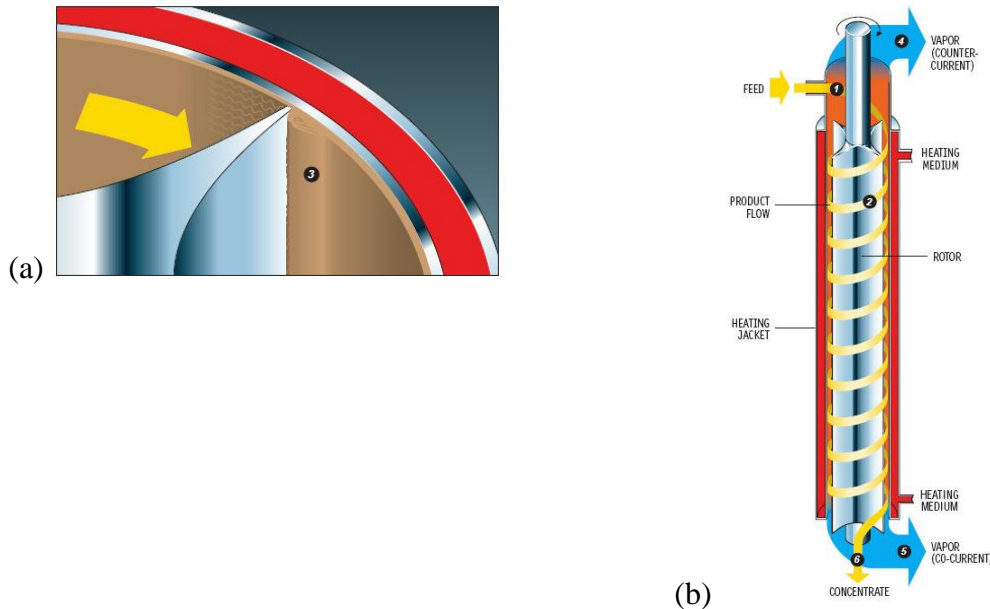


Figure 2-26 Schematic of the WFE (a) Scrapper spreading a thin film on the walls; (b) Direction of liquid flow (FoodProcessingTechnologies, 2017)

2.3.25 Agitated Thin Film Dryer

The main application of ATFD (Figure 2-27) is to turn a concentrated solution into dry powder. There are three types of film dryers – vertical and horizontal and a combination of both. The dryer consists of cylindrical, vertical/horizontal body with rows and wiper blades all over the length of dryer. The hinged blades spread the wet feed product in a thin film over the heated wall. As the solvent evaporates, the solution will convert to slurry and to cake and scrapped off the wall surface as dry power. The solvent vapour travels counter-current to the solution flow and will be condensed in the condenser. The system is usually operated under vacuum for temperature sensitive products. The advantages of this system are gentle evaporation due to short residence time, one step operation from solution to solid in one pass, fouling of surface prevented by wiper blades and minimal product hold-up (KetavConsultant, 2017).

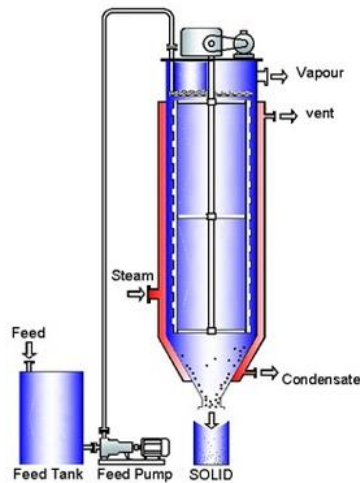


Figure 2-27 Schematic of agitated thin film dryer (Aquacare, 2017)

2.3.26 Spray Dryer

The most common method of drying API has been batch drying either by tray or fluid bed dryers (Sharratt, 1997). The solution is atomised into fine droplets in the spray dryer and dispersed radially to a moving stream of hot gas (Figure 2-28). The temperature of the droplets is immediately increased and fine droplets get dried instantaneously. This process is completed in a few seconds before the droplets reach the wall of the dryer. There are many advantages in using spray dryer which include rapid drying, excellent particle size control and low labour costs as it integrates the function of an evaporator, crystalliser, dryer and size reduction unit. However, it is bulky and complex equipment that is not always easy to operate. It is not only expensive but also suffers from low thermal efficiency as much heat is lost in the discharged gases. It is commonly used in pharmaceutical process (Patel et al., 2009).

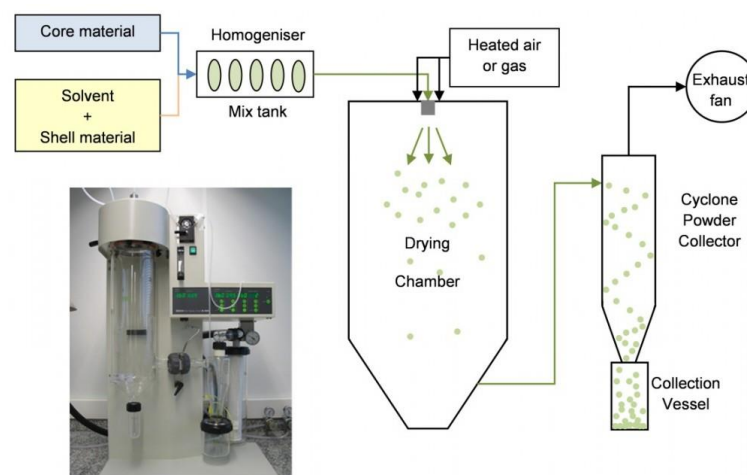


Figure 2-28 Example of spray drying technology (Sonarome, 2017)

2.3.27 Microwave Drying

Microwave dryer is used in pharmaceutical industry as it provides rapid drying at low temperature and uniform heating of the wet mass. However the batch size of microwave dryer is usually smaller than the fluidized bed dryer. The coupling between continuous flow and microwave heating can overcome the scalability issue (Wiles and Watts, 2012). The main advantage of microwave drying is the shortening of drying time from hours to minutes. It is not energy efficient to depend solely on microwave heating to completely dry the product. Rather, it should be used to complement conventional heating where non-uniform heating tends to occur (Walters et al., 2014).

Table 2-1 List of PI and conventional equipment for pharmaceutical applications

	Unit operations	PI options	Examples of pharmaceutical applications	Examples of commercial suppliers
1	Reaction (Gas-liq)	Microreactor	Organometallic (Yoshida <i>et al.</i> , 2013; Nagaki <i>et al.</i> , 2014a; Nagaki <i>et al.</i> , 2015)	Syrris (2017) Uniqsis (2017)
2	Reaction (Gas-liq)	Spinning tube in tube reactor	Oxidation of alcohol (Hampton <i>et al.</i> , 2008) Synthesis of imidazolium (Gonzalez and Ciszewski, 2008)	Costello (2017)
3	Reaction (Gas-liq-solid)	Gas-liquid-solid trickle flow reactor	Selective hydrogenation (Ouchi <i>et al.</i> , 2014)	-
4	Reaction (Gas-liq-solid)	Catalytic foam stirrer reactors	Hydrogenation of functionalised alkyne (Leon <i>et al.</i> , 2011)	-
5	Reaction (Gas-liq)	Heat exchanger (HEX) reactors	Oxidation of sodium thiosulfate (Prat <i>et al.</i> , 2005) Esterification (Benaïssa <i>et al.</i> , 2008)	BHR (2017)
6	Reaction Mixing (Gas-liq)	Static mixer and static mixer reactor	Liquid-liquid mixing (Kiss <i>et al.</i> , 2011) Boc protection of amine (Brechtelsbauer and Ricard, 2001)	Sulzer (2017a) Noritake (2017a)
7	Reaction Crystallisation (Gas-liq-solid)	Oscillatory baffled reactor	Crystallisation of APIs (Lawton <i>et al.</i> , 2009; McGlone <i>et al.</i> , 2015)	Nitech (2017)
8	Reaction Crystallisation (Gas-liq-solid)	Thin-film spinning disc reactor	Crystallisation of API (Oxley <i>et al.</i> , 2000) Organometallic (Feng <i>et al.</i> , 2017)	Flowid (2015)
9	Reaction Separation (Gas-liq-solid)	Rotor-stator spinning disc		
10	Reaction Waste treatment (Gas-liq-solid)	Hydrodynamics cavitation reactor	Synthesis of pharmaceutical nanoemulsions (Sivakumar <i>et al.</i> , 2014) Applications of cavitation in biotechnology (Gogate and Kabadi, 2009)	Hydrodynamics (2017)
11	Reaction	Taylor-Couette reactor	Crystallisation (Nguyen <i>et al.</i> , 2012)	-

	Crystallisation (Gas-liq)		Fast competitive reactions (Forney <i>et al.</i> , 2005)	
12	Reaction Separation (Gas-liq)	Monolithic reactor	Selective oxidation of benzyl alcohol (Al Badran <i>et al.</i> , 2013) Organocatalysis (Chiroli <i>et al.</i> , 2014) Chromatography (Viklund <i>et al.</i> , 1996)	PSE (2017) Techninstro (2017)
13	Reactive Crystallisation (Gas-liq)	Impinging jets reactor	Reactive crystallisation (Lince <i>et al.</i> , 2009; Liu <i>et al.</i> , 2017)	-
14	Reactive precipitation (Gas-liq-solid)	Rotating packed bed	absorption of VOCs(Chen and Liu, 2002) absorption of CO ₂ with ionic liquid (Zhang <i>et al.</i> , 2011) Reactive precipitation (Chen <i>et al.</i> , 2000)	(life, 2017)
15	Reactive separation (Gas-liq)	Reactive distillation	Esterification (Steinigeweg and Gmehling, 2004; Liu <i>et al.</i> , 2005)	Sulzer (2017c) (Chemoxy, 2017)
16	Reaction Separation Purification (Liq-liq)	Simulated moving bed (reactor)	Separation of racemic mixture (Guest, 1997) Nucleophilic substitution (O'Brien <i>et al.</i> , 2012)	(Chemito, 2017) (technology, 2017) (KNAUER, 2017)
17	Reaction Separation Purification (Liq-liq)	Rotating annular chromatographic reactor	Hydrolysis of methformate (Cho <i>et al.</i> , 1980)	(Biofilm, 2017)
18	Liquid-liquid extraction	Centrifugal extractor	Recovery of penicillin (Likidis and Schügerl, 1987) Pharmaceutical processes (Meikrantz <i>et al.</i> , 2002)	(CINC, 2017) (B&PLittleford, 2017) (RousseletRobotel, 2017)
19	Liquid-liquid extraction	Scheibel column	Preparing arylalkanoic acid derivatives (Amin and Walker, 1979)	(KMPS, 2017c)
	Liquid-liquid extraction	Kuhni column	Extraction of zinc sulfate (Mansur <i>et al.</i> , 2003)	(Sulzer, 2017b)

	Liquid-liquid extraction	Asymmetrical rotating disc contactor	Synthesis of pharmaceutical intermediate (Teoh <i>et al.</i> , 2015)	(KMPS, 2017b)
	Liquid-liquid extraction	Karr column	Extraction of fermentation broth (Karr <i>et al.</i> , 1980)	(Karr <i>et al.</i> , 1980)
20	Filtration	Nutsche filters	Vacuum contact drying of pharmaceutical compounds (Murru <i>et al.</i> , 2011) Removal of solvent in pharmaceuticals manufacturing (Mudryk <i>et al.</i> , 1999)	(Heinkel, 2017b)
21	Filtration	Centrifugal filters	Common pharmaceutical filters (Sharratt, 1997)	(Heinkel, 2017a)
22	Filtration	Rotary vacuum drum filter	Recovery of biomass (Grima <i>et al.</i> , 2003)	(Komline-Sanderson, 2017)
23	Drying	Tray dryer (optional vacuum)	Drying sensitive drug (Roy, 2002)	(WALDNER, 2017)
	Drying	Fluid bed dryer	Pharmaceutical granules (Leuenberger, 2001)	(Glatt, 2017)
	Drying	Belt dryer	Continuous pharmaceutical granules (Ghebre-Sellassie <i>et al.</i> , 2002)	(TheilenMaschinenbau, 2017)
	Drying	Drum dryer	Coating of pharmaceutical tablets (Denis <i>et al.</i> , 2003)	(FEECO, 2017)
24	Solvent evaporation	Wiped film evaporator (WFE)	Concentrate clopidogrel base (Turgeman and Malachi, 2006) Synthesis of N-acetylneuraminic acid (Mahmoudian <i>et al.</i> , 1997)	(POPEscientific, 2017) (Pfaudler, 2017) (PMMixers, 2017) (SMS, 2017)
25	Solvent evaporation Drying	Agitated thin film dryer	Drying of API (Kumar and Dixit, 2007)	(KetavConsultant, 2017) (LCIcorp, 2017) (GIGKarasek, 2017) (SMS, 2017)
26	Solvent evaporation Drying	Spray dryer	Pharmaceutical application (Broadhead <i>et al.</i> , 1992; Tarara <i>et al.</i> , 2003; Vehring, 2008; Sollohub and Cal, 2010)	(Hovione, 2017) (GEA, 2017) (Capsugel, 2017) (Juniper, 2017)
27	Drying	Microwave drying	Drying of pharmaceutical powder (McMinn <i>et al.</i> , 2005)	(LinnHighTherm, 2017)

2.4 Pharmaceutical Plant-wide Process Intensification – Batch to continuous

Continuous process (CP) is one of the forms of process intensification which aims to reduce costs, reduce the size of process equipment, improve product quality, and reduce energy consumption, solvent usage and waste generation. Ideally, the continuous process is constrained only by the chemistry and physics of the reaction, whilst batch process is usually limited by the equipment constraints. In the pharmaceutical context, PI brings several advantages:

2.4.1 Economics

Lower operational cost (OPEX) can be obtained from reduced inventory, processing equipment footprint, waste and emissions and energy consumption. One commercial example from Lonza describes a case where the cryogenic lithiation reaction and coupling reactions are replaced by a microreactor in a flow system to run higher temperature and avoid long residence time. The yield is also increased by 5% compared to the batch result. The reaction time is no longer the bottleneck of the process as the reaction rate is increased dramatically. The operational cost saving of this process is estimated to be 10% versus batch (Roberge *et al.*, 2008).

2.4.2 Quality

Continuous processing offers improved mass and heat transfer and the ability to operate more intensely at higher temperatures which can improve product quality compared to batch. Furthermore, process deviations in CP can be less detrimental since there is small inventory, resulting in less product loss. More precise control of temperature, pressure and heat transfer can improve yields and selectivity and reduce process deviations. For example, a continuously operating spinning disc reactor (SDR) achieved 93% reduced impurity level for a phase-transfer-catalyzed (PTC) Darzen's reaction to prepare a drug intermediate and recrystallization of an API (Oxley *et al.*, 2000). With contact time of under 1s, the impurity arise from prolonged contact of desired product with other reagent can be minimized drastically.

2.4.3 Safety

Smaller reactor volumes and inventory offers process safety especially when dealing with hazardous reagents or solvents. Usually the smaller equipment or flexible modular setup require smaller containment facilities (walk-in fumehood) which provide a reduced potential for exposure to chemicals. CP can minimise the risks with hazardous chemistry that otherwise would have been impossible in batch processing. For example in the synthesis of 1H-4-substituted imidazoles, high temperature and backpressure of 17 bar in a stainless steel coil reactor with a residence times of 2 to 5 minutes afforded the desired products in high purity (Carneiro *et al.*, 2015). CP allows implementation of "Novel Process Windows" (Hessel *et al.*,

2013) which enhance reaction performance under a safer environment. Other examples of implementation of a continuous flow reactor driven by safety concerns are the nitration bromination reactions (Pelleter and Renaud, 2009).

2.4.4 *Environmental*

The application of rapid mixing and heat transfer in complex pharmaceuticals synthesis offers the possibility to run concentrated reaction which minimizes the use of solvent. Thus, significant reduction can be recognised in Process Mass Intensity (PMI). Compared to high frequency of cleaning in batch, CP steady-state operations should require less frequent shutdown and cleaning. In return, the solvent usage and emissions can also be reduced. For example, the reduction of ethyl nicotinate was performed solvent-free without the need for further downstream processing (Ouchi *et al.*, 2016).

However, it should be noted that not all reactions are suitable for continuous processing. When the reaction times are longer than several minutes, flow reactors start to become increasingly impractical. There are very few reactions that take hours to perform continuously (Boodhoo and Harvey, 2013).

In summary, the pharmaceutical industry requires methodology for in-depth analyses of existing processes and new processes to identify opportunities to sustainability metrics by intensifying steps. In the pharmaceutical development, time to market is paramount and new technologies are perceived as high risk so there is usually hesitance to apply them; hence, PI implementation can be very difficult.

Additionally, there are so many ways to intensify a process, it is often difficult for the typical project technical team to swiftly identify what option might be best within the time constraints and capability (Jiménez-González *et al.*, 2011). Despite the many options available, only 22% of all PI equipment are categorised as highly mature while around 60% of the PI equipment are considered as low or medium maturity (Lutze *et al.*, 2010; Lutze *et al.*, 2012; Lutze *et al.*, 2013).

To overcome these barriers, the ACS GCI Pharmaceutical Roundtable has made suggestions for research opportunities (Jiménez-González *et al.*, 2011) to develop guidance and tools to assist with the selection of the best intensification option. This includes the development of methodologies to integrate intensification considerations into a given process from early stage of process development. Also, establish procedures of analysis for production processes to define opportunities to identify opportunities to intensify unit operations to improve their sustainability metrics.

2.5 PI of ortho-Lithiation

Ortho-lithiation is an important class of reaction for the synthesis of regioselectively substituted aromatics, and it is an emerging method to prepare phthalides which are common pharmaceutically active compounds (de Silva *et al.*, 1992; Roberge *et al.*, 2008; Faigl *et al.*, 2010; Karmakar *et al.*, 2014; Newby *et al.*, 2014; Laue *et al.*, 2016). Ortho-lithiation is typically conducted in batch mode under cryogenic temperatures (-78 to -40 °C) (Desai, 2012) to minimize the side reactions arising from the highly reactive organolithium intermediates. Although this process produces high purity compounds, it requires the use of large reaction vessels and long cycle time to achieve the required throughput. The challenges of safely handling both the highly reactive chemicals and a highly energetic reaction in scaled-up operations constitute a major disadvantage of such batch processes. One solution to overcome these safety related issues is to implement continuous flow processes (Anderson, 2012).

There are examples of deploying flow processing for lithiation reaction as a process intensification (PI) technique. The Yoshida group demonstrated several lithiation reactions using different electrophiles in microstructured flow devices (consisting of micromixers and microtube reactors) to be superior to batch protocols (Nagaki *et al.*, 2011; Yoshida *et al.*, 2011; Nagaki *et al.*, 2014a; Nagaki *et al.*, 2014b; Nagaki *et al.*, 2015).

Several successful studies have been performed to scale up continuous lithiation using tubular flow reactors (Newby *et al.*, 2014; Laue *et al.*, 2016). These flow reactors offer superior control of process parameters like mixing, residence time and temperature. Roberge *et al.* (2008) and Laue *et al.* (2016) have both demonstrated the possibility to scale up lithiation reactions in flow reactors for pharmaceutical manufacturing. However, both authors reported challenges in handling plugging due to precipitation of salts. Kockmann *et al.* (2011) evaluated the feasibility to scale up the lithiation reaction using tubular flow reactors with different channel diameters and flow rates to avoid parallelization.

2.6 Review of PI Methodology

In general, the identification of a feasible intensified process is not easy and intuitive (Harmsen, 2010). Existing methodologies for process synthesis can be categorized into either heuristics, thermodynamic insights (Jakslund *et al.*, 1995), mathematical programming such as superstructure optimisation (Franke *et al.*, 2008) or combinations of these into hybrid methods (Lutze *et al.*, 2010). Most of the process synthesis methodologies have been developed based on unit operations. However, innovative concepts have been used to synthesize processes as well, for example methodologies for synthesizing processes based on elementary process functions (Freund and Sundmacher, 2008, Peschel *et al.*, 2010, Peschel *et al.*, 2011a, Peschel *et al.*

al., 2011b); modularisation (Arizmendi-Sánchez and Sharratt, 2008) mass and heat building blocks (Papalexandri and Pistikopoulos, 1996; Proios and Pistikopoulos, 2005; Alguasane et al., 2006); phenomena (Ben-Guang *et al.*, 2000; Rong *et al.*, 2004; Rong *et al.*, 2008) have been proposed. The common bottleneck among these methodologies is the lack of details on algorithms to select suitable PI equipment and methods. The IMPULSE project (Bayer *et al.*, 2005) called for cooperation of equipment manufacturers to characterise the equipment according to standardised methods, so that a database of equipment characteristics can be created.

The PI concept is complex and covers multiple aspects and one of the focus is the integration of reaction and separation. For example, the process synthesis framework for reactive separation (Schembecker, 2002); design and optimisation of hybrid separation processes based on integration (Franke et al., 2008) and integration of superstructure optimisation and thermodynamic insights (Marquardt, 2008). Optimisation function is usually performed using MINLP methods. Another PI strategy is continuous processing which has been claimed to be more efficient at batch processes, examples of guideline on the benefits and feasibility of converting a batch to continuous process is discussed by (Teoh *et al.*, 2016), Plouffe *et al.* (2014) and Kockmann *et al.* (2011). The following summarises the reviews on reported methodologies.

2.6.1 Phenomena Approach

The approach classified process phenomena into “chemistry and chemical reaction phenomena, materials phases and transport phenomena, phase behaviour and separation phenomena etc.” Process phenomena are further characterised by surface materials, operation modes, flow pattern, facility medium, geometry, energy sources, key variables as well as components and phases. This systematic methodology based on phenomena approach was given by Rong (Ben-Guang *et al.*, 2000; Rong *et al.*, 2004; Rong *et al.*, 2008). The methodology decomposes the synthesis problem into 10 hierarchical steps. The heart of their method consists of trial and error variations of the characteristics for the identified key process phenomena through seven different suggested PI principles. Despite a systematic approach, there are gaps that the methodology did not address: (1) Identification of phenomena; (2) strategies for variations of these phenomena; (3) techniques on how to find all currently available options; (4) identification of the best option.

2.6.2 Framework for Choice of Intensified Equipment

This methodology have been proposed by Commenge and Falk (2014) aims to provide a decision tool that relates directly and rapidly the specifications of a given problem to the best

technologies available commercially. Two intermediate steps are included between initial problem that engineering tends to intensify, and the best available technologies to solve this problem. The first one consist in identify limitation of a problem. The second step is based on a set of intensification strategies. Two matching matrix are built between the lists of limitations and strategies. The first matrix relates limitations to strategies. In each cell, a mark is attributed to describe the relevance of this strategy with respect to this limitation. The marks range from 0 (no impact) up to 5 (Very strong impact). The second matrix relates the strategies to a list of technologies. The relevance of each technology as an application of each strategy is assessed by attributing marks to each cell of the matrix. A mark equal to 0 indicates that this strategy cannot be applied in this equipment, whereas a mark of 5 indicates that this equipment is ideally suited to apply this strategy. After calculation, a sorted list of the most-promising technologies is provided. Unfortunately, the marks included in the matrices only assessed the degree of relevance of strategies with respect to limitations and technologies, but did not take into account the quantitative data of the initial problem. The search space was based on a small selection of predefined PI equipment and strategies. This was no guidance on how to gauge the weightage of new limitations and strategies to a problem to maintain consistency when extending this methodology to new case studies.

2.6.3 Local and Global Process Intensification Approach

Portha *et al.* (2014) have proposed the global process intensification approach as more superior to local process intensification as the local process intensification approach tends to present several limitations when compared to the more holistic global intensification. It is because when PI focuses on single units, the strong interactions among all units within the process are ignored, resulting in weak improvement of the whole process. The global intensification evaluates a multi-dimensional aspect of the whole process where different drivers (economic, safety eco-efficiency and sustainability) are included. The downside of this methodology was the lack of algorithms, necessary tools and solution techniques to implement global intensification. The application of this data-intensive approach was also more challenging for new processes.

Ponce-Ortega *et al.* (2012) have reclassified the local and global process intensification into two main categories called unit intensification and plant intensification. A general mathematical formulation for each intensification process was proposed considering the intensification of existing units and installation of new units. The study uses the methodologies of process systems engineering (including modelling, optimisation, control and integration) to achieve intensification objectives. Although this methodology used algorithms for

intensification, it relied heavily on process system engineering, there was insufficient PI strategies (e.g. batch to continuous, reactive separation, etc.) incorporated. The application was not straightforward as it required intensive modelling (General Algebraic Modelling Systems, GSMS, BARON, etc.) which can only be used by expert in the field.

2.6.4 Thermodynamics Approach

Jaksland *et al.* (1995) have developed a methodology for synthesis/design of separation systems by linking physicochemical properties of pure components as well as mixtures to select suitable unit operations in a database. The mixture properties is retrieved from a database or generated using property prediction methods. For all binary pairs, the difference in binary ratio of each pair is analysed to identify a set of potentially suitable equipment. Unfortunately, the property prediction and equipment database were not updated so new chemistry transformations and separation methods (e.g. reactive separation) were not captured in the database.

2.6.5 Modularisation Approach

The modularisation approach is defined by several authors (Papalexandri and Pistikopoulos, 1996; Proios and Pistikopoulos, 2005; Alguasane *et al.*, 2006) as process synthesis based on heat and mass building blocks instead of specified unit operations. Given the connections between the building blocks produce a feasible solution, then in a subsequent step, unit operations are identified. The selection of initial search space of building blocks is based on heuristics and thermodynamics insights. Arizmendi and Sharratt (2008) classified description of mass transfer, phase change, energy, change conditions and mechanical operations into phenomena which are aggregated to form phases. Phases can be aggregated to form tasks. Task can be aggregated to represent the whole process. However, majority of the methodologies did not provide tools to identify PI options

2.6.6 Decomposition Based Solution Approach

This is a systematic computer aided model-based methodology have been proposed by Lutze *et al.* (Lutze *et al.*, 2010; Lutze *et al.*, 2012; Lutze *et al.*, 2013). Instead of solving the whole synthesis problem, the problem is decomposed into subsets of process options at the phenomena level. For each process option, operational constraints and short-cut phenomena model are solved and known unit operations are identified which then make up the process. The resulting feasible process is ranked according to performance criteria. Rigorous modelling is used to further optimise the top-ranked feasible alternatives to determine the optimal solution. The methodology decomposed the problem into 6 steps. In each step, the user needs to make decisions, use algorithms and tools to proceed to the next step. One obstacle in applying this methodology is the use of many algorithms and modelling software (e.g. ICAS Databases,

ProcAMD, ProII, ProPed, ICAS MOT, etc.) which is usually inaccessible by the industry. Although the methodology provided a PI knowledge base which contain a long list of equipment (>100), the equipment description is qualitative and general which might not generate meaningful result.

The sustainability/LCA factors have been excluded from the performance criteria used to rank processes in the methodology presented by Lutze. Babi *et al.* (Babi *et al.*, 2014; Babi *et al.*, 2015) have focused on comparison of PI options based on sustainability/LCA factors along with criteria related to economic (e.g. utility, cost, operational cost, profit, etc.). To perform the economic, sustainability and LCA analysis, the respective tools were used- ECON (Kalakul *et al.*, 2014), SustainPro (Carvalho *et al.*, 2013), LCSOFT (Kalakul *et al.*, 2014).

A similar method for reaction synthesis is proposed recently (Živković and Nikačević, 2016) as it establishes interaction between PI principles and process system engineering (PSE) techniques. The method consists of three stages: (1) reaction screening where the phenomenological modules are defined; (2) reaction system superstructure and mathematical modelling in which modules are connected in a generic reactor superstructure and (3) Optimisation in which optimal structure and operational regime is derived, using techno-economical objective function and different optimisation methods.

Benneker *et al.* (2016) have recently applied the PI methodology developed by Lutze in an industrial process (production of DADPM) of the Huntsman with the goal of reducing operating costs. It is demonstrated that the DTU method is unable to detect the bottleneck accurately, whilst heuristics and good engineering practices are able to provide additional insight and trace the process limitations. It is concluded that the combination of both heuristic and methodology-based intensification would be able to provide more efficient analysis and synthesis and reduces calculations.

2.6.7 Elementary Process Function Approach

The approach (Freund and Sundmacher, 2008; Peschel *et al.*, 2010; Peschel *et al.*, 2011a; Peschel *et al.*, 2011b) tracks a fluid element through a reactor with possibilities to integrate separation and heating/cooling (thermal). Starting from a definition of the objective of the investigation, the method decomposes the problem into three levels: 1) Level of integration in which the optimal route in the state space is identified; 2) Operational constraints based on detailed mass and energy transport calculations are integrated within the design of level 1; 3) Unit operation is identified to screen for technical constraints of the design.

Reactor parameters such as interfacial areas, residence time and number of units are not chosen a priori but are investigated through a stepwise procedure, identifying resistances in individual process steps. The performance of innovative reaction concepts were benchmarked against reference reactors for comparison. This approach tend to depend strongly on chemical engineering experiment to make preliminary decisions to focus or eliminate initial possible reaction concepts.

2.6.8 Optimisation and Integration for Reactive Separation

Schembecker (2002) has developed a systematic framework focusing on assessing the feasibility of reactive separation in the early stages of process development. This involves defining the operation windows for reaction and separation and only if an overlap is identified, reactive separation process is feasible. Another group of researchers (Franke et al., 2008; Marquardt, 2008) have proposed a three-step systematic framework for the design of separation flowsheets. 1) UNIFAC and Computer-Aided Molecular Design (CAMD) are used to predict mixture properties based on group contribution methods when database is not available. (2) Alternative flow sheets are evaluated with shortcut methods and narrowed down to best alternatives with minimum energy demand. (3) A rigorous mixed-integer nonlinear programming (MINLP) optimisation of the entire flow sheet is executed to determine the best alternative. This approach requires expertise in the field of programming and computation like MINLP.

2.6.9 Framework for Batch to Continuous

Recently, (Teoh *et al.*, 2016) have proposed a practical methodology to assess the feasibility of converting a batch process into a continuous one. The methodology guides user to make swift decision at the beginning of the evaluation state on either to proceed with or kill the idea at early stage to avoid wasted effort. The ordered approach also provides a whole process assessment and decision making for the appropriate choice of continuous or hybrid processing mode. The methodology was applied to three case studies (the Reformatsky reaction, the synthesis of 4,D-erythronolactone and the phase transfer catalysed O-alkylation of 3-phenyl-1-propanol). This methodology may also be extended to incorporate a wider spectrum of PI strategies (use of alternative energy, membrane separation, reactive distillation, etc.).

Plouffe *et al.* (2014) have proposed an approach by considering reaction kinetics (Type A, B, C), reacting phases and the reaction network in order to select the most appropriate reactor module (Plate, Coil or CSTR) for continuous operation. The very fast (in seconds), intermediate and slow reactions were classified in types A, B and C respectively. Kockmann *et al.* (2011) described an additional Type D reaction which requires harsher reaction conditions to be treated

as at least a Type C reaction. Three case studied were presented (1. Reaction of dimethyl-oxalate with ethylmagnesium chloride; 2. Nitration of salicylic acid; 3. Ring-closing metathesis reaction). The classification of reaction may simplify the evaluation of the complex and broad spectrum of pharmaceutical reactions. Although the Plate, Coil and CSTR were more accessible by the industry, the reactor module considered in the study was very limited.

2.6.10 PI Equipment Database Focused Approach

The IMPULSE project (Bayer et al., 2005) has called for cooperation of equipment manufacturers to characterise the equipment according to standardised methods, so that a database of equipment characteristics can be created. The information collected is concerned with reaction, mixing, heat and mass transfers, phases to be processed, flow patterns and operability. The database is captured in a user-friendly manner enabling user to input critical parameters and the database would generate a list of possible equipment. Currently, the database has collected more than 400 equipment information. However, some of the entries apply to very specific model of equipment provided by the equipment manufacturer which may not be a good representation of the generic class of equipment when used in the initial equipment screening stage. The entries are only limited to commercially available equipment (mainly reactors), they do not extend to novel equipment reported in literature and do not include equipment used in separation and purification. Overall, this project offered a good approach to benchmark the equipment in an accurate and practical manner.

In summary, the synthesis of a holistic PI methodology is not easy and requires enormous effort and interdisciplinary collaborations. Most of the existing methodologies reviewed in this chapter encountered common limitations and gaps when applied to industrial pharmaceutical processes. Some of the common limitations include the need to perform optimisation using programming tools like MINILP, property prediction tools like UNIFAC and CAMD and modelling software like ICAS Databases, ProII, etc. and these are usually inaccessible by the industry. Furthermore, due to the complexity of the pharmaceutical reactions, the application of these modelling/prediction tools are often restrictive due to the lack of information on the new chemical reaction. This is a serious challenge as the accuracy of the results from these modelling-based methodologies is directly dependent on the reliability of the data input which is known to be hard to obtain.

Often, the existing PI methodologies do not include database for PI equipment and strategy although this database is pivotal to the selection of optimum PI option. Currently, the applications of PI equipment and strategy are reported independently in literature which leads to a scattered and fragmented database where benchmarking of PI equipment is hard. This is

the reason for the strong reliance on chemical engineers' experience when it comes to equipment selection.

Chapter 3. Amidation Process – Synthesis and Evaluation for Intensification and Sustainability Benefits

3.1 Introduction

Amide bond formation is one of the most frequent transformations in the pharma industry and amide bonds are very often part of active pharmaceutical ingredients (API) (Roughley and Jordan, 2011). The most common practice is to perform amidation through the acylation of commercially available acid chloride on a large scale, as this approach avoids the need for acid activation (Carey *et al.*, 2006; Hong *et al.*, 2013; Ishimoto *et al.*, 2013; Yoshida *et al.*, 2014).

Direct amidation using commercially purchased 4-chlorobenzoyl chloride with diisopropylamine (Faigl *et al.*, 2010) is chosen as an example for this case study. One reason for selecting this reaction is because the product, 4-chloro-N,N-diisopropylbenzamide (amide 1), is a potential building block for the synthesis of many natural molecules. This reaction is considered for intensification because it demonstrates sufficiently complex process behaviours. For example, the reaction involves multiple phases consisting of sticky gel-like solids and is moderately fast and exothermic. The separation and purification processes also present a realistic representation of a large number of processes commonly seen in pharmaceutical processing that involve extraction, handling of sticky solids and drying.

3.2 Aims and Objectives

The objective of this work is to evaluate the sustainability benefits of the intensification of a conventional batch amidation process. In this study, the sustainability performance of different systems (Table 3-1) under various intensification scenarios for the whole process (reaction and separation) is assessed and compared at a hypothetical design scale of 3 tons per year. The benefits that could potentially be achieved are minimization of solvents, reagents and wastes, improved mixing performance and better process safety.

Table 3-1 Four amidation cases to be evaluated

	Cases	Potential intensification options
1	Batch base case	Conventional batch manufacturing process following the literature procedure reported by Faigl <i>et al.</i> (2010)
2	Intensified batch case	1) Reduce the number and amount of reagents used 2) Reduce toluene usage by using toluene-water mixture as solvent 3) Reduce the wash mediums in workup 4) Consecutive reactions from amidation to ortho-lithiation

3	Continuous reaction (workup in batch mode)	Continuous reaction in static mixer reactor
4	Continuous whole process	Continuous reaction + Continuous separation operations using centrifugal extractor and wiped film evaporator

The batch base case, which is developed from a lab-scale procedure (Faigl *et al.*, 2010), serves as a benchmark for the intensified cases. Since there is no side product formation in amidation reaction, the material efficiency of the reaction is close to 100%. Hence, it is difficult to reduce the operational costs by increasing reaction efficiency. Only contributions from reduction in wash solvents and waste treatment and solvent recycling would make a difference. Therefore, the intensification efforts should be focused on these areas as described in the intensified batch base case. Attempts are made to perform consecutive reactions from amidation to ortho-lithiation without solvent swap and product isolation. This involves drying the reaction mixture to a moisture level suitable for the next reaction (ortho-lithiation).

Switching from batch to continuous reaction, higher reaction volume efficiency is expected as the residence time required is shorter. The amidation reaction is estimated to have a reaction time in the order of minutes, so flow reactors with extremely short residence time (in the order of seconds) like the microreactor and SDR are unsuitable. The static mixer reactor is selected in this study as it can provide flexible residence time by extending the length of the reactor and sufficient mixing. The workup process in the continuous reaction case is performed in batch mode. The continuous whole process case extends continuous processing from reaction to workup. This is achieved with the use of centrifugal extractor and wiped film evaporator, which are suitable for pharmaceutical application.

3.3 Experimental Apparatus and Procedures

3.3.1 Batch base case experiment/RC1 Experiment

Calorimetry was carried out using a Mettler Toledo RC1 in a 500 mL volume baffled reactor (6 cm i.d., AP01-0.5-RTC), glass 4-pitch blade turbine agitator (4 cm i.d.), RD10 control box and RC1 software. The RC1 reactor was charged with 233 g of toluene and 30 g of diisopropylamine (DIPA) (1.1 M) as shown in Figure 3-1. The temperature of the reaction mixture was stabilized at 25 °C and was stirred at 450 rpm for 5 minutes before calibration and determination of the initial reaction mixture heat capacity. 24 g of 4-chlorobenzoyl chloride (AC) (0.5 M) was charged into the reactor over 15 minutes using a New Era 1000 syringe pump. 1 mL GC samples were drawn via a syringe every 30 min for conversion measurement. Full conversion was observed after 2 h of reaction time and the heat capacity of the final reaction

mixture was calibrated. Large excess of 1 M HCl solution was added to quench the reaction by reacting with the excess DIPA.



Figure 3-1 Base case amidation reaction in a 500 mL RC 1 reactor.

3.3.2 *Amidation mixing study in toluene solvent system*

21.7 g of triethylamine (TEA) (1.5 mol eqv w.r.t. AC) and 21.7 g of DIPA (1.5 mol eqv with respect to AC) were charged into a 500 mL round bottom flask (RBF) and mixed with 269 mL of toluene using a magnetic stirrer. A temperature sensor connected to a data logger was submerged in the solution. The agitation speed of the magnetic stirrer was set at 100 rpm. The stopwatch was started once 25 g of AC was added into the solution in one shot. After three minutes, the reaction was quenched by adding 100 mL of 1 M HCl solution the reaction mixture in one shot and the agitation speed was increased to 1000 rpm. Although HCl was also produced as the byproduct, the amine bases were present in excess. The large excess of quench HCl ensured the neutralization of all the excess bases. The quenched reaction mixture was allowed to stir vigorously for about 5 min before sample was taken from the organic layer for GC analysis. The experiment was repeated using two other agitation speeds at 500 rpm and 1000 rpm.

3.3.3 *Amidation kinetic study in toluene solvent system*

A 150 mL baffled stirred tank reactor (4 cm i.d.) (Figure 3-2) was charged with 60 g of toluene and selected amounts of AC and DIPA were added successively according to Table 3-2. The toluene solution of DIPA was stirred at 400 rpm using a 2 blade pitched propeller stainless steel agitator (2 cm i.d.) for 5 min. The jacket temperature was set at 20 °C. The stop watch was started once AC was added in one-shot manually via a syringe. 1 mL samples were drawn from the reaction mixture at fixed irregular time intervals and immediately quenched with an excess of 1 M HCl solution. The GC samples were taken from the organic phase to quantify the respective reaction conversions.



Figure 3-2 Amidation kinetic study in a 150 mL stirred tank reactor

Table 3-2 Initial AC and DIPA concentrations used for amidation kinetic study

Run	Temperature (°C)	Initial AC [M]	Initial DIPA [M]
1	20	0.042	0.11
2	20	0.042	0.20
3	20	0.055	0.20
4	35	0.042	0.11
5	6	0.042	0.11

3.3.4 Intensified Batch Case Experiment in Toluene-Water Solvent System

The 150 mL baffled stirred tank reactor (4 cm i.d.) (Figure 3-2) was charged with 40 g of toluene and 10 g of DIPA (2.1 M in toluene), followed by 7 g of water. The liquid-liquid mixture was stirred at 400 rpm using a 4 blade pitched stainless steel agitator (2 cm i.d.) for 5 min. The jacket temperature was set at 20 °C. The stop watch was started once 8.5 g of AC (1 M in toluene) was added dropwise manually via a syringe and the addition took less than a minute. The reaction was quenched after 5 min, upon addition of excess 1 M HCl solution under vigorous agitation. Samples from the organic phase were taken for GC analysis to quantify the reaction conversion.

3.3.5 Continuous Reaction in Static Mixer

In the setup shown in Figure 3-3, two peristaltic pumps (Watson Marlow 520S/R peristaltic pumps) were used to deliver toluene solution of AC (1 M) and aqueous solution of DIPA (1.1 M) respectively. The two tubing carrying the two streams of solutions were connected in a head-on manner to a Tee-joint (CTA-2-STEL, 1/8 in, Hylok) and the combined outlet was connected to three Noritake static mixers (T3-17R-S) in series with a combined length of about 1 m, followed by a 24.5 m long bare 1/8 in i.d. PTFE tubing to provide a residence time of 5 min. The long coils of PTFE tubing is shown in Figure 3-4. Each static mixer (Figure 3-5) was 10 cm in length and equipped with 17 rod-like elements positioned

perpendicular to the flow direction of liquid. The peristaltic pumps were calibrated and dried by pumping air through prior to the experiment. The static mixer setup was dried prior to each experiment by pushing compressed air through.

2 L of AC in toluene (1 M) and 6 L of aqueous solution of DIPA (1 M) were prepared. The flow rate of the AC stream into the reactor was set at 32.3 mL/min, while the flow rate of DIPA stream was set at 67.7 mL/min. Flow through the two pumps was started simultaneously and a combined flow rate of 100 mL/min was collected at the reactor outlet. The reaction mixture was collected in two 5 L schott bottle prefilled with 1 L of 2 M HCl solutions. The reaction mixture was mixed vigorously with the quench solution using a magnetic stirrer. The experiment was conducted for about 40 min as the first 10 min were discarded to minimize collection during unsteady-state. The samples were taken from the organic phase at different time intervals and sent for GC analysis to quantify the reaction conversion.

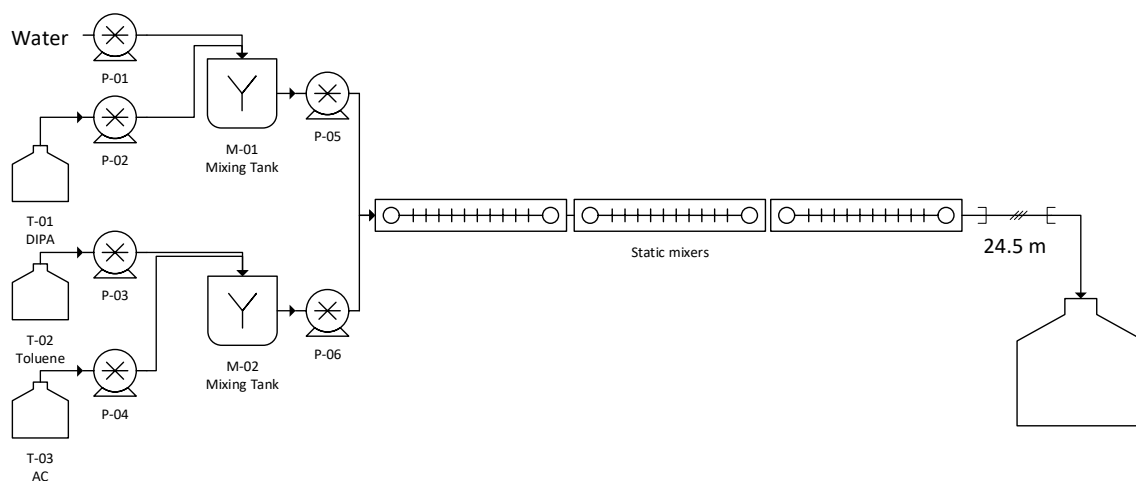


Figure 3-3 Schematic of the continuous static mixer setup.

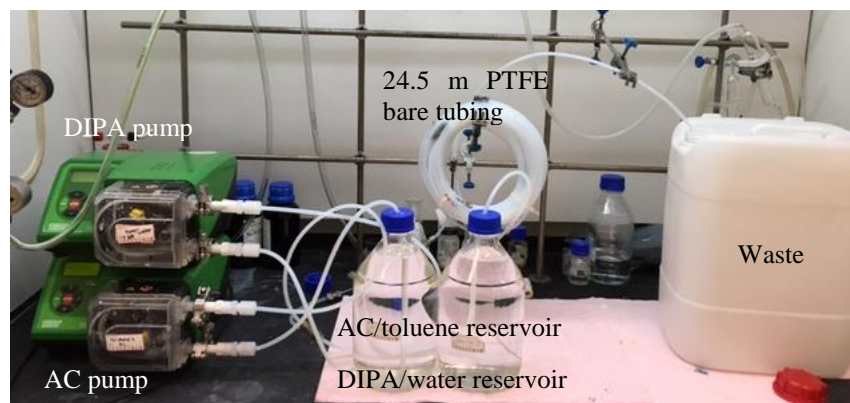


Figure 3-4 Continuous amidation reaction in static mixer setup (Static mixers not visible)



Figure 3-5 A single Noritake static mixer (Source: Noritake (2017a))

3.3.6 Continuous Extraction using Centrifugal Extractor

A schematic of a centrifugal extractor (CE) (CINC, V02) is shown in Figure 3-6 (a). Prior to the experiment, trials were conducted with toluene/water mixture and different weir sizes under a fixed rotational speed of 4000 rpm (maximum) to obtain suitable weir size aimed at obtaining clear separation of the two phases. A weir size of 2.1 cm was found to be the most robust and effective weir size to separate toluene/water mixture. All experiments were carried out in a single stage CINC V02, which was washed with toluene and water between the experiments. The experiment was initiated by switching on the agitator at 4000 rpm and pumping the heavy phase (aqueous) first, followed by the lighter phase (organic). After reaching steady state at the outlet flows, the experiment went on for several minutes. The CE was tested under three different operating conditions:

- 1) Separation of liquid-liquid reaction mixture directly from the output of static mixer setup into organic and aqueous phase. The objective was to ensure clear separation of the phases. The outlet of the static mixer setup flowed directly into the CE at 100 mL/min and the respective phases were collected at separate outlets as seen in Figure 3-6 (b). The rate of collection of the organic phase was at about 30 mL/min, while

the collection rate of the aqueous phase was 70 mL/min and clear phase separation was obtained.

- 2) Extraction of excess DIPA from organic phase into HCl solution. The objective was to ensure majority of DIPA was removed in the aqueous phase. The organic phase from previous extraction and 1 M HCl solution were both pumped (Watson Marlow 520S/R peristaltic pumps) into the CE at 30 mL/min each via two separate inlets. The collection rates of both organic and aqueous phases were observed to be 30 mL/min. Samples for analysis were taken from the organic phase for the detection of DIPA by qualitative NMR analysis.
- 3) Extraction of amine salt (if any) from organic phase into 1 M NaCl solution. As there was no suitable analytical method to quantify amine salt in organic solvent, so it was assumed that the quantity of NaCl solution used according to literature (Faigl *et al.*, 2010) would be sufficient to remove all the amine salt from the organic phase. The organic phase from previous extraction and 1 M NaCl were pumped into the CE at 30 mL/min and 15 mL/min respectively. The collection rates remained at 30 mL/min for the organic phase and 15 mL/min for the aqueous phase.

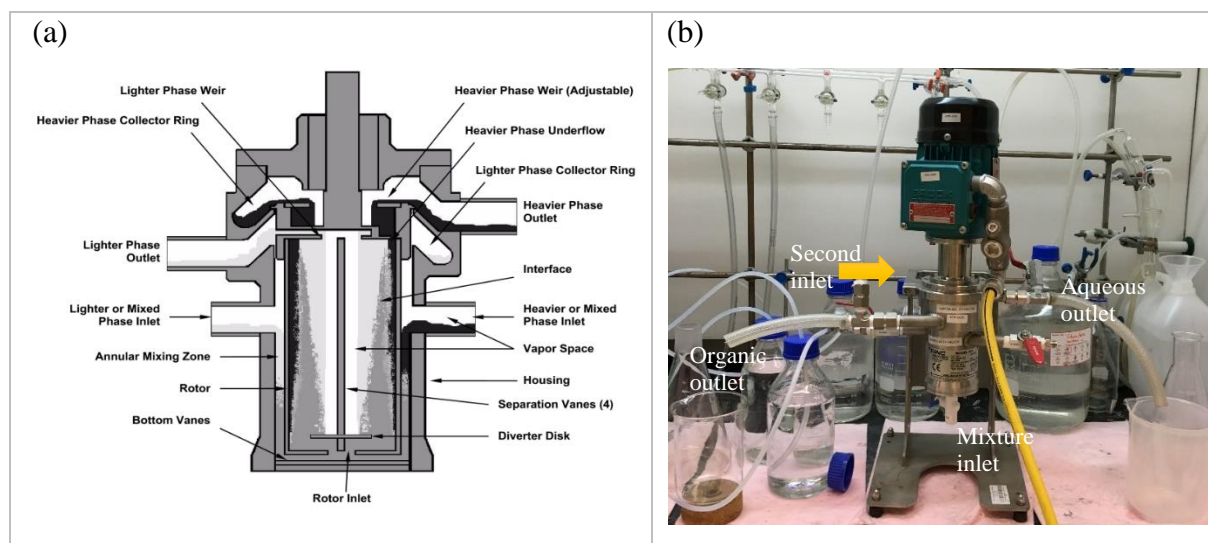


Figure 3-6 (a) Schematic of CINC V02 centrifugal extractor (Source: CINC (2017)); (b) Actual setup used in experiment.

3.3.7 Wiped Film Evaporator

The wiped film evaporator (WFE) from Pope Scientific Inc., USA was used in continuous solvent evaporation as seen in Figure 3-7. The temperature of the still jacket was set at 70°C with a pressure of 0.09 bar and agitator speed of 250 rpm. The organic feed, obtained from the multiple CE washes, was admitted into the still at two different flow rates – 43 and 100 mL/min using a Watson Marlow 520S/R peristaltic pump. The feed flowed down the evaporative surface, where the more volatile toluene vaporized, while the less volatile amide 1

concentrate continued flowing down the cylinder into the concentrate collector. The toluene was collected in the distillate receiver after passing through the condenser. The equipment dimensions were:

- 1) Distance from evaporation surface to agitator tips: 1 mm;
- 2) evaporator heated surface area: 0.108 m²;
- 3) evaporator cylinder internal diameter: 10.16 cm;
- 4) condenser surface area: 0.390 m².



Figure 3-7 POPE Wiped Film Evaporator used in actual experiments.

3.3.8 Feasibility Study of Consecutive reactions from amidation to ortho-lithiation: THF drying study

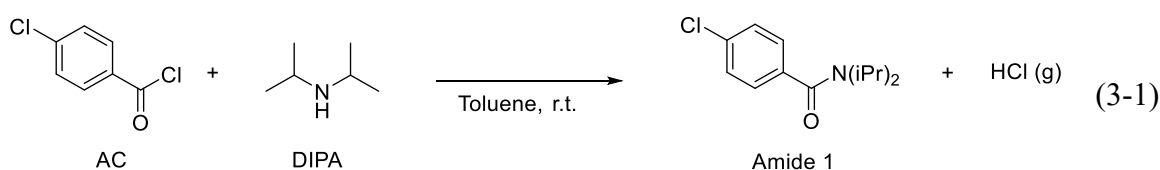
Analytical grade THF (100 mL) was washed with 1 M NaCl (33 mL) and the aqueous layer was separated. The volume of the 'wet' THF was measured and the required amount of desiccant was weighed and packed in a glass column. The 'wet' THF was then passed through the desiccant plug and the volume of solvent collected was noted. This process was repeated, if required, with a second batch of fresh desiccant.

The water content of THF was determined via Karl Fischer titration (Mettler Toledo Karl Fischer Titrator V20, using HYDRANAL®-Solvent, and HYDRANAL®-Titrant 5 pre-calibrated with HYDRANAL®-Water Standard 10).

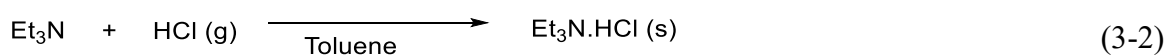
3.4 Reaction Understanding

According to Faigl *et al.* (2010), the overall stoichiometries of amidation between 4-chloro benzoyl chloride (AC) and diisopropylamine (DIPA) and of neutralization reaction between trimethylamine (TEA) and by-product HCl are given by Eqs. (3-1) to (3-3) below.

Synthesis of amide 1 via amidation reaction between AC and DIPA:



By-product HCl neutralised by TEA to form amine salts:



By-product HCl neutralised by DIPA to form amine salts:



Amide 1 was obtained from the reaction between AC and DIPA in the presence of TEA at ambient temperature. During the reaction, stoichiometric amounts of amine salts were formed while the HCl released were ‘captured’ by the amine bases. The amine salts were insoluble in toluene and presented as solids. This reaction had no side product formation according to GC analysis.

The RC 1 experiment revealed a heat of reaction of 105 kJ/mol AC, with a potential adiabatic temperature rise of 56 K. During the addition of bases (DIPA and TEA mixture) to AC in toluene and depending on the addition rate and agitation speed, evolution of HCl fume was observed. Caution was exercised during the RC 1 experiment to ensure minimum release of HCl fume into reactor headspace by optimizing the agitation speed and reagent dosing rate. Good ventilation was ensured during the reaction and the headspace was constantly purged by nitrogen gas, which bubbled through sodium hydroxide solution before exiting to the surrounding. Preliminary study from RC 1 experiment showed that the amidation reaction, following the procedure from Faigl *et al.* (2010), did not seem entirely safe due to release of HCl fume. Therefore, slight modifications were made to the literature procedure to enhance it into a safe and scalable base case.

According to Faigl *et al.* (2010), the mixture of DIPA and TEA was added slowly to a solution of AC in toluene. The reason for using two different amine bases was to ensure that

sufficient TEA is available to quench the HCl byproduct as DIPA react with AC. The quenching of HCl was made more efficient by changing the addition sequence – AC added slowly to a solution of bases in toluene. With this modification, noticeably lesser HCl fume was released during the reaction because AC was added to a large excess of bases where the concentration of amine bases is significantly higher than AC and HCl. As a result, HCl was quickly ‘taken’ by the bases that are present in abundance.

It was also visually observed during the RC 1 experiment that there was a layer of stagnant solid-liquid suspension close to the reactor wall and the only moving section was in the center of the reactor where the impeller was. This phenomena is very similar to the description of a cavern in Figure 3-8 (Paul et al., 2004), which is a physical characteristic of viscoelastic/yield-stress fluid when the minimum shear stress in a vessel is lower than the fluid yield stress. This raised concerns that the poor mixing close to the wall could have led to accumulation of unreacted AC in the reactor and potential exothermic runaway should all the unreacted materials suddenly make contact, mix rapidly and react.

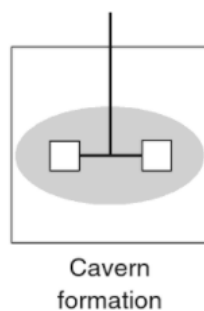


Figure 3-8 Schematic of cavern formation (Paul et al., 2004)

In order to validate whether the formation of amine salts could result in mixing limitation during the reaction, experiments were conducted at different agitation speeds. Results in Figure 3-9 (a) shows that the conversion was dependent on agitation speed; this was supported by their respective temperature profiles in Figure 3-9 (b). The initial temperature rise in 100 rpm was noticeably slower than those at higher agitation speeds, indicating that the initial rate of reaction is affected by agitation speed. Based on these observations, it is clear that mixing is paramount to the scalability of this process.

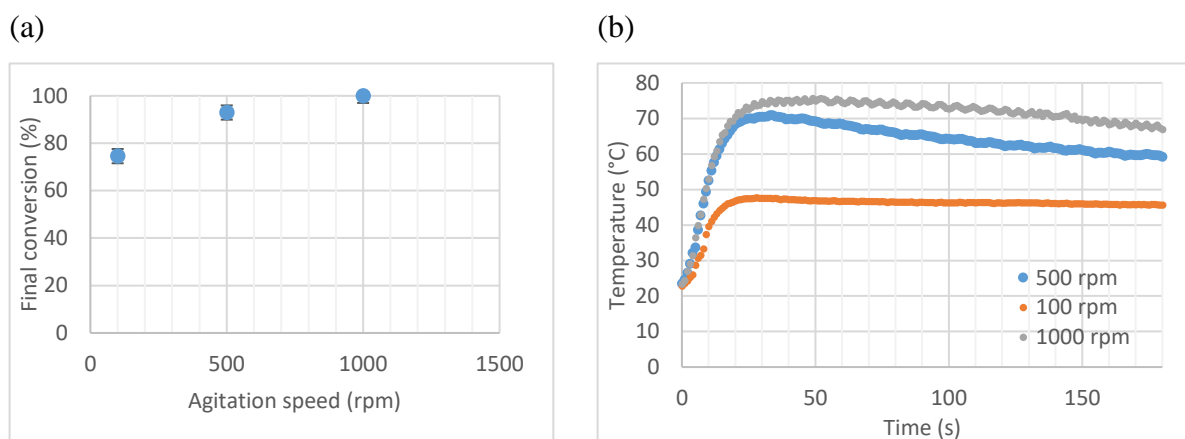


Figure 3-9 a) Mixing dependency of the amidation experiments; b) Temperature profile of the experiments

A series of rheology tests were performed to characterise the flow behaviour of the reaction mixture through analysis of the material's storage and loss moduli (Appendix A.1). The rheology results revealed that the suspension behaved as a viscoelastic solid at low strains and began to flow at higher strains after a long period of yield as it turned into a viscoelastic liquid. A microscope photo of the gel-like suspension (Figure 3-10) was taken to gain an insight to its physical structure. The amine salts (TEA.HCl and DIPA.HCl) formed rod-like crystalline dispersion in toluene. According to a study by Solomon and Spicer (2010), one common feature of rod-shaped particle systems is their ability to form space-filling networks, to efficiently create elasticity and to trigger a solid-like rheological response. For example, a network of rod-shaped particles could increase the yield stress by orders of magnitude for a given concentration compared to a close packing of spherical shaped particles. This suggests that the extensive network of rods might be responsible for the physical properties such as viscosity and yield-stress. However, if the solid concentration falls below a certain concentration or minimum percolation volume fraction such that the number density of the rods is too low to contact each other, the rods would likely lose their structural impact on the suspension. Under such a condition, the intrinsic reaction kinetics could be achieved without the effect of mixing limitation.

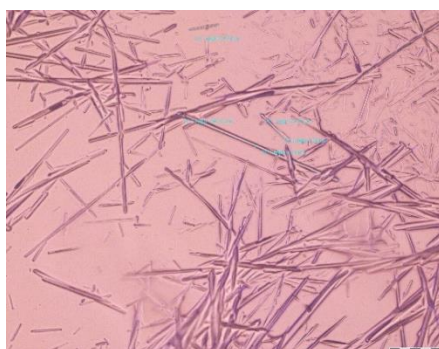


Figure 3-10 Microscope photography of the final reaction mixture slurry at 6 w/w%

Given the mixing limitation, one possible solution was to increase the volume of cavern by employing multiple impellers as shown in Figure 3-11 (Arratia et al., 2006). Although the bulk of the vessel seemed to be well mixed, the volume close to the wall might still be poorly mixed. The impeller shaft needed to be carefully designed and positioned to ensure consistent mixing throughout the vessel. Due to equipment constraint (no suitable multiple impellers), this method could not be proven experimentally. It is assumed to be a practical and effective solution to the mixing problem and could potentially be applied in the batch base case for a safe and scalable batch process.

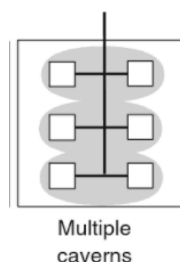


Figure 3-11 Schematics of cavern observed in mixed tanks, where grey areas indicate regions that are well mixed and white indicates unmixed areas. (Kresta et al., 2015)

Based on the experimentally obtained reaction kinetics in Table 3-3 (Appendix A.2) using very low reagent concentration (~ 0.5 w/w% solid loading), the reaction time for the original AC concentration of 0.5 M could be extrapolated. It was estimated that the intrinsic reaction time required to obtain 99% conversion at 20 °C was about 183 s (3 min) while Faigl *et al.* (2010) reported a residence time of 24 h at similar concentration and temperature. Under the assumption that the use of multiple impellers eliminated mixing limitation, the residence time was assumed to be solely dependent on AC dosing rate, which was controlled by the heat of reaction.

Table 3-3 Kinetic parameters of amidation reaction

Batch base case	Kinetic data
Order of 4-chlorobenzoyl chloride	1
Order of DIPA	2
k, rate constant at 20 °C ($L^2 s^2/mol^2$)	2.1
Ea (kJ/mol)	20
k_0 , pre-exponential ($L^2 s^2/mol^2$)	5581
Overall rate equation at 20 °C	$-r_{AC} = 2.1C_{AC}C_{DIPA}^2$

Isolation of amide 1 from the solution was carried out as described by Faigl *et al.* (2010) where the organic solvent was evaporated under reduced pressure. The resultant ‘wet’ solid (amide 1) was triturated with hexane and filtered. However, these steps were unsuitable for large scale process as amide 1 was quite soluble in hexane, with a recovery of only 30-40% of

the reaction yield after filtration. Nevertheless, it is concluded that purification and trituration are unnecessary as the reaction does not produce side products.

Another major challenge was the evaporation of the crude reaction mixture. The minute amounts of water present during solvent evaporation resulted in the formation of hard and clumpy solid that was not readily transferrable from the reactor vessel. It was found that ‘drying’ of the reaction mixture using anhydrous magnesium sulfate allowed the formation of easy-to-flow crystalline solid product as seen in Figure 3-12 and there was no solid sticking to the wall of the round bottom flask.



Figure 3-12 Crystalline solid amide 1 obtained after workup under anhydrous condition

Based on the experiments and experiences during the base case development, the following pitfalls/bottlenecks/limitations in the process were identified:

- Large amount of DIPA and TEA excesses used which led to unnecessary wastage of reagents.
- Unnecessary complication by using two types of bases (DIPA and TEA) which required additional premixing step.
- Maximum initial AC concentration capped at 0.5 M due to mixing limitation which led to the use of large amount of solvent and high energy consumption for solvent evaporation in workup.

3.5 Investigation of process intensification options

Based on the above identified bottlenecks, possible PI options were proposed to remove bottlenecks in the process and improve process performance. In the following section, several process intensification options were discussed, followed by propositions of three intensified cases. The PI options investigated were:

- 1) Reduce the number and amount of reagents used
- 2) Reduce toluene usage
- 3) Reduce the wash mediums in workup
- 4) Consecutive reactions from amidation to ortho-lithiation
- 5) Continuous reaction

6) Continuous whole process (including workup)

3.5.1 Reduce Number and Amount of Reagents Used

As DIPA has similar basicity as TEA, the TEA in the amine reagent mixture was replaced by an equal amount of DIPA without affecting the reaction performance. The premixing of DIPA and TEA prior to the reaction was avoided.

Attempts to reduce the usage of DIPA from 3 to 2.1 mol eqv (with respect to moles of AC) did not affect the efficiency of capturing HCl. This was done by quantifying the amount of DIPA.HCl present in the first aqueous wash medium through conductivity tests (Appendix A.3) and assuming that all DIPA.HCl salt dissolved in the aqueous layer. The result showed that 97% of the HCl was converted to DIPA.HCl, which indicated that the reduction of DIPA did not compromise on safety as majority of the HCl byproduct was efficiently captured by the DIPA. Table 3-4 shows the material costs for different quantities and types of amines used. Option 3 gives about \$26 to \$36 savings in reagent cost when compared to options 1 and 2. Therefore, the decision is to use 2.1 mol equivalent of DIPA as it appears to be the most cost saving option.

Table 3-4 Cost comparison of amine reagents

	Options	Cost (USD/kg amide 1)	Cost Saving (%)
1)	3 mol eqv DIPA	122	N.A.
2)	1.5 mol eqv TEA+ 1.5 mol eqv DIPA	112	8.2
3)	2.1 mol eqv DIPA	86	29.5

3.5.2 Reduce Toluene Usage

To eliminate mixing limitation caused by amine salt (solid), water could be added to the solvent (toluene) as the amine salt was highly soluble in water (approximately 500 g/L). Without mixing limitation, higher initial AC concentration in toluene could be used.

To test this, 1.05 M of DIPA was prepared in toluene followed by addition of minimum amount of water needed to dissolve the amine salt. Subsequently, AC (0.5 M in toluene) was added to the toluene-water solvent system and the reaction was monitored through regular sampling and GC analysis. Based on visual observation during the reaction, there was no formation of solid and the reaction mixture appeared cloudy as the organic and aqueous phases appeared to be well dispersed under the agitation of a single impeller at 450 rpm. The result indicated that full conversion was reached in less than 5 min (Appendix A.4) and it proved that the use of toluene-water mixture as solvent can effectively avoid mixing limitation.

In light of this promising result, the initial AC and DIPA concentrations in toluene were doubled to 1 M and 2.1 M respectively. Under these conditions, complete conversion was achieved in less than 90 s, which was expected as the rate of reaction increases at higher concentrations. This proved that the toluene-water system was robust even with more concentrated reaction mixture. Even though the toluene-water system might be capable of operating at even higher reagent concentrations, the decision is to cap the initial AC and DIPA concentrations at 1 M and 2.1 M, as AC has limited solubility in toluene and it might take a longer time for complete dissolution of the AC in toluene if higher concentrations were used.

3.5.3 Reduce Wash Medium in Separation Process

The amounts of wash solvents (e.g. water, NaCl solution and HCl solution) used in the safe and scalable batch process were investigated (Table 3-5). Based on the solubility of DIPA.HC in water (500 g/L), the required amount of water to dissolve the salts was calculated to be only 45% of the reported value (219 g/L) by Faigl *et al.* (2010).

Based on section 4.5.1, since the required mol eqv of DIPA was decreased from 3 to 2.1, the excess DIPA correspondingly decreased from 1 to 0.1 mol eqv. As a consequence, the amount of HCl wash required for neutralization of excess DIPA was reduced significantly.

The brine wash reported in literature (Faigl *et al.*, 2010) was replaced by 1 M NaCl extraction because brine has a higher tendency to corrode stainless steel in the long term. Unfortunately, there was no suitable analytical equipment to quantify the amount of amine salt and DIPA that remained in the organic phase. In order to ensure that the majority of the amine salt and the DIPA were removed from the organic phase, a conservative decision is to use the same volume equivalent with respect to AC of 1 M NaCl solution as reported in the literature (Faigl *et al.*, 2010).

Although the amide 1 yield residing in the organic phase decreased after each aqueous wash (Table 3-5), no traces of amide 1 was observed in the GC analysis of the respective discarded aqueous phases after phase separations. This suggested that the loss of amide 1 was more likely due to handling.

Table 3-5 Summary of the improvement actions taken to minimise amount of wash medium used.

Workup step	Reagents	Literature data (Faigl <i>et al.</i> , 2010)	PI option	Crude sustainability benefits	Amide 1 yield in organic phase (%)
Water wash and phase separation	Water	0.63 L/mol AC	0.28 L/mol AC (minimum)	55% reduction in volume of water usage	98

HCl wash and phase separation	5 w/w% (1.44M) HCl	0.47 L/mol AC	0.07 L/mol AC	85% reduction in volume of HCl solution usage	96
NaCl wash and phase separation	1 M NaCl solution	0.47 L/mol AC	0.47 L/mol AC is the minimum amount required to remove the remaining salt in toluene	-	94

3.5.4 Consecutive Reaction from Amidation to ortho-Lithiation

With the intent to minimise amide 1 yield loss in the workup steps, attempts were made to carry the amidation crude to consecutive ortho-lithiation reaction. Since ortho-lithiation was performed in THF, the amidation was also carried out in THF. The use of THF as amidation reaction solvent was demonstrated to be feasible. However, one important criterion for amidation crude to go on to ortho-lithiation was to have a very low water content of approximately 0.04 w/w% as observed from lab-scale experiments. A technology search was done and some common dehydration techniques using desiccants like anhydrous magnesium sulfate and neutral alumina were assessed through preliminary lab-scale experiments (Appendix A.5).

To assess the drying efficiency of various desiccants, pure THF was first washed with 1 M NaCl solution and the organic phase ('wet' THF) was isolated and analysed via Karl Fischer titration. This step 'simulated' the water content in the amidation reaction crude after the aqueous extractions which were necessary steps before carrying on to ortho-lithiation. Subsequently, the desiccant was added to the wet THF and THF was dried over the selected desiccants. Unfortunately, the results showed that both drying agents were unable to reduce the water content in the THF to 0.04 w/w% as they were limited to 1 w/w%. Another general problem faced was the significant loss of reaction crude within the desiccant matrix which not only trapped water but also amide 1 and THF. The loss of amide 1 whilst passing it through the packed drying agents would be too high to make this a viable process. Unless a more efficient drying method could be found, performing consecutive reactions from amidation to ortho-lithiation would not be feasible. Amide 1 had to be isolated as dry crystalline solid for use in the next reaction step.

3.5.5 Continuous reaction

The use of toluene-water solvent system in the intensified case was able to avoid the formation of solid amine salt, which made it compatible with continuous mode of reaction. The proof of concept was experimented with static mixers. The objective of the static mixer

experiment was to prove the feasibility of operating amidation in continuous flow reactor. The static mixer setup offers flexible residence time as it could be extended using longer PTFE bare tubing.

The schematic diagram of the continuous static mixer reactor setup is shown in Figure 3-4, where the two reagent streams (AC in toluene, DIPA in water) were mixed in a T-mixer, after which the liquid-liquid mixture were mixed in three static mixers connected in series (1 m in length, 12 s of residence time) and a long stretch of bare tubing (24.5 m) which provided the required residence time of about 5 min with a flow rate of 100 mL/min.

The issue with this setup was the poor mixing in the bare tubing where the toluene-water mixture flowed through as large biphasic slugs were observed in Figure 3-13. This might explained the longer residence time required to obtain complete conversion in contrast to a batch reactor. Although this setup was not optimised in terms of mixing efficiency, throughput and residence time, the applied reaction condition was able to obtain full conversion within a reasonable range of residence time. Based on this encouraging result, the static mixer reactor setup is used as a feasible example of the continuous reaction.

Improvements to improve the mixing performance in the setup could be made by extending the length of static mixer length longer or reducing the diameter of the bare tubing. Given better mixing capability, a shorter residence time and smaller reactor volume would be expected (Ghaini *et al.*, 2011; Hartman *et al.*, 2011; Ufer *et al.*, 2011).



Figure 3-13 Photo of large biphasic slugs of toluene and water phases in the bare PTFE tubing section. Large liquid-liquid slugs observed in red circle

3.5.6 Continuous whole process

In view of a continuous flow reaction, a continuous operation incorporating continuous workup was proposed. A potential continuous process involved a static mixer reactor (section 4.5.5) and subsequent continuous separation equipment such as centrifugal extraction, Karr column, agitated thin film dryer, spray dryer and wiped film evaporator. There are many other possible continuous workup equipment that might be applicable. For the ease of determining

the feasibility of the equipment, experiments were performed with technologies that were available in-house such as the centrifugal extractor (CE) and the wiped film evaporator (WFE).

The CE was used in three liquid-liquid phase separation steps involving 1) separation of aqueous and organic phase; 2) extraction of excess DIPA from the organic phase using 1 M HCl solution; and 3) removal of any remaining salts in the organic phase using 1 M NaCl solution. For all the phase separations, clear organic and aqueous streams were collected from the outlets. Nearly complete removal of DIPA from organic phase was achieved for the given operating condition according to NMR analysis of the organic phase. Due to lack of analytical method to quantify amine salt in the organic phase, it was conservatively assumed that the CE would be equally efficient in amine salt extraction as STR. In general, the extraction using CE is considered superior to batch as the mixing and phase separation was completed in seconds compared to more than 10 mins in STR.

The use of Wiped Film Evaporator (WFE) was aimed at obtaining amide 1 as free-flowing dry solid by efficiently removing toluene continuously through a heated column under reduced pressure continuously. The pressure in the WFE was set at 0.09 bar and the estimated boiling point of toluene at this pressure is about 35 °C. In order to increase the rate of evaporation, the WFE jacket was set at 70 °C which is still below the boiling point of amide 1 at about 85 °C. In the first trial with a reaction mixture flow rate of 100 mL/min in a single pass, only 24 v/v% of toluene was removed. Despite operating at the highest temperature and lowest pressure possible, this result was far from ideal. It was believed that the residence time of the reaction mixture in the heated column was too short for evaporation. In order to extend the residence time in the fixed length column, the lowest possible flow rate of 43 mL/min was used and the result improved as 33 v/v% of toluene was removed. A second pass was made under the same condition and a further 22 v/v% was removed. At this point, the existing WFE had removed more than half of the solvent in two passes. Although multiple passes were required to obtain the desired product specification, WFE has shown promising and optimistic results.

3.5.7 Summary of PI options

After assessing the feasibility of the proposed PI options 1 to 6, the experimental conditions for the following four cases (batch base case, intensified batch case, continuous reaction case and continuous process case) are summarised in Table 3-6. It was noted that the operating conditions and results reported were not optimised, but experimentally proven as feasible.

The batch base case is a modification from the literature procedure (Faigl *et al.*, 2010) to obtain a safe and scalable process. It is also virtually designed under the assumption of no

mixing limitation with the use of multiple impellers during the reaction. An intensified batch case is developed by retrofitting PI options 1-4 on the batch base case.

For the continuous reaction case and the continuous process case, the pre-mixing of DIPA in water to obtain an aqueous stream of DIPA and AC in toluene are required. However, this raised concern that increased quantity of water is required to dissolve DIPA because DIPA has limited solubility in water (100 g/L or 1 M). A brief water consumption comparison is also shown in Table 3-6.

Table 3-6 Summary of reaction and separation information in literature, base case and intensified batch case, continuous reaction and continuous process

	Literature case (not scalable)	Batch base case	Intensified batch case	Continuous reaction	Continuous whole process
Mode of reaction	Batch			Continuous	Continuous
Mode of separation	Batch				Continuous
Solvent system	Toluene	Toluene	Toluene-water		
Recycling of solvent	No	No	Yes		
Required residence time	24 h	3 min (Theoretical)	90 s	5 min	
Sequence of addition	Mixture of TEA & DIPA added to a mixture of AC in toluene	AC added to a mixture of TEA & DIPA in toluene	AC added to DIPA in toluene-water mixture	AC in toluene mixed with DIPA in water	
Concentration of limiting reagent (AC)	0.5 M	0.5 M	1 M		
Reagents	TEA – 1.5 mol. eq. DIPA – 1.5 mol. eq.	TEA – 1.5 mol. eq. DIPA – 1.5 mol. eq.	DIPA – 2.1 mol. eq.		
Reaction yield	>99%				
Work up	Water wash	Water wash	HCl wash		HCl wash in CE
	HCl wash	HCl wash	1 M NaCl solution wash		1 M NaCl wash in CE
	Brine wash	1M NaCl solution wash	Anhydrous MgSO ₄ addition		Anhydrous MgSO ₄ addition in CSTR
	MgSO ₄ drying	Anhydrous MgSO ₄ addition	Filtration		Continuous filtration

	Filtration	Filtration	Evaporation of toluene		Wiped film dryer
	Distillation	Evaporation of toluene	Drying		-
	Trituration with Hexanes	Drying	-	-	-
	Filtration	-	-	-	-
	Drying	-	-	-	-
Recycling of solvent	No	No	Yes		
Water consumption	0.7 L/mol AC	0.7 L/mol AC	0.3 L/mol AC	2.1 L/mol AC	

3.6 Design of batch base case, intensified batch case, continuous reaction case and continuous whole process case for 3 tons per year production (amide 1)

In order to compare the sustainability benefits between the batch base case, intensified batch case, continuous reaction case and continuous whole process case, the plants were designed to produce about 3 tons per year of amide 1 from AC and DIPA (Reaction scheme), with product purity of about 99 w/w% and less than 0.1 w/w% of residual toluene. The following assumptions were made based on lab-scale experimental work:

- 1) There was no side product observed from the reaction based on ^1H NMR spectra.
- 2) There was no observable degradation of AC when in contact with water based on the amide 1 yield obtained.
- 3) There was no observable heat of neutralisation when excess DIPA and HCl solution are mixed together.
- 4) During the HCl wash step, all the excess DIPA was assumed to be reacted and removed in the aqueous phase as observed from ^1H NMR spectra.
- 5) During the NaCl solution wash step, all the amine salt was assumed to be removed in the aqueous phase.
- 6) All amide 1 losses were assumed to be due to handling as no organics is observed in the aqueous phase based on GC analysis.
- 7) 90% of the toluene used in intensified batch case, continuous reaction and continuous process was assumed to be recycled.
- 8) The reactors were assumed to have good containment so there was no loss of volatile amines to the atmosphere.
- 9) For the batch base case, it was assumed that three agitators of 3 pitched blade turbine impellers would provide good mixing performance.
- 10) Total number of operation hours per year was assumed to be 8000 h.

Heat and mass balances of the process were carried out based on lab scale experimental data as well as the above assumption. Both the batch base case and intensified case consisted of one-pot integrated reaction and separation process where the reactor vessel is used for reaction and workup extraction (water, HCl and HCl washes). The solvent evaporation, filtration and drying unit operations are not performed in the reactor. The schematic diagrams of all the four cases are shown in Appendix A.6.

The base case used more reagents (DIPA and TEA) and solvents (toluene, water, HCl solution) than the intensified batch case where the reaction is performed at higher concentrations. Due to the higher reaction concentration, the volume of the reactor in the intensified batch case is designed to be relatively smaller than that in the batch base case. It is also verified experimentally that there was no mixing limitation in the intensified batch case due to the presence of water which dissolved the amine salt during the reaction. The condensation and recycling of evaporated toluene for subsequent batches is incorporated in the design of the intensified batch and continuous cases.

The reaction conditions used in the continuous reaction case is based on the actual static mixer experiment which obtained 100% conversion at a residence time of 5 min and a combined AC and DIPA flow rate of 100 mL/min. The reactor design consisted of three Noritake static mixers connected in series to a 24.5 m long PTFE tube. The separation operations are performed in batch mode where the reaction mixture had to be collected in a decanter for phase separation. After accumulation to a certain volume, the organic phase is pumped from the top layer into the next reactor for washes in batch mode, while the aqueous phase in the bottom layer is discarded.

The continuous whole process case consisted of continuously reaction and separation. The continuous extractions are designed to be performed using three CE in series. Although the WFE did not obtain satisfactory result, it showed potential for continuous solvent removal. For the purpose of design, it is assumed that a state-of-the-art agitated thin film dryer which operated based on the same principle as the WFE would be able to meet the expectation. Other conceptually developed continuous operations included the continuous feed of anhydrous magnesium sulfate using an automatic screw feeder, a well-mixed CSTR to suspend the magnesium sulfate and a continuous filtration of the slurry.

For all these plants, the utilities used would be electricity for pumping/agitation/heating and chilled water for cooling/condensation. All the organic, aqueous and solid waste generated are assumed to be drained into the Intermediate Bulk Containers (IBCs) and sent off for treatment/disposal by a waste management contractor.

3.7 Comparisons of sustainability performance

Based on the process design for the four cases, their sustainability performances in terms of economy, mass, energy and environmental efficiencies are summarized in Table 3-7 (Appendix A.7). The continuous cases have higher reaction volume efficiency than the batch cases. The static mixer reactor volume is much smaller than the batch reactors because the batch cases have relatively longer cycle times (one-pot reaction) which require larger reactor volumes in order to cope with the required throughput. When comparing the volume efficiency of the separation process, the continuous process case has the smallest equipment volume (CE, Wiped film dryer, etc.). The batch base case has the lowest volume efficiency because it needed to process more solvent (toluene) than the other cases.

Table 3-7 Comparisons of sustainability metrics between batch base case, intensified case, continuous reaction, continuous whole process at design scale of about 3 ton amide 1 per year.

	Batch base Case	Intensified batch case	Continuous reaction	Continuous whole process
Reaction volume efficiency (kg amide 1 /h/m ³)	3	17	835	835
Reaction and separation volume efficiency (kg amide 1 /h/m ³)	0.001	0.007	0.013	5.644
Max processing inventory at any point of time (L/kg amide 1/h)	993	203	293	225
Total material efficiency (kg material/kg amide 1)	21	6	15	15
E-factor (kg waste/kg amide 1)	20	5	14	13
Total energy efficiency (kJ/kg amide 1)	454,784	149,927	167,069	420,338
CAPEX (USD/kg amide 1)	76	63	68	145
Economic savings in CAPEX (%)	Benchmark	17	10	-91
OPEX (USD/kg amide 1)	369	220	227	253
Economic savings in OPEX (%)	Benchmark	40	39	32

The maximum processing inventory at any point of time refers to the total inventory in all the processing equipment which includes the storage and mixing tanks. Despite providing the best volume efficiency, the continuous reaction and continuous whole process cases did not provide overall smaller inventory in the plant compared to the intensified batch case. This is because of the additional volumes of the DIPA/water and AC/toluene mixing tanks and the decanter in the continuous cases that are not required in the batch cases. Nevertheless, the three intensified cases would still provide safety benefits compared to the batch base case when dealing with hazardous chemicals.

In terms of the material efficiency and E-factor, the intensified batch case appears to have the best performance because recycling of toluene is incorporated in the design conceptually. For the continuous cases, the poorer performance is due to significant amount of water used to dissolve DIPA in order to introduce DIPA as an aqueous stream to the organic stream containing AC. This is unnecessary in the intensified batch case where toluene, DIPA, water and AC are added separately into the batch reactor and significantly lesser amount of water is required as the amine salt is highly soluble in water.

The two most energy intensive cases are the batch base case and the continuous whole process case. The majority of the energy consumption for the batch base case is invested in toluene evaporation; as its AC concentration was more dilute than in other the cases. For the continuous whole process case, most of the continuous equipment, including the centrifugal extractors, the screw feeder and the agitated thin film dryer, required mechanical movement/agitation that is energy intensive.

Costing of the plants is based on process designs (Appendix A.6) and it is assumed to be operating on existing plant area which is fully facilitated with utility infrastructure. Apart from the centrifugal extractor and the static mixer, most of the general equipment like storage vessel is priced on the same costing basis using Matches' Process Equipment Cost Estimates (Matche, 2017). As for the specialized state-of-the-art equipment like the agitated thin film dryer, the equipment quotations are obtained from Alibaba (2017a). The absolute capital expenditure (CAPEX) calculated in this section might not reflect the actual CAPEX of a plant because many of the equipment are not customized and installation costs are not included. However, the percentage CAPEX reduction relative to the batch base case cost would provide a sensible comparison. The slight CAPEX reduction in the intensified batch case and the continuous reaction case is mainly due to the decrease in equipment volume since the reactor volume is reduced significantly compared to the batch base case. As expected, the CAPEX of the continuous process case appears to be most expensive and is 90% higher than the batch base case. This was due to the costly specialized continuous equipment involved such as the agitated thin film dryer, the rotary vacuum drum filter, three centrifugal extractors and an automatic screw feeder.

The operational expenditure (OPEX) derived in this study included the cost of raw materials, utilities/energy and waste treatment. They are priced based on the same source of costing database. In general, the cost of raw material constituted majority of the operating cost in this process is as summarized in Figure 3-14. AC is the most expensive reagent among the chemicals used, followed by toluene and the amine bases. Since all the cases have the same AC input, the difference in raw material cost is due to varied quantities of toluene and amine used.

The intensified batch base case obtains the lowest CAPEX of 220 USD/kg amide 1 because of the reduction in solvents and DIPA used, which also leads to reduction in waste treatment and energy consumption for solvent evaporation. For the continuous reaction case and the continuous whole process case, the water consumptions are much higher than the intensified batch case, hence the aqueous waste treatment costs in the continuous cases are also indirectly higher. The main OPEX difference between the continuous reaction case and the continuous whole process case is in the workup energy cost as significant amount of energy is supplied to the continuous workup equipment. Despite having higher CAPEX than the batch base case, the continuous process offered a lower operating cost which might still justify the adoption of continuous process in the long run. Furthermore, labor cost is not considered in this study but it is generally observed that labor cost is lower in continuous process compared to batch (Denčić et al., 2014) and it might compensate for the higher energy cost. Nevertheless, all the cases summarized in Table 3-7 are still considered profitable according to the market price of 4300 USD/kg amide 1 (Apolloscientific, 2017).

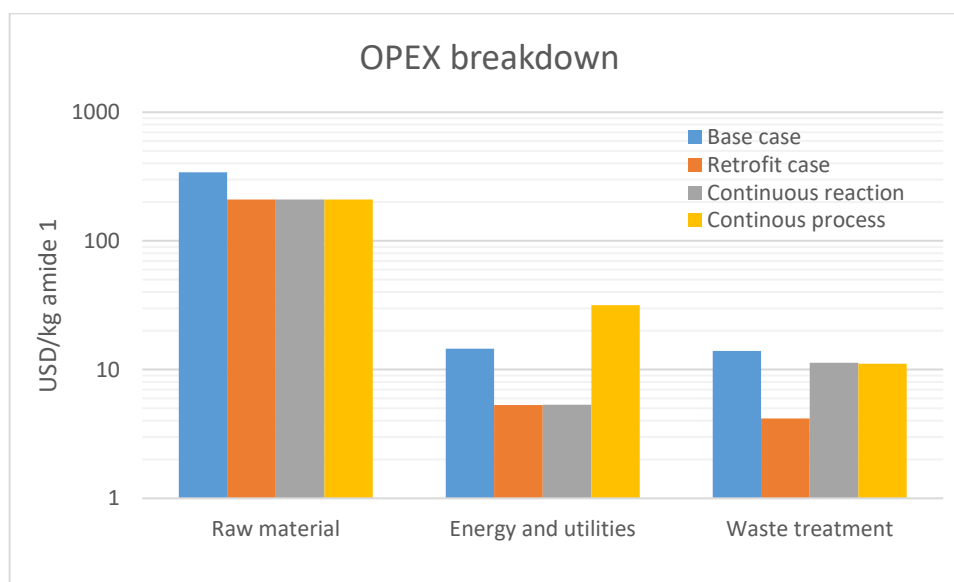


Figure 3-14 Breakdown of OPEX for all 4 cases.

In this study, the continuous whole process did not bring the most benefits. It is recognized that the continuous cases resulted in higher water consumption and solvent waste generation due to low DIPA water solubility. Although this did not negatively affect OPEX to a great extent, the effect on E-factor and material efficiency is significant. The continuous operation of the entire process has not been practiced yet and the actual operation might be different or there could be consequences not predicted by the preliminary process design discussed here. However, in the context of sustainable processing, the continuous cases are likely to be considered as feasible development options.

The result of this study indicates that the largest overall cost reduction potential is the intensified batch case as the waste and energy costs are relatively low compared to the continuous reaction and continuous process cases. It uses the least amount of reagents and solvents among all the cases leading to least material processed and least energy demanded overall, which is significant from an environmental point of view. The impact of several process improvement actions using the batch process can sum up to a greener process.

3.8 Conclusion

The amidation reaction of 4-chlorobenzoyl chloride with DIPA is successfully developed and improved based on the implementation of a number of processing and operational modifications in order to achieve sustainability benefits. The thick, gel-like, solid-liquid suspension that exhibited viscoelastic liquid properties was challenging to scale up due to poor mixing. By changing the phase of reaction mixture to liquid-liquid through addition of water during the reaction, the major mixing limitation is eliminated and the reaction is performed at higher reagent concentrations over a much shorter residence time. Several PI options, proven feasible in lab-scale experiments are adopted. These included reducing the amount of DIPA and solvents used in washes and carrying out continuous flow reaction in static mixers. A systematic series of washes and phase separation are also performed in a centrifugal extractor, which enabled a continuous extraction process to be developed. Promising experimental results are obtained from the WFE but it was not efficient enough to obtain dry solid product. Instead, a conceptual agitated thin film dryer is assumed to be able to meet the drying specifications. Attempts are also made to avoid tedious workup steps by performing the subsequent reaction (ortho-lithiation) directly on amidation reaction mixture. However, this required the THF solvent to be dried to 0.04 w/w%, which was difficult to achieve due to the common drying agents failing to efficiently remove water without excessive loss of amide 1.

In order to evaluate the sustainability performance of the batch base case, the intensified batch case, the continuous reaction case and the continuous process case, the respective plants were designed at the same basis of about 3 ton per year throughput. Overall, the intensified batch case provides the most benefits, in terms of higher material and energy efficiency, lower E-factor, smaller processing inventory and lower CAPEX and OPEX. It is noted that the reason for the poorer performance of the continuous cases is because of the larger amount of water used to dissolve DIPA due to the difference in the mode of reagent addition between the batch and continuous cases. On the basis of the sustainability analysis undertaken in this study, it is demonstrated that continuous processing might not always be the best process intensification option.

Chapter 4. Ortho-Lithiation process – Part 1: Process Understanding

4.1 Introduction

Ortho-lithiation is an important class of reaction for the synthesis of regioselectively substituted aromatics, and it is an emerging method to prepare phthalides which are common pharmaceutically active compounds (de Silva *et al.*, 1992; Roberge *et al.*, 2008; Faigl *et al.*, 2010; Karmakar *et al.*, 2014; Newby *et al.*, 2014; Laue *et al.*, 2016). Ortho-lithiation is typically conducted in batch mode under cryogenic temperatures (-78 to -40 °C) (Desai, 2012) to minimize the side reactions arising from the highly reactive organolithium intermediates. Although this process produces high purity compounds, it requires the use of large reaction vessels and long cycle time to achieve the required throughput. The challenges of safely handling both the highly reactive chemicals and a highly energetic reaction in scaled-up operations constitute a major disadvantage of such batch processes. One solution to overcome these safety related issues is to implement continuous flow processes (Anderson, 2012).

Indeed, several successful studies have been performed to scale up continuous lithiation using tubular flow reactors (Newby *et al.*, 2014; Laue *et al.*, 2016). These flow reactors offer superior control of process parameters like mixing, residence time and temperature. There are examples of deploying flow processing for lithiation reaction as a process intensification (PI) technique. The Yoshida group demonstrated several lithiation reactions using different electrophiles in microstructured flow devices (consisting of micromixers and microtube reactors) to be superior to batch protocols (Nagaki *et al.*, 2011; Yoshida *et al.*, 2011; Nagaki *et al.*, 2014a; Nagaki *et al.*, 2014b; Nagaki *et al.*, 2015). Roberge and co-workers (Roberge *et al.*, 2008) and Stephan and co-workers (Laue *et al.*, 2016) have both demonstrated the possibility to scale up lithiation reactions in flow reactors for pharmaceutical manufacturing. However, both authors reported challenges in handling plugging due to precipitation of salts. Kockmann and co-workers (Kockmann *et al.*, 2011) evaluated the feasibility to scale up the lithiation reaction using tubular flow reactors with different channel diameters and flow rates to avoid parallelization.

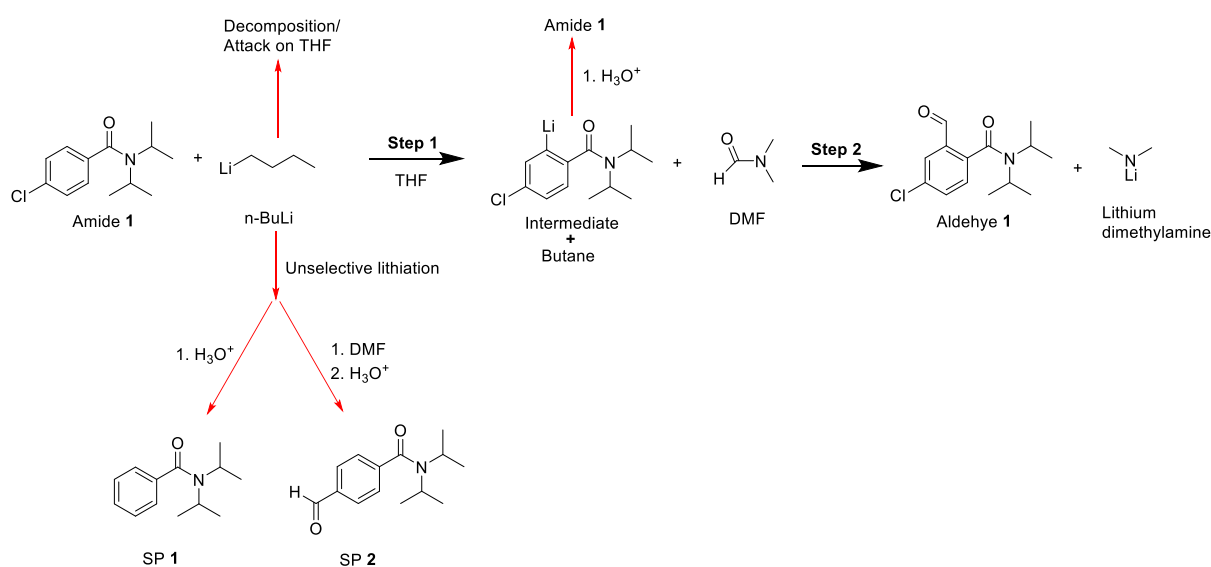
One major problem with adopting flow processing in enclosed microchannels is the possibility of deposition of the intermediate lithium salts, which can lead to clogging of such flow reactors (Laue *et al.*, 2016). It is envisioned overcoming this limitation by the use of the SDR which allows a free surface film flowing over the disc surface instead of through an enclosed channel. The SDR also possesses a number of characteristics which make it a potential intensification tool for ortho-lithiation reaction, such as the capability of achieving rapid mixing with an estimated micromixing time in the range of 0.125 to 0.02 s (Jacobsen and Hinrichsen,

2012) and high mass and heat transfer rates in the free flowing thin film of liquid produced owing to centrifugal acceleration created by rotation (Boodhoo, 2013). Various examples in the literature demonstrate the advantages of performing fast reactions in the SDR (Boodhoo et al., 2006; Vicevic et al., 2007; Mohammadi et al., 2014).

The objective of this work is to minimize side product formation by the use of continuous flow PI reactors at ambient temperature. Inspired by the success of performing ortho-lithiation reaction in microreactors, feasibility study using microreactors (microchips 1 and 2) and stainless steel reactor is conducted. From the reaction understanding gained from the feasibility study, a customized PI reactor – T-reactor, is assembled in-house. In depth reactor study on the two most promising PI reactors (T-reactor and SDR) is performed. Comparison of the experimental result between the stirred tank reactor (STR), the T-reactor and the SDR is shown.

4.2 Reaction System

A typical ortho-lithiation reaction is taken from the literature (Scheme 5-1) (Faigl et al., 2010) where the 4-chloro-N,N-diisopropylbenzamide (amide 1) was treated with n-Butyllithium (n-BuLi, 1.6 M in hexane) in tetrahydrofuran (THF) at -70 to -75 °C and the lithiation occurred selectively at the ortho-position to the amide group. The subsequent treatment with dimethylformamide (DMF) in step 2 produced 4-chloro-N,N-diisopropyl-2-formylbenzamide (aldehyde 1). Step 1 was a very fast reaction with an adiabatic temperature rise of more than 55 °C (230 kJ/mol n-BuLi) (Godany et al., 2011). The second step was less demanding in terms of heat exchange and mixing and had a lesser possibility for new side product formation (Kockmann et al., 2011).



Scheme 4-1 Reaction used in this study and possible side reactions.

Unfortunately the side reaction mechanism of ortho-lithiation is not yet fully understood. Only partial information was obtained in the study using liquid chromatography-mass spectrometry (LC-MS) which nevertheless provided some useful insight into the possible side products formed. As shown in Scheme 1, two possible side reactions had been proposed based on identification by LC-MS of two molecular masses which had been matched to the anticipated molecular structures SP 1 and SP 2. It was noted that versions of other structural isomers of these molecules were also possible. It was postulated that these side products arise from unselective lithiation reactions competing with the desired ortho-lithiation in step 1. The mixing performance in step 2 determined the formation of either SP 1 or SP 2. Poor mixing in step 2 tended to generate SP 1 as DMF failed to react with the lithiated species before contacting water, while good mixing in Step 2 allowed the lithiated species to undergo electrophilic addition to form SP 2. Certain processing conditions may also affect the overall amide conversion. For instance, n-BuLi tended to decompose or get consumed in the reaction with THF (Stanetty and Mihovilovic, 1997) when n-BuLi was not well-mixed. A lesser quantity of n-BuLi available for reaction with amide 1 led to low overall conversion. Similarly low overall conversion was expected when the DMF failed to mix homogeneously with the reaction mixture in step 2, so the intermediate was converted back to amide 1 upon contact with water during separation process. The step 1 reaction in a batch reaction at -60 °C was monitored by in situ IR measurement (Appendix B.1). Although accurate reaction kinetic was not obtained, the experimental result showed that step 1 reaction was very fast and it was estimated to reach 99% conversion at 20 °C in 2.6×10^{-6} s.

4.3 Experimental Apparatus and Procedures

4.3.1 Microreactors

Microchip 1 used in this study is made of borosilicate glass and has a reaction volume of 250 μ L, as shown in Figure 4-1. The 4-chloro-N,N-diisopropylbenzamide and n-BuLi were delivered into the microchip with a nominal cross sectional area of 0.075 mm² via its two inlets, while the third inlet was blocked off. The two streams were mixed in the mixing channel (40 μ L) followed by the reaction channel (210 μ L). It was noted that only the reaction channel is encased on the temperature control module while the mixing channel is not. After passing through the reaction channel, the reaction mixture was immediately quenched with the DMF in a Tee-joint after leaving the glass microchip outlet.

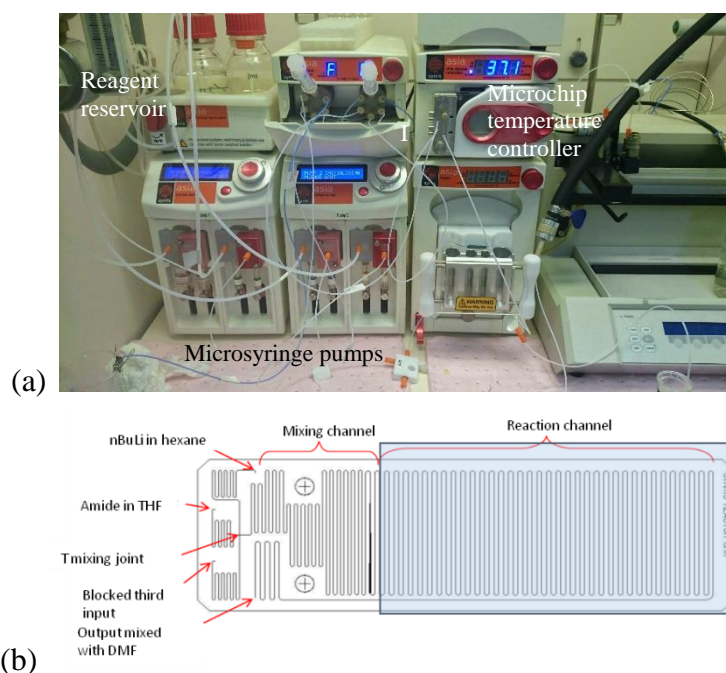
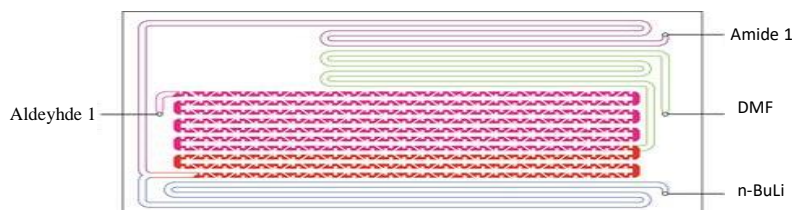


Figure 4-1 (a) Setup of the entire microreactor system; (b) Schematic of glass microchip 1 with two inlets in use

Microchip 2 used in this study is also made of glass but it has a larger nominal cross section area of 1 mm^2 . The point of contact between the *n*-BuLi and the 4-chloro-*N,N*-diisopropylbenzamide is similar to a Y-junction. The walls of the glass microchip were lined with static elements (step and rotating), after the Y-junction. As seen in Figure 4-2, the 4-chloro-*N,N*-diisopropylbenzamide and the *n*-BuLi were mixed together in the initial section of the channel labelled in red which occupied $300 \mu\text{L}$. Subsequently, DMF was added via the third inlet and quenched the reaction along the purple channel which occupied $700 \mu\text{L}$. Microchip 2 was submerged in constant temperature cooling bath. At least 4 samples, at fixed time intervals, were collected to check if steady-state has been reached during each sample collection.

Figure 4-2 Schematic of glass microchip 2 with three inlets



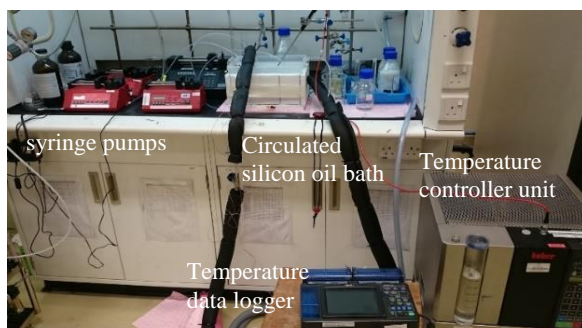
The preparation steps for all flow reactors were similar. 0.4 M of amide 1 solution was prepared by dissolving amide 1 (24 g) in THF (230 mL) using a 250 mL volumetric flask. About 120 mL of the amide 1 solution, 40 mL of *n*-BuLi in hexanes (1.6M) and 10 mL of DMF were drawn using syringes (HSW syringes) and loaded onto syringe pumps (NE 1010 dual, NE 1000, NE300 respectively). The chip reactor was flushed and filled with anhydrous THF for at least 10 min before experiments to ensure anhydrous environment. The output of the reactor was

collected in fixed time intervals of about every 30 s for up to 5 min. All collected samples were analysed and unsteady-state sample data were excluded (e.g. increasing/decreasing trend in the initial/final sample data). From experience, the unsteady-state condition usually occurred in the first 30 s and last 30 s of each run. However, due to limited volume of the syringe, the flow reactors could only be operated for a short time (about 5 min). Samples were taken at different time intervals to ensure steady state has been reached.

4.3.2 *Stainless Steel Reactor*

The stainless steel reactor was assembled in house from commercially available stainless steel tubing (1.75 mm i.d., 3.17 mm o.d.) and the tubing was fitted with Hy-Lok stainless steel nuts and ferrules and connect to the Hy-Lok union Tee fitting (CTA-2-S316, 2.28 mm i.d., 3.17 mm o.d.). The T-reactor setup, included three precooling coils of 1 m each (for amide 1 in THF, n-BuLi in hexanes and DMF streams) and the reactor tubing, R1, ranged from 0.26 to 5.55 m. The n-BuLi in hexanes and the amide 1 in THF streams were pumped into the first T-mixer from opposite directions and the DMF stream merged with the reaction mixture in the second T-mixer. Other than the syringe pumps and the outlet tubing, the stainless steel reactor was immersed in a circulated silicone oil bath using Huber temperature control unit. The flow diagram is depicted in Figure 4-3.

(a)



(b)



Figure 4-3 (a) Setup of the stainless steel reactor; (b) Reagents delivered into stainless steel reactor via syringe pumps, submerged in circulated silicone oil bath.

4.3.3 *PTFE T-reactor*

The T-reactor was assembled in house from commercially available PTFE tubing (Sigma Aldrich, 1.6 mm I.D.) and connected to of two PTFE T-mixers (Upchurch Scientific P-713, 1.25 mm i.d., 17.5 μ L swept volume) as shown in Figure 4-4. The T-reactor setup, included a reactor tubing, R1, ranged from 0.06 to 2 m. The n-BuLi in hexanes and the amide 1 in THF streams were pumped into the first T-mixer from opposite directions and the DMF stream

merged with the reaction mixture in the second T-mixer. Other than the syringe pumps and the outlet tubing, the T-reactor was immersed in a circulated silicone oil bath using Huber temperature control unit.

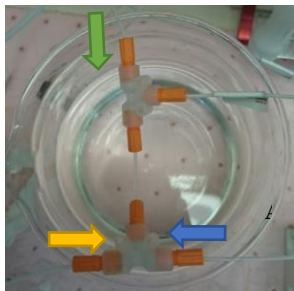


Figure 4-4 PTFE T-reactor setup

4.3.4 *Spinning Disc Reactor (SDR)*

For the SDR, the stainless-steel disc of 10 cm in diameter was driven by an electric motor which operates in the range of 400-2,400 rpm. The SDR was tightly enclosed and purged with nitrogen prior to the experiment and kept at positive nitrogen gas pressure throughout the experiment. Cooling water was recirculated underneath the disk surface through a temperature-controlled water bath to keep the disc temperature constant. The three reagents were delivered via syringe pumps onto the rotating disk through three feed pipes. The two center feed pipes delivering amide 1 in THF and n-BuLi in hexanes were located at the center of the disc. The third feed pipe delivering DMF was located at a radial distance of 45 mm from the centre of the disc. All the feed pipes were fixed at a distance of 5.0 mm above the surface. The feed tube diameter was approximately 1.6 mm for the starting material stream and 1.0 mm for the n-BuLi in hexanes and DMF streams where the flow rates were slower. The reactor diagram is depicted in Figure 4-5.

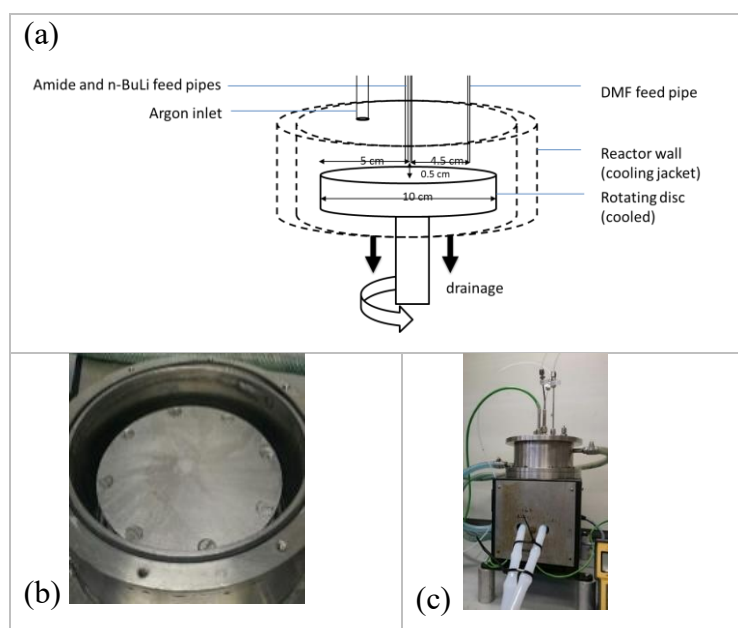


Figure 4-5 (a) Schematic of the SDR (10 cm diameter) set-up; (b) view of disc surface; (c) picture of the set-up.

Details on analytical methods, n-BuLi titration and stability of aldehyde 1 are presented in Appendix B.2.

4.4 Feasibility Study of Flow Process

4.4.1 Microreactors (*Microchip 1 and 2*) Results and Discussions

The main objective of the feasibility study was to ensure no clogging occurs during the flow process and reasonably good reaction yield could be obtained at higher temperature under similar reagent concentrations as the batch system.

Unfortunately, the initial trial with microreactor using Microchip 1 (nominal cross section area 0.2 mm^2) resulted in blockages as seen in Figure 4-6. The possible reasons for this could be the formation of solids due to moisture in feed streams, impurities, formation of salt, solid formation in the hot spots or polymerization. Attempts to avoid moisture was made by drying the reagents and using anhydrous solvents but still, the formation of solids could not be totally eliminated.

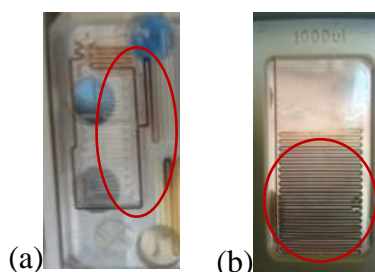


Figure 4-6 Microchip 1 – (a) Clogging in premixing region; (b) clogging in entire microchip

Microchip 1 was replaced by Microchip 2 (1 mm^2) which has a channel cross sectional area five times larger than Microchip 1 and equipped with static elements. The intention was to

provide large enough passage space for fine solids to pass through. This method worked well for a short period of time before pressure started to build up as particle accumulation was observed in Figure 4-7 in the channel. It was speculated that the solid particles were trapped between the narrow gaps of the static elements.

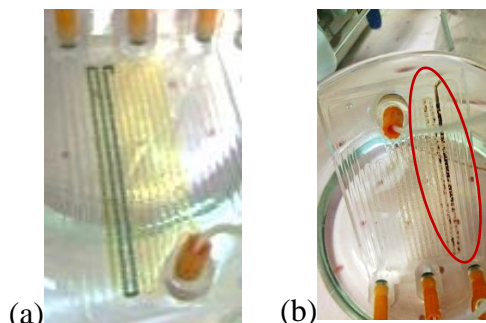


Figure 4-7 (a) Smooth run; (b) particle accumulation in Microchip 2 channel

Although the Microchip 2 setup faced issues with clogging, the result appears promising (Table 4-1), obtaining aldehyde 1 yield of 90% at the highest step 1 combined flow rate. Despite a shorter step 1 residence time, the high flow rate provided better mixing performance. The result indicated that the reaction was most likely a mixing controlled.

Table 4-1 Microchip 2 result at 20 °C

Run	Step 1 combined flow rate (mLs ⁻¹)	Step residence time (s)	Re	Aldehyde 1 yield (%)	Overall conversion (%)	Impurity* (%)
1	0.002	144	4	55	99	44
2	0.01	28	20	67	99	32
3	0.06	5	108	76	99	23
4	0.1	3	187	83	99	16
5	0.15	2	284	90	99	9

(*) % impurity = % overall conversion - % aldehyde 1 yield

4.4.2 Stainless Steel Reactor Results and Discussions

Based on the experience working with Microchips 1 and 2, it was gathered that increasing the channel size and avoiding the use of static elements might reduce the extent of clogging. Therefore, a stainless steel reactor setup (Figure 4-8) consisting of even larger dimensioned stainless steel bare tubing (R1, i.d.=1.75 mm) and Tee-mixer (i.d.=2.28 mm) was assembled. The use of stainless steel was intended to improve the heat transfer capability of the reactor given its lower surface area to volume ratio as compared to the microchips.

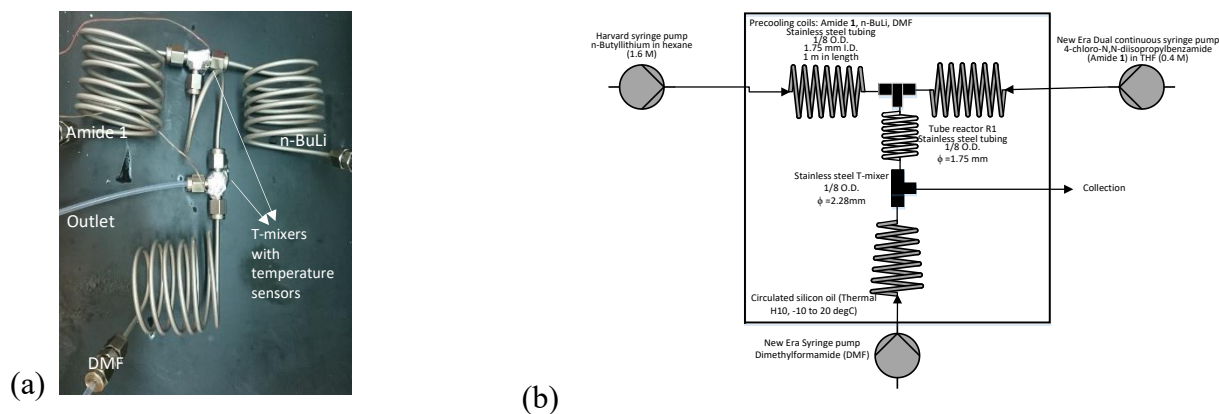


Figure 4-8 (a) Stainless steel reactor setup; (b) Schematic of stainless steel reactor setup

The flow experiments showed that the stainless steel reactor flow experiments did not cause any clogging issues. This was because the fine solids were able to flow through the relatively large reactor channel smoothly. However, for similar step 1 combined flow rates, the stainless steel reactor (Table 4-2) obtained in poorer yield compared to Microchip 2. This could be due to the less efficient mixing and temperature control in the large reactor channel.

The reactor surface temperature profiles of Run 1 and 7 (Table 4-2) are shown in Figure 4-9. The R1 surface temperature difference between the two flow rates was almost 10 °C. The surface temperature of inlet R1 was observed to be higher than that of T-mixer in both flow rates. This might be because the T-mixer wall was thicker and more insulated than R1 (bare tubing) wall. It is interesting to observe that although the reaction temperature was higher than 30 °C in Run 7, the corresponding aldehyde 1 yield was still the highest. This finding seemed to contradict the general statements found in the literature that ortho-lithiation reaction requires accurate control of the inner temperature to stabilize the intermediate.

Table 4-2 Effect of flow rate at constant residence time and temperature for stainless steel reactor

Run	Step 1 combined flow rate (mL s ⁻¹)	Residence time (s)	R1 length (m)	Re	Aldehyde 1 yield (%)	Overall conversion (%)	Impurity* (%)
1	0.12	11	0.6	133	26	42	16
2	0.14	11	0.65	145	28	46	18
3	0.16	11	0.75	169	63	93	30
4	0.18	11	0.85	193	77	97	20
5	0.23	11	1.05	242	79	99	20
6	0.54	11	2.55	580	81	97	16
7	1.18	11	5.55	1263	82	99	17

(*) % impurity = % overall conversion - % aldehyde 1 yield

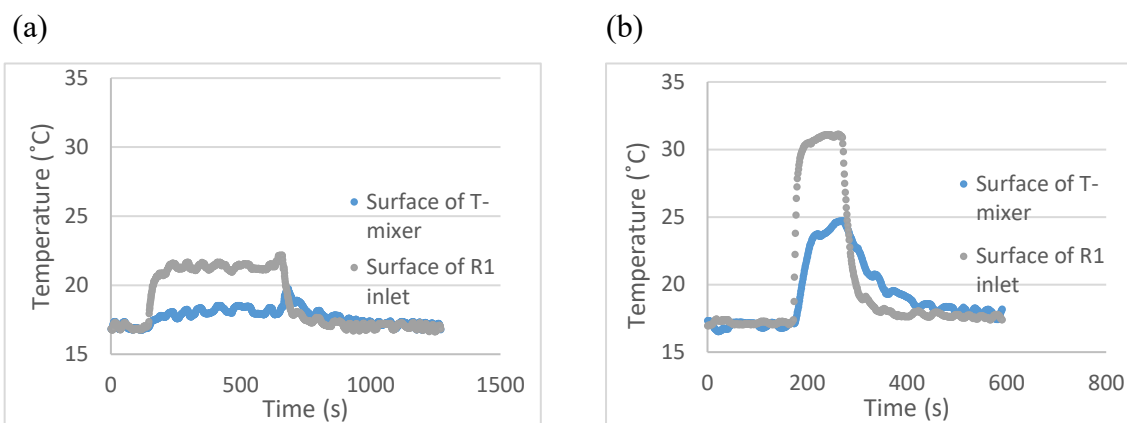


Figure 4-9 Temperature profile on the surface of the T-mixer and surface of inlet of R1 tube for (a) 0.12 mL/s and (b) 1.18 mL/s respectively (Bath temperature was at 17 °C)

Another approach was taken to study the temperature sensitivity of the reaction. The reaction profiles at different bath temperatures were studied using the stainless steel reactor. As shown in Table 4-3, the reaction proved to be robust over a range of about 50 °C as the reaction yield decreased only slightly from 92% to 85% as the bath temperature increased from -20 °C to 35 °C.

Table 4-3 Reaction profile at different temperatures

Run	Bath temperature (°C)	Tres (s)	Flow rate in first T-joint (mL/s)	Flow rate in second T-joint (mL/s)	Aldehyde 1 yield (%)	Overall conversion (%)	Impurity* (%)
1	-20	0.5	1.22	1.27	92	99	7
2	0	0.5	1.22	1.27	91	99	8
3	17	0.5	1.22	1.27	89	99	10
4	35	0.5	1.22	1.27	85	97	12

(*) % impurity = % overall conversion - % aldehyde 1 yield

This result is consistent with the finding in Figure 4-9 and this is referred to as Flash Chemistry (Yoshida *et al.*, 2008) where reaction time is usually less than a second, given highly efficient mixing on a time scale with similar order of magnitude or even shorter. For this type of condition, the mixing efficiency is more important than temperature control as the residence times are very short and the time taken for decomposition of the intermediate is less of a concern. Due to the short residence times, even high reaction temperatures, e.g. 30 °C, could be tolerated. The reaction yields obtained in continuous reactor are significantly more superior to the yields obtained in stirred tank reactor. This is because of the poor mixing and residence time control in the semi-batch stirred tank reactor, where the high reactive n-BuLi was rapidly consumed in side reactions or over reaction, accounting for the low conversion and yield.

Based on these experiments and experiences during the feasibility study, the following could be concluded:

- 1) The problem of clogging could be avoided by using larger dimension channel as long as the fine solids were able to flow freely through.
- 2) The reaction in flow (~90% at 20 °C) is superior to batch (3% at 20 °C) as the formation of side products was greatly minimized.
- 3) Mixing efficiency was more important than temperature control given short residence time. Poor mixing performance resulted in low overall conversion due to decomposition of n-BuLi and formation of impurities.
- 4) Both step 1 and step 2 were mixing sensitive. Step 1 reaction time to achieve 99% overall conversion was estimated to be 2.6×10^{-6} s.

4.5 Development of T-reactor (PTFE) Flow Process

From the stainless steel reactor experiments, it was found that the reaction in flow was not very sensitive to temperature, high reaction temperatures, for example close to adiabatic temperature could even be used, as long as the stability of intermediates and aldehyde 1 at the maximum internal temperature (MISR) were ensured. The thermal stabilities of aldehyde 1 and amide 1 up till 300 °C are determined using differential scanning calorimetry (DSC) (Appendix B.3). Although there was no secondary decomposition observed, it was difficult to conduct thermal stability test on the reaction intermediate as it was unstable and decompose instantaneously in air. It was important to determine the possibility to perform the reaction at adiabatic conditions (or worst case scenario). The reason for this is so that simple and inexpensive PTFE tubing and Tee-mixers could be used instead of the stainless steel reactor which was less flexible and more costly, since better heat transfer property was not much of an advantage in this case.

Commercially available PTFE T-mixers (i.d.= 1.25 mm) were used and joined together with PTFE tubing (i.d.= 1.6 mm) where its length could be adjusted to provide desired residence times. The final reactor setup for the two step ortho-lithiation reaction is depicted in Figure 4-4. The feeds enter the T-mixers from opposing direction and the combined stream exited in a 90° angle for both step 1 and step 2.

4.5.1 Effect of DMF Addition Mode

The addition mode/mixing of DMF in step 2 played an important part on determining the overall aldehyde 1 yield and overall conversion. It is evident from Table 4-4 that the DMF flow rate could influence the aldehyde 1 yield. Beyond a ‘minimum’ DMF quantity, the mixing limitation in step 2 diminished and reaction profile depended solely on the flow conditions in step 1. However, the ‘minimum’ DMF quantity was likely to be a variable which was dependent on step 1 flow rate.

Table 4-4 Experiments using different quantities of DMF carried out under constant step 1 residence time of 0.4 s and bath temperature set at 17 °C

Run	DMF flow rate (mL/s)	DMF mole eqv to amide 1	Step 1 combined flow rate (mL/s)	Step 2 combined flow rate (mL/s)	Aldehyde 1 yield (%)	Overall conversion (%)	Impurity (%)
1	0.01	1.3	0.65	0.66	74	97	23
2	0.02	1.7	0.65	0.67	90	99	9
3	0.03	2	0.65	0.68	92	99	7
4	0.05	4	0.65	0.70	91	99	8
5	0.08	6	0.65	0.73	90	99	9
6	DMF reservoir	~ Infinity	0.65	NA	91	99	8

(*) % impurity = % overall conversion - % aldehyde 1 yield

For simplicity of scale-up and material efficiency, DMF of 2 mole equivalent with respect to amide 1 was used in all flow experiments. For T-reactor, the same mixing principles in step 1 could be applied to step 2 as the reaction mixture met ‘head on’ with the DMF feed in the second T-mixer. The speeds of the feeds in the second T-mixer mixing channel were dependent on the combined flow speed in the first T-mixer. Thus, it was expected that mixing time in the second T-mixer is of similar order of magnitude as the first T-mixer. Therefore, good mixing performance in the first T-mixer was likely to improve mixing in the second T-mixer and vice versus. It was also noted that poor reaction performance could be a result of poor mixing contributed by both steps.

4.5.2 Effect of Bath Temperature in step 1

Attempts were made to change the reaction temperature of T-reactor by adjusting the bath temperature. Figure 4-10 shows that the reaction seemed robust over a range of bath temperature from 0 °C to 40 °C. Assuming that the system was adiabatic as PTFE is a good insulator, the temperature rise was expected to be more than 50 °C and yet there was no significant deterioration in aldehyde 1 formation observed in Figure 4-10. The poor heat transfer capability of the T-reactor may be compensated by improving the mixing performance and

shortening the residence time. The circulated silicon bath temperature was maintained at 17 °C for subsequent experiments.

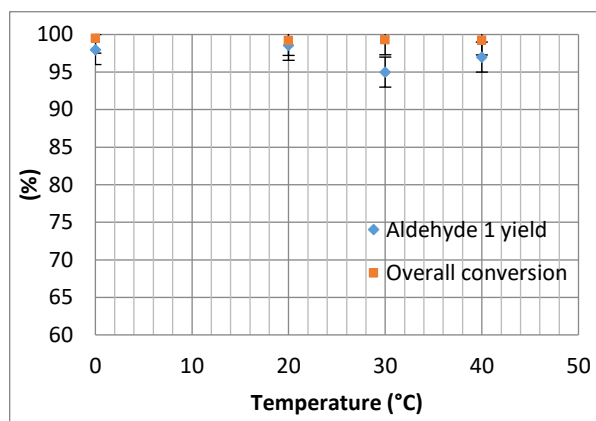


Figure 4-10 Effect of circulation bath temperature on step 1 under constant residence time (0.4 s) and combined flow speed.

4.5.3 Effect of Residence Time in Step 1

Figure 4-11 shows the effect of residence time for two different flow speeds and it was demonstrated that shorter step 1 residence time improved aldehyde 1 yield. The longer than desired residence time could result in poorer yield due to prolonged exposure to high temperature which might cause decomposition of intermediate or overreaction.

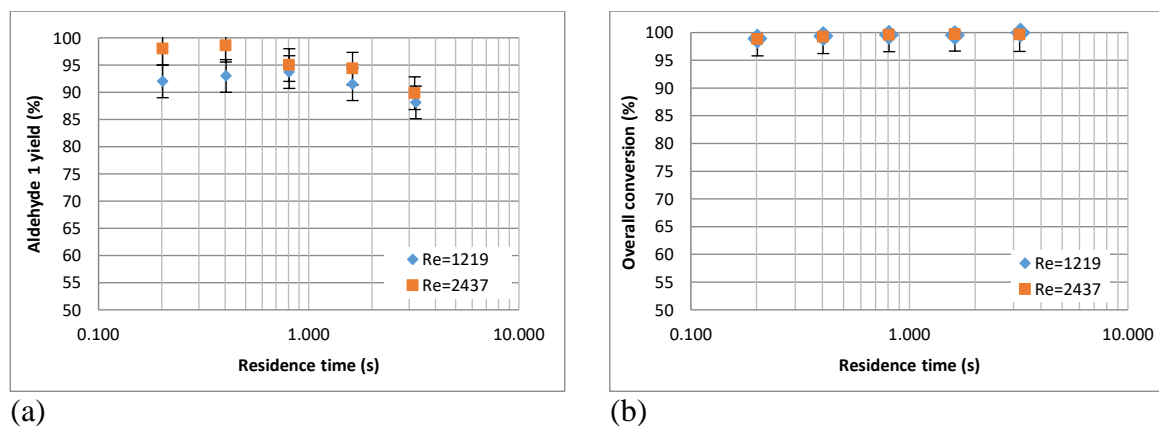


Figure 4-11 (a) Aldehyde 1 yield; (b) Overall conversion against residence time (Step 1) using T-reactor for different Re numbers of 1219 and 2437

One observation made from Figure 4-11 (a) was that the gap in aldehyde 1 yield between Re of 1219 and 2437 appeared more significant at shorter residence times. One possible reason could be the effect of mixing limitation was more prominent at low flow speed (Re=1219) and short residence times (below 0.8 s). As the residence time increased for Re of 1219, there was a subtle improvement in aldehyde 1 yield as there was more time available for mixing to occur until over-reaction kicked in as characterized by the drop in yield. Therefore, the optimum residence time was very much mixing dependent.

4.5.4 CFD Simulation of Mixing in T-mixer

To achieve realistic simulations, the dimensions of the T-mixer chosen were as close to the actual dimension of the T-mixer used as possible. The geometrical setup of the channel structure in the T-mixer with circular cross sections is displayed in Figure 4-12. The reactor geometry consisted of a mixing channel with a length of 6 mm and uniform diameter of 1.25 mm. Each inlet channel is 4.75 mm long with the same diameter as the mixing channel. The focus was on the mixing within the T-mixer and in order to avoid perturbations of the flow behavior due to the outflow conditions, the outlet of the T-mixer was connected to a PTFE tube with diameter of 1.6 mm which was similar to the actual experimental case.

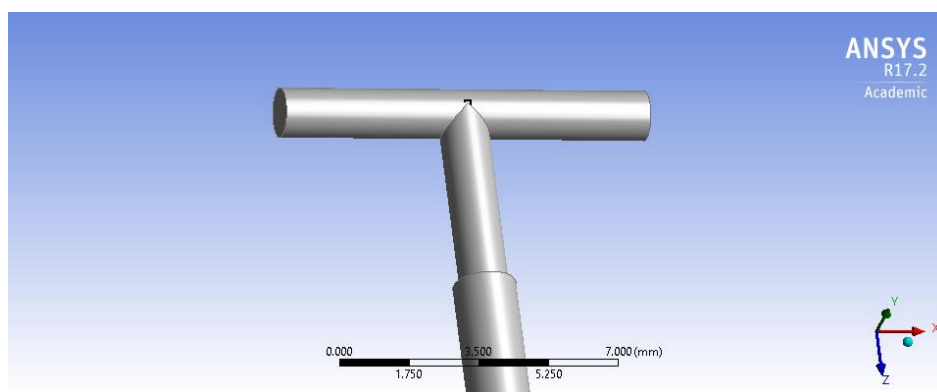


Figure 4-12 Schematic picture of T-mixer used in step 1 in T-reactor

For the inlet velocity profile, a fully developed duct flow was used. At outlet, the pressure was set to atmospheric pressure. No slip boundary condition at the side walls was applied. The numerical simulations were performed with the CFD software FLUENT 17.2 (Ansys Academic). The simulations were performed with approximately 60,000 elements. THF and hexane at 20 °C were simulated to mix in the T-mixer. THF was specified to enter the T-mixer from the right inlet and hexane on the left inlet. Three different scenarios were simulated and summarized in the Table 4-5.

Table 4-5 Simulated flow conditions in T-reactor using three different flow speeds

Scenario	Velocity at right inlet (m/s) in x-direction	Velocity at left inlet (m/s) in x-direction	Re in mixing channel of T-mixer	Model
1	0.002	-0.0006	6	Laminar
2	0.1	-0.03	305	Laminar
3	0.81	-0.24	2437	Laminar

In the experimental study the lowest Re used was about 305, corresponding to the simulation in Figure 4-13 (Scenario 2) where the two feed streams swap to the opposite sides. This is known as the secondary flow which is first defined by Prandtl (Prandtl and Deans, 1953)

as the result of centrifugal force when fluid flows in a curved path. This results in cross flow which is good for mixing as it creates a larger area of contact between the two liquids for mixing. This observation is similar to that seen by Kockmann, Engler, Wong and co-workers in T-mixers using similar Re, which they described as engulfment flow, characterized by distinct rapid increase of mixing quality with Re (Engler *et al.*, 2004; Wong *et al.*, 2004; Kockmann *et al.*, 2006).

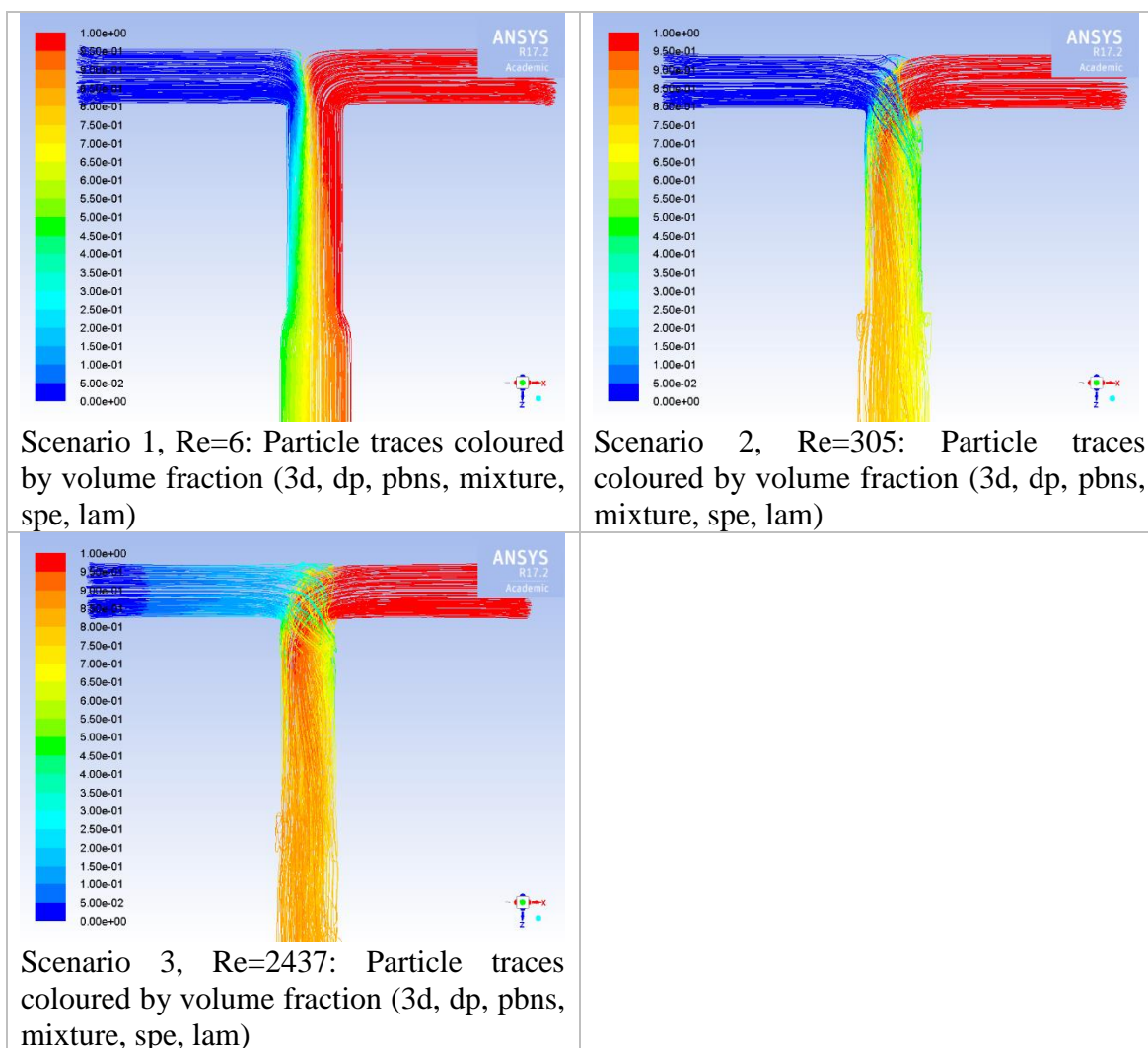


Figure 4-13 Simulation result of scenarios 1 to 3 showing particle traces and contour plots of volume fraction. (Red: THF stream; Blue: Hexane stream)

Even though all the runs are likely to be operating in the engulfment flow regime, the mixing performance is still dependent on Re as seen in Figure 4-14. At low Re where the two feeds are not efficiently mixed, the n-BuLi may get consumed by reacting unselectively with THF and DMF that are present in abundance. This leaves the bulk of amide 1 unreacted which accounts for the low overall conversion in Figure 4-14 (b).

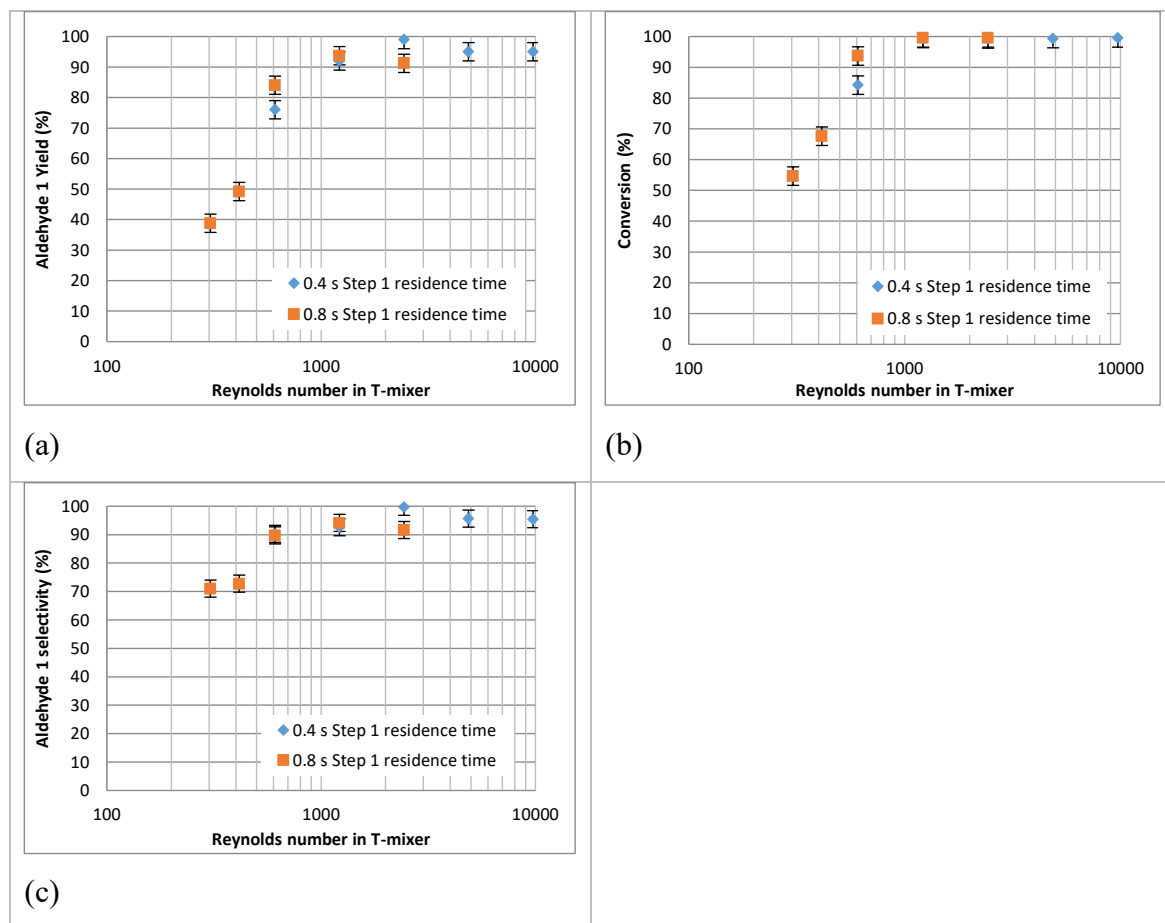


Figure 4-14 (a) Aldehyde 1 yield; (b) overall conversion; (c) Aldehyde 1 selectivity against Re (Step 1) using T-reactor under constant residence times of 0.4 s and 0.8 s

Comparing the simulated flow patterns between Re of 305 and 6, a large contrast in mixing can be seen in Figure 4-13 (Scenario 1) at very low Re where there was a distinct boundary between the blue (hexane) and red (THF) streams when they came together at the T-mixer. This indicates no extensive mixing, except for diffusion, at the low flow speed as the streams flow in a laminar mode at low Re. It is expected that none of the runs in Figure 4-14 falls into this flow pattern.

As the Re increased beyond 2400, aldehyde 1 yield reached a plateau or is slightly decreased (Figure 4-14 (a)). One possible reason could be the back-mixing effect in the n-BuLi/hexane feed arm as seen in Figure 4-13 (Scenario 3), as it caused small quantity of amide 1/THF to travel into n-BuLi feed arm where the n-BuLi localized concentration is high and tend to encourage side reactions. This might account for the lower aldehyde 1 yield observed in Figure 4-14 (a) at Re above 4800. Similar observation is made by Kockmann and co-workers (Kockmann *et al.*, 2006) where the segregation index is increased for higher Re. Another possible explanation put forward by Kockmann and co-workers is the formation of transient, fluctuating vortices, at the entrance of the feed inlets at higher flow speed, which transport unmixed feed through the mixing chamber.

4.6 Development of Spinning Disc Reactor (SDR) Flow Process

4.6.1 Mode of DMF Addition

The DMF feed was added close to the edge of the disc (4.5 cm radial distance away from the center of the disc) where the mixing performance should be better compared to other parts of the disc. While the residence time of step 2 on the disc was expected to be even shorter than step 1 as it had only a radial distance of 5 cm to mix and react, the step 2 reaction was expected to be faster than step 1 (Kockmann et al., 2011). Thereafter, the reaction mixture was flown off the disc and splashed onto the wall which was, in fact, a form of mixing as well. Theoretically, SDR offered relatively better mixing for step 2 reaction than step 1 provided that the DMF feed contacted the disc as a continuously stream rather than dropwise. Therefore, Step 1 was deemed as ‘bottleneck’ in term of mixing performance and it was also the step that aldehyde 1 yield and overall conversion were most dependent upon. Through visual observation, a minimum flow rate of 2 mole equivalent (0.06 mL/s) of DMF was required for the lowest Step 1 combined flow rate of 1.3 mL/s was needed to ensure a continuous stream of DMF from the feed pipe.

4.6.2 Position of *n*-BuLi Feed

Theoretically, the mixing of the amide 1 and *n*-BuLi feeds could be improved by moving one of the feed (e.g. *n*-BuLi) away from the center of the disc, where the mixing was poor, to a higher radial position where the film thickness is smaller (Jacobsen and Hinrichsen, 2012). However, the result obtained for *n*-BuLi feed placed 2.5 cm from center of the disc were worse than position at center of disc (Table 4-6). The poorer overall conversion could be explained by the reduction in residence time as the *n*-BuLi feed moves 2.5 cm closer to the edge of the disc.

Table 4-6 Effect of position of *n*-BuLi feed on reaction profile

Position of <i>n</i> -BuLi feed	Flow rate (mL/s)	Disc speed (rpm)	Aldehyde 1 yield (%)	Overall conversion (%)	Impurity* (%)
Center of disc	1.3	1400	87	97	10
2.5 cm away from center of the disc	1.3	1400	66	90	24

(*) % impurity = % overall conversion - % product 1 yield

4.6.3 Effect of SDR Coolant Temperature

The coolant temperature dictates the disc surface temperature in the SDR. Figure 4-15 shows that aldehyde 1 yield was only marginally affected by the coolant temperature. Similar explanation as in the T-reactor could be applied where the effect of temperature was limited by the short contact time between the reagents and the disc. Although compared to the T-reactor, the SDR was expected to have a better heat transfer capability where the coolant was supplied directly beneath the metal rotating disc which had a relatively large surface area for heat transfer; the SDR had even shorter residence time and thus shorter exposure time to the higher surface temperature than the T-reactor.

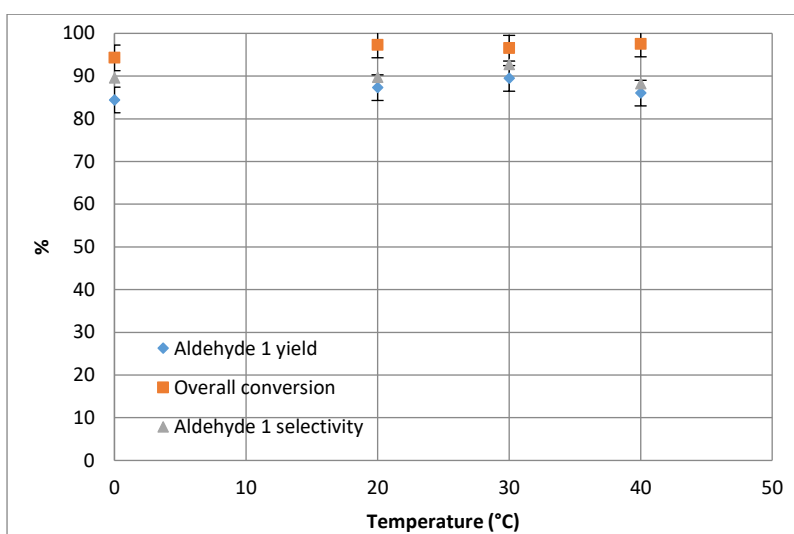


Figure 4-15 Effect of circulated bath temperature under constant residence time (0.4 s), total flow rate (1.2 mL/s) and disc speed (1,400 rpm).

4.6.4 Effect of Total Flow Rate

Figure 4-16 shows a steady decrease in aldehyde 1 yield and overall conversion with the increase in flow rate from 1.2 to 5 mL/s at a disc speed of 1400 rpm.

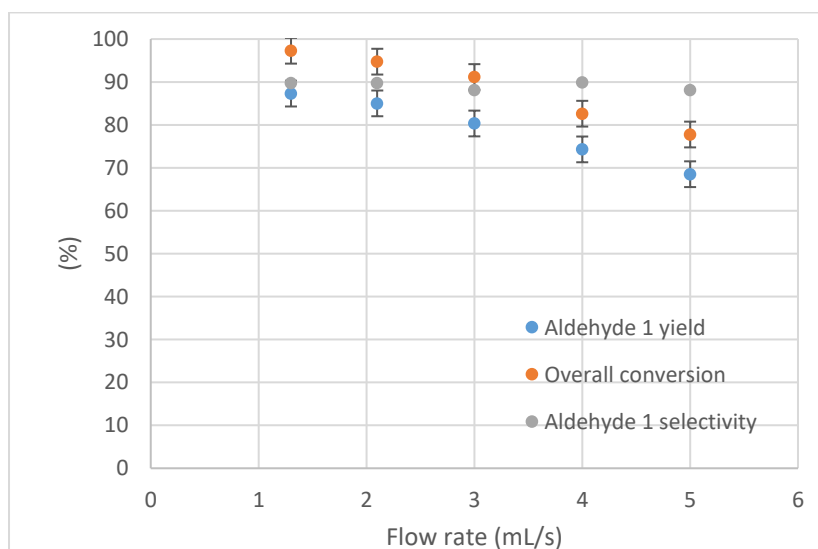


Figure 4-16 Effect of total flow rate (step 1) under constant disc speed of 1400 rpm.

Under the same disc speed, Figure 4-17 shows the corresponding residence time (Eqs. 2-1) (Boodhoo and Al-Hengari, 2012) for the flow rates in Figure 4-16 at 1,400 rpm. The residence time decreased with increasing flow rates, from 0.15 s at lowest flow rate to 0.05 s at the highest flow rate. It is known that ortho-lithiation reaction time is very fast especially at high temperature, so the reaction is most likely mixing limited in this regime. The micromixing time reported by Hinrichsen (Jacobsen and Hinrichsen, 2012) using similar operating conditions and disc size, is in the range of 0.125 to 0.02 s. If a conservative estimate of 0.125 s was taken to be the average micromixing time regardless of flow rate and disc speed, Figure 4-17 shows that for disc speed of 1,400 rpm and flow rates above 1.2 mL/s, the corresponding residence times could be shorter than the micromixing time (represented by the dotted line). This suggested that the mixing controlled reaction might be indirectly limited by the short residence time. Therefore, the longer residence time benefits the mixing as it allows more time for molecular contact. This trend was similarly observed in the T-reactor with low flow rates.

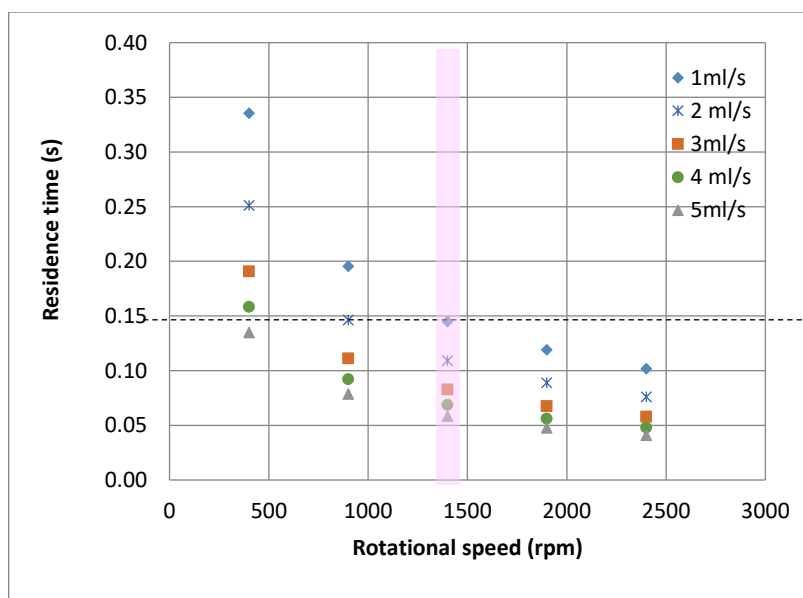


Figure 4-17 Estimated residence time (Boodhoo and Al-Hengari, 2012) of Step 1 on the disc at different flow rates and disc speeds. Data within the pink area represents the corresponding residence times at 1400 rpm

Although the SDR residence time could be extended by reducing the disc speed, the mixing intensity might be compromised even further. Compared to the T-reactor which offered residence times of 0.2 to 3 s, the estimated range of residence time of 0.05 to 0.15 s used in the existing SDR was much shorter. The shorter residence time on the SDR was more likely to minimize over-reaction at the expense, however, of insufficient mixing.

4.6.5 Effect of Disc Speed

Attempts were made to improve the mixing and thus, the reaction dependency on residence time. From Figure 4-18 and Figure 4-19, it could be inferred that aldehyde 1 yield

and overall conversion were inversely proportional to the film thickness for flow rates at 3 and 5 mL/s. In the lower disc speed range, typically between 400 and 1400 rpm, the film thickness decreased considerably and the corresponding yield increases significantly. Beyond 1,400 rpm, there was only a marginal decrease in film thickness from about 30 to 20 μm which was accompanied by a minimal increase in yield. This seemingly direct correlation between film thickness decrease and yield increase highlighted more rapid mixing and mass transfer taking place across the reduced path length of thinner films.

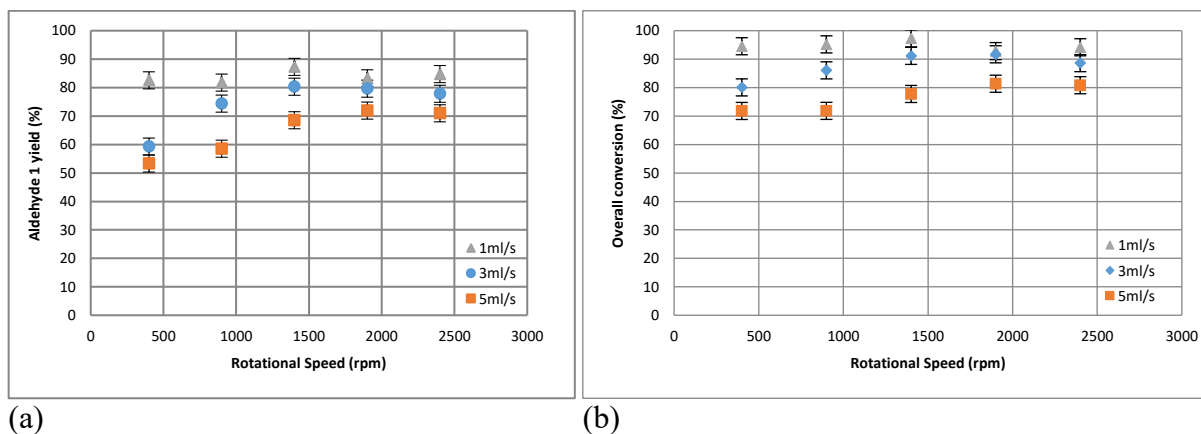


Figure 4-18 (a) Aldehyde 1 yield; (b) overall conversion against disc speeds of 400 to 2400 rpm at different flow rates

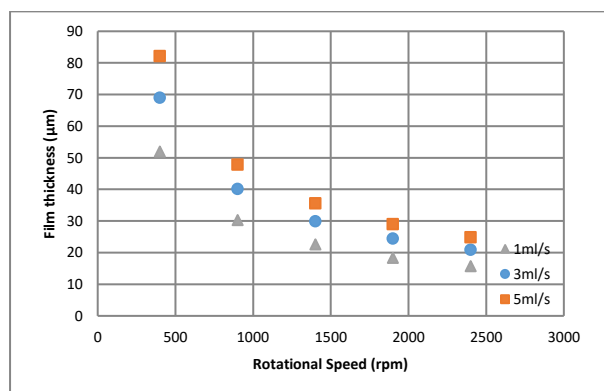


Figure 4-19 Estimated film thickness (Boodhoo, 2013) at different disc speed at constant total flow rates.

The film thickness depended on disc speed and flow rate as seen in Figure 4-19 is described in Eqs. (2-2). The convergence of the film thickness profiles at high disc speeds in Figure 4-19 also matched aldehyde 1 yield trends seen in Figure 4-18 (a), suggesting that the limit of highest mixing/mass transfer had been reached for the process under consideration. Similar convergence profiles were observed at high disc speeds in micromixing studies conducted in the SDR (Boodhoo and Al-Hengari, 2012). This observation is in agreement with the findings made by Jacobsen and Hinrichsen (2012) that the micromixing segregation index is directly correlated to the calculated film thickness.

4.6.6 Visual Observations

Besides considerations to change reagent concentrations, some observations were made during the experiments. During SDR experiments, a thin film of white precipitate tended to form on the surface of the disc and walls where there were still traces of moisture present but once the moisture was consumed by n-BuLi, there was minimum accumulation of precipitate in the subsequent reaction as seen in Figure 4-20. Therefore, the advantages of the SDR include less fouling and the formation of the precipitate is not disruptive to the reaction and cleaning of the disc surface is relatively easy.

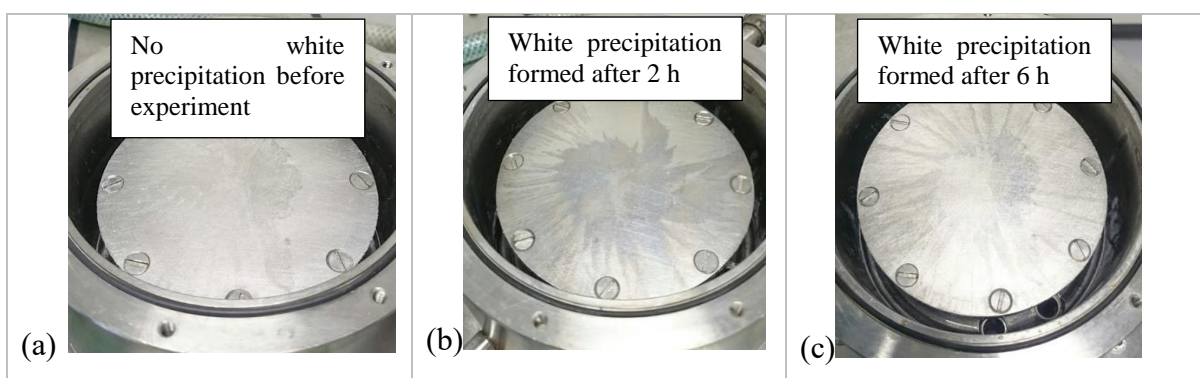


Figure 4-20 (a) SDR disc before experiment; (b) SDR after 2 hours of usage; (c) SDR disc after 6 hours of usage

Attempts to use higher initial amide 1 concentration were made in both T-reactor and SDR, with the intent to reduce the amount of THF used. Unfortunately, the yields in both flow reactors dropped drastically when higher concentrations were used (Figure 4-21) so the decision is to keep to the current amide 1 concentration of 0.4 M in THF.

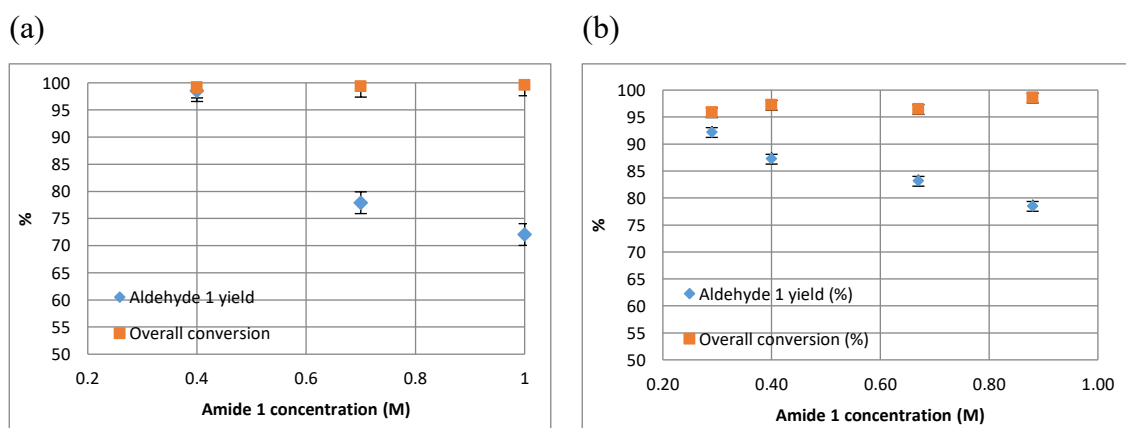


Figure 4-21 (a) T-reactor under constant residence time (0.4 s) and total flow rate (1.3 mL/s); (b) SDR under constant total flow rate (1.2 mL/s) and disc speed (1,400 rpm). (Circulated bath at 17 °C)

At higher amide 1 concentrations (e.g. 0.7 M and above), the reaction selectivity in the T-reactor was worse than in the SDR. It may be due to the better heat transfer capability in SDR

which was enhanced at higher temperature where the temperature difference between the reaction and disc surface was sufficiently large. Although higher aldehyde 1 yield could be achieved in the SDR using lower concentration of 0.3 M and below, this would compromise the throughput based on the current operating condition.

4.7 Summary

The feasibility of performing the ortho-lithiation reaction in the T-reactors and the SDR at ambient temperature was demonstrated. The conventional method was to operate the reaction at -70 °C in a fed-batch mode which was challenging to scale up. A continuous flow PI reactor – T-reactor is developed and obtained a highest aldehyde 1 yield of 99% at ambient temperature by providing short residence time (flash chemistry concept) and efficient mixing (CFD simulation).

The early feasibility study using the microreactors (chips 1 and 2) demonstrated constraints like clogging of the narrow channel and non-adjustable channel length which resulted in inflexible residence time given a fixed flow rate. To overcome these limitations, a stainless steel reactor was assembled in-house which provided sufficiently large channel size to avoid clogging, flexible reactor length and made of good heat transfer material. Unfortunately, the large channel size resulted in poor mixing, hence the relative low aldehyde 1 yield.

In depth reactor study was performed on the two most promising PI reactors – the T-reactor and the SDR. Although the T-reactor obtained higher aldehyde 1 yield than the SDR, further optimization of the SDR operating conditions was expected to offer distinct potentials of improvement in the aldehyde 1 yield to a level similar to the T-reactor. More importantly, the free surface film characteristics of the SDR, in contrast to the fully enclosed volume of the T-reactor, could render the SDR more advantageous if other processing capabilities were desirable- for example, handling a reaction with solid formation or requiring rapid heat removal through evaporation or formation and removal of gas that the T-reactor cannot do.

The experimental operating conditions of the best runs of the STR, the T-reactor and the SDR are summarized in

Table 4-7. The STR experimental results and discussions is presented in Appendix B.4. The experience gained from these experiments should provide adequate basis to illustrate the critical differences in performance that would be expected between batch and flow processes at industrial scale.

Table 4-7 presents the operating conditions that would be used in the batch and flow process designs for the comparison of their sustainability performance which is investigated in Chapter 5.

Table 4-7 Highest yield obtained in the different reactors and their respective operating conditions

	STR	T-reactor	SDR
Mode of operation	Batch/semi-batch	Flow	Flow
Coolant temperature (°C)	-80 °C	17 °C	17 °C
Aldehyde 1 yield (%)	96	99	87
Impurity (%)	4	<1	10
Step 1 combined flow rate (mL/s)	-	1.2	1.2
Residence time (s)	Mins (depends on dosing rate)	~0.4 s	~0.14 s
BuLi mol eqv	1.2	1.2	1.2
DMF mol eqv	1.3	2	2

Chapter 5. Ortho-lithiation Process – Part 2: Assessment of Sustainability Benefits for Reaction

As a continuation from Chapter 4, the objective of this chapter is to evaluate the sustainability benefits of operating ortho-lithiation reaction in different process intensification (PI) reactors as compared to the conventional batch reactor (Teoh *et al.*, 2015). This work focuses on the comparison of the sustainability performance of a batch and two intensive continuous reactors (the T-reactor and the spinning disc reactor) for the reaction step excluding workup at a hypothetical design scale of 3 tons per year. The potential benefits that could be achieved are higher reaction selectivity and material efficiency, lower energy consumption, improved safety and economic savings.

5.1 Design of STR Reaction System for 3 tons per year Production

Having obtained laboratory data for the three process technology options in Table 4-7, the designs for operation at a nominal 3 tons per year scale were generated. For each technology, considerations were made to whether the laboratory data were representative of what could be achieved at the larger scale.

For the batch STR, due to lack of suitable large equipment that can provide a proper cooling system (-80 °C), experiments were unable to perform ortho-lithiation at the designed industrial scale of 28 L. However, it would still be possible to design the STR batch process by making some realistic assumptions based on the laboratory results at 50 mL Multi-max™ scale. It is identified that the reaction was most sensitive to temperature which is directly controlled by the n-BuLi dosing rate. To ensure the cooling capacity of the reactor is sufficient to cope with the n-BuLi dosing rate, a conservative overall heat transfer coefficient value is assumed. In addition, good mixing is required to avoid temperature gradient. The power dissipation of the 50 mL Multi-max™ at its maximum achievable agitation speed is used as a basis for providing sufficient mixing required for the 28 L reactor. The refrigeration method is one of the biggest differences between the laboratory Multimax™ and designed industrial process. The vapor-compression refrigeration system is selected for the large scale cryogenic reactor design which is based on highly idealized model.

A two-stage selected cascade system schematic is shown in Figure 5-1. The refrigeration system consists of two compressor units, two heat exchangers, two throttles and an evaporator is required to achieve a refrigeration temperature of -80 °C. Refrigerants R-32 and R-23 are selected for the cascade cycle to provide maximum thermodynamic efficiency and recycled

after each batch. An ideal cycle model was assumed, taking into account the compressor in the cryogenic reactor is driven by an electric motor with an efficiency of 0.72. The utilities consumed will be mainly for compressor duties, pumping, agitation and chilled water for condensation. In order to achieve similar mixing intensity, the agitation power of the large scale STR is designed to have similar agitation power as the bench scale of 0.053 W/kg.

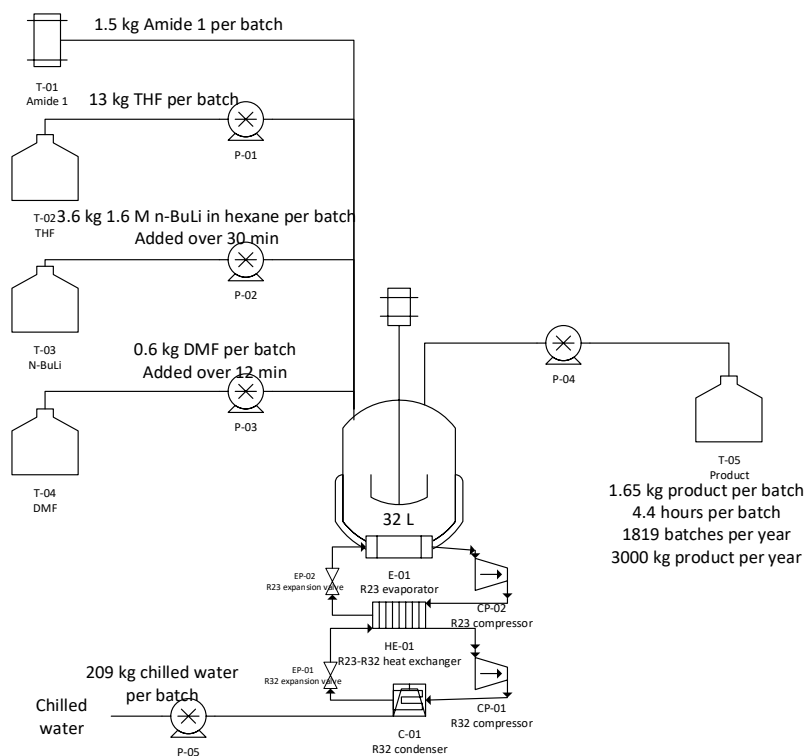


Figure 5-1 Schematic process diagram for batch process

5.2 Design of T-reactor and SDR Reaction Systems for 3 tons per year Production

For both the T-reactor and the SDR flow processes, their process designs would be based on the actual laboratory operating conditions (flow rate, temperature, residence time, etc.) used in their best runs in

Table 4-7 that are able to deliver an annual production of about 3 tons per year. This provides a more realistic operating conditions on the flow reactors, rather than artificially trying to predict the yield at other operating conditions. One point to note is that for all the flow experiments conducted either in the T-reactor or the SDR, the maximum duration of the run is about 5 min due to volume limitation of the syringe pump. However, the large scale design requires the run duration to be extended to 8000 h.

Although there was no clogging in the T-reactor experiments as the runs performed were very short, there could be a possibility of agglomeration of the precipitate (Cafiero *et al.*, 2002b) over time and result in clogging of the mixing chamber. One possible option to get

around this problem is to build in several T-reactors that can be easily switched to another when pressure build up is sensed. The clogged T-reactors can then be disposed and replaced swiftly as the T-mixers and tubes are relatively cheap. In this way, sudden disruption to the process due to clogging and maintenance of the T-reactor can be avoided entirely.

Even though a small amount of lithium salt was observed on the surface of the disc after the experiments, the SDR is clearly less prone to clogging. The SDR maintenance can be scheduled regularly without the worry of sudden severe pressure drop as seen in the T-reactors (Cafiero *et al.*, 2002a). Another operational advantage of the SDR is the variation in rotational speed which offers an additional degree of freedom as the disc speed can be controlled independently of the flow rate to achieve target mixing intensity without affecting the throughput.

One common drawback in the flow processes is the less efficient method to prepare amide 1 solution as additional equipment are required to dissolve amide 1 in THF. The respective reactor setups are shown in Figure 5-2 and Figure 5-3. 32 L of amide 1 solution (0.4 M) will be prepared in a 41 L mixing tank (M-01) in batch mode which will provide 8 hours of amide 1 solution supply for the T-reactor. To ensure continuous supply of amide 1 solution, two mixing tanks are required to alternate between each other when one is consumed. Similarly, two product storage tanks (T-05) will be required.

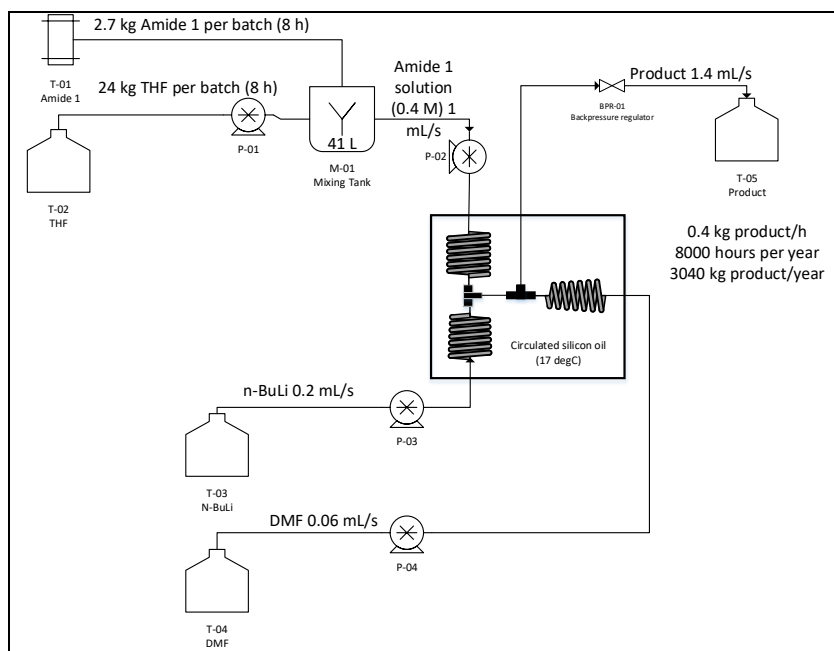


Figure 5-2 Schematic process diagram for T-reactor flow process

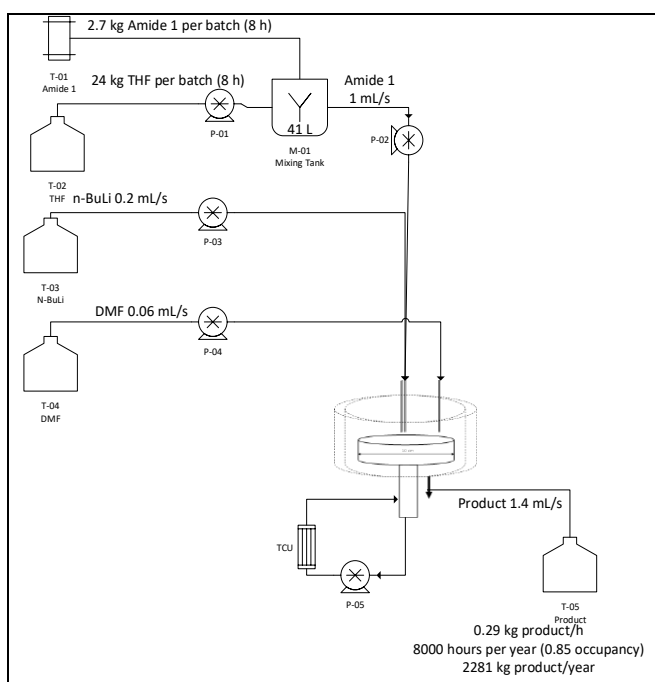


Figure 5-3 Schematic process diagram for SDR flow process

For the T-reactor system (Figure 5-2), the utilities used will be mainly the electricity for silicone oil bath cooling, pumping and agitation for mixing tanks. To avoid evaporation of butane during the reaction, a back pressure of 2 bars is applied.

For the SDR flow process (Figure 5-3), the utilities used will be mainly the electricity for rotating the disc, silicone oil bath cooling, pumping and agitation for mixing tanks. No backpressure is applied in this system, so butane is expected to evaporate from the surface of the disc and which will be diluted by the continuous supply of nitrogen gas. The mixture of gas then escapes together with the final reaction mixture through the sink underneath the SDR. Although argon gas was used in experiments, nitrogen gas can also be used and is considered in the reactor design.

Following general design assumptions were made:

- 1) No loss of aldehyde 1 yield due to workup, all aldehyde 1 were assumed to be recovered. (workup is excluded from the study)
- 2) All reactors were assumed to be air- and moisture-free during the course of the reaction.
- 3) At the end of the reaction, butane gas (byproduct) was assumed to be diluted and discharged via nitrogen purge.
- 4) All chemicals were at ambient temperature which is at 20 °C.
- 5) Concentration of purchased n-BuLi in hexane was always 1.6 M.
- 6) Total number of operation hours per year in a plant was 8000.

- 7) T-reactor and SDR reached steady state in less than a minute observed from experiment data, insignificant aldehyde 1 loss due to unsteady state flow during start up and shut down was assumed.
- 8) No observable degradation of aldehyde 1 after addition of DMF during storage based on GC.
- 9) Pump efficiency was assumed to be 50 %.
- 10) Specifications of purchased raw materials were assumed as in Table 5-1.

Table 5-1 Specifications of the raw materials

Raw materials	Specifications
4-chloro-N,N-diisopropylbenzamide (amide 1)	Solid, >99% pure
n-BuLi in Hexane	Liquid solution, 1.6 M
Tetrahydrofuran (THF)	Liquid, anhydrous, 99.9% stabilized with BHT
Dimethylformamide (DMF)	Liquid, anhydrous, 99.8%

Material cost is calculated as 1/10 of a catalogue price (Laird, 2005). Cost of labour are not considered. The equipment capital cost are estimated based on online catalogue from suppliers like Alibaba, Coleparmer, etc. Waste treatment cost and utility consumption are estimated based on charges in Singapore. The sizing of the equipment is sized on the cycle time and production capacity. Lang factor of 4.7 is factored into the overall capital cost to account for liquid system (Sinnott, 1999). All costs are expressed in USD to avoid conversion factors. Detailed cost tables are presented in Appendix C.

5.3 Comparisons of Sustainability Performance

Based on the above process designs, the sustainability performance is evaluated in terms of volume, mass and energy efficiencies and estimated the expected operational expenditure (OPEX) and capital expenditure (CAPEX) respectively (Table 5-2). The reactor volumes in the flow processes are smaller than the equivalent batch process because of the shorter residence time. In terms of the footprint of the major equipment, the T-reactor and SDR process are only 20 % of the batch equivalent.

Table 5-2 Comparisons of sustainability metrics between STR, T-reactor and SDR process at design scale of about 3 tons per year aldehyde 1

	STR	T-reactor	SDR
Operation time fraction	0.5	1	1
Throughput (kg aldehyde 1/h)	0.38	0.38	0.29
Processing equipment footprint ratio	1	0.2	0.2
Max processing inventory at any point of time (L/kg aldehyde 1/h)	59	0.01	0.06
Total material efficiency (kg aldehyde 1/kg material*)	0.087	0.090	0.079
Material efficiency (%)	-	4	-8

Total energy efficiency (kJ/kg aldehyde 1)	3,956	1,321	2,173
CAPEX (USD/kg aldehyde 1)	48	31	40
Economic savings in CAPEX (%)	-	36	16
OPEX (USD/kg aldehyde 1)	456	406	466
Economic savings in OPEX (%)	-	11	-4

(*) kg material consists of masses of amide 1, n-BuLi, DMF and THF.

Maximum processing inventory at any point of time for batch process includes the stirred tank reactor volume. As for the T-reactor and the SDR flow processes, it refers to the volume of the reactor and the piping of the reactor system. The mixing tanks are excluded from the process equipment as they do not deal with n-BuLi and are not involved any reactions; they are instead considered as part of the storage unit. On this basis, the T-reactor and SDR flow processes provide much smaller processing inventory as compared to batch process. This would provide significant safety benefit especially when dealing with hazardous chemical like n-BuLi.

With the T-reactor operating at a flow rate of 1.3 mL/s, it is able to handle the throughput of a 32 L stirred tank reactor which would require strict safety measures to be in place. However, one possible safety concern when operating the flow reactors could be the incomplete quench of n-BuLi during unsteady state flow which may occur during the reactor start-up or shut down phases. This could lead to unreacted n-BuLi to exit from the flow reactors and get into direct contact with water during the downstream separation process. This scenario could be avoided by starting the n-BuLi feed pump last during start-up and stopping it first during shut down, this ensures sufficient quantities of amide 1 and DMF are present to react with and quench n-BuLi.

Comparing the process safety considerations of the T-reactor and SDR, the T-reactor presented a higher risk of leakage of reaction mixture if the system was pressurized due to clogged channel. This is an unlikely situation in SDR where even if there was precipitation on the disc it would not affect the system pressure. To minimize the danger of n-BuLi leaking from the T-reactor into the environment, silicon oil was used as coolant in the circulated cooling system as its moisture content is lower (especially at 20 °C – minimum condensation) and it is less reactive towards n-BuLi.

As for the SDR, the major safety concern lies with the presence of vapor space in the reactor, unlike T-reactor, the butane gas produced in SDR is allowed to escape from the liquid film and the large surface area of the liquid film also promoted evaporation of the volatile solvents. If there was failure in the inert gas supply or insufficient inert gas to dilute the organic vapor, there would be accumulation of flammable vapor in the SDR vapor space. This risk can be mitigated by setting up an alternative inert gas supply which can be placed in operation if failure in primary inert supply was detected. Moreover, the SDR reactor volume is much smaller

than the batch reactor volume and this put a limit to the maximum quantity of flammable vapor that can be accumulated, so it can be diluted fairly quickly and has a less catastrophic consequence.

There is hardly any difference in total material efficiency between the STR and T-reactor because both processes have similar aldehyde 1 yield. The SDR is less material efficient due to lower reaction selectivity. Even though the quantity of DMF used in the T-reactor and SDR flow processes is slightly higher than in the batch process, it appears that its impact on the total material efficiency is minimal.

Figure 5-4 shows the energy consumption breakdown of the processes. Compressor duties in the two-stage cascade refrigeration system consume the most energy to maintain the reaction temperature at $-70\text{ }^{\circ}\text{C}$. Although the two-stage cascade refrigeration system is more energy efficient than direct cooling with electricity, the energy required in the batch process is still much higher than in the flow processes because it needs to maintain at a very low temperature. In addition, the pumping duty required in batch process is also much higher than in the flow processes because the material flow rate is higher than in the flow reactors where the flow rate is averaged and becomes smaller. The T-reactor flow process gives the best energy efficiency where the overall energy consumption is about 65 % lesser than the batch equivalent. The avoidance of the use of cryogenic temperature in the flow reactors resulted in tremendously energy savings. The sources of energy usage for the T-reactor and the SDR processes are similar with the exception of additional energy required for disc rotation in the SDR and extra pump duty needed to overcome the backpressure (2 bars) in T-reactor. The SDR process requires about 50 % more energy than the T-reactor to account for the disc rotational energy which consist of the rotational energy of the dry disc, overall kinetic energy supplied to the fluid and frictional energy dissipation of the fluid on the disc (Ghiassy and Boodhoo, 2013).

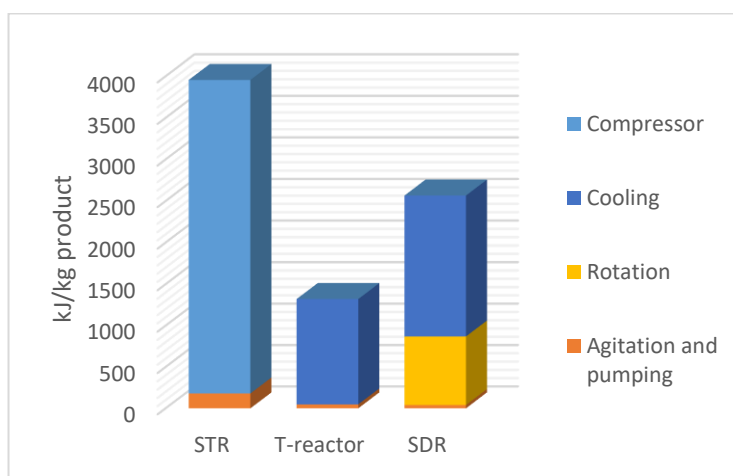


Figure 5-4 Breakdown of the energy consumption

The calculation of the operating cost (OPEX) in Figure 5-5 is based on the cost of raw materials and utilities which consists of electricity, chilled water and nitrogen cost. It is found that the raw materials cost represents the bulk of the OPEX. Amide 1 is the most expensive reagent among the chemicals used. The cost analysis shows cost saving of 10 % for the T-reactor in OPEX which is mainly contributed by the increased in aldehyde 1 yield (99 %) as compared to 96 % in the STR. Despite lowering the energy consumption by more than 50 %, the SDR incurred a higher OPEX than the STR. The cost savings from reduced energy consumption is meager compared to the cost of amide 1 due to the lower yield in the SDR (86 %). The reaction yield will also affect the downstream process (workup) which is critical to the overall process cost. A higher yield could mean a less tedious workup and waste treatment procedure that leads to further cost reduction. However, the impact of yield on subsequent workup is not included in the scope of our current study.

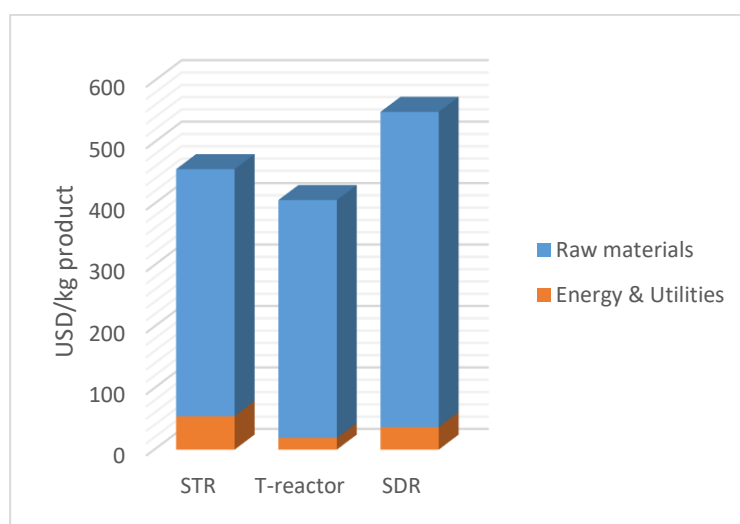


Figure 5-5 Cost breakdown of the OPEX

A rough estimation of the capital cost investment is done based on new major equipment and setup required to operate the processes respectively. Costing of common equipment like the storage vessels, heat exchangers, compressor, etc. is obtained from online suppliers. For the STR, the cryogenic reactor makes up more than 50 % of the CAPEX. For the flow reactors, the increased proportion of tanks in CAPEX is due to the additional mixing tanks and product storage tanks which are required to ensure continuous production. The CAPEX of the T-reactor includes the reactor and an open silicone oil temperature controlled circulated bath. The T-reactor is assembled in-house so it is relatively cheap considering only the cost of T-mixers and tubes which is insignificant compared to the cost of the temperature controlled circulated bath. The SDR is currently commercially unavailable so assumption is made regarding its selling price which includes the cost of material (316 stainless steel), electric motor, labor and frame cost. Since reaction can be performed at ambient temperature in flow reactors, costly

refrigeration equipment (e.g. compressors, heat exchangers, condenser and evaporator) and cold resistant reactor vessel could be avoided which leads to lower CAPEX in flow reactors compared to STR as shown in Figure 5-6.

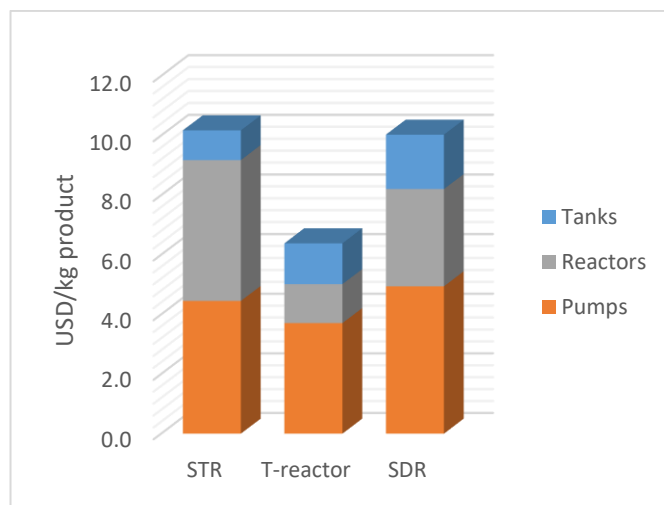


Figure 5-6 Cost breakdown of the CAPEX

5.4 Summary

The feasibility of performing the ortho-lithiation reaction in the T-reactors and the SDR at ambient temperature was demonstrated in Chapter 4. The conventional method is to operate the reaction at $-70\text{ }^{\circ}\text{C}$ in a fed-batch mode which is challenging to scale up. By performing the reaction in flow reactors, similar yields were achieved with a much shorter residence time at ambient temperature.

Compared to batch process, significant process intensification is achieved in the flow reactors which demonstrated higher energy efficiency, better volume efficiency, smaller processing inventory, smaller equipment footprint.

The performance of the T-reactor was particularly outstanding among the three reactors leading to much lower CAPEX and OPEX. Based on these promising results, the use of T-reactor presents a commercial viable alternative to the conventional batch processing. The SDR also performs well and brings additional energy-saving benefits

Chapter 6 would involve the study of the whole process including workup for the batch and flow processes. The reaction yield would affect the downstream processes which is critical to the overall process cost.

Chapter 6. Ortho-lithiation to Reduction Process – Part 3: Assessment of Sustainability Benefits for Whole Process Featuring Consecutive Reaction from ortho-Lithiation to Reduction

6.1 Introduction

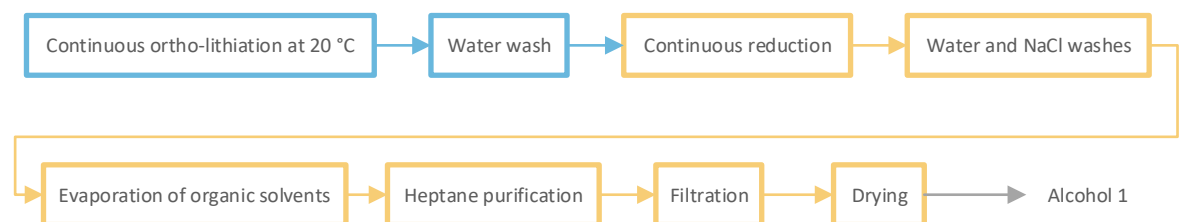
As an extension from Chapter 5, this chapter studies the sustainability performance of the whole process including workup for the batch (STR) and flow (T-reactor) processes. Given that the T-reactor is able to obtain higher reaction yield than the STR, it would be interesting to investigate the impact of reaction yield on downstream processes. The manufacturing process of the typical pharmaceutical plant involves multiple reaction steps with intermediate separation steps. The separation process is usually the most time consuming, energy and material intensive step and it is expected to be where the bottleneck resides. The purposes for product isolation between reactions are for solvent switch and product purification.

The products, classified as phthalide, from ortho-lithiation are useful building blocks in the synthesis of common pharmaceutically active compounds (Castaner and Roberts, 1979; Sorbera *et al.*, 2001; Hilden *et al.*, 2004), which are used widely in a number of subsequent reactions. These include ortho-carboxylation (Kosaka *et al.*, 2005), acidic treatment (Snieckus, 1990) and reduction (Faigl *et al.*, 2010). In this study, the reduction reaction is selected as the subsequent reaction as described by Faigl *et al.* (2010).

The objective of this study is to evaluate the sustainability benefits through intensification of the ortho-lithiation workup steps by avoiding the isolation of product (aldehyde 1) and directly transferring it into the next reactor for subsequent reduction reaction in a continuous mode. This is summarized in

Figure 6-1 (a) as the continuous consecutive reaction case. The continuous consecutive reaction case is benchmarked against the combined batch base case (Figure 6-1(b)), which consists of conventional batch ortho-lithiation reaction and aldehyde 1 isolation, followed by similar conventional batch reduction reaction and alcohol 1 isolation. The potential benefits of the continuous consecutive reaction case are significant savings from wash solvents and energy consumption, higher material efficiency and reduction in loss of product.

(a) Continuous consecutive reaction case



(b) Combined batch base case

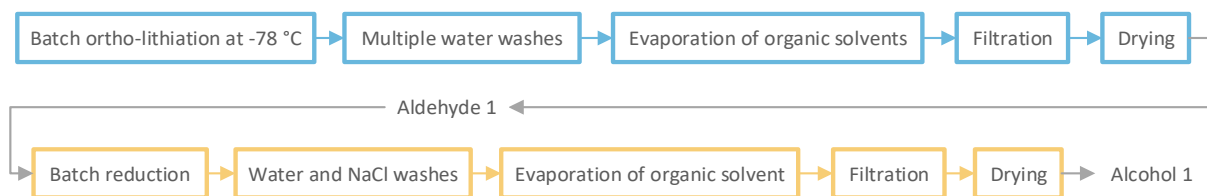


Figure 6-1 Summary of major process steps in (a) continuous consecutive reaction. Blue boxes indicate ortho-lithiation related steps; yellow boxes indicate reduction related steps; (b) combined base case process;

A detailed study of the selected reduction reaction was performed to assess its compatibility and identify any constraints in performing the consecutive reactions. Upon validating the feasibility of the consecutive reaction, a comparison between the combined batch base case (ortho-lithiation followed by reduction in batch mode) and the conceptually synthesized continuous consecutive reaction process at a hypothetical design scale of 3 tons per year would be made based on sustainability performance.

6.2 Experimental Apparatus and Procedures

6.2.1 Method of analysis in ortho-lithiation and reduction workup

The same method of GC analysis was used in ortho-lithiation and reduction workup. Organic and aqueous samples were collected after every separation step and analyzed using the internal standard method. The quantities of aldehyde 1 and alcohol 1 were determined by Gas Chromatography (GC) using Agilent Technologies 6890N GC system with 7693 autosampler and a HP-5 column. Temperature ramp: 150 to 210 °C, 25 °C/min; run time: 15 min; post run: 280 (5 min); injection volume: 1 μ L; detector temperature: 280 °C, control mode: constant pressure; pressure: 11.02 psi. Response factors of aldehyde 1 and alcohol 1 were determined by calibration using n-hexadecane as the internal standard in Appendix D.1.

After each separation step, about 1 mL of reaction mixture was taken and weighed. 50 mg of internal standard was added to the sample. Lastly, 20 μ L of the organic layer was drawn and diluted in 1 mL of ethyl acetate.

6.2.2 *Ortho-lithiation laboratory-scale workup according to literature procedure*

After the ortho-lithiation reaction, the reaction mixture was diluted with a saturated aqueous solution of ammonium chloride and the aqueous phase was extracted three times with ethyl acetate. The combined organic phase was then washed with brine, dried over MgSO_4 and evaporated. The residue was triturated with heptane. The crystalline aldehyde 1 was collected by filtration. The workup steps for ortho-lithiation reactions in both the cryogenic batch reactor and T-reactor were the same.

6.2.3 *Modified safe and scalable ortho-lithiation workup*

The literature lab-scale workup steps in section 6.2.2 were modified to ensure a safe and scalable ortho-lithiation separation process. After the reaction, the reaction mixture was quenched with water, followed by phase separation and the aqueous phase was discarded. A second water wash was introduced to ensure the removal of all salts and excess DMF and the second aqueous phase was discarded. The organic solvents were evaporated and water was slowly added during the evaporation until complete evaporation of the organic solvents and precipitation of aldehyde 1 in water as a solid-liquid suspension. The solid aldehyde 1 was collected after filtration and purified with heptane, followed by a second filtration to obtain the residue. The aldehyde 1 was then dried in oven.

6.2.4 *Reduction experiments (in-situ IR)*

A three-necked baffled jacketed 150 mL glass reactor was used to carry out the reduction experiments. The reactor has three glass baffles and its internal diameter is 0.06 m. The impeller is made up of a 4-pitched blade with diameter of 0.03m that is attached to an overhead stirrer through the middle neck of the reactor.

Two reduction reactions were performed using different forms of NaBH_4 – option 1: solid NaBH_4 ; option 2: 25w/w% NaBH_4 dissolved in 1 M NaOH solution. Table 6-1 shows the summary of the reaction conditions for the two experiments. 20 mL of 0.3 M aldehyde 1 solution in THF was charged into the reactor. A nitrogen blanket was introduced through one of the remaining necks. NaBH_4 was added in one-shot as the formation of alcohol 1 was monitored in-situ using IR spectroscopy measurement. The setup is shown in Figure 6-2.

Table 6-1 Lab-scale batch reduction reaction conditions using different forms of NaBH_4

Options	Agitation speed (rpm)	Reaction components (molar ratio)	Solvent (mL)	Temperature ($^{\circ}\text{C}$)	Time (min)
1 (S-L)	450	Aldehyde 1 / NaBH_4 (1:1.3)	THF (20 mL)	20	~16

2 (L-L)	450	Aldehyde 1 /NaBH ₄ (1:0.5)	THF- 1 M NaOH (20:0.3 mL)	20	~2
---------	-----	--	---------------------------------	----	----

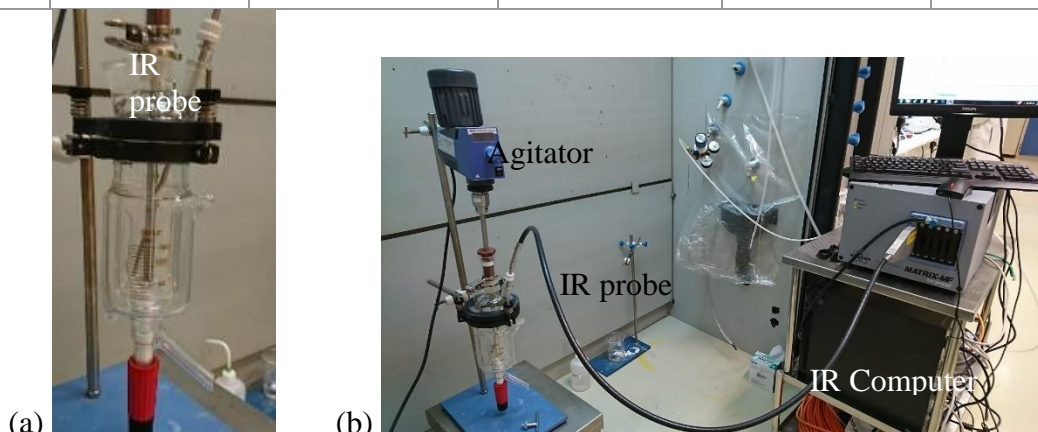


Figure 6-2 (a) 150 mL stirred tank reactor (STR) used for performing batch IR experiments; (b) STR connected to IR computer via IR probe

The IR spectroscopy was carried out using Bruker Matrix-MR-ex, Mid IR ATR-FTIR with the IN350-T Fiber Probe that measures spectra range from 3500 to 720 cm^{-1} . An exposure of 1 s with 64 acquisitions was employed for a single scan in this study. The IR probe was submerged in the solution through the third neck and the background spectra were taken using the initial reaction mixture as a reference.

The IR spectra shows that the C=O bond stretching in the aldehyde 1 occurred at a frequency of between 1700 and 1620 cm^{-1} and gave a distinct peak (Figure D-1 in Appendix D.1). Calibrations based on the area of the peak corresponding to different starting aldehyde concentrations in the THF were obtained (Appendix D.1).

6.2.5 Reduction laboratory-scale workup

The reaction progress was tracked using in-situ IR spectroscopy. The reaction was deemed to be complete once no more aldehyde 1 could be detected according to IR spectroscopy. Water was added to quench the excess unreacted NaBH₄ and also to provide a heat sink for the quench reaction. Caution was taken to maintain good ventilation as hydrogen gas was evolved during the quench. After fully quenching the NaBH₄, phase separation of the organic and aqueous phase was performed. The aqueous phase containing the salts was discarded. A second wash using 1 M NaCl solution was added to the remaining organic phase to remove any remaining salts in the organic phase, followed by a second phase separation where the second aqueous phase was discarded. Anhydrous magnesium sulfate was added to the final organic reaction mixture to remove as much water from the organic phase as possible, followed by filtration to collect the filtrate. The filtrate was evaporated in a rotor-evaporator under vacuum and 40 °C water bath.

6.3 Bottlenecks in ortho-lithiation Batch Base Case Separation Process

The key steps in proposed safe and scalable batch whole process for ortho-lithiation are summarized in Table 6-2. To ensure a safe and scalable batch base case, the key process steps were modified from the lab-scale procedure reported by Faigl *et al.* (2010) (Appendix D.2).

Table 6-2 Summary of ortho-lithiation safe and scalable base case operations

Steps	Aldehyde 1 yield (%)
1) Ortho-lithiation reaction	96 (crude yield)
2) First water wash	90.3
3) Second water wash	90.1
4) Evaporation of organic solvents and addition of water	90.1 (assumed)
5) First filtration	90.1 (assumed)
6) Heptane wash	72.3
7) Second filtration	72.3 (assumed)
8) Drying	72.3 (assumed)

Upon completion of the ortho-lithiation reaction at very low temperature, the reaction mixture was warmed to ambient temperature. In step 2, water was added to dissolve lithium dimethylamine and excess DMF and was discarded as the aqueous phase after phase separation. The second water wash in step 3 ensured the removal of any remaining lithium dimethylamine and DMF from the organic phase. One major issue observed during lab-scale evaporation of solvent (step 4) using the rotor-evaporator was the formation of sticky solid that hardened on the wall of the glass vessel. This would be a problem at large scale during the transfer of solid product out of the reactor vessel. Therefore, this step was conceptually modified by adding water during evaporation of the organic solvents. The solid product (aldehyde 1), which was insoluble in water, is expected to precipitate out and form a solid-liquid suspension as all the organic solvents evaporate. The suspension was filtered in Step 5 and aldehyde 1 was obtained as solid residue while the aqueous filtrate was discarded. The solid aldehyde 1 was purified using small amount of heptane as the side products are expected to be more soluble in heptane than aldehyde 1 in step 6. Finally, aldehyde 1 was filtered and dried to a moisture content of 0.1%.

The aldehyde 1 yield loss specified in steps 1, 2, 3 and 6 was based on lab-scale experiment and assumptions. For workup steps 4, 5, 7 and 8, the yield loss was assumed to be negligible at large scale because the loss was believed to be attributed to handling, which could be greatly minimized in actual large-scale operation that is much more efficient compared to lab-scale experiment.

In step 6, it was observed experimentally that the solubility of aldehyde 1 in heptane varied with the level of impurity in the mixture. Table 6-3 provides a rough estimation on the effect of impurity on aldehyde 1 recovery. It was decided that for reaction where the aldehyde

1 yield was below 90%, the decision is not to proceed with separation process as a yellow oil would be obtained and the aldehyde 1 recovery would be insignificant. For this reason, the SDR reactor system, which obtained a highest yield of 87%, was not considered in this whole process comparison. As expected, the major bottleneck of the whole process was in the separation process and specifically the heptane purification step (step 6 in Table 6-2) where there was an almost 20% aldehyde 1 yield loss. Since the raw material cost (amide 1) accounted for the greatest operating cost, the considerable yield loss would raise the operating cost significantly. This step justified the need for intensification as major value could be gained.

Table 6-3 Effect of amount of side product on purification

Reaction aldehyde 1 yield	Side products (mol%)	Aldehyde 1 recovered (mol%)
>90%	<10%	>80% 
<90%	>10%	Cannot recover (yellow oil) 

6.4 Feasibility of performing consecutive reactions from ortho-lithiation to reduction in batch mode

The two important requirements for integrated, two-step consecutive reactions of ortho-lithiation and reduction were solvent compatibility and ease of isolation of product (alcohol 1) after the two reactions. A detailed study of the selected reduction reaction was thus performed to assess its compatibility and limitations in performing the consecutive reactions.

6.4.1 Solvent compatibility

According to Faigl *et al.* (2010), the reduction of aldehyde 1 using sodium borohydride (NaBH_4) was carried out in methanol where 1.3 mol eqv of NaBH_4 was used. To avoid solvent swap between ortho-lithiation and reduction, the original reduction solvent, methanol, was replaced by THF (solvent used in ortho-lithiation). As for the form of NaBH_4 used, two options were investigated as highlighted in Table 6-4. Option 1 uses solid NaBH_4 while option 2 involves dissolution of NaBH_4 in aqueous sodium hydroxide solution (1 M NaOH) to form a fully dissolved aqueous basic solution. The result showed that both options were feasible in THF, achieving complete conversion with no side product formation.

Table 6-4 Comparison of reduction rate between solid and liquid form NaBH₄ used

Options	Agitation speed (rpm)	Reaction components (molar ratio)	Solvent (mL)	Temperature (°C)	Time (min)	Conversion (%)
1 (Solid-Liq)	450	Aldehyde 1 /NaBH ₄ (1:1.3)	THF (20 mL)	20	~16	99
2 (Liq-Liq)	450	Aldehyde 1 /NaBH ₄ (1:0.5)	THF- 1 M NaOH (20:0.3 mL)	20	~2	100

The reaction rate for option 1 appeared to be almost independent of the reactant concentrations with a likely overall reaction order of zero as seen in Figure 6-3. One possible explanation put forward by Ward and Rhee (1989) is that in the absence of dissolved NaBH₄ species, heterogeneous (solid-liquid) reduction is likely to occur, which might further inhibit the dissolution of NaBH₄. This suggested that the rate of reduction was limited by the dissolution rate of the solid NaBH₄ in THF as a solid-liquid suspension was observed during the reaction.

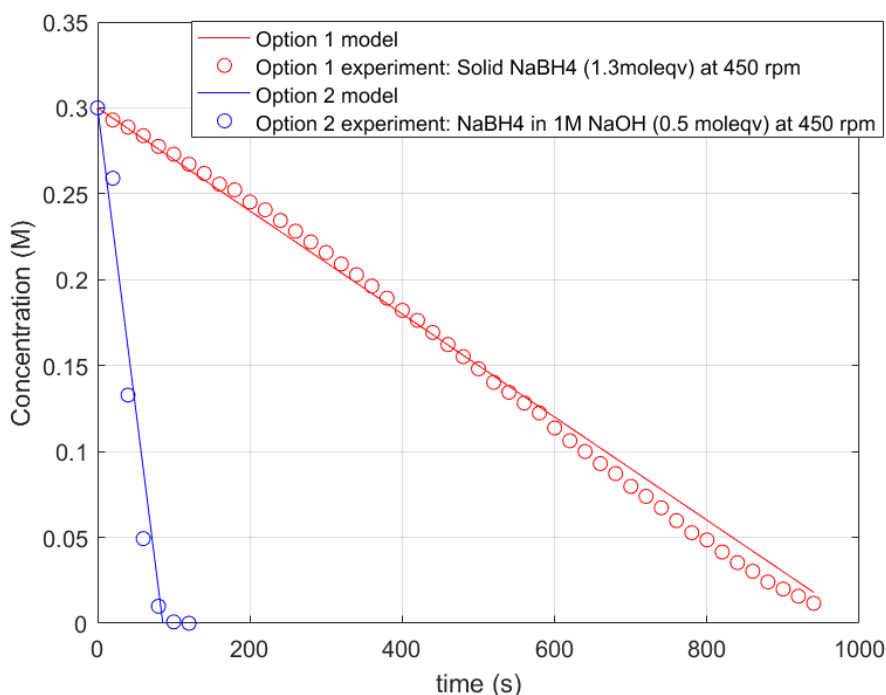


Figure 6-3 Aldehyde 1 concentration profiles tracked by in-situ IR measurement for two different forms of NaBH₄ used

The rate of reduction in option 2 was faster than option 1 as shown in Figure 6-3. As NaBH₄ is known to be more stable in high pH, the use of NaOH solution in option 2 enabled the dissolution of NaBH₄ in the aqueous alkaline solution without undergoing rapid hydrolysis. Without the inhibition from the heterogeneous reduction, the reaction was likely to be much

faster even though a lower stoichiometric ratio of NaBH_4 (0.5 mol eqv) was used since the alkaline solution was pre-saturated with dissolved NaBH_4 . The reduction reaction mechanism using aqueous base NaBH_4 is proposed in Appendix D.3.

A comparison between the options is summarized in Table 6-5. Due to the fast rate of reaction, the release of flammable hydrogen gas and large heat of reaction, the literature case (Faigl *et al.*, 2010) was deemed as unsafe for scale-up. Options 1 and 2 appeared to be the safer options, especially in terms of mitigating safety concerns from the generation of hydrogen gas during the reaction and quench.

Table 6-5 Summary of the advantages and disadvantages of different reduction cases

Case	Solvents	Reagent	Advantages	Disadvantages
Literature (Faigl <i>et al.</i> , 2010)	Methanol (0.45 M)	Solid NaBH_4 (1.3 mol eqv)	<ul style="list-style-type: none"> Fast rate of reaction (~instantaneous). 	<ul style="list-style-type: none"> Consume large excess of NaBH_4. Large heat of reaction released (RC 1, $\Delta H_r = 453$ kJ/mol aldehyde). Flammable hydrogen gas generated during reaction. Heat may ignite hydrogen gas. Precooling (0 °C) required.
Option 1	THF (0.3 M)	Solid NaBH_4 (1.3 mol eqv)	<ul style="list-style-type: none"> No loss of NaBH_4 to reaction with solvent. Lesser hydrogen gas and heat of reaction generated during reduction. 	<ul style="list-style-type: none"> Relatively slow rate of reaction. No reduction in quantity of NaBH_4 used as it would result in even slower rate of reduction. Quench reaction between excess NaBH_4 with water, generates hydrogen gas.
Option 2	THF-NaOH (0.3 M)	Aqueous NaBH_4 (0.5 mol eqv)	<ul style="list-style-type: none"> Fast rate of reaction (~2 min). Smaller quantity of NaBH_4 required. No significant loss of NaBH_4 to reaction with solvent. Lesser hydrogen gas and heat of reaction 	<ul style="list-style-type: none"> Required an extra step of dissolving NaBH_4 in NaOH solution. Addition of NaOH solution.

			generated during reduction and quench reaction.	
--	--	--	---	--

A brief material cost comparison between options 1 and 2 is presented in Table 6-6. Although an additional reagent (NaOH solution) is required in option 2, it was still cheaper than option 1 because NaBH₄ is more costly than NaOH. The decision is to go with option 2 for reduction in THF.

Table 6-6 Material cost comparison between options 1 and 2

Materials	Option 1		Option 2	
	Mol eqv	Cost (USD/kg alcohol 1)	Mol eqv	Cost (USD/kg alcohol 1)
4-chloro-N,N-diisopropyl-2-formylbenzamide	1	-	1	-
NaBH ₄	1.3	61.71	0.5	23.74
Sodium hydroxide solution (1 M)	-	-	3 times w/w% of NaBH ₄	0.16
	Total	\$61.71	Total	\$23.90

6.4.2 Feasibility of workup after the consecutive reactions in batch mode

After verifying the feasibility of performing reduction in THF, actual ortho-lithiation reaction mixtures from the STR and T-reactor with composition as shown in Table 6-7 were used to perform reduction in batch mode. It was noted that the water washes after ortho-lithiation reaction were necessary to remove excess DMF, which could react with NaBH₄, and to remove lithium dimethylamine, which might reduce the solubility of NaBH₄ in the reaction mixture. The average water content in the respective reaction mixtures after the two water washes were obtained experimentally from Karl Fischer.

Table 6-7 Composition of reaction mixtures from STR and T-reactor after ortho-lithiation reaction and two water washes.

Compounds	STR reaction mixture (96% crude yield)	T-reactor reaction mixture (99% crude yield)
	w/w%	w/w%
4-chloro-N,N-diisopropyl-2-formylbenzamide (Aldehyde 1)	8.9 (~0.3 M)	9.2 (~0.3 M)
Unknown side products	0.4	0.1
THF	70	70
Hexane	18	18
Water	2.7	2.7

As expected, complete reductions of aldehyde 1 were achieved in both reaction mixtures. Other than the side products from ortho-lithiation reaction, there was no new side

products observed from GC analysis after the reduction reaction. The lab-scale reduction workup, as described in Table 6-8, was performed on both the ‘STR’ and ‘T-reactor’ reaction mixtures after reduction reaction. It was observed that the product (alcohol 1) from the ‘STR’ reaction mixture existed as an ‘oil’ even after trituration with heptane (step 5), forming a liquid-liquid mixture with heptane as the lighter phase and ‘oil’ as the heavier phase. On the other hand, the product (alcohol 1) from the T-reactor reaction mixture had successfully precipitated as white solid. One reason for this difference could be the higher proportion of side products in the STR reaction mixture that might have inhibited the precipitation of the alcohol 1. Therefore, it was concluded that only ortho-lithiation reaction mixture with high product purity (~99%) is suitable for the consecutive reduction reaction. Otherwise, the alcohol 1 isolation step in reduction would be problematic.

Table 6-8 Reduction laboratory scale experiments and observations

	STR reaction mixture	T-reactor reaction mixture
Steps	Observations	
Reaction	Complete reduction of aldehyde 1 after an hour. No additional side products observed.	
1) First water wash	Rapid formation of hydrogen gas as excess sodium borohydride reacted with water.	
2) Second water wash	Clear phase separation due to presence of hexane, minimized loss of organic in aqueous.	
3) Additional of anhydrous magnesium sulfate and filtration	Filtrates collected. Residue discarded.	
4) Rotor-evaporation	Colorless oil obtained.	White solids formed on the wall.
5) Heptane wash	Liquid-liquid mixture. ‘Oil’ was heavier phase. 	Solid slightly soluble in heptane. 

6.5 Design of combined batch base case and continuous consecutive reaction processes for 3 ton per year production

The major process steps in the combined base case is summarised in

Figure 6-1 (b). The combined base case consisted of two independently operated conventional batch processes (ortho-lithiation and reduction) with a production target of about 3 tons products (aldehyde 1 and alcohol 1) per year. The proposed safe and scalable batch whole processes for ortho-lithiation and reduction are summarised in Appendix D.4. After the ortho-lithiation workup, the aldehyde 1 was isolated in the form of ‘white powder’ before

commencing with the reduction reaction. Unlike the continuous consecutive reaction case where the aldehyde 1 concentration was fixed by the upstream ortho-lithiation reaction concentration, the aldehyde 1 concentration in the reduction reaction of the combined batch base case did not have such constraint. Although the concentration of aldehyde 1 in THF used in lab-scale experiments (section 6.4.1) was 0.3 M, theoretically higher aldehyde 1 concentration in THF could be used as aldehyde 1 is very soluble in THF. A conservative assumption of 1 M aldehyde 1 in THF was used in the reduction reaction of the combined batch base case.

The key unit operations of the continuous consecutive reaction case are summarized in Figure 6-1(a). The continuous ortho-lithiation reaction was performed in the T-reactor, which had the best reactor performance (Chapter 4). Although the reduction reaction was performed solely in batch mode in this study, a continuous reduction process was conceptually developed to ensure a smooth process integration from a continuous ortho-lithiation to reduction.

A potential continuous process would involve ortho-lithiation reaction in T-reactor and the subsequent water washes using mixer-settler column, reduction reaction in static mixer, followed by workup steps consisting of continuous extractions with water and NaCl solution, agitated thin film dryer to remove the organic solvent, continuous filtration with heptane and drying. Some possible examples of the commercially available, state-of-the-art continuous equipment (Description in Chapter 2) for each unit operation are listed in Table 6-9. It is assumed that the performance of the continuous equipment is at least equivalent to that of the batch process in terms of energy consumption, efficiency and alcohol 1 recovery. The continuous equipment cost is assumed to be 110% of batch equipment cost of equivalent production rate (Schaber *et al.*, 2011).

Table 6-9 Summary of small-scale continuous consecutive reaction operations

Steps	Examples of continuous equipment
1) Ortho-lithiation reaction	T-reactor (in-house)
2) Water washes	Karr column (KMPS, 2017a)
3) Reduction reaction	Static mixer (Noritake, 2017b; Sulzer, 2017a)
4) Water wash	Karr column (KMPS, 2017a) Centrifugal extractor (CINC, 2017)
5) 1 M NaCl wash	
6) Evaporation of organic solvents	Agitated thin film dryer (KetavConsultant, 2017; systems, 2017a)
7) Heptane wash	Rotary pressure filter (Komline-Sanderson, 2017)
8) Filtration	
9) Drying	Belt dryer (TheilenMaschinenbau, 2017)

Following general design assumptions were made:

- 1) No observable degradation of aldehyde 1 and alcohol 1 during the course of the reactions.
- 2) No scheduling of the reactions was required in the combined base case as the ortho-lithiation and reduction processes were operated in different plants.
- 3) All chemicals were at ambient temperature which was at 20 °C.
- 4) Total number of operation hours per year in a plant was 8000.
- 5) No product loss in evaporation of solvent, filtration and drying operations as product loss due to handling was assumed to be minimal in large scale operations.
- 6) Byproducts such as salts and excess reagents were assumed to be completely removed during water washes.
- 7) Pump efficiency was assumed to be 50 %.

6.6 Comparison of process performance between combined base case and continuous consecutive reaction

Based on the process designs (Appendices D.4 and D.5), the whole process performance metric for combined base case and continuous consecutive reaction case were estimated based on alcohol 1 throughput of 3 tons per year. Table 6-10 presents the comparison of sustainability metrics between the combined base case and continuous consecutive reaction in terms of volume, mass and energy efficiencies and operational and capital expenditures. The performance metric of the combined base case is derived from the sum of the individual ortho-lithiation and reduction batch base cases. For the reduction whole process, it is noted that the material cost does not include the cost of aldehyde 1 as it was produced in-house through ortho-lithiation reaction and was not commercially available. This explains the relatively low reduction OPEX obtained as cost of raw material is often one of the major process cost. Based on the assumption that the energy consumption of the continuous equipment in consecutive reaction is the same as the batch equipment in the combined base case, both cases have the same electricity cost and energy efficiency.

Table 6-10 Performance metrics of combined ortho-lithiation and reduction base case at design scale of about 3 tons per year alcohol 1

Performance metric	Ortho-lithiation whole process*	Reduction whole process*	Combined base case	Continuous consecutive reaction
Total material efficiency (kg material/kg product)	37	14	51	44

E-factor (kg waste/kg product)	35	13	48	43
Material cost (USD/kg product)	634	33	667	583
Energy and utilities cost (USD/kg product)	111	20	131	131
Waste treatment cost (USD/kg product)	27	14	41	34
Total energy efficiency (kJ/kg product)	13,745	6,592	20,337	20,337
CAPEX (USD/kg product)	85	38	123	75
% CAPEX reduction	-	-	Benchmark	-39%
OPEX (USD/kg product)	771	48	819	656
% OPEX reduction	-	-	Benchmark	-20%

(*) Refer to Appendix D.4 for the synthesis of the ortho-lithiation and reduction whole processes

A 20% reduction in operating cost (OPEX) is expected in the continuous consecutive reaction case because of the avoidance of the ortho-lithiation heptane purification step, which resulted in significant aldehyde 1 loss given that material cost accounts for the largest contribution in the process cost. The other major cost saving in the continuous consecutive reaction case is contributed by reduced energy cost as the three most energy and time intensive separation operations (present in the combined base case) are avoided: 1) the use of very low reaction temperature in ortho-lithiation; 2) the evaporation of solvents (THF and hexane); and 3) the drying of solid aldehyde 1.

Although the aldehyde 1 concentration in the combined batch base case could be conceptually increased to 1 M, the continuous consecutive reaction still resulted in lower solvent demand. The material efficiency is improved in the continuous consecutive reaction mainly due to reduction in solvent usage (THF) as no additional solvent was required for reduction reaction. In addition, the relatively lower product loss in the continuous consecutive reaction case has also improved the material efficiency. Consequently, the improvement in material efficiency led to lower E-factor and waste treatment cost since the amount of organic waste was directly reduced.

It is noted that the CAPEX shown is only a vague estimation. For more accurate estimation, detailed equipment sizing, material of construction and technical specifications have to be taken into consideration. The main reason for the much lower CAPEX in the continuous consecutive reaction compared to the combined base case was because of the significantly lower capital cost of T-reactor compared to a batch cryogenic reactor. The

continuous consecutive operation of the entire process have not been demonstrated yet, although in the context of cost saving and sustainable processing, it is likely to be considered as future development options.

6.7 Conclusion

As demonstrated in Chapter 4, the ortho-lithiation reaction yield difference between the STR and T-reactor was not significant as the respective yields were 96% and 99%. The improvement in yield achieved by the T-reactor was insignificant compared to the amount of aldehyde 1 loss (~20%) during heptane purification step, which drastically decreased the overall process efficiency. The most time consuming operation was found to be drying and the most energy intensive operation was the evaporation of organic solvents. It was clear that the separation process was the bottleneck of the whole ortho-lithiation process. To avoid dealing with inefficient separation process, the feasibility of performing consecutive reactions (ortho-lithiation followed by reduction) in the same solvent without major intermediate workup was investigated. The consecutive reaction has been proven feasible using THF as the common solvent. However, the reaction mixture from batch ortho-lithiation (STR) was unable to obtain solid alcohol 1 after the reduction work-up because of the higher amount of impurities/side products present.

This illustrated the direct impact of reaction yield on downstream processes and subsequent reaction. Although the difference in ortho-lithiation reaction yield between the STR and T-reactor was less than 5%, its impact on subsequent reduction reaction and separation was significant. It was concluded that the consecutive reaction was only suitable to be carried out in ortho-lithiation reaction mixture with product purity of 99%. This intensification strategy (\$656 USD/kg alcohol 1) was theoretically estimated to be more competitive in terms of OPEX than the combine base case (\$819 USD/kg alcohol 1). The cost savings mainly come from 1) greater aldehyde 1 recovery and 2) significant reduction in energy cost in ortho-lithiation reaction. The consecutive reaction also contributes to a greener process as solvent usage is greatly reduced by conducting the reactions in the same solvent.

Key separation process technologies operating in continuous mode, which are commercially available on the market, have been identified in a conceptual fully continuous process to produce alcohol from amide. Although continuous operation of the entire process including the separation stages has yet to be demonstrated in practice, it is likely to be considered as future development options.

Chapter 7. General Framework

Based on the experience gained working with different processes, a general framework is presented by summarizing the approach to PI for pharmaceutical processes. The framework is developed primarily based on the work covered Chapters 3, 4, 5 and 6, and its scope is limited to some of the common problems faced in pharmaceutical processing, such as solid handling, challenging purification, sensitive reactions, etc.

The overall work-flow for this framework is given in the Figure 7-1. The starting point of a new process is usually from a lab-scale procedure and in the cases of amidation and ortho-lithiation, this was obtained from a lab-scale procedure reported by Faigl *et al.* (2010). Therefore, the first step relies heavily on lab-scale experiments, with the objective of process definition. This is followed by the development of a safe and scalable batch base case to establish a benchmark. Based on the issues encountered in lab-scale experiments, possible PI options/solutions are proposed and evaluated based on preliminary experimental results. Intensified cases are developed by incorporating the promising PI options. Finally, the base case and the intensified cases are compared based on techno-economic-sustainability metrics.

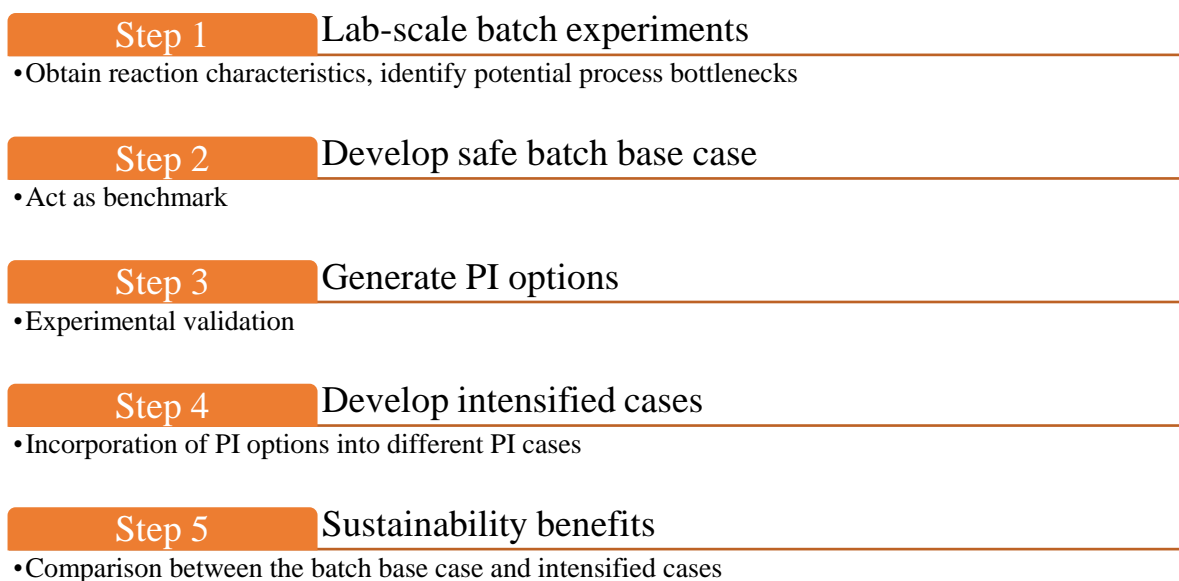


Figure 7-1 Stepwise framework for intensification

The constraints of this approach include 1) tedious multiple lab-scale experiment and 2) equipment constraint due to lack of resources. It is envisioned that the framework proposed would address these potential issues by providing guidance on prioritization of crucial experiment based on mapping of PI options to techno-economic sustainability drivers and identify the potential barriers. The initial evaluation would be primarily based on lab-scale

experiments, although simple engineering calculations (e.g. Dynochem modelling), rule-of-the-thumb and best practice did get involved to provide indicative numbers for further evaluations. As for equipment constraint, this is a very realistic problem often faced by many in industries and academia alike. It is encouraged to perform experiments with available in-house resources or alternatives in order to provide analogous assessment of the potential of the actual state-of-the-art equipment. The intention is to provide an accurate assessment of the feasibility of the PI option rather than to provide the best and most optimized solution. This framework is therefore complementary to other methodologies.

7.1 Lab-scale Batch Experiments

Information regarding the basic physical behavior of the reaction mixture (e.g. evolution of gas, formation of solids, phase behavior or interaction etc.) is often unavailable in the literature procedure and experiments needs to be performed to bridge the gap. Other than the usual lab-scale batch experiments (e.g. RC 1 to obtain heat of reaction), for some characteristics additional investigations need to be carried out. For instance, the determination of mixing sensitivity requires additional mixing study to make a more informed assessment and to predict whether a reaction would face mixing limitation at large scale. Table 7-1 lists the available literature procedures and the findings from actual lab-scale experiments for the amidation and ortho-lithiation processes.

Besides the inherent reaction characteristics, potential side reaction formation, safety, phase complexity and workup performance are also considered in order to have a holistic view of the whole process to be developed. For workup, the tracking of product yield is performed by taking organic sample after every workup step (i.e. reaction, extraction, filtration, etc.). It is noted that the amount of product lost at lab-scale might not be reflective of the equipment performance at large-scale as large-scale equipment are usually more efficiency than that at lab-scale. For example, centrifugal filter is more efficient in solid-liquid separation as compared to filter paper and funnel. Therefore, it is assumed that product loss is minimal during large-scale unit operations like filtration, solvent evaporation and drying, even though the product lost at lab-scale is significant.

Table 7-1 Initial evaluation of characteristics of lab-scale batch chemical systems

	Amidation		Ortho-lithiation	
Reaction	A given literature procedure	Information from laboratory experiment	A given literature procedure	Information from laboratory experiment
Order of addition	A mixture of diisopropylamine (1.5 mol. eq.) and triethylamine (1.5 mol. eq.) was added dropwise to 4-chlorobenzoyl chloride (limiting reagent) in toluene (17.8 mol. eq.)	Same procedure as literature. HCl fume was emitted depending on addition rate and agitation speed. Not a robust procedure for scale up.	n-BuLi (1.2 mol eqv) added slowly to a solution of amide 1 in THF at -78 °C. After 1 h, temperature of reaction mixture was raised to -50 °C followed by the addition of DMF (1.3 mol eqv).	Same procedure as literature.
Use of reagent(s)	Use of two types of base Large excess of DIPA and TEA used.	TEA and DIPA were mixed together before addition to a solution of AC in toluene. Corrosive HCl fume released if it is not fully neutralised.	2.5 M of n-BuLi in THF was used.	Due to lack of supply, 1.6 M of n-BuLi in THF was used. Although the reaction concentration changed, it was assumed that the reaction would not be affected
Phase complexity & physical properties	Not reported.	Large amount of amine salt (DIPA.HCl) formed when AC was added. The thick suspension exhibited complex viscoelastic/yield stress liquid properties which resulted in poor mixing during RC 1 experiment. The solid loading is approx. 0.069 g/mL (6 % w/w, calculated from a 8 g scale batch reaction).	Not reported.	Particulates observed when n-BuLi reacts with residual moisture in the solvent to form lithium salt.
Mixing	Not reported.	Mixing limited.	Not reported.	Mixing limited.
Use of solvent(s)	Toluene is used as the solvent	Toluene used as solvent but further increase in reagent concentrations was unlikely due to high solid loading.	Anhydrous THF used as solvent	Unlikely to increase reaction concentration further as it would either require a longer dosing time to control the exotherm or cause more side reactions.
Heat generation	Slow reagent addition to control exotherm. Keep reaction at room temperature.	Moderately exothermic (~105 kJ/mol AC). Although amidation is not a highly exothermic reaction, poor mixing can raise safety concerns with sudden contact between accumulated, unreacted reagents which could react rapidly and cause fast heat released.	Not reported.	No experimental calorimetric data. Significant heat released during ortho-lithiation according to literature (>200 kJ/mol)
Reaction rate	Long residence time of 24 h reported	Fast reaction of within 5 min. Long residence time required due to poor mixing.	Not reported.	Step 1 (lithiation) – Fast (<1 s) Step 2 (DMF) addition – Faster than step 1
Hazards	Not reported.	Corrosive HCl fume released if it is not fully neutralised.	Not reported.	n-BuLi is pyrophoric which ignite in air/water

		Large excess of DIPA (50 mol%) used. Harmful to aquatic lives if it is not disposed properly.		
Side reaction(s)	Not reported	100% conversion to amide 1	Not reported.	Side reactions dominate in high n-BuLi concentration, inefficient mixing and higher temperature.
Workup	A given literature procedure	Information from laboratory development	A given literature procedure	Information from laboratory experiment
Water wash	After 24 h, toluene and water were added. Phase separation to remove and dispose the aq. layer.	The actual reaction time was found to be less than 5 mins. Amine salt has high solubility in water of ~500 g/L DIPA has low solubility in water of ~100 g/L No significant amide 1 loss observed	Quench with water, followed by phase separation (remove aqueous layer)	Follow the literature procedure.
HCl wash	The organic layer was separated, washed with an aqueous solution of 5wt/wt% HCl. Phase separation to remove and dispose the aqueous layer.	HCl 5 wt/wt% added to organic layer to neutralise the excess amine base. No significant amide 1 loss observed	Multiple extraction of aqueous layer to retrieve aldehyde 1. The organic layers were combined.	The amount of aldehyde 1 recovered from multiple ethyl acetate extraction was insignificant.
NaCl wash	The organic layer was further separated and washed with brine. Phase separation to remove and dispose the aqueous layer.	Brine was used to remove salt from the org layer. No significant amide 1 loss observed	Anhydrous MgSO ₄ was added to organic phase to remove residual water followed by filtration where the filtrate was collected.	Not necessary as water was required in the next step.
Drying of mixture	Dried the organic layer over MgSO ₄ .	Add anhydrous MgSO ₄ to dry the organic layer. Filter to discard the hydrated solid MgSO ₄ . No significant amide 1 loss observed	Evaporation of solvent from filtrate.	After solvent evaporation, aldehyde 1 was present as a sticky solid which was difficult to transfer.
Solvent removal	Evaporated solvent from the organic layer.	Evaporated solvent from the organic layer. No significant amide 1 loss observed	Purification by triturating residue with hexane.	Significant amount of aldehyde 1 lost (>50%) as it was slightly soluble in hexane/heptane. The amount of purified aldehyde 1 crystallised depended the amount of side products in the mixture.
Purification	The residue was triturated with hexane. The crystalline product was collected by filtration.	Significant amount of amide 1 lost (40%) during trituration as amide 1 was quite soluble in hexane. Trituration was found to be unnecessary as there was no formation of side products.	Filtration and collect the residue followed by drying.	

7.2 Safe and Scalable Batch Base Case

Since the given literature procedures are done in lab-scale, some processes possess characteristics that cannot be run efficiently or safely when scaled up. For example, the formation of thick solid-liquid suspension in amidation reaction requires more effective mixing than what a conventional stirred tank reactor is capable of and the release of corrosive HCl fume also presents challenges. In addition, the formation of sticky solid product in ortho-lithiation after solvent evaporation made transfer challenging. These problems are not reported in literature and were only detected after initial lab-scale experiments. In order to obtain safe and scalable base cases, modifications to the lab-scale procedure are required where necessary.

The conventional typical pharmaceutical manufacturing process in batch mode is assumed (i.e. one-pot reaction, liquid-liquid extractions, evaporation, solvent swap, filtration and drying). It is also assumed that the reaction chemistry is fixed but there is flexibility to modify solvent types.

7.3 Generation of PI Options

The initial findings from step 1 made it easier to identify process issues and process steps where there is value to be gained (e.g. low yield, loss of product, generate too much waste, etc.). Table 7-2 and Table 7-3 present the PI options that can potentially address the process issues in amidation and ortho-lithiation processes respectively.

The approach taken to generate PI options starts with addressing the issues in the process and that is where the primary PI options are proposed as illustrated in Figure 7-2. However, the primary PI options might not be successfully applied all the time as there may be barriers and roadblocks during the execution of the primary PI options. A qualitative rating of 3 levels, “high”, “medium” and “low”, is used to assess the potential benefits and effort required to execute the PI option and “negative” is used for identified barrier when executing the PI option. Given that the execution of a primary PI option would yield ‘high’ benefits with the presence of a barrier, an extended PI option (1) can be generated as a potential solution to overcome the barrier.

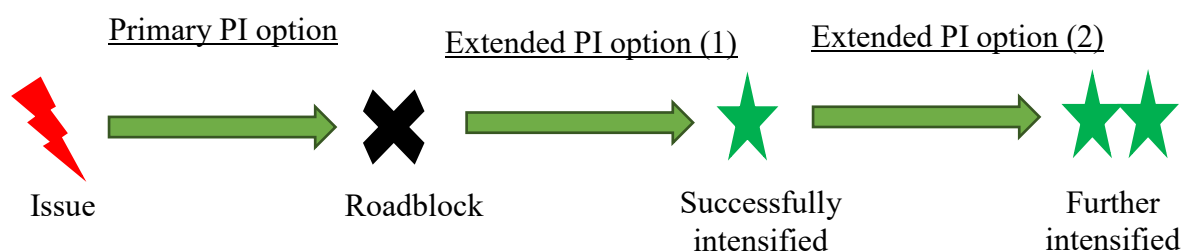


Figure 7-2 Thought process for the generation of PI options

In a situation where there are both benefits and hindrances but minimum effort is required to perform it in the laboratory, it would be very useful to base the decision on lab-scale experimental results – “experiment”, which would present a realistic and accurate assessment of the technical feasibility of the PI option. When there is no hindrance and minimum effort is required to execute the PI option, the decision would naturally be “Yes”. The final decision to execute the PI option depends on stakeholder’s business objective.

As an illustration (Table 7-2), in order to avoid pre-mixing of TEA and DIPA in the amidation process, one possible primary PI option is to replace TEA by DIPA. However, this resulted in an increase in overall reagent cost as DIPA is more costly than TEA and a roadblock is met. An extended PI option (1) to overcome the roadblock is generated through the lowering of the mol eqv of DIPA used. Yet again, this extended PI option raised concerns on whether there is sufficient base to capture HCl. At this stage, it is difficult to decide how much DIPA could be reduced without compromising the efficiency of HCl neutralisation. Instead of trying to model the outcome, an experiment would be able to provide a quick and relatively more accurate assessment of the situation. In the case of amidation, the experiment gave satisfactory result that shown almost 97% of the HCl released was captured by DIPA. A swift decision to reduce the mole equivalent of DIPA used could be made based on the experimental result.

Extended PI option (2) is built upon the success of the primary PI option. In the case of ortho-lithiation process (Table 7-3), the success of the PI reactor to achieve better product selectivity would generate extended PI options focusing on downstream process, such as elimination of purification step or continuation with consecutive reduction reaction using crude reaction mixture. In general, the potential benefits in product quality, efficiency, cost and safety are significant enough to make a strong case to carry out experiments using the PI reactors even though it might take effort to setup the reactors.

As mentioned previously, the identification of suitable PI reactor will depend on the process engineers’ knowledge of the capabilities (e.g. heat transfer, mass transfer, mixing efficiency, residence time etc.) and availability of the PI reactor at the desired scale. It is noted that some barriers are unknown or unexpected until they are discovered during experiments, such as the problem of clogging in the microreactor. In the case where the microreactor did not meet the requirement of the reaction, another PI reactor can be built in-house and customized to the reaction specifications (e.g. T-reactor in this particular case). In view of the presence of unexpected barriers, it is important to verify the feasibility of the extended PI options (1) and (2) through experiments where possible.

Table 7-2 Potential benefits and barriers to PI options for amidation process

Issues identified	PI options	Safety	Quality	Cost	Efficiency	Environmental impact	Time to market	Effort to execute	Decision
Two types of base used	Replace TEA with DIPA (Primary)			Negative DIPA is slightly more costly than TEA	High Avoid premixing of TEA with DIPA			Low	Experiment
Large excess of costly DIPA was used	Reduce the quantity of DIPA from 3 to 2.1 mol eqv.(Extended)			High Cost reduction from lesser DIPA usage		High Amine salts are bad for aquatic life if the waste is not treated.		Low	Experiment
Mixing limitation due to solid suspension	Reduce toluene usage by increasing reagent concentrations in toluene-water solvent system (Primary)		Negative Possible degradation of starting material upon contact with water	Medium Cost reduction from less toluene usage		Medium Higher material efficiency		Low	Experiment
No recycling of solvent	Toluene recycling (Primary)			High Cost reduction from toluene recycling		High Higher material efficiency		Low	Yes
Long batch residence time due to poor mixing	Continuous reaction (Primary)	Medium Higher reaction volumetric efficiency			Neutral Might require continuous separation	Negative Consume more water to dissolve DIPA	High Throughput can be adjusted by flow rate using existing flow setup	Medium	Experiment
Loss of amide 1 in workup	Consecutive reaction from amidation to ortho-lithiation (Primary)			High Cost saving from energy and utilities used for solvent evaporation and condensation in amidation workup	High No tedious workup and loss of product through handling	High Lesser solvent usage and reduced waste generated.	High Significant time saving from avoidance of workup steps, especially drying.	Low	Yes

Unnecessary large amount of wash solvents used	Reduction of solvents used in washes (Primary)			High Wash solvents like water, HCl and NaCl solutions are relatively cheaper than reagents so the cost impact might not be great. Waste treatment cost might be reduced.		High Reduction in aqueous waste generated.		Low	Yes
Batch workup is a potential barrier to continuous reaction	Continuous workup (Extended)	High Higher workup volumetric efficiency			High Process integration from continuous reaction to workup.		Neutral Greater flexibility as throughput might be adjusted by changing flow rate. Might be time consuming to obtain an optimum operating condition due to potential technical barriers.	High Require PI equipment like CE, WFE, continuous filtration, etc.	Experiment

Table 7-3 Potential benefits and barriers to PI options for ortho-lithiation process

Issues identified	Preliminary PI options	Safety	Quality	Cost	Efficiency	Environmental impact	Time to market	Effort	Decision
High energy consumption due to -70 °C Mixing limitation due to fast reaction	Suitable PI reactor that provide better heat control and efficient mixing can reduce side reactions (Primary)	High Better heat control in flow equipment	Medium Improve product selectivity	Medium Reduce energy consumption by performing reaction at higher temperatures	High Avoid long waiting time for reaction mixture to cool and warm Negative Clogging likely to occur in microreactor	Medium Less energy consumption	High Flow equipment allows the development of scalable processes in the laboratory.	Medium	Experiment
Clogging in flow reactor as potential barrier to PI reactor	Flow reactor with larger diameter (Extended)		Negative Larger channel 'microreactor' might compromise on product quality		High Issue of clogging might be resolved			Medium	Experiment
	Spinning disc reactor (Extended)	High Better heat control in flow equipment	Medium Improve product selectivity	Medium Reduce energy consumption by performing reaction at higher temperatures	High Avoid long waiting time for reaction mixture to cool and warm		High Flow equipment allows the development of scalable processes in the laboratory.	Medium	Yes
n-BuLi is pyrophoric	PI reactor with lower inventory (Extended)	High Inherently safer process via lower inventory						Medium	Yes
Significant heat released during lithiation	PI reactor with good heat control (Extended)	High Reduces the risk of runaway reactions						Medium	Experiment

Loss of product during purification	Make purification redundant by minimising side reactions (Extended)		High Improve product quality	High Minimise loss of high value product	High Simplification by skipping purification step		Medium Simplification of workup step	Low	Yes
Loss of product during workup	Consecutive reaction from ortho-lithiation to reduction using crude reaction mixture (Extended)		Negative Side products crude ortho-lithiation reaction mixture might be detrimental to reduction	Medium Cost saving in reducing wash solvents and energy consumption during workup	High Avoid workup steps	High Reduce solvent usage in reduction	High Avoidance of tedious workup	Low	Experiment

7.4 Synthesis of Intensified Cases (Whole Process)

After generation of PI options and assessment of their feasibility through experiments, it is essential to consider the development of the whole process including the workup steps. For the ortho-lithiation process, it has been demonstrated that the continuous flow PI reactors can bring significant benefits by minimizing side product formation due to shorter contact time. This prompted the need for continuous workup to improve the overall process efficiency. The subsequent batch extraction, solvent evaporation and filtration can be eliminated by using continuously operated centrifugal extractor, wiped film evaporator, rotary drum filter, etc. In cases where experimental demonstration is lacking due to equipment constraint or unavailability such as for continuous workup operations in amidation and ortho-lithiation as highlighted in Chapters 3 and 6, assumptions are made to fill in the process gaps.

7.5 Comparison of Sustainability Metrics

According to the process intensification strategy, an intensified process should provide higher production capacities, reduced energy and raw materials consumption, increased safety and reduced equipment volume and waste generation. Under these definitions, a set of metrics has been selected and weighted as shown in Table 7-4. The weightage is determined based on individual project goals and overall strategy of the company. For the purpose of this project, operational cost, material efficiency and E-factor have been selected as the most relevant indicators for intensification. The capital cost and energy efficiency do not have large impact on the overall production cost in the long term, hence they are assigned lower weightage. Similarly, safety is not a main objective for process intensification though compromise in safety is definitely unacceptable.

The sustainability metrics of the intensified cases would be compared to the batch base case at the designated manufacturing scale. The result of the comparison would support a decision to implement the selected process/case on a plant based on their overall business drivers.

Table 7-4 Sustainability metrics

Metric	Class	Weight
Capital cost	Economic	+
Operational cost	Economic	+++
E-factor	Environmental	++
Material efficiency	Environmental/ economic	+++
Energy efficiency	Environmental	+
Volume efficiency	Safety	+
In-process inventory	Safety	+

Chapter 8. Conclusions and Recommendations

This research deals with intensification of industrial API synthesis, with a focus on two particular process – the amidation of 4-chlorobenzoyl chloride in the presence of amine base; and ortho-lithiation of 4-chloro-N,N-diisopropylbenzamide, and evaluate the sustainability benefits of various process options. The impact of reaction mode, operating mode, solvent evaporation, purification and drying method on the overall operating costs have been investigated.

8.1 Conclusions

1. The amidation process is successfully intensified with the implementation of a number of Process Intensification (PI) options, proven feasible in lab-scale experiments. These options are represented in terms of three intensified cases - the intensified batch case, the continuous reaction case and the continuous process case, are compared to the batch base case. To compare their sustainability performance, the respective plants are designed at a hypothetical throughput of 3 tons per year. The sustainability metrics used in this study are volume efficiency, maximum processing inventory at any point of time, material efficiency, E-factor, energy efficiency, capital and operating expenditure. Overall, cost savings of up to 40% is estimated for the intensified batch case, indicating that batch mode operation in this particular process is more suitable than continuous mode. It is noted that the main reason for the poorer performance of the continuous cases is because of the larger amount of water used to dissolve DIPA due to the difference in the mode of reagent addition between the batch and continuous cases.
2. In the first part of the ortho-lithiation process, the feasibility of performing the ortho-lithiation reaction in continuous flow reactors at ambient temperature is investigated in Chapter 4. The conventional method is to operate the reaction at -70 °C in a fed-batch mode which is challenging to scale up. A continuous flow PI reactor – T-reactor was developed and obtained the highest reaction yield of 99% at ambient temperature by providing short residence time (flash chemistry concept) and efficient mixing (CFD simulation). In depth reactor study was performed on the two most promising PI reactors – the T-reactor and the SDR. Although the T-reactor obtained higher aldehyde 1 yield than the SDR, further optimization of the SDR operating conditions is expected to offer distinct potentials of improvement in the aldehyde 1 yield to a level similar to the T-reactor.

3. In the second part of the ortho-lithiation process, a comparison of the T-reactor, the SDR and the Stirred Tank Reactor (STR) based on the sustainability metrics is made. Compared to the STR, significant process intensification is achieved in the flow reactors which demonstrate higher energy efficiency, better volume efficiency, smaller processing inventory and smaller equipment footprint. The performance of the T-reactor is particularly outstanding among the three reactors leading to 66% and 11% reduction in energy consumption and operating expenditure compared to the STR process respectively. Based on these promising results, the use of T-reactor presents a commercial viable alternative to the conventional batch processing. The SDR also performs well and brings additional energy-saving benefits
4. The last part of the ortho-lithiation process focuses on the study of the whole process including workup for the batch and flow processes. For the batch production, it is clear that the separation process is the bottleneck of ortho-lithiation whole process. To avoid dealing with challenging and inefficient operations during the purification stages of the aldehyde product obtained from the ortho-lithiation reaction, the feasibility of performing consecutive reactions (ortho-lithiation followed by reduction) in the same solvent without major workup in between is investigated. This example illustrated the direct impact of reaction yield on downstream processes and subsequent reaction. Although the difference in ortho-lithiation reaction yield between batch and continuous (T-reactor) was less than 5%, its impact on subsequent reduction reaction and separation is significant. Theoretical estimation for the continuous consecutive reaction (\$656 USD/kg alcohol 1) highlight that it is likely to be more competitive than the combined base case (\$819 USD/kg alcohol 1). The cost savings mainly come from 1) greater aldehyde 1 recovery; 2) significant reduction in energy cost in ortho-lithiation reaction.
5. Lastly, based on the experience gained in different processes, a general framework which summarizes the approach to PI for pharmaceutical processes is developed. It aims to facilitate the early state of process development by offering the first estimation of benefits versus costs and providing suggestions on possible intensification options through an experimental approach.

8.2 Recommendations for Future Work

One of the objectives set for the project was to identify gaps to be covered in future work or in alternative projects.

1. It has been mentioned in the framework that key missing data can be obtained through laboratory experiments when information in the form of mathematical models is limited or not available. Laboratory protocols are not included in the framework, so these should be developed and integrated with process development. It can provide guidance to capture critical data while performing fewer numbers of experiments.
2. The framework presented depends largely on process engineers' experience, resources and knowledge to select suitable PI technology. Although there are several organizations involved in cataloguing the capabilities of intensified devices (Bayer *et al.*, 2005), it is not designed for pharmaceutical industry which often require dealing with challenging workup steps and handling with solids, etc. The generation of such a database is not included in the project scope. As the PI concept is continuously expanded and new devices and designs are developed, there should be knowledge base dedicated to the pharmaceutical application.
3. The work presented features the two chemical transformations and the proposed framework is adapted to the needs of these specific industrial applications. Essential refinement of the framework should be done by application of more challenging transformations such as the Heck coupling which has long reaction time and involves catalytic reaction, Friedel-Crafts which is exothermic and involves 'messy' workup, etc. This should improve the robustness of the framework. It is further suggested to extend the analysis to more process steps including formulation of the final drug and to perform life cycle analysis for the selected process options.
4. Previous research has shown that process bottlenecks tend to occur in the separation process. Although preliminary experiments has been performed with the centrifugal extractor and the wiped film evaporator, future experimental work should also extend to continuous intensified filtration and drying operations. This will potentially bring further improvements and intensification benefits.
5. Challenges come from the selection of 'optimum' operating condition for the PI reactors can be enhanced by obtaining the reaction kinetics. It is vital that the PI reactor operates in the right process conditions as minor variations may have a significant influence on the overall system (i.e. incomplete reaction due to insufficient residence time, etc.). However, it is also equally important to ensure that the reaction kinetics obtained is accurate which is very difficult to obtain for fast

reactions (reaction time in seconds). Otherwise, the use of inaccurate kinetic data may result in greater deviation from optimum result. A sensible decision has to be made on whether to focus and prioritize the effort to obtain the reaction kinetics or perform trial and error experiments to scan for the optimum process condition.

6. Additional gaps that have to be covered in future work are related to the solvent selection. Given the sustainability consideration, the feasibility of performing reactions with greener solvents (i.e. 2-methyl tetrahydrofuran versus tetrahydrofuran) should be incorporated in the initial stage. Apart from the one-parameter-at-the-time analysis performed here, design of experiment (DOE) can be performed instead to identify critical factors that can be enhanced to give the maximum overall process yields.

References

- Al Badran, F., Awdry, S. and Kolaczowski, S. (2013) 'Development of a continuous flow reactor for pharmaceuticals using catalytic monoliths: Pt/C selective oxidation of benzyl alcohol', *Catalysis Today*, 216, pp. 229-239.
- Algusane, T.Y., Proios, P., Georgiadis, M.C. and Pistikopoulos, E.N. (2006) 'A framework for the synthesis of reactive absorption columns', *Chemical Engineering and Processing: Process Intensification*, 45(4), pp. 276-290.
- Alibaba (2017a) *Products*. Available at: https://www.alibaba.com/?src=sem_ggl&cmpgn=678190955&adgrp=34276573373&fditm=&tgt=aud-362622410597:kwd-14739453&locintrst=&locphyscl=9062499&mtchtyp=e&ntwrk=g&device=c&dvcmdl=&creative=148007444336&plcmnt=&plcmntcat=&p1=&p2=&aceid=&position=1t1&gclid=CjwKC_AjwrO_MBRBxEiwAYJnDLA5fm-ARaIgIEQ-rDQOdt-qZ_D9DvRyKRV18DXJAdFCkZcqiTzPV-xoCWLUQAvD_BwE (Accessed: 17 Jan).
- Alibaba (2017b) *SCD Series Conveyor dryer*. Available at: https://www.alibaba.com/product-detail/SCD-IR-Hot-Drying-Tunnel-drying_60271980760.html (Accessed: 8 Jan).
- Amin, S.I. and Walker, J.A. (1979) 'Process for preparing arylalkanoic acid derivatives'. Google Patents.
- Anderson, N.G. (2012) 'Using Continuous Processes to Increase Production', *Organic Process Research & Development*, 16(5), pp. 852-869.
- Anlauf, H. (2007) 'Recent developments in centrifuge technology', *Separation and Purification Technology*, 58(2), pp. 242-246.
- Anxionnaz, Z., Cabassud, M., Gourdon, C. and Tochon, P. (2008) 'Heat exchanger/reactors (HEX reactors): Concepts, technologies: State-of-the-art', *Chemical Engineering and Processing: Process Intensification*, 47, pp. 2029-2050.
- ApolloScientific (2017) *4-chloro-N,N-diisopropylbenzamide*. Available at: http://www.apolloscientific.co.uk/display_item.php?id=43422 (Accessed: 24 Aug).
- Aquacare, U. (2017) *agitated thin film dryer*. Available at: <http://www.unitopaquacare.in/agitated-thin-film-dryer-3884177.html> (Accessed: 8 Jan 2017).
- Arizmendi-Sánchez, J.A. and Sharratt, P.N. (2008) 'Phenomena-based modularisation of chemical process models to approach intensive options', *Chemical Engineering Journal*, 135(1–2), pp. 83-94.
- Arratia, P., Kukura, J., Lacombe, J. and Muzzio, F. (2006) 'Mixing of shear-thinning fluids with yield stress in stirred tanks', *AIChE Journal*, 52(7), pp. 2310-2322.
- B&PLittleford (2017) *Liquid liquid extraction*. Available at: <http://www.bplittleford.com/pod-centrifuge.html> (Accessed: 17 Aug).
- Babi, D.K., Holtbruegge, J., Lutze, P., Gorak, A., Woodley, J.M. and Gani, R. (2015) 'Sustainable process synthesis–intensification', *Computers & Chemical Engineering*, 81, pp. 218-244.
- Babi, D.K., Lutze, P., Woodley, J.M. and Gani, R. (2014) 'A process synthesis-intensification framework for the development of sustainable membrane-based operations', *Chemical Engineering and Processing: Process Intensification*, 86, pp. 173-195.
- Bayer, T., Jenck, J. and Matlosz, M. (2005) 'IMPULSE—A new approach to process design', *Chemical Engineering & Technology*, 28(4), pp. 431-438.
- Beak, P. and Snieckus, V. (1982) 'Directed lithiation of aromatic tertiary amides: an evolving synthetic methodology for polysubstituted aromatics', *Accounts of Chemical Research*, 15(10), pp. 306-312.
- Ben-Guang, R., Fang-Yu, H., Kraslawski, A. and Nystrom, L. (2000) 'Study on the methodology for retrofitting chemical processes', *Chemical Engineering and Technology*, 23(6), pp. 479-484.
- Benaïssa, W., Gabas, N., Cabassud, M., Carson, D., Elgue, S. and Demissy, M. (2008) 'Evaluation of an intensified continuous heat-exchanger reactor for inherently safer characteristics', *Journal of Loss Prevention in the Process Industries*, 21(5), pp. 528-536.
- Benneker, A.M., van der Ham, L.G., de Waele, B., Zeeuw, A.J. and van den Berg, H. (2016) 'Design and intensification of industrial DADPM process', *Chemical Engineering and Processing: Process Intensification*, 109, pp. 39-50.

- BHR (2017) *HEX reactors for fast exothermic reactions*. Available at: <http://www.bhrgroup.com/Portals/5/Documents/Case%20Studies/HexReactor.pdf> (Accessed: 16 Aug).
- Biofilm (2017) *Biofilm annular reactor*. Available at: <http://biofilms.biz/products/biofilm-reactors/biofilm-annular-reactor/> (Accessed: 16 Aug).
- Boodhoo, K. (2013) 'Spinning disc reactor for green processing and synthesis', *Process Intensification for Green Chemistry: Engineering Solutions for Sustainable Chemical Processing*, pp. 59-90.
- Boodhoo, K. and Harvey, A. (2013) 'Process Intensification: An Overview of Principles and Practice', in *Process intensification technologies for green chemistry: engineering solutions for sustainable chemical processing*. John Wiley & Sons, pp. 1-31.
- Boodhoo, K.V. and Al-Hengari, S.R. (2012) 'Micromixing Characteristics in a Small-Scale Spinning Disk Reactor', *Chemical Engineering & Technology*, 35(7), pp. 1229-1237.
- Boodhoo, K.V., Dunk, W.A., Vicevic, M., Jachuck, R.J., Sage, V., Macquarrie, D.J. and Clark, J.H. (2006) 'Classical cationic polymerization of styrene in a spinning disc reactor using silica-supported BF₃ catalyst', *Journal of Applied Polymer Science*, 101(1), pp. 8-19.
- Brechtelsbauer, C. and Ricard, F. (2001) 'Reaction engineering evaluation and utilization of static mixer technology for the synthesis of pharmaceuticals', *Organic Process Research and Development*, 5(6), pp. 646-651.
- Broadhead, J., Edmond Rouan, S. and Rhodes, C. (1992) 'The spray drying of pharmaceuticals', *Drug Development and Industrial Pharmacy*, 18(11-12), pp. 1169-1206.
- Burchat, A.F., Chong, J.M. and Nielsen, N. (1997) 'Titration of alkylolithiums with a simple reagent to a blue endpoint', *Journal of Organometallic Chemistry*, 542(2), pp. 281-283.
- Cafiero, L., Baffi, G., Chianese, A. and Jachuck, R. (2002a) 'Process intensification: precipitation of barium sulfate using a spinning disk reactor', *Industrial & Engineering Chemistry Research*, 41(21), pp. 5240-5246.
- Cafiero, L., Baffi, G., Chianese, A. and Jachuck, R. (2002b) 'Process intensification: precipitation of barium sulfate using a spinning disk reactor', *Industrial and Engineering Chemistry Research*, 41(21), pp. 5240-5246.
- Capsugel (2017) *Pharmaceutical spray drying*. Available at: <http://www.bendresearch.com/drug-delivery-technologies/spray-dried-dispersion> (Accessed: 17 Aug).
- Cárdenas-Guerra, J.C., López-Arenas, T., Lobo-Oehmichen, R. and Pérez-Cisneros, E.S. (2010) 'A reactive distillation process for deep hydrodesulfurization of diesel: Multiplicity and operation aspects', *Computers and Chemical Engineering*, 34(2), pp. 196-209.
- Carey, J.S., Laffan, D., Thomson, C. and Williams, M.T. (2006) 'Analysis of the reactions used for the preparation of drug candidate molecules', *Organic and Biomolecular Chemistry*, 4(12), pp. 2337-2347.
- Carneiro, P.F., Gutmann, B., de Souza, R.O. and Kappe, C.O. (2015) 'Process Intensified Flow Synthesis of 1 H-4-Substituted Imidazoles: Toward the Continuous Production of Daclatasvir', *ACS Sustainable Chemistry & Engineering*, 3(12), pp. 3445-3453.
- Carvalho, A., Matos, H.A. and Gani, R. (2013) 'SustainPro—A tool for systematic process analysis, generation and evaluation of sustainable design alternatives', *Computers & Chemical Engineering*, 50, pp. 8-27.
- Castaner, J. and Roberts, P. (1979) 'Citalopram', *Drugs of the future*, 4, p. 407.
- Chemito (2017) *Simulated moving bed*. Available at: <http://chemito.net/ps/simulated-moving-bed.htm> (Accessed: 16 Aug).
- Chemoxy (2017) *Reactive distillation*. Available at: <http://www.chemoxy.com/reactive-distillation/> (Accessed: 16 Aug).
- Chen, J.-F., Wang, Y.-H., Guo, F., Wang, X.-M. and Zheng, C. (2000) 'Synthesis of nanoparticles with novel technology: high-gravity reactive precipitation', *Industrial and Engineering Chemistry Research*, 39(4), pp. 948-954.
- Chen, Y.-S. and Liu, H.-S. (2002) 'Absorption of VOCs in a Rotating Packed Bed', *Industrial & Engineering Chemistry Research*, 41, pp. 1583-1588.
- Chiroli, V., Benaglia, M., Puglisi, A., Porta, R., Jumde, R.P. and Mandoli, A. (2014) 'A chiral organocatalytic polymer-based monolithic reactor', *Green Chemistry*, 16(5), pp. 2798-2806.
- Cho, B.K., Carr Jr, R.W. and Aris, R. (1980) 'A continuous chromatographic reactor', *Chemical Engineering Science*, 35(1-2), pp. 74-81.

- CINC (2017) *Extraction*. Available at: <http://www.cincind.com/index.php/opmodes/extractop> (Accessed: 17 Aug).
- ColeParmer (2017) *Centrifugal separator*. Available at: <https://www.coleparmer.com/p/cinc-v2-centrifugal-multipurpose-separator-extractors/51089> (Accessed: 8 Jan).
- Commonge, J.M. and Falk, L. (2014) 'Methodological framework for choice of intensified equipment and development of innovative technologies', *Chemical Engineering and Processing: Process Intensification*, 84, pp. 109-127.
- Costello (2017) *Spinning tube in a tube - HOLL-REACTOR* Available at: http://www.rccostello.com/spinning_tube.html (Accessed: 16 Aug).
- de Silva, S.O., Reed, J.N., Billedeau, R.J., Wang, X., Norris, D.J. and Snieckus, V. (1992) 'Directed ortho metalation of n,n-diethyl benzamides. Methodology and regiospecific synthesis of useful contiguously tri- and tetra-substituted oxygenated aromatics, phthalides and phthalic anhydrides', *Tetrahedron*, 48(23), pp. 4863-4878.
- Delsman, E.R., de Croon, M.H.J.M., Kramer, G.J., Cobden, P.D., Hofmann, C., Cominos, V. and Schouten, J.C. (2004) 'Experiments and modelling of an integrated preferential oxidation-heat exchanger microdevice', *Chemical Engineering Journal*, 101(1), pp. 123-131.
- Dencic, I. and Hessel, V. (2013) 'Industrial Microreactor Process Development up to Production', in *Microreactors in Organic Chemistry and Catalysis*. Wiley-VCH Verlag GmbH & Co. KGaA, pp. 373-446.
- Denčić, I., Ott, D., Kralisch, D., Noël, T., Meuldijk, J., de Croon, M., Hessel, V., Laribi, Y. and Perrichon, P. (2014) 'Eco-efficiency analysis for intensified production of an active pharmaceutical ingredient: a case study', *Organic Process Research & Development*, 18(11), pp. 1326-1338.
- Denis, C., Hemati, M., Chulia, D., Lanne, J.-Y., Buisson, B., Daste, G. and Elbaz, F. (2003) 'A model of surface renewal with application to the coating of pharmaceutical tablets in rotary drums', *Powder Technology*, 130(1), pp. 174-180.
- Desai, A.A. (2012) 'Overcoming the Limitations of Lithiation Chemistry for Organoboron Compounds with Continuous Processing', *Angewandte Chemie International Edition*, 51(37), pp. 9223-9225.
- Deviatkin, I. (2013) 'Wastewater treatment and deinking sludge utilization possibilities for energy and material recovery in the Leningrad region'.
- Engler, M., Kockmann, N., Kiefer, T. and Woias, P. (2004) 'Numerical and experimental investigations on liquid mixing in static micromixers', *Chemical Engineering Journal*, 101(1), pp. 315-322.
- Faigl, F., Thurner, A., Molnár, B., Simig, G. and Volk, B. (2010) 'Manufacturing synthesis of 5-substituted phthalides', *Organic Process Research & Development*, 14(3), pp. 617-622.
- Faure, A., York, P. and Rowe, R. (2001) 'Process control and scale-up of pharmaceutical wet granulation processes: a review', *European Journal of Pharmaceutics and Biopharmaceutics*, 52(3), pp. 269-277.
- FEECO (2017) *Rotary dryers*. Available at: http://feeco.com/rotary-dryers/?gclid=CjwKCAjw_dTMBRBHEiwApIzn_JPSb8dshs2oViWvvyUSpe9KaXbkrqDVV9xymdHYDLn2QqPIAssJ_xoCtYsQAvD_BwE (Accessed: 17 Aug).
- Feng, R., Ramchandani, S., Ramalingam, B., Tan, S.W.B., Li, C., Teoh, S.K., Boodhoo, K. and Sharratt, P.N. (2017) 'INTENSIFICATION OF CONTINUOUS ORTHO-LITHIATION AT AMBIENT CONDITIONS-Process Understanding and Assessment of Sustainability Benefits', *Organic Process Research & Development*.
- Flowid (2015) *The SpinPro R300*. Available at: <https://www.flowid.nl/spinpro-reactor-compared-to-thin-film-spinning-disc-reactor/> (Accessed: 16 Aug).
- FoodProcessingTechnologies (2017) *concentration wiped film*. Available at: http://foodtechinfo.com/foodpro/index_gas_technologies/concentration_-_wiped_film/ (Accessed: 8 Jan).
- Forney, L., Ye, Z. and Georges, A. (2005) 'Fast competitive reactions in Taylor- Couette flow', *Industrial & Engineering Chemistry Research*, 44(19), pp. 7306-7312.
- Franke, M.B., Nowotny, N., Ndocko, E.N., Górak, A. and Strube, J. (2008) 'Design and optimization of a hybrid distillation/melt crystallization process', *AIChE Journal*, 54(11), pp. 2925-2942.
- Freund, H. and Sundmacher, K. (2008) 'Towards a methodology for the systematic analysis and design of efficient chemical processes', *Chemical Engineering and Processing: Process Intensification*, 47(12), pp. 2051-2060.
- Friedle, U. and Vesper, G. (1999) 'A counter-current heat-exchange reactor for high temperature partial oxidation reactions', *Chemical Engineering Science*, 54(10), pp. 1325-1332.

- Gavi, E., Di Giacobbe, F., Marchisio, D.L., Barresi, A.A., Olsen, M.G. and Fox, R. (2007) *The 2007 Annual Meeting*.
- GEA (2017) *Spray dryers*. Available at: http://www.gea.com/en/productgroups/dryers_particle-processing-systems/spray-dryers/pharmaceutical-products/index.jsp (Accessed: 17 Aug).
- Ghaini, A., Mescher, A. and Agar, D.W. (2011) 'Hydrodynamic studies of liquid–liquid slug flows in circular microchannels', *Chemical Engineering Science*, 66(6), pp. 1168-1178.
- Ghebre-Sellassie, I., Mollan Jr, M.J., Pathak, N., Lodaya, M. and Fessehaie, M. (2002) 'Continuous production of pharmaceutical granulation'. Google Patents.
- Ghiassy, D. and Boodhoo, K. (2013) 'Opportunities for Energy Saving from Intensified Process Technologies in the Chemical and Processing Industries', *Process Intensification for Green Chemistry: Engineering Solutions for Sustainable Chemical Processing*, pp. 379-392.
- GIGKarasek (2017) *thin film drying plant*. Available at: <http://www.gigkarasekusa.com/thin-film-drying-plants/> (Accessed: 17 Aug).
- Glatt (2017) *Fluidized bed drying*. Available at: <https://www.glatt.com/en/processes/fluidized-bed-drying/> (Accessed: 17 Aug).
- Godany, T.A., Neuhold, Y.-M. and Hungerbühler, K. (2011) 'Combined in situ monitoring method for analysis and optimization of the lithiation-fluoroacetylation of n-(4-chlorophenyl)-pivalamide', *Industrial & Engineering Chemistry Research*, 50(10), pp. 5982-5991.
- Gogate, P.R. and Kabadi, A.M. (2009) 'A review of applications of cavitation in biochemical engineering/biotechnology', *Biochemical Engineering Journal*, 44(1), pp. 60-72.
- Goldberg, E. (2012) *Handbook of downstream processing*. Springer Science & Business Media.
- Gonzalez, M.A. and Ciszewski, J.T. (2008) 'High conversion, solvent free, continuous synthesis of imidazolium ionic liquids in spinning tube-in-tube reactors', *Organic Process Research & Development*, 13(1), pp. 64-66.
- Grima, E.M., Belarbi, E.-H., Fernández, F.A., Medina, A.R. and Chisti, Y. (2003) 'Recovery of microalgal biomass and metabolites: process options and economics', *Biotechnology Advances*, 20(7), pp. 491-515.
- Guest, D.W. (1997) 'Evaluation of simulated moving bed chromatography for pharmaceutical process development', *Journal of Chromatography A*, 760(1), pp. 159-162.
- Hampton, P.D., Whealon, M.D., Roberts, L.M., Yaeger, A.A. and Boydson, R. (2008) 'Continuous organic synthesis in a spinning tube-in-tube Reactor: TEMPO-catalyzed oxidation of alcohols by hypochlorite', *Organic Process Research & Development*, 12(5), pp. 946-949.
- Harmsen, G.J. (2007a) 'Reactive distillation: The front-runner of industrial process intensification A full review of commercial applications, research, scale-up, design and operation', *Chemical Engineering and Processing*, 46, pp. 774-780.
- Harmsen, G.J. (2007b) 'Reactive distillation: The front-runner of industrial process intensification: A full review of commercial applications, research, scale-up, design and operation', *Chemical Engineering and Processing: Process Intensification*, 46(9), pp. 774-780.
- Harmsen, J. (2010) 'Process intensification in the petrochemicals industry: Drivers and hurdles for commercial implementation', *Chemical Engineering and Processing: Process Intensification*, 49(1), pp. 70-73.
- Hartman, R.L., McMullen, J.P. and Jensen, K.F. (2011) 'Deciding whether to go with the flow: evaluating the merits of flow reactors for synthesis', *Angewandte Chemie International Edition*, 50(33), pp. 7502-7519.
- Heinkel (2017a) *Inverting filter centrifuges*. Available at: <http://www.heinkel.com/products/centrifuges/inverting-filter-f.aspx> (Accessed: 17 Aug).
- Heinkel (2017b) *Nutsche filter*. Available at: <http://www.heinkel.com/products/nutsche-filters-en-filter-dryers.aspx> (Accessed: 17 Aug).
- Hessel, V., Kralisch, D., Kockmann, N., Noël, T. and Wang, Q. (2013) 'Novel Process Windows for Enabling, Accelerating, and Uplifting Flow Chemistry', *ChemSusChem*, 6(5), pp. 746-789.
- Hilden, L., Huuhtanen, T., Rummakko, P., Grumann, A. and Pietikainen, P. (2004) 'Process for the preparation of 1-(3-dimethylaminopropyl)-1-(4-fluorophenyl)-1, 3-dihydroisobenzofuran-5-carbonitrile'. Google Patents.
- Hong, J.-B., Davidson, J.P., Jin, Q., Lee, G.R., Matchett, M., O'Brien, E., Welch, M., Bingenheimer, B. and Sarma, K. (2013) 'Development of a Scalable Synthesis of a Bruton's Tyrosine Kinase Inhibitor via C–N and C–C Bond Couplings as an End Game Strategy', *Organic Process Research & Development*, 18(1), pp. 228-238.

- Hovione (2017) *Spray drying*. Available at: <http://www.hovione.com/products-and-services/contract-manufacturing-services/particle-engineering/technologies/spray-drying> (Accessed: 17 Aug).
- Hydrodynamics (2017) *Cavitation technology*. Available at: <http://hydrodynamics.com/cavitation-technology/> (Accessed: 16 Aug).
- Ishimoto, K., Fukuda, N., Nagata, T., Sawai, Y. and Ikemoto, T. (2013) 'Development of a Scalable Synthesis of a Vascular Endothelial Growth Factor Receptor-2 Kinase Inhibitor: Efficient Construction of a 6-Etherified [1, 2, 4] Triazolo [1, 5-a] pyridine-2-amine Core', *Organic Process Research & Development*, 18(1), pp. 122-134.
- Jacobsen, N.C. and Hinrichsen, O. (2012) 'Micromixing Efficiency of a Spinning Disk Reactor', *Industrial & Engineering Chemistry Research*, 51(36), pp. 11643-11652.
- Jakslund, C.A., Gani, R. and Lien, K.M. (1995) 'Separation process design and synthesis based on thermodynamic insights', *Chemical Engineering Science*, 50(3), pp. 511-530.
- Jiménez-González, C., Poehlauer, P., Broxterman, Q.B., Yang, B.-S., am Ende, D., Baird, J., Bertsch, C., Hannah, R.E., Dell'Orco, P. and Noorman, H. (2011) 'Key green engineering research areas for sustainable manufacturing: a perspective from pharmaceutical and fine chemicals manufacturers', *Organic Process Research & Development*, 15(4), pp. 900-911.
- Johnston, A.M., Levy, W. and Rumbold, S.O. (2001) *AICHE Annual Meeting*.
- Juniper (2017) *Pharmaceutical spray drying*. Available at: <http://www.juniperpharma.com/pharmaceutical-development-services/pharmaceutical-spray-drying/> (Accessed: 17 Aug).
- Kalakul, S., Malakul, P., Siemanond, K. and Gani, R. (2014) 'Integration of life cycle assessment software with tools for economic and sustainability analyses and process simulation for sustainable process design', *Journal of Cleaner Production*, 71, pp. 98-109.
- Karmakar, R., Pahari, P. and Mal, D. (2014) 'Phthalides and Phthalans: Synthetic Methodologies and Their Applications in the Total Synthesis', *Chemical Reviews*, 114(12), pp. 6213-6284.
- Karr, A., Gebert, W. and Wang, M. (1980) 'Extraction of whole fermentation broth with karr reciprocating plate extraction column', *The Canadian Journal of Chemical Engineering*, 58(2), pp. 249-252.
- Katsuragi (2017) *Rotary vacuum drum dryer*. Available at: <http://www.katsuragi.co.jp/en/products/01/drumdryer.html> (Accessed: 8 Jan).
- KetavConsultant (2017) *Agitated thin film dryer*. Available at: <http://www.evaporatorplants.com/agitated-thinflim-dryer-atfd.html> (Accessed: 16 Aug).
- Kiss, N., Brenn, G., Pucher, H., Wieser, J., Scheler, S., Jennewein, H., Suzzi, D. and Khinast, J. (2011) 'Formation of O/W emulsions by static mixers for pharmaceutical applications', *Chemical Engineering Science*, 66(21), pp. 5084-5094.
- KMPS (2017a) *KARR column*. Available at: <https://modularprocess.com/liquid-liquid-extraction/extraction-column-types/karr-columns/> (Accessed: 17 Aug).
- KMPS (2017b) *Rotating disc contactor*. Available at: <https://modularprocess.com/liquid-liquid-extraction/extraction-column-types/rdc/> (Accessed: 17 Aug).
- KMPS (2017c) *Scheibel column*. Available at: <https://modularprocess.com/liquid-liquid-extraction/extraction-column-types/scheibel-columns/> (Accessed: 17 Aug).
- KNAUER (2017) *Simulated moving bed chromatography*. Available at: <http://www.knauer.net/systems-solutions/multicolumn-applications-smb/smb/smb-technique.html> (Accessed: 8 Jan 2017).
- Kockmann, N., Gottsponer, M. and Roberge, D.M. (2011) 'Scale-up concept of single-channel microreactors from process development to industrial production', *Chemical Engineering Journal*, 167(2-3), pp. 718-726.
- Kockmann, N., Kiefer, T., Engler, M. and Woias, P. (2006) 'Convective mixing and chemical reactions in microchannels with high flow rates', *Sensors and Actuators B: Chemical*, 117(2), pp. 495-508.
- Kockmann, N. and Roberge, D.M. (2011) 'Scale-up concept for modular microstructured reactors based on mixing, heat transfer, and reactor safety', *Chemical Engineering and Processing: Process Intensification*, 50(10), pp. 1017-1026.
- Komline-Sanderson (2017) *Rotary drum vacuum filters*. Available at: http://www.komline.com/docs/rotary_drum_vacuum_filter.html (Accessed: 17 Aug).
- Kosaka, M., Sekiguchi, S., Naito, J., Uemura, M., Kuwahara, S., Watanabe, M., Harada, N. and Hiroi, K. (2005) 'Synthesis of enantiopure phthalides including 3-butylphthalide, a fragrance

- component of celery oil, and determination of their absolute configurations', *Chirality*, 17(4), pp. 218-232.
- Kresta, S.M., Etchells III, A.W., Atiemo-Obeng, V.A. and Dickey, D.S. (2015) *Advances in industrial mixing: a companion to the handbook of industrial mixing*. John Wiley & Sons.
- Kuczynski, M., Oyevaar, M.H., Pieters, R.T. and Westerterp, K.R. (1987) 'Methanol synthesis in a countercurrent gas-solid-solid trickle flow reactor. An experimental study', *Chemical Engineering Science*, 42, pp. 1887-1898.
- Kumar, B. and Dixit, G. (2007) 'Amorphous pregabalin and process for the preparation thereof'. Google Patents.
- Laird, T. (2005) 'Cost Estimates for New Molecules', *Organic Process Research & Development*, 9(2), pp. 125-126.
- Laue, S., Haverkamp, V. and Mleczko, L. (2016) 'Experience with Scale-Up of Low-Temperature Organometallic Reactions in Continuous Flow', *Organic Process Research & Development*, 20(2), pp. 480-486.
- Lawton, S., Steele, G., Shering, P., Zhao, L., Laird, I. and Ni, X.-W. (2009) 'Continuous crystallization of pharmaceuticals using a continuous oscillatory baffled crystallizer', *Organic Process Research & Development*, 13(6), pp. 1357-1363.
- LCIcorp (2017) *thin film dryer*. Available at: http://lxicorp.com/assets/documents/thin_film_drying.pdf (Accessed: 17 Aug).
- Leon, M.A., Maas, R.J., Bieberle, A., Schubert, M., Nijhuis, T.A., van der Schaaf, J., Hampel, U. and Schouten, J.C. (2013) 'Hydrodynamics and gas-liquid mass transfer in a horizontal rotating foam stirrer reactor', *Chemical Engineering Journal*, 217(0), pp. 10-21.
- Leon, M.A., Nijhuis, T.A., van der Schaaf, J. and Schouten, J.C. (2012) 'Mass transfer modeling of a consecutive reaction in rotating foam stirrer reactors: Selective hydrogenation of a functionalized alkyne', *Chemical Engineering Science*, 73(0), pp. 412-420.
- Leon, M.A., Tschentscher, R., Nijhuis, T.A., van der Schaaf, J. and Schouten, J.C. (2011) 'Rotating foam stirrer reactor: effect of catalyst coating characteristics on reactor performance', *Industrial & Engineering Chemistry Research*, 50(6), pp. 3184-3193.
- Leuenberger, H. (2001) 'New trends in the production of pharmaceutical granules: batch versus continuous processing', *European Journal of Pharmaceutics and Biopharmaceutics*, 52(3), pp. 289-296.
- Levenspiel, O. and Levenspiel, C. (1972) *Chemical reaction engineering*. Wiley New York etc.
- life, T.i.f. (2017) *HIGEE Technology*. Available at: <https://www.tno.nl/en/focus-areas/industry/sustainable-chemical-industry/efficient-processing/higee-technology/> (Accessed: 16 Aug).
- Likidis, Z. and Schügerl, K. (1987) 'Recovery of penicillin by reactive extraction in centrifugal extractors', *Biotechnology and Bioengineering*, 30(9), pp. 1032-1040.
- Lince, F., Marchisio, D. and Barresi, A. (2009) 'Smart mixers and reactors for the production of pharmaceutical nanoparticles: Proof of concept', *Chemical Engineering Research and Design*, 87(4), pp. 543-549.
- LinnHighTherm (2017) *Microwave heating*. Available at: <https://www.linn-high-therm.de/products/microwave-heating/others.html> (Accessed: 17 Aug).
- Liu, H.-S., Lin, C.-C., Wu, S.-C. and Hsu, H.-W. (1996) 'Characteristics of a Rotating Packed Bed', *Industrial & Engineering Chemistry Research*, 35, pp. 3590-3596.
- Liu, K., Tong, Z., Liu, L. and Feng, X. (2005) 'Separation of organic compounds from water by pervaporation in the production of n-butyl acetate via esterification by reactive distillation', *Journal of Membrane Science*, 256(1), pp. 193-201.
- Liu, W.J., Ma, C.Y., Liu, J.J., Zhang, Y. and Wang, X.Z. (2017) 'Continuous reactive crystallization of pharmaceuticals using impinging jet mixers', *AIChE Journal*, 63(3), pp. 967-974.
- Lode, F., Mazzotti, M. and Morbidelli, M. (2001) 'A new reaction-separation unit: the simulated moving bed reactor', *Chimia*, 55, pp. 883-886.
- Lutze, P., Babi, D.K., Woodley, J.M. and Gani, R. (2013) 'Phenomena Based Methodology for Process Synthesis Incorporating Process Intensification', *Industrial & Engineering Chemistry Research*, 52(22), pp. 7127-7144.
- Lutze, P., Gani, R. and Woodley, J.M. (2010) 'Process intensification: A perspective on process synthesis', *Chemical Engineering and Processing: Process Intensification*, 49(6), pp. 547-558.

- Lutze, P., Román-Martinez, A., Woodley, J.M. and Gani, R. (2012) 'A systematic synthesis and design methodology to achieve process intensification in (bio) chemical processes', *Computers & Chemical Engineering*, 36, pp. 189-207.
- Mahmoudian, M., Noble, D., Drake, C., Middleton, R., Montgomery, D., Piercey, J., Ramlakhan, D., Todd, M. and Dawson, M. (1997) 'An efficient process for production of N-acetylneuraminic acid using N-acetylneuraminic acid aldolase', *Enzyme and Microbial Technology*, 20(5), pp. 393-400.
- Majekodunmi, S.O. (2015) 'A review on centrifugation in the pharmaceutical industry', *American Journal of Biomedical Engineering*, 5(2), pp. 67-78.
- Mansur, M.B., Slater, M.J. and Biscaia Junior, E.C. (2003) 'Reactive extraction of zinc sulfate with bis (2-ethylhexyl) phosphoric acid in a short Kühni column used in batch mode', *Industrial and Engineering Chemistry Research*, 42(17), pp. 4068-4076.
- Marquardt, W.S., Kossack, K., Kraemer (2008) 'A Framework for the Systematic Design of Hybrid Separation Processes', *Chinese Journal of Chemical Engineering*, 16(3), pp. 333-342.
- Matche (2017) *Matches' process equipment cost estimates*. Available at: <http://www.matche.com/equipcost/Default.html>.
- McGlone, T., Briggs, N.E., Clark, C.A., Brown, C.J., Sefcik, J. and Florence, A.J. (2015) 'Oscillatory flow reactors (OFRs) for continuous manufacturing and crystallization', *Organic Process Research & Development*, 19(9), pp. 1186-1202.
- McMinn, W., McLoughlin, C. and Magee, T. (2005) 'Microwave-convective drying characteristics of pharmaceutical powders', *Powder Technology*, 153(1), pp. 23-33.
- Mederos, F.S., Ancheyta, J. and Chen, J. (2009) 'Review on criteria to ensure ideal behaviors in trickle-bed reactors', *Applied Catalysis A: General*, 355(1), pp. 1-19.
- Meeuwse, M., Schaaf, J.v.d. and Schouten, J.C. (2011) 'Multistage Rotor-Stator Spinning Disc Reactor', *AIChE Journal*, 58.
- Meikrantz, D., Macaluso, L., Flim, W., Heald, C., Mendoza, G. and Meikrantz, S. (2002) 'A new annular centrifugal contactor for pharmaceutical processes', *Chemical Engineering Communications*, 189(12), pp. 1629-1639.
- Migliorinia, C., Fillinger, M., Mazzottia, M. and Morbidellib, M. (1999) 'Analysis of simulated moving-bed reactors', *Chemical Engineering Science*, 54, pp. 2475-3480.
- Mohammadi, S., Harvey, A. and Boodhoo, K.V.K. (2014) 'Synthesis of TiO₂ nanoparticles in a spinning disc reactor', *Chemical Engineering Journal*, 258(0), pp. 171-184.
- Molga, E., Lewak, M. and Ciach, M. (2009) *GPE-EPIC Congress*. Venice.
- Mudryk, B., Dung, J.-S., Sapino, C. and Guro, J. (1999) 'Method for removal of residual organic solvents and use thereof in manufacturing pharmaceuticals'. Google Patents.
- Mujumdar, A.S. and Menon, A.S. (1995) 'Drying of solids: principles, classification, and selection of dryers', *Handbook of industrial drying*, 1, pp. 1-39.
- Murphy, D.M., Parker, M. and Sullivan, N.P. (2014) 'The interplay of heat transfer and endothermic chemistry within a ceramic microchannel reactor', *Journal of Thermal Science and Engineering Applications*, 6(3), p. 031007.
- Murru, M., Giorgio, G., Montomoli, S., Ricard, F. and Stepanek, F. (2011) 'Model-based scale-up of vacuum contact drying of pharmaceutical compounds', *Chemical Engineering Science*, 66(21), pp. 5045-5054.
- Nagaki, A., Ichinari, D. and Yoshida, J.-i. (2014a) 'Three-component coupling based on flash chemistry. carbolithiation of benzyne with functionalized aryllithiums followed by reactions with electrophiles', *Journal of the American Chemical Society*, 136(35), pp. 12245-12248.
- Nagaki, A., Imai, K., Ishiuchi, S. and Yoshida, J.i. (2015) 'Reactions of difunctional electrophiles with functionalized aryllithium compounds: remarkable chemoselectivity by flash chemistry', *Angewandte Chemie*, 127(6), pp. 1934-1938.
- Nagaki, A., Takahashi, Y. and Yoshida, J.i. (2014b) 'Extremely Fast Gas/Liquid Reactions in Flow Microreactors: Carboxylation of Short-Lived Organolithiums', *Chemistry—A European Journal*, 20(26), pp. 7931-7934.
- Nagaki, A., Yamada, S., Doi, M., Tomida, Y., Takabayashi, N. and Yoshida, J.-i. (2011) 'Flow microreactor synthesis of disubstituted pyridines from dibromopyridines via Br/Li exchange without using cryogenic conditions', *Green Chemistry*, 13(5), pp. 1110-1113.
- Newby, J.A., Blaylock, D.W., Witt, P.M., Turner, R.M., Heider, P.L., Harji, B.H., Browne, D.L. and Ley, S.V. (2014) 'Reconfiguration of a Continuous Flow Platform for Extended Operation:

- Application to a Cryogenic Fluorine-Directed ortho-Lithiation Reaction', *Organic Process Research & Development*, 18(10), pp. 1221-1228.
- NewcastleUniversity (2017) *Process Intensification*. Available at: <http://www.ncl.ac.uk/engineering/research/chemical/process-intensification/#overview> (Accessed: 8 Jan).
- Nguyen, A.-T., Joo, Y.L. and Kim, W.-S. (2012) 'Multiple feeding strategy for phase transformation of GMP in continuous Couette–Taylor crystallizer', *Crystal Growth & Design*, 12(6), pp. 2780-2788.
- Nijhuis, T.A., Kreutzer, M.T., Romijn, A.C.J., Kapteijn, F. and Moulijn, J.A. (2001) 'Monolithic Catalysts as More Efficient Three-Phase Reactors', *Catalysis Today*, 66, pp. 2-4.
- Nitech (2017) *Examples of NiTech solutions*. Available at: <http://www.nitechsolutions.co.uk/examples-of-nitech-solutions/> (Accessed: 16 Aug).
- Noritake (2017a) *Product information*. Available at: <http://www.noritake.co.jp/eng/products/eeg/mixing/mixer/mix/> (Accessed: 16 Aug).
- Noritake (2017b) *Static mixer T series*. Available at: <http://noritake-engineering.com/mixing-technology/static-mixer/mixing/t-series/> (Accessed: 10 Jan).
- O'Brien, A.G., Horváth, Z., Lévesque, F., Lee, J.W., Seidel-Morgenstern, A. and Seeberger, P.H. (2012) 'Continuous Synthesis and Purification by Direct Coupling of a Flow Reactor with Simulated Moving-Bed Chromatography', *Angewandte Chemie International Edition*, 51(28), pp. 7028-7030.
- Ouchi, T., Battilocchio, C., Hawkins, J.M. and Ley, S.V. (2014) 'Process intensification for the continuous flow hydrogenation of ethyl nicotinate', *Organic Process Research & Development*, 18(11), pp. 1560-1566.
- Ouchi, T., Mutton, R.J., Rojas, V., Fitzpatrick, D.E., Cork, D.G., Battilocchio, C. and Ley, S.V. (2016) 'Solvent-Free Continuous Operations Using Small Footprint Reactors: A Key Approach for Process Intensification', *ACS Sustainable Chemistry & Engineering*, 4(4), pp. 1912-1916.
- Oxley, P., Brechtelsbauer, C., Ricard, F., Lewis, N. and Ramshaw, C. (2000) 'Evaluation of Spinning Disk Reactor Technology for the Manufacture of Pharmaceuticals', *Industrial & Engineering Chemistry Research*, 39(7), pp. 2175-2182.
- Papalexandri, K.P. and Pistikopoulos, E.N. (1996) 'Generalized modular representation framework for process synthesis', *AIChE Journal*, 42(4), pp. 1010-1032.
- Parthasarathy, S., Siah Ying, T. and Manickam, S. (2013) 'Generation and optimization of palm oil-based oil-in-water (O/W) submicron-emulsions and encapsulation of curcumin using a liquid whistle hydrodynamic cavitation reactor (LWHCR)', *Industrial & Engineering Chemistry Research*, 52(34), pp. 11829-11837.
- Patel, R., Patel, M. and Suthar, A. (2009) 'Spray drying technology: an overview', *Indian Journal of Science and Technology*, 2(10), pp. 44-47.
- Paul, E.L., Atiemo-Obeng, V.A. and Kresta, S.M. (2004) *Handbook of industrial mixing: science and practice*. John Wiley & Sons.
- Pelleter, J. and Renaud, F. (2009) 'Facile, fast and safe process development of nitration and bromination reactions using continuous flow reactors', *Organic Process Research & Development*, 13(4), pp. 698-705.
- Peschel, A., Freund, H. and Sundmacher, K. (2010) 'Methodology for the design of optimal chemical reactors based on the concept of elementary process functions', *Industrial & Engineering Chemistry Research*, 49, pp. 10535-10548.
- Peschel, A., Hentschel, B., Freund, H. and Sundmacher, K. (2011a) 'Optimal Reactor Design for the Hydroformylation of Long Chain Alkenes in Biphasic Liquid Systems', in E.N. Pistikopoulos, M.C.G. and Kokossis, A.C. (eds.) *Computer Aided Chemical Engineering*. Elsevier, pp. 1246-1250.
- Peschel, A., Karst, F., Freund, H. and Sundmacher, K. (2011b) 'Analysis and optimal design of an ethylene oxide reactor', *Chemical Engineering Science*, 66(24), pp. 6453-6469.
- Pfautler (2017) *Wiped film evaporator*. Available at: <https://www.pfautler.com/en/products/wiped-film-evaporators> (Accessed: 16 Aug).
- Phillips, C.H. and Symonds, K.T. (2007) *Development of a novel integrated chemical reactor-heat exchanger*. [Online]. Available at: <http://lorien.ncl.ac.uk/ming/pdfs/bhrpaper1.pdf>.
- Plouffe, P., Macchi, A. and Roberge, D.M. (2014) 'From Batch to Continuous Chemical Synthesis—A Toolbox Approach', *Organic Process Research & Development*, 18(11), pp. 1286-1294.

- PMMixers (2017) *Agitated thin film evaporators*. Available at: <http://www.pmmixers.com/evaporators.html> (Accessed: 16 Aug).
- Poehlauer, P., Manley, J., Broxterman, R., Gregertsen, B. and Ridemark, M. (2012) 'Continuous Processing in the Manufacture of Active Pharmaceutical Ingredients and Finished Dosage Forms: An Industry Perspective', *Organic Process Research & Development*, 16(10), pp. 1586-1590.
- Ponce-Ortega, J.M., Al-Thubaiti, M.M. and El-Halwagi, M.M. (2012) 'Process intensification: New understanding and systematic approach', *Chemical Engineering and Processing: Process Intensification*, 53, pp. 63-75.
- POPEscientific (2017) *Wiped film evaporator and vacuum distillation*. Available at: <http://www.popeinc.com/still-products/wiped-film-stills-evaporators> (Accessed: 16 Aug).
- Porta, R., Benaglia, M. and Puglisi, A. (2016) 'Flow chemistry: Recent developments in the synthesis of pharmaceutical products', *Organic Process Research and Development*, 20(1), pp. 2-25.
- Portha, J.-F., Falk, L. and Commenge, J.-M. (2014) 'Local and global process intensification', *Chemical Engineering and Processing: Process Intensification*, 84, pp. 1-13.
- Prandtl, L. and Deans, W. (1953) 'Essentials of fluid dynamics'. JSTOR.
- Prat, L., Devatine, A., Cognet, P., Cabassud, M., Gourdon, C., Elgue, S. and Chopard, F. (2005) 'Performance evaluation of a novel concept "open plate reactor" applied to highly exothermic reactions', *Chemical Engineering and Technology*, 28(9), pp. 1028-1034.
- PRISMpharma (2017) *mixer blender dryer*. Available at: <http://www.mixerblenderdryer.com/tray-dryer.html> (Accessed: 8 Jan).
- Proios, P. and Pistikopoulos, E.N. (2005) 'Generalized Modular Framework for the Representation and Synthesis of Complex Distillation Column Sequences', *Industrial & Engineering Chemistry Research*, 44(13), pp. 4656-4675.
- PSE (2017) *Monolith reactor*. Available at: <https://www.psenderprise.com/sectors/chemicals/reaction/cases/catalyst-monolith-reactors> (Accessed: 16 Aug).
- Pudjiono, P. and Tavare, N. (1993) 'Residence time distribution analysis from a continuous Couette flow device around critical Taylor number', *The Canadian Journal of Chemical Engineering*, 71(2), pp. 312-318.
- Ramshaw, C. (1999) 'Process intensification and green chemistry', *Green Chemistry*, 1(1), pp. G15-G17.
- Rao, D.P., Bhowal, A. and Goswami, P.S. (2004) 'Process Intensification in Rotating Packed Beds (HIGEE): An Appraisal', *Industrial & Engineering Chemistry Research*, 43(4), pp. 1150-1162.
- Rebrov, E.V., de Croon, M.H.J.M. and Schouten, J.C. (2001) 'Design of a microstructured reactor with integrated heat-exchanger for optimum performance of a highly exothermic reaction', *Catalysis Today*, 69(1), pp. 183-192.
- Roberge, D.M., Zimmermann, B., Rainone, F., Gottsponer, M., Eyholzer, M. and Kockmann, N. (2008) 'Microreactor technology and continuous processes in the fine chemical and pharmaceutical industry: is the revolution underway?', *Organic Process Research & Development*, 12(5), pp. 905-910.
- Rong, B.-G., Kolehmainen, E. and Turunen, I. (2008) 'Methodology of conceptual process synthesis for process intensification', in Bertrand, B. and Xavier, J. (eds.) *Computer Aided Chemical Engineering*. Elsevier, pp. 283-288.
- Rong, B.-G., Kolehmainen, E., Turunen, I. and Hurme, M. (2004) 'Phenomena-based methodology for process intensification', in Barbosa-Póvoa, A. and Matos, H. (eds.) *Computer Aided Chemical Engineering*. Elsevier, pp. 481-486.
- Roughley, S.D. and Jordan, A.M. (2011) 'The medicinal chemist's toolbox: an analysis of reactions used in the pursuit of drug candidates', *Journal of medicinal chemistry*, 54(10), pp. 3451-3479.
- Rouhi, A. (2003) 'Innovations bridge batch and continuous processing', *Chemical Engineering News*, 81(28), p. 14.
- RousseletRobotel (2017) *Multistage centrifugal extractors*. Available at: <http://www.rousselet-robotel.com/chemical-fine-chemical-pharmaceutical/multistage-centrifugal-extractors-type-ix/> (Accessed: 17 Aug).
- Roy, J. (2002) 'Pharmaceutical impurities—a mini-review', *AAPs PharmSciTech*, 3(2), pp. 1-8.
- Sapse, A.-M. and Schleyer, P.v.R. (1995) *Lithium chemistry: a theoretical and experimental overview*. John Wiley & Sons.

- Schaber, S.D., Gerogiorgis, D.I., Ramachandran, R., Evans, J.M.B., Barton, P.I. and Trout, B.L. (2011) 'Economic Analysis of Integrated Continuous and Batch Pharmaceutical Manufacturing: A Case Study', *Industrial & Engineering Chemistry Research*, 50(17), pp. 10083-10092.
- Schembecker, G.S.T. (2002) 'Process synthesis for reactive separations', *Chemical Engineering and Processing*, (42), p. 11.
- Schwolow, S., Neumüller, A., Abahmane, L., Kockmann, N. and Röder, T. (2016) 'Design and application of a millistructured heat exchanger reactor for an energy-efficient process', *Chemical Engineering and Processing: Process Intensification*, 108, pp. 109-116.
- Separationprocesses (2017) *Mechanically agitated extractors*. Available at: http://www.separationprocesses.com/Extraction/SE_Chp03c.htm (Accessed: 8 Jan 2017).
- Sharratt, P.N. (1997) *Handbook of batch process design*. Springer Science & Business Media.
- Siddiqui, S.W., Zhao, Y., Kukukova, A. and Kresta, S.M. (2009) 'Characteristics of a Confined Impinging Jet Reactor: Energy Dissipation, Homogeneous and Heterogeneous Reaction Products, and Effect of Unequal Flow', *Industrial & Engineering Chemistry Research*, 48, pp. 7945-7958.
- Sigma-Aldrich (2017) *Micoreactor Technology*. Available at: <http://www.sigmaaldrich.com/technical-documents/articles/chemfiles/micoreactor-technology.html> (Accessed: 8 Jan).
- Sinnott, R. (1999) *Coulson & Richardson's Chemical Engineering: Volume 6/Chemical Engineering Design*. Elsevier Butterworth Heinemann.
- Sivakumar, M., Tang, S.Y. and Tan, K.W. (2014) 'Cavitation technology—a greener processing technique for the generation of pharmaceutical nanoemulsions', *Ultrasonics Sonochemistry*, 21(6), pp. 2069-2083.
- SMS (2017) *Thin film evaporator*. Available at: <http://www.sms-vt.com/technologies/evaporation-technology/thin-film-evaporator/> (Accessed: 17 Aug).
- Snieckus, V. (1990) 'Directed ortho metalation. Tertiary amide and O-carbamate directors in synthetic strategies for polysubstituted aromatics', *Chemical Reviews*, 90(6), pp. 879-933.
- Sollohub, K. and Cal, K. (2010) 'Spray drying technique: II. Current applications in pharmaceutical technology', *Journal of Pharmaceutical Sciences*, 99(2), pp. 587-597.
- Solomon, M.J. and Spicer, P.T. (2010) 'Microstructural regimes of colloidal rod suspensions, gels, and glasses', *Soft Matter*, 6(7), pp. 1391-1400.
- Sonarome (2017) *Spray drying technology*. Available at: <http://sonarome.com/2014/12/02/spray-drying-technology/> (Accessed: 8 Jan).
- Sorbera, L., Revel, L., Martin, L. and Castaner, J. (2001) 'Escitalopram oxalate', *Drugs Future*, 26(2), pp. 115-120.
- Stanetty, P. and Mihovilovic, M.D. (1997) 'Half-Lives of Organolithium Reagents in Common Ethereal Solvents', *The Journal of Organic Chemistry*, 62(5), pp. 1514-1515.
- Stankiewicz, A.I. and Moulijn, J.A. (2000) 'Process intensification: transforming chemical engineering', *Chemical Engineering Progress*, 96(1), pp. 22-34.
- Steinigeweg, S. and Gmehling, J. (2004) 'Transesterification processes by combination of reactive distillation and pervaporation', *Chemical Engineering and Processing: Process Intensification*, 43(3), pp. 447-456.
- Stemmet, C.P., Schaaf, J.V.D., Kuster, B.F.M. and Schouten, J.C. (2006) 'Solid Foam Packings for Multiphase Reactors: Modelling of Liquid Holdup and Mass Transfer', *Chemical Engineering Research and Design*, 84, pp. 1134-1141.
- Sulzer (2017a) *General purpose mixers*. Available at: <http://www.sulzer.com/ms/Products-and-Services/Mixpac-Cartridges-Applications-Static-Mixers/Static-Mixers/General-Purpose-Mixers> (Accessed: 16 Aug).
- Sulzer (2017b) *Kuhni agitated column*. Available at: <http://www.sulzer.com/en/Products-and-Services/Separation-Technology/Liquid-Liquid-Extraction/Kuehni-Agitated-Columns-ECR> (Accessed: 17 Aug).
- Sulzer (2017c) *Reactive distillation technology*. Available at: <https://www.sulzer.com/nl/Products-and-Services/Process-Technology/Reaction-Technology/Reactive-Distillation-Technology> (Accessed: 16 Aug).
- Syrris (2017) *Asia*. Available at: <http://syrris.com/product/asia/> (Accessed: 16 Aug).
- systems, C.p. (2017a) *agitated thin film dryer*. Available at: <http://www.chemprosys.com/products/evaporators/agitated-thin-film-dryer/> (Accessed: 17 Aug).

- Systems, D.P. (2017b) *Nutsche filtration and drying process*. Available at: <http://www.ddpsinc.com/blog-0/understanding-the-nutsche-filtration-and-drying-process> (Accessed: 8 Jan).
- Tarara, T.E., Weers, J.G., Kabalnov, A., Schutt, E.G. and Dellamary, L.A. (2003) 'Methods of spray drying pharmaceutical compositions'. Google Patents.
- Techninistro (2017) *Ceramic honeycomb*. Available at: <https://www.indiamart.com/techinstroexhaustcontrol/ceramic-honeycomb.html> (Accessed: 16 Aug).
- technology, p. (2017) *SepTor Technologies*. Available at: http://www.pharmaceutical-technology.com/contractors/process_automation/sep/ (Accessed: 16 Aug).
- Teoh, S.K., Rathi, C. and Sharratt, P. (2016) 'Practical Assessment Methodology for Converting Fine Chemicals Processes from Batch to Continuous', *Organic Process Research & Development*, 20(2), pp. 414-431.
- Teoh, S.K., Sa-ei, K., Noorulameen, M.S., Toh, Q.Y., Ng, Y.L. and Sharratt, P.N. (2015) 'Sustainability benefits of a continuous phase transfer catalyzed process for a model pharmaceutical intermediate', *Chemical Engineering Research and Design*, 100, pp. 467-480.
- TheilenMaschinenbau (2017) *Belt dryer*. Available at: <http://www.belt-dryer.com/EN/English.html> (Accessed: 17 Aug).
- Tran, T.S., Park, S.J., Yoo, S.S., Lee, T.-R. and Kim, T. (2016) 'High shear-induced exfoliation of graphite into high quality graphene by Taylor–Couette flow', *RSC Advances*, 6(15), pp. 12003-12008.
- Tschentscher, R., Nijhuis, T.A., van der Schaaf, J., Kuster, B.F.M. and Schouten, J.C. (2010a) 'Gas–liquid mass transfer in rotating solid foam reactors', *Chemical Engineering Science*, 65(1), pp. 472-479.
- Tschentscher, R., Spijkers, R.J.P., Nijhuis, T.A., van der Schaaf, J. and Schouten, J.C. (2010b) 'Liquid–Solid Mass Transfer in Agitated Slurry Reactors and Rotating Solid Foam Reactors', *Industrial & Engineering Chemistry Research*, 49(21), pp. 10758-10766.
- Turgeman, E. and Malachi, O. (2006) 'Clopidogrel base suitable for pharmaceutical formulation and preparation thereof'. Google Patents.
- Ufer, A., Mendorf, M., Ghaini, A. and Agar, D.W. (2011) 'Liquid/liquid slug flow capillary microreactor', *Chemical Engineering & Technology*, 34(3), pp. 353-360.
- Uniqsis (2017) *FlowSyn mixer blocks*. Available at: http://www.uniqsis.com/paProductsDetail.aspx?ID=ACC_MIX (Accessed: 16 Aug).
- University, C. (2017) *Oscillatory flow mixing*. Available at: <https://www.ceb.cam.ac.uk/research/groups/rg-p4g/archive-folder/pfg/ofm-folder> (Accessed: 8 Jan 2017).
- Van Gerven, T. and Stankiewicz, A. (2009) 'Structure, energy, synergy, time – The fundamentals of process intensification', *Industrial & Engineering Chemistry Research*, 48(5), pp. 2465-2474.
- Vaxelaire, J. and Puiggali, J. (2002) 'Analysis of the drying of residual sludge: From the experiment to the simulation of a belt dryer', *Drying Technology*, 20(4-5), pp. 989-1008.
- Vehring, R. (2008) 'Pharmaceutical particle engineering via spray drying', *Pharmaceutical research*, 25(5), pp. 999-1022.
- Vicevic, M., Boodhoo, K.V. and Scott, K. (2007) 'Catalytic isomerisation of α -pinene oxide to campholenic aldehyde using silica-supported zinc triflate catalysts: II. Performance of immobilised catalysts in a continuous spinning disc reactor', *Chemical Engineering Journal*, 133(1), pp. 43-57.
- Viklund, C., Svec, F., Fréchet, J.M. and Irgum, K. (1996) 'Monolithic, “molded”, porous materials with high flow characteristics for separations, catalysis, or solid-phase chemistry: control of porous properties during polymerization', *Chemistry of Materials*, 8(3), pp. 744-750.
- Vilar, G., Williams, R.A., Wang, M. and Tweedie, R.J. (2008) 'On line analysis of structure of dispersions in an oscillatory baffled reactor using electrical impedance tomography', *Chemical Engineering Journal*, 141(1), pp. 58-66.
- Visscher, F., van der Schaaf, J., Nijhuis, T.A. and Schouten, J.C. (2013) 'Rotating reactors – A review', *Chemical Engineering Research and Design*, 91(10), pp. 1923-1940.
- Wakeman, R. (1995) 'Selection of equipment for solid/liquid separation processes', *Filtration & Separation*, 32(4), pp. 337-341.

- WALDNER (2017) *Vacuum tray dryer VTP*. Available at: <http://www.processsystems.de/English/Products/Dryingtechnology/VacuumtraydryerVTP/tabid/1326/language/en-US/Default.aspx> (Accessed: 17 Aug).
- Walters, R.H., Bhatnagar, B., Tchessalov, S., Izutsu, K.I., Tsumoto, K. and Ohtake, S. (2014) 'Next generation drying technologies for pharmaceutical applications', *Journal of Pharmaceutical Sciences*, 103(9), pp. 2673-2695.
- Wang, H., Mustaffar, A., Phan, A., Zivkovic, V., Reay, D., Law, R. and Boodhoo, K. (2017) 'A review of process intensification applied to solids handling', *Chemical Engineering and Processing: Process Intensification*, 118, pp. 78-107.
- Ward, D.E. and Rhee, C.K. (1989) 'Chemoselective reductions with sodium borohydride', *Canadian Journal of Chemistry*, 67(7), pp. 1206-1211.
- Wiles, C. and Watts, P. (2012) 'Continuous flow reactors: a perspective', *Green Chemistry*, 14(1), pp. 38-54.
- Williams, D.B.G. and Lawton, M. (2010) 'Drying of Organic Solvents: Quantitative Evaluation of the Efficiency of Several Desiccants', *The Journal of Organic Chemistry*, 75(24), pp. 8351-8354.
- Wong, S.H., Ward, M.C. and Wharton, C.W. (2004) 'Micro T-mixer as a rapid mixing micromixer', *Sensors and Actuators B: Chemical*, 100(3), pp. 359-379.
- Yadav, G.D., Jadhav, Y.B. and Sengupta, S. (2003) 'Selectivity engineered phase transfer catalysis in the synthesis of fine chemicals: reactions of p-chloronitrobenzene with sodium sulphide', *Journal of Molecular Catalysis A: Chemical*, 200(1), pp. 117-129.
- Yadav, G.D. and Lande, S.V. (2006) 'Novelties of kinetics of chemoselective reduction of citronellal to citronellol by sodium borohydride under liquid-liquid phase transfer catalysis', *Journal of Molecular Catalysis A: Chemical*, 247(1), pp. 253-259.
- Yoshida, J.-i., Kim, H. and Nagaki, A. (2011) 'Green and Sustainable Chemical Synthesis Using Flow Microreactors', *ChemSusChem*, 4(3), pp. 331-340.
- Yoshida, J.-i., Takahashi, Y. and Nagaki, A. (2013) 'Flash chemistry: flow chemistry that cannot be done in batch', *Chemical communications*, 49(85), pp. 9896-9904.
- Yoshida, J.i., Nagaki, A. and Yamada, T. (2008) 'Flash chemistry: fast chemical synthesis by using microreactors', *Chemistry—A European Journal*, 14(25), pp. 7450-7459.
- Yoshida, S., Marumo, K., Takeguchi, K., Takahashi, T. and Mase, T. (2014) 'Development of a practical and scalable synthetic route to YM758 monophosphate, a novel if channel inhibitor', *Organic Process Research & Development*, 18(12), pp. 1721-1727.
- Zeynizadeh, B. and Behyar, T. (2005) 'Wet THF as a suitable solvent for a mild and convenient reduction of carbonyl compounds with NaBH₄', *Bulletin of the Chemical Society of Japan*, 78(2), pp. 307-315.
- Zhang, L.-L., Wang, J.-X., Xiang, Y., Zeng, X.-F. and Chen, J.-F. (2011) 'Absorption of Carbon Dioxide with Ionic Liquid in a Rotating Packed Bed Contactor: Mass Transfer Study', *Industrial & Engineering Chemistry Research*, 50, pp. 6957-6964.
- Zhang, Z., Wang, G., Nie, Y. and Ji, J. (2016) 'Hydrodynamic cavitation as an efficient method for the formation of sub-100nm O/W emulsions with high stability', *Chinese Journal of Chemical Engineering*, 24(10), pp. 1477-1480.
- Živković, L.A. and Nikačević, N.M. (2016) 'A method for reactor synthesis based on process intensification principles and optimization of superstructure consisting of phenomenological modules', *Chemical Engineering Research and Design*, 113, pp. 189-205.

Appendices

Appendix A. Amidation Process - Synthesis and Evaluation for Intensification and Sustainability Benefits

A.1 Rheometer study

Shear measurements were performed to evaluate the flow behavior of the solid-liquid reaction mixture. Apparent viscosity and shear elastic modulus were measured at 25 °C using rheometer (Anton Paar MCR 301), using parallel plate geometry (50 mm diameter) as shown in Figure A-1. Samples of different solid concentrations were prepared and poured slowly onto the bottom plate and the upper plate was lowered to the fixed position, leaving 1 mm gap in between. Immediately after the sample was spread onto the rheometer plates, an external casing was lowered to cover the plates to minimize evaporation of solvent into the surrounding. The sample was allowed to rest for 5 minute before commencing the tests. The oscillation frequency was fixed at 10 rad/s and shear strain was varied from 0.0001 to 1. Reaction mixtures with different solid loading were tested: 2.0, 2.5 and 3.5 w/w%. These solid suspensions were prepared individually with lower AC and DIPA concentrations.

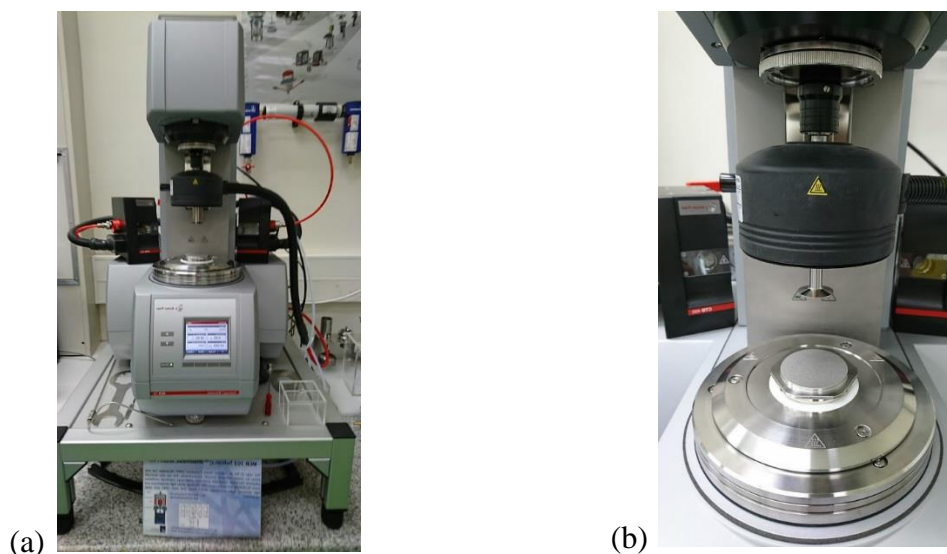


Figure A-1 (a) Anton Paar rheometer; (b) Sample was placed on the plate with an external black casing that can be lowered to minimise solvent evaporation from the sample.

Attempts were made to perform rheological analysis to characterise the flow behaviour of the reaction mixture. However, it was quickly realised that the handling of the sample was challenging. The rheology testing required the suspension to be spread into a thin layer over the plate, it resulted in rapid evaporation of toluene. Dry white powder, which was believed to be a mixture of amine salts and amide 1, was observed on the plate after leaving the sample to settle for 5 minutes before testing despite covering the plates with an external housing.

Unfortunately, it was impossible to perform tests on the white powder as it would not be representative of the original reaction mixture. In order to prevent excessive solvent evaporation, more dilute suspensions of solid loading of 2.0, 2.5, 3.5 w/w% were tested instead of the original 6 w/w%. However, the reproducibility of the tests were not ideal. Figure A-2 shows three repeated test conducted with three different samplings from the same 2 w/w% suspension. It was observed that during sampling, the sample bottles contained precipitant that was difficult to remove from the wall and this might had significant impact on the solid loading of the sample which could affect the consistency.

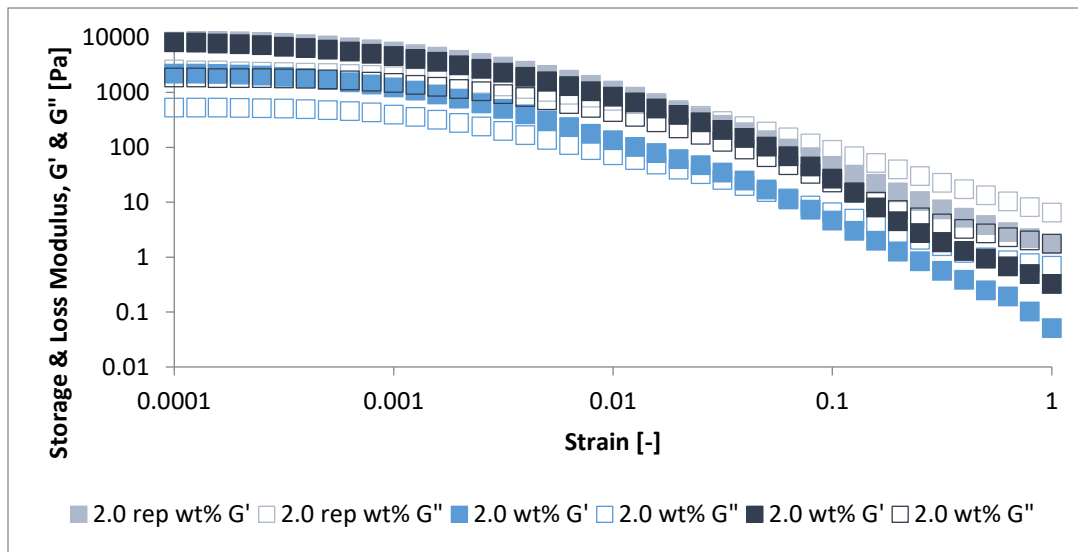


Figure A-2 Sampling reproducibility 2w/w% repeated 3 times

It can be seen from Figure A-3(a) that the suspension becomes more viscous as the solid loading increases. In Figure A-3 (b), the complex viscosity was taken at 100% and plotted against respective samples with different solid loadings and an extrapolated value can be obtained for 6 w/w%, shown in orange, giving a complex viscosity at about 4.5 kPa s, which is considered very viscous (i.e. peanut butter typically liquid viscosity is 250 Pa s at 35 °C). Although the general trend of complex viscosity increasing with higher solid loading, the absolute value of the complex viscosity of suspension at 6 w/w% is questionable due to low reproducibility of the test results.

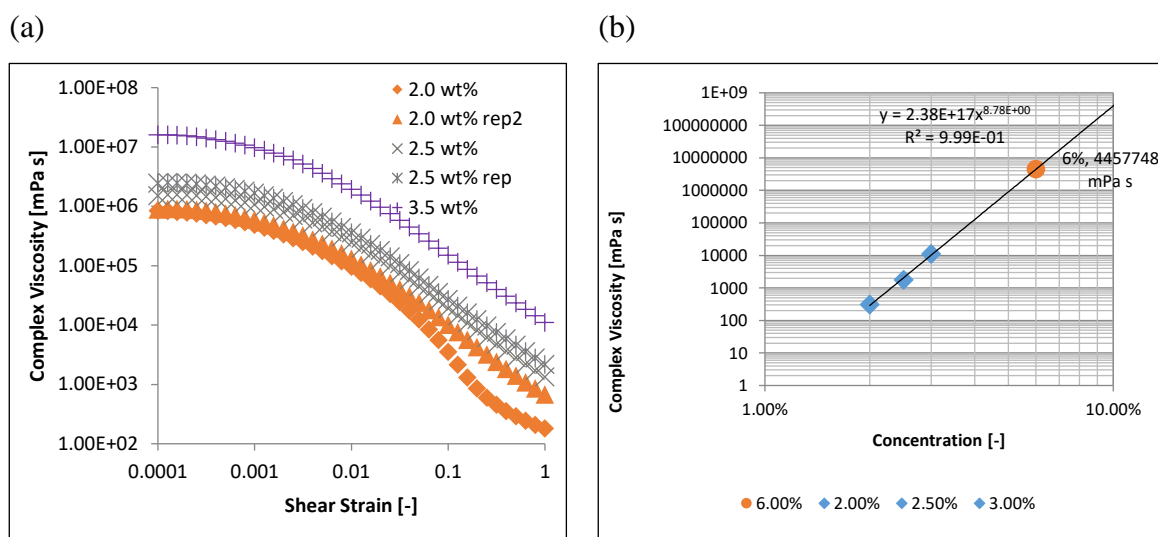


Figure A-3(a) Change in complex viscosity across strain for suspensions with different solid loadings; (b) Complex viscosity for suspensions with different solid loadings at 100% strain.

Nevertheless, the rheology study revealed some insightful understanding about the general physical properties of the suspensions. For example, Figure A-4 shows the storage and loss moduli, G' and G'' , of 2 w/w% suspension against strain. Generally, storage modulus, G' [Pa] is a measure of the material's ability to elastically store energy, which is the solid characteristics of the material. Loss modulus, G'' [Pa] is the material's ability to flow and this is liquid behaviour. The behaviour of the suspension follows the more dominant moduli (greater value). The strain is the amount of deformation (i.e. horizontal displacement divided by vertical sample gap height) the material experiences. It starts from almost undisturbed (i.e. 0.0001) to complete deformation (i.e. 1).

Normally for polymeric gel-like material, it would have a constant G' under very small strain where reversible elastic deformation occurs and the intermolecular interaction would not be disrupted. However, it can be seen in Figure A-4 that the G' has started to decline even at 0.001 strain, signifying weak interactions. The orange zone shows yield zone where strain increase successively disrupts more interactions, hence solid in the suspension loses the ability to elastically store energy.

It can be seen that G' continues to decrease until it is equal to G'' and this is called the flow point, where any increase in strain beyond this point induces flow. This is when all intermolecular interactions are completely broken and the solids in the suspension begin to flow like fluid. It is also the minimum strain required to ensure good mobility and mixing. The green zone shows the flow zone.

In general, it can be observed that the suspension behaved as a viscoelastic solid at low strains, and after a long period of yielding, and began to flow at higher strains, turning into a

viscoelastic liquid. The suspension was identified as yield-stress fluid by its gel-like characteristics and initial resistance to motion (Kresta et al., 2015).

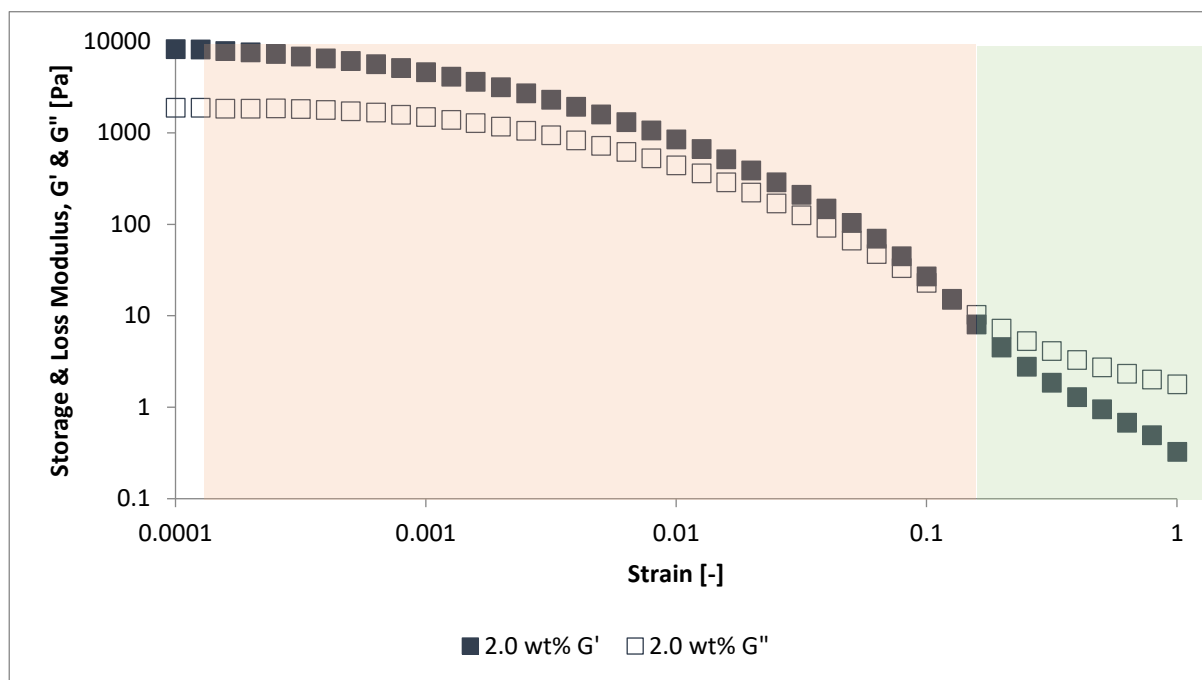


Figure A-4 Change in storage and loss modulus for suspension at 2w/w% solid loading.

A.2 Amidation kinetic study (Batch base case)

Based on the understanding of the microstructure of the suspension, the reaction kinetic study was carried out at a lower AC concentration of 0.04 M (0.5 w/w% solid loading) instead of the literature value of 0.5 M (6 w/w% solid loading). As mentioned earlier, a very dilute suspension is unable to form highly interconnected crystalline structures and would solely behave like a fluid without yield stress properties. This would ensure a homogeneous reaction without the complication of dealing with yield stress fluids so that intrinsic reaction kinetics could be obtained. After several trials with different AC concentrations, 0.04 M was chosen as it resulted in a sufficiently low solid loading of 0.5 w/w% where the reaction mixture appeared non-viscous and translucent. Due to lack of suitable analytical method to identify AC and DIPA, their quantities in the samples could not be quantified, only amide 1 concentration was monitored against time as shown in Figure A-5 below. The respective reaction conditions were tabulated in Table A-1.

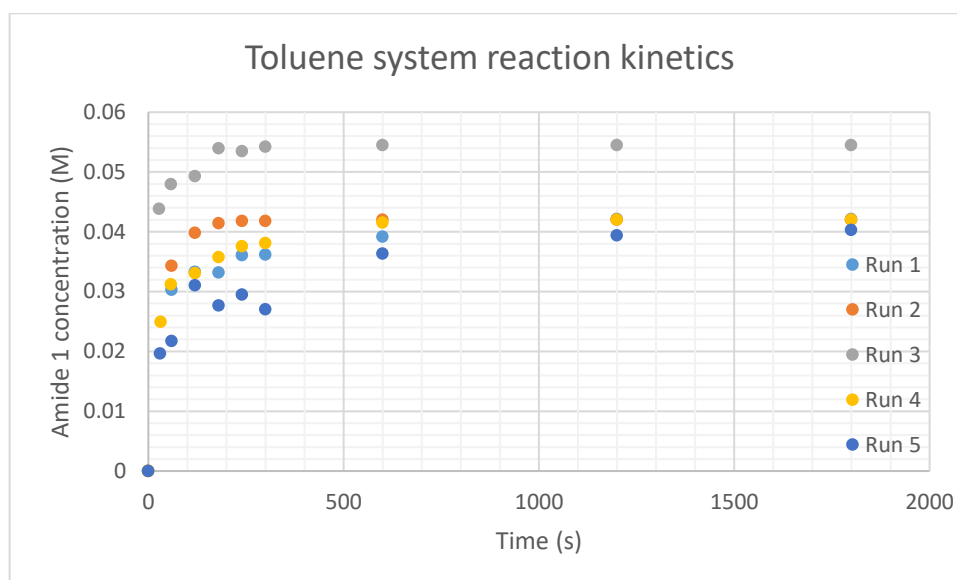
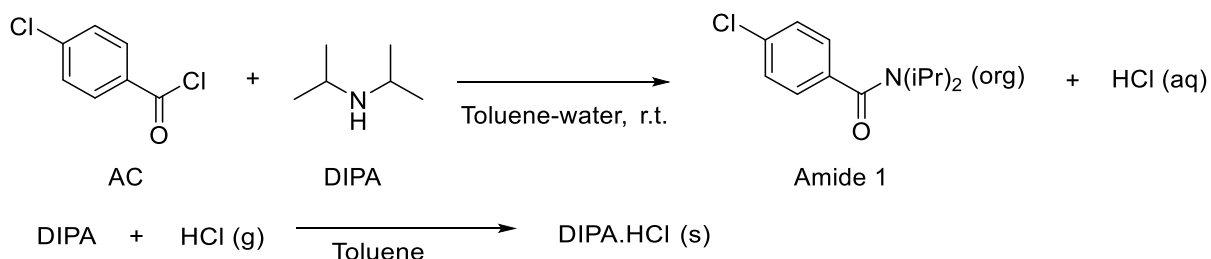


Figure A-5 Kinetic experiments of amidation in the toluene system

Table A-1 Respective reaction conditions of the kinetic experiments

Run	Temperature (°C)	Initial [M]	AC	Initial [M]	DIPA	Rate constant (3 rd order rate equation)	Average rate constant at 20 °C
1	20	0.042		0.11	3.16	2.1	
2	20	0.042		0.20	1.29		
3	20	0.055		0.20	1.83		
4	35	0.042		0.11	6.45		
5	6	0.042		0.11	0.98		

The data obtained from the kinetics study was fitted to kinetic models using the integral analysis method. It was assumed that the second reaction between DIPA and HCl as shown in Scheme A-1 was very fast, with the first step as the rate determining step.



Scheme A-1 “two-step” amidation reaction being considered

The first iteration was undertaken with the simplest form of the irreversible bimolecular-type second order reaction. Unfortunately, the result from the first iteration of overall second-order kinetics cannot reasonably represent the data as shown in Figure A-6 so third-order kinetics was assumed. Figure A-6 (b) showed that the third order kinetics fitted the data better.

First iteration:



$$-r_{\text{AC}} = k[\text{C}_{\text{AC}}][\text{C}_{\text{DIPA}}]$$

Second iteration:



$$-r_{\text{AC}} = k[\text{C}_{\text{AC}}][\text{C}_{\text{DIPA}}]^2$$

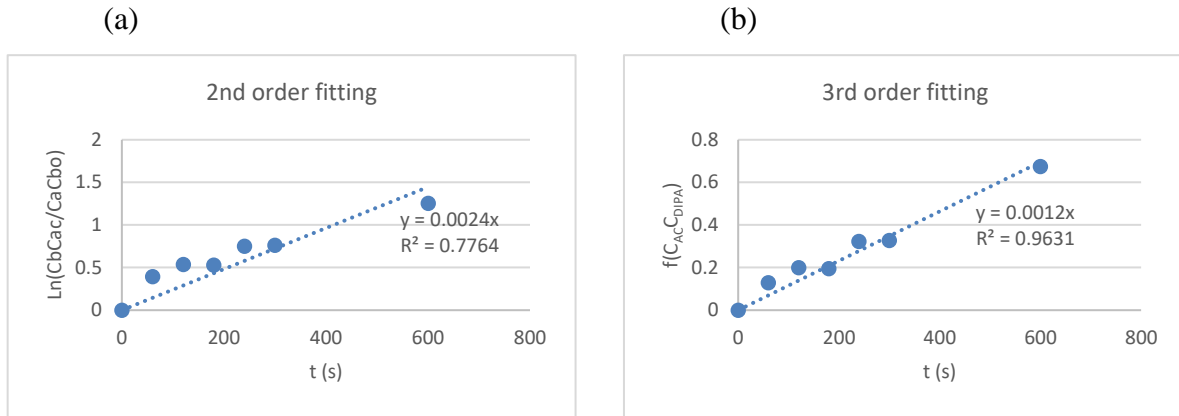


Figure A-6 Test of rate equation by integral analysis method using data from Run 1 as an example of the fittings. (a) Second order rate fitting; (b) third order rate fitting

Therefore, the rate equation that represents the amidation reaction in toluene system is assumed as irreversible trimolecular-type third-order reaction:

$$-r_{\text{AC}} = k C_{\text{AC}} C_{\text{DIPA}}^2 \quad \text{A-2}$$

In terms of conversions the rate of reaction becomes

$$\frac{dX_{\text{AC}}}{dt} = k C_{\text{AC}0}^2 (1 - X_{\text{AC}})(M - 2X_{\text{AC}})^2 \quad \text{A-3}$$

where, $M = \frac{C_{\text{DIPA}0}}{C_{\text{AC}0}}$ (Levenspiel and Levenspiel, 1972)

On integration this gives

$$f(C_{\text{AC}} C_{\text{DIPA}}) = \frac{(2C_{\text{AC}0} - C_{\text{DIPA}0})(C_{\text{DIPA}0} - C_{\text{DIPA}})}{C_{\text{DIPA}0} C_{\text{DIPA}}} + \ln\left(\frac{C_{\text{AC}0} C_{\text{DIPA}}}{C_{\text{AC}} C_{\text{DIPA}0}}\right) = (2C_{\text{AC}0} - C_{\text{DIPA}0})^2 kt \quad \text{A-4}$$

where $(2C_{\text{AC}0} - C_{\text{DIPA}0})^2$ is a constant and k is the gradient.

Using Run 1 in Figure A-5 as an example to obtain rate constant is by plotting $f(C_{\text{AC}} C_{\text{DIPA}})$ against t , k can be found based on the gradient of the line. This was repeated for run 2 to 5 to obtain their respective rate constants as shown in Table A-1. An average rate constant of 2.1 was taken for runs at 20 °C.

Based on the reaction rate constants obtained at 6, 20, 35 °C (279, 293 and 308 K), a graph of $\ln(k)$ against $1/T$ is plotted in Figure A-7. The pre-exponential factor (k_0) was obtained

and the activation energy (E_a) were obtained from the intercept and gradient respectively according to following Arrhenius' Law:

$$k = k_0 e^{\left(-\frac{E_a}{RT}\right)}$$

A-5

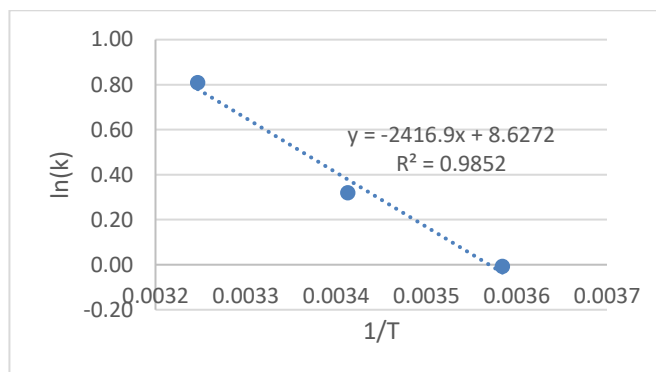


Figure A-7 Temperature dependency of the reaction based on Arrhenius Law

The kinetics parameters of the amidation reaction at 20 °C are summarized in Table A-2.

Table A-2 Kinetics parameters of amidation reaction in toluene system.

Toluene system	Kinetic data
Order of 4-chlorobenzoyl chloride	1
Order of DIPA	2
k at 20°C (L² s²/mol²)	2.1
E_a (kJ/mol)	20
k₀	5581

A.3 Analytical methods

Determination of DIPA.HCl salt concentration

A conductivity meter (Yokogawa FLXA21 Two-wire analyzer, with SC42-EP15 epoxy probe) was calibrated using different concentration of DIPA.HCl solutions as shown in Figure A-8. Prior to this, an amidation experiment was performed to obtain DIPA.HCl solids by filtering the reaction mixture, wash with toluene and oven dried. The calibration sample solutions were prepared by weighing exact amounts of DIPA.HCl dissolved in deionised water. To determine the DIPA.HCl formed during the amidation reaction, minimum volume of water (0.28 L/mol AC) was added to the reaction mixture slurry to dissolve the DIPA.HCl, followed by phase separation to obtain the mass of the aqueous layer. Assuming 100 % conversion and all the HCl formed is converted to DIPA.HCl and dissolved in the aqueous layer, the aqueous DIPA.HCl concentration is expected to be about 490 g/L. A 20x dilution of the aqueous layer

with water brought the concentration to within the detection range for the conductivity meter (about 25 g/L).

The equation for the calibration curve (Figure A-8) is obtained as follows:

$$\text{Conductivity reading (mS/cm)} = 0.80205 (\text{aq. DIPA.HCl})^{0.8665}$$

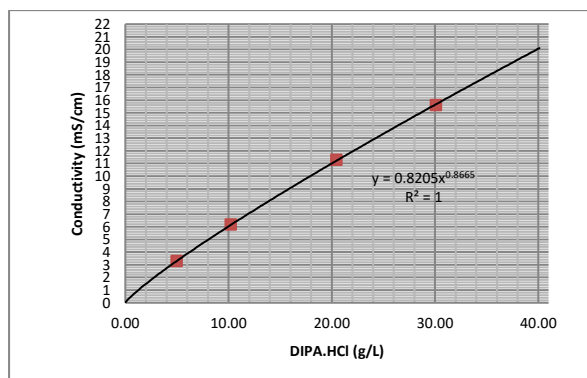


Figure A-8 Conductivity calibration for aqueous solution of DIPA.HCl salt

Method of analysis and sample collection

Samples were collected at particular time intervals and analyzed using the internal standard method. The amide 1 yield/ determined by Gas Chromatography (GC) using Agilent Technologies 6890N GC system with 7693 autosampler and a HP-5 column. Temperature ramp: 150 to 210 °C, 25 °C/min; run time: 15 min; post run: 280 (5 min); injection volume: 1 µl; detector temperature: 280 °C, control mode: constant pressure; pressure: 11.02 psi. Response factor of amide 1 was determined by calibration using n-hexadecane as the internal standard as shown in Figure A-9.

First, the samples were collected for a fixed time interval and weighed. About 1 mL of reaction mixture was taken and weighed separately, to which 1 mL of quench water was added. Followed by the addition of 50 mg of internal standard and mixed well. Lastly, 20 µL of the organic layer was drawn and diluted in 1 mL of ethyl acetate.

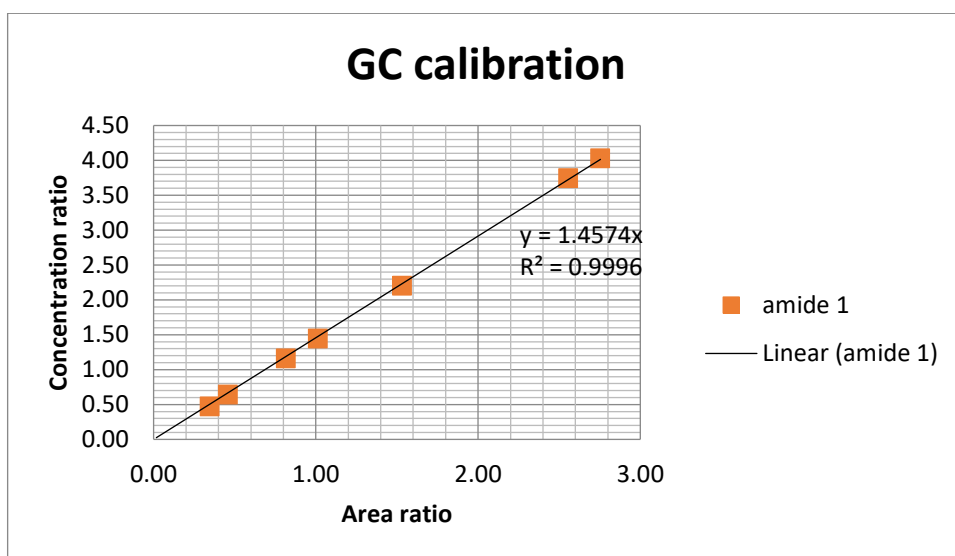


Figure A-9 Response factor for amide 1 using internal standard method

A.4 Amidation in toluene-water solvent system (*Intensified batch case*)

For toluene-water system, the main aim is to minimise the mixing limitation experienced in the toluene system at high AC concentration by dissolving the solid amine salt in the water present in the system during the reaction. The experiment was conducted by preparing DIPA in toluene. Water was subsequently added to the DIPA solution, where minimum amount of water needed to dissolve all the amine salt was used, based on solubility of DIPA.HCl in water (500 g/L).

The experimental data is as shown in Figure A-10 and the reaction was completed within 5 min which is likely to be faster than reaction in the toluene system with solid loading of 6 w/w%. Based on visual observation during the reaction, there was no accumulation of amine salt, the reaction mixture appeared cloudy as the organic and aqueous phases seemed well dispersed. This indicated that the absence of amine salt during the reaction is able to minimise the mixing limitation significantly. With this understanding higher reaction concentrations can be considered, primarily aimed at reducing the toluene usage and increasing material efficiency while maintaining good mixing. To validate this idea, the amount of toluene was reduced by half so the AC and DIPA initial concentrations (in toluene) became 1 M and 2.1 M respectively. The experimental data in Figure A-10 shows that full conversion was reached in less than 90 s, which did not deviate too much from the calculated reaction time of 72 s based on the rate equation (Table A-2). This proved that the toluene-water system is robust and does not encounter significant deterioration in mixing performance even with more concentrated reaction mixture. Even though the toluene-water system might be capable of operating at even higher reagent concentrations, the decision is to maintain the initial AC and DIPA

concentrations at 1 M and 2.1 M, as AC had limited solubility in toluene and it might require a longer time for complete dissolution of the reagents in toluene.

Based on the rate equation in Eqs. (A-5), the apparent rate constant, k_{TW} , obtained at 20 °C for the toluene-water system is $1.3 \text{ L}^2\text{s}^2/\text{mol}^2$. Compared to the ‘intrinsic’ rate constant of $2.1 \text{ L}^2\text{s}^2/\text{mol}^2$, the value of k_{TW} is smaller as the reaction in the toluene-water system is slower than in the toluene system (without mixing limitation). One possible reason for this could be that DIPA is also soluble in water (100 g/L) so the concentration of DIPA in toluene could be diluted by the addition volume of water. Consequently, DIPA dissolved in the aqueous phase might experience liquid-liquid mass transfer limitation as it is required to diffuse back into organic phase to react with AC which is insoluble in the aqueous layer.

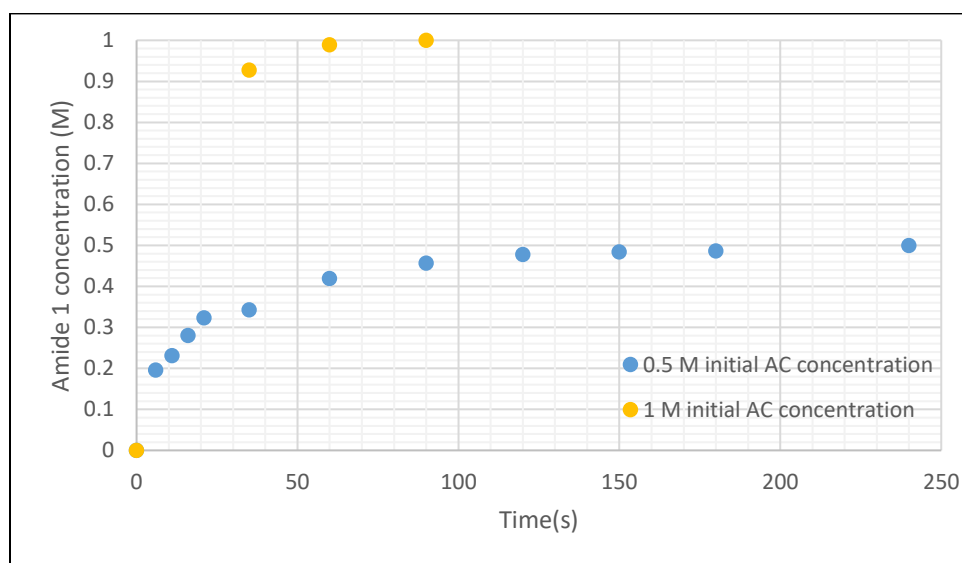


Figure A-10 Rate of amidation reaction in toluene-water solvent system in batch.

$$-r_{AC} = 1.3C_{AC}C_{DIPA}^2$$

A-6

A.5 THF drying study

To assess the drying efficiency of various desiccant, pure THF was washed with 1 M NaCl solution, and the organic layer (‘wet’ THF) isolated and analysed via Karl Fischer titration. Preliminary results with anhydrous MgSO_4 as the drying agent (Figure A-11), shows that a water content of 1 w/w% is the limit. Also, the greater the desiccant loading, the more solvent is lost as it is being trapped within the desiccant matrix.

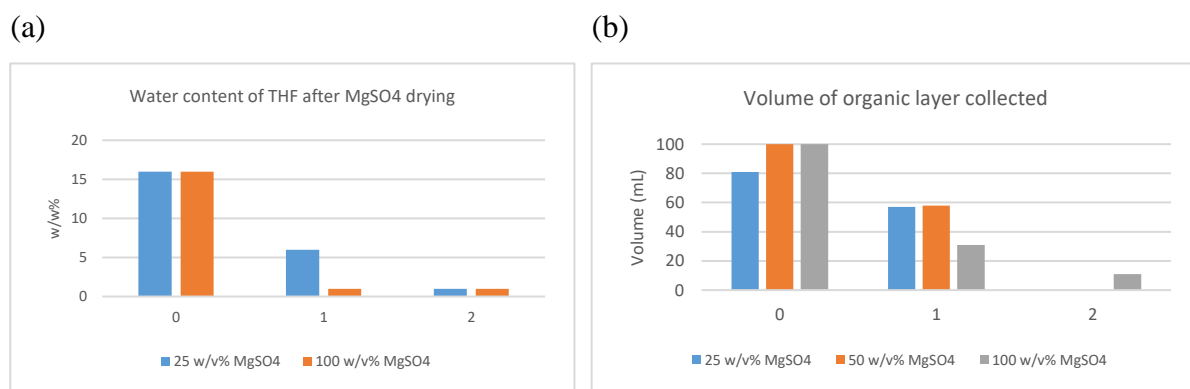


Figure A-11 Drying of 'wet' THF with various loading of MgSO₄. x-axis means 0- after separation from 1 M NaCl; 1- after 1st pass through desiccant; 2- after 2nd pass through fresh desiccant.

Following this, using neutral alumina as the drying agent, as shown in Figure A-12, gave disappointing results as well. It was not able to obtain the results as reported in the literature (Williams and Lawton, 2010).

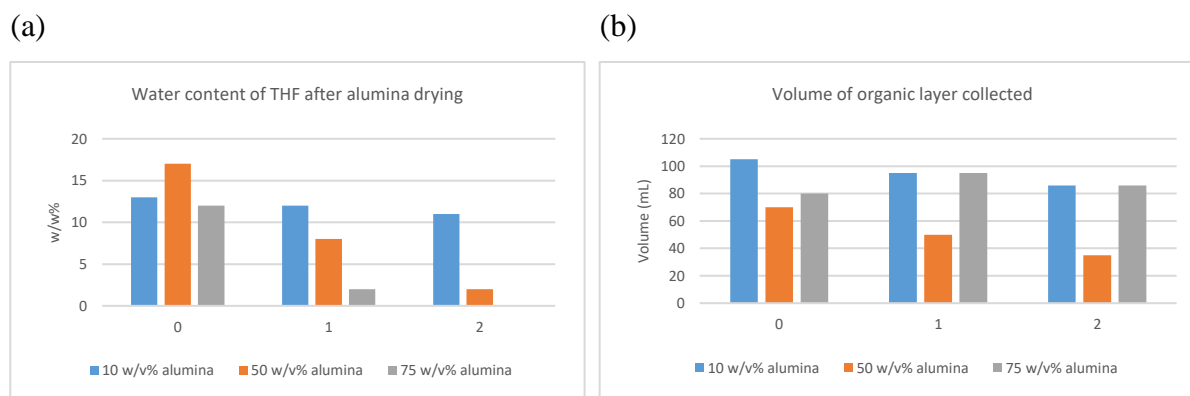


Figure A-12 Drying of 'wet' THF with various loading of neutral alumina. x-axis means 0- after separation from 1 M NaCl; 1- after 1st pass through desiccant; 2- after 2nd pass through fresh desiccant.

Subsequently it was found that the solvent that was trapped within the alumina plug should not be eluted during the process as that would increase the water content of the collected solvent significantly. It is reasoned that alumina acts as a desiccant by adsorption of water present in the solvent; hence drying the alumina plug by eluting the residual solvent would elute the adsorbed water as well. By only collecting the THF that passes through the alumina plug without the need to apply additional pressure, it is able to obtain a THF solvent that meets the specification for the subsequent lithiation reaction. Unfortunately, the high loading of alumina required suggests that the loss of amide product whilst passing it through the alumina plug would be too high to make this a viable process.

A.6 Sustainability performance

1. Batch base case

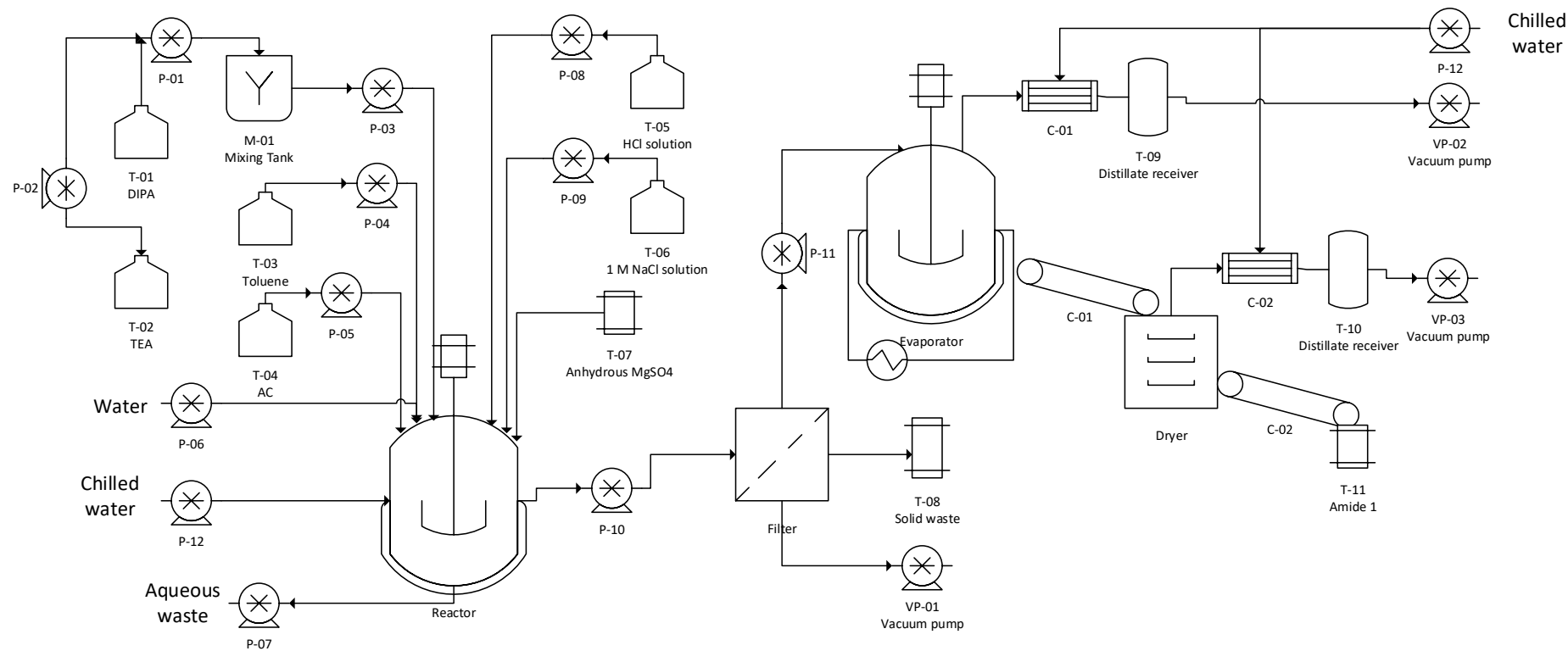


Figure A-13 Schematic process diagram for base case

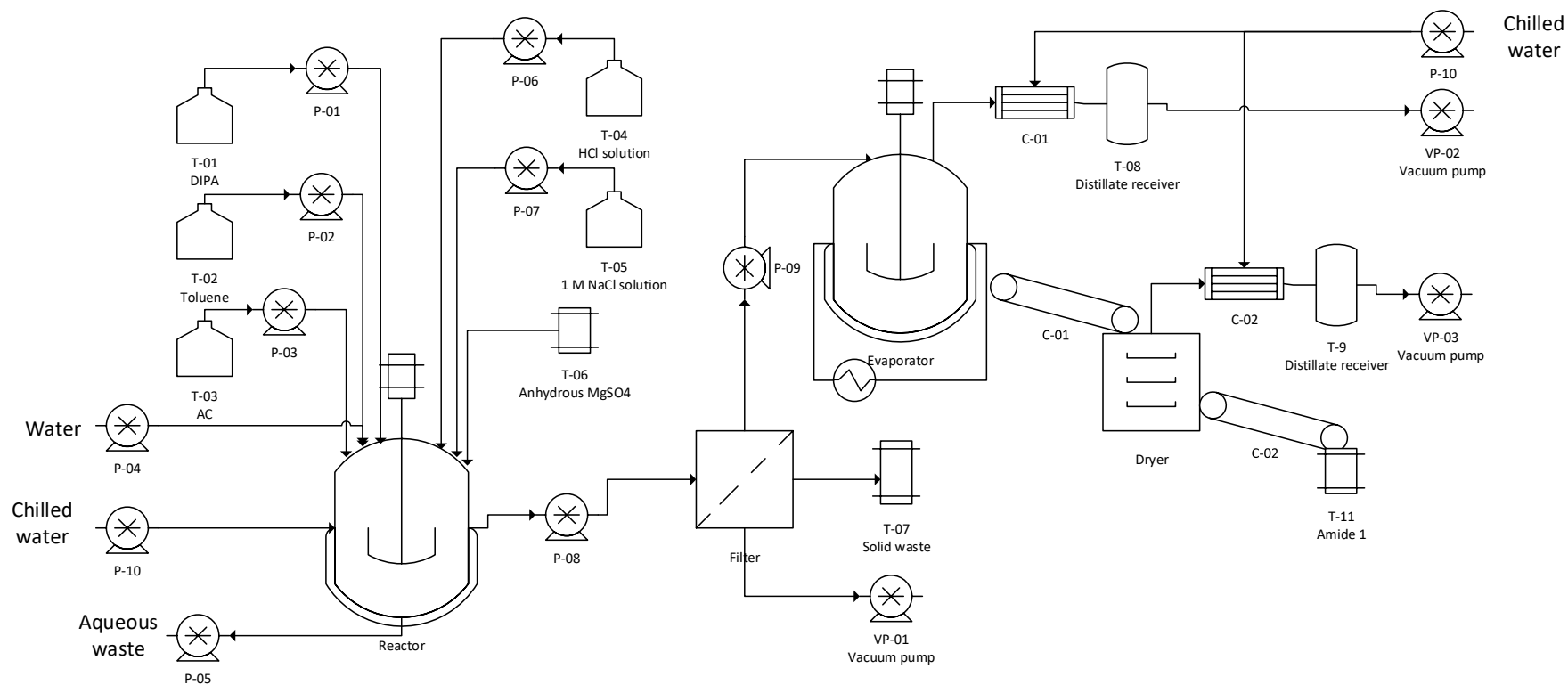
2. *Intensified batch case – similar to batch base case*

Figure A-14 Schematic process diagram for base case

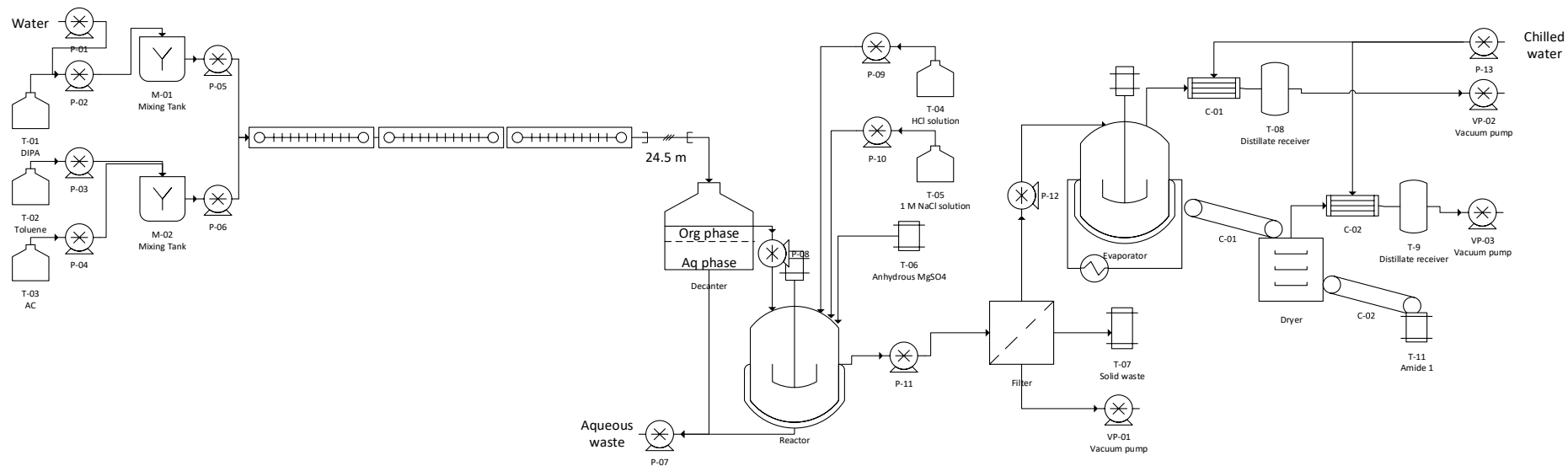
3. *Continuous reaction case*

Figure A-15 Schematic process diagram for continuous reaction case

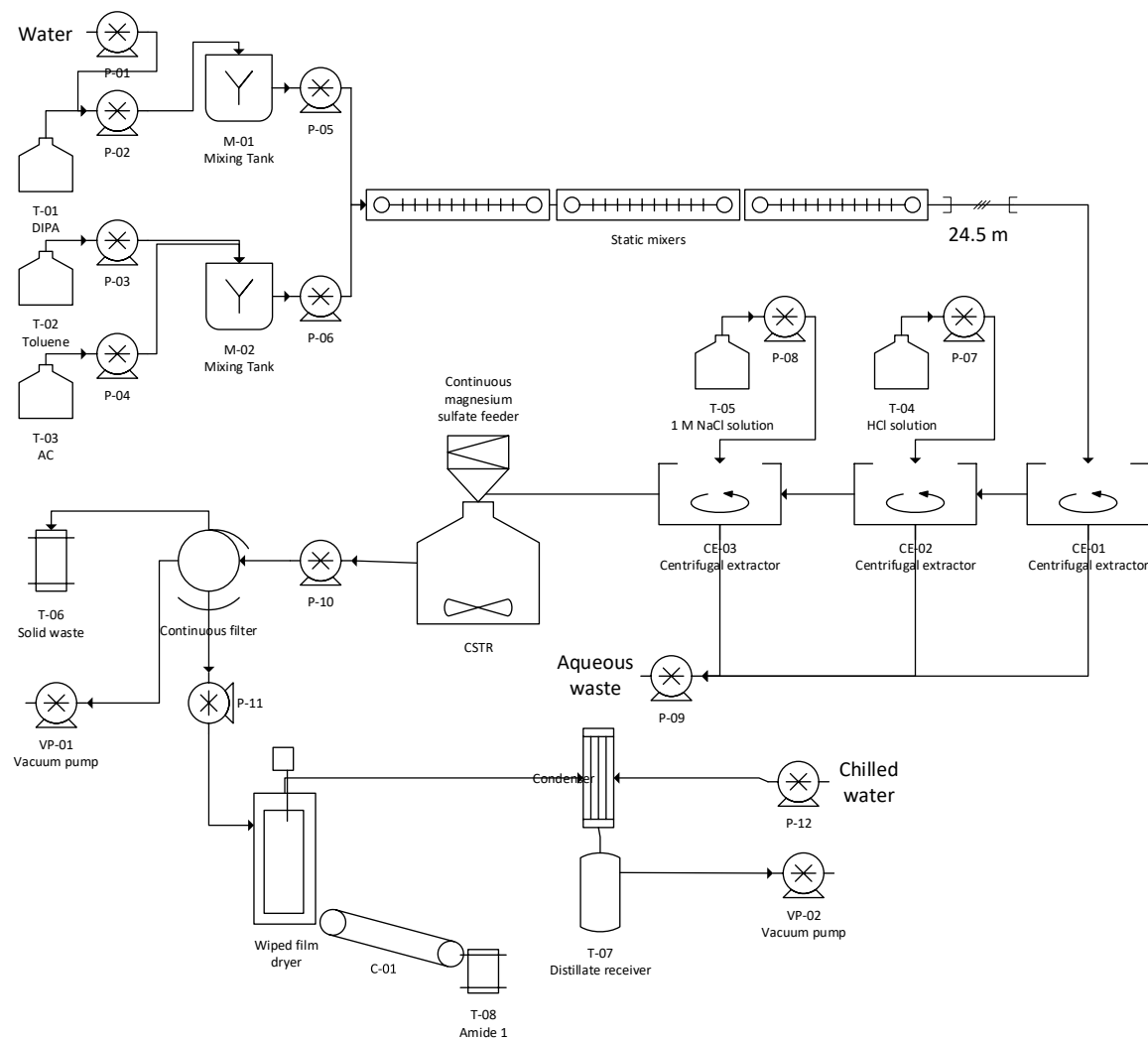
4. *Continuous process case*

Figure A-16 Schematic process diagram for continuous process.

A.7 Sustainability metrics

1. Batch base case

Total material efficiency (kg material/kg product)	20.8	Raw materials	kg/year	kg material/kg prod	Weightage
Total material efficiency (kg product/kg material)	0.047985	Toluene	31263	9	45
		AC	2708	1	4
		DIPA	2350	1	3
		TEA	2350	1	3
		Water	10273	3	15
		HCl solution	11266	3	16
		NaCl solution	8158	2	12
		MgSO4	1257	0	2
			69626	21	100

Total Energy Efficiency (kJ/kg prod)	454784	Energy	kJ/year	kJ/kg product	Weightage
		Agitation	498157264	149103	33
		Pump duties	2160000	647	0
		Heating	1019130372	305035	67
			1519447636	454784	100

Waste index		Waste	kg/year	kg/kg prod	weightage
Total waste/total product	19.81787	Aqueous waste	33587	10	51
		Org waste	31262.71241	9	47
		solid waste	1362.590047	0	2
			66212.13586	20	100
Total OPEX per year (USD)	1234196	Raw materials	USD/year	USD/kg prod	weightage
Total OPEX per year (USD/kg prod)	369.4055	Toluene	319954	96	28
Weightage		AC	426865	128	37
Waste treatment	3.785902	DIPA	158321	47	14
energy and utilities	3.934994	TEA	132967	40	12
raw materials	92.2791	Water	9	0	0
		HCl solution	39945	12	4

		NaCl solution	13978	4	1
		MgSO4	46867	14	4
			1138905	341	100
		Energy and Utilities	USD/year	USD/kg prod	Weightage
		Electricity consumption	48017	14	99
		Chilled water consumption	549	0	1
			48566	15	100
		Waste treatment	USD/year	USD/kg prod	Weightage
		Aqueous waste	23321	7	50
		Organic waste	12697	4	27
		Solid waste	958	0	2
		IBC	9750	3	21
			46725	14	100

Total CAPEX	253762	Equipment	USD
Reaction eqpt (%)	93	Pumps	19630
workup eqpt (%)	6	vacuum pump	10740
CAPEX per kg prod (USD/kg prod)	75.95326	Toluene storage tank (for 1 week)	751.9698017
		DIPA storage tank	217.828306
		TEA storage tank	217.828306
		AC storage tank	165.9574856
		Distillate receiver 1	247.8629509
		Distillate receiver 2	5.968728004
		Condenser	2000
		Reactor jacketed, agitated	4184
		Evaporator jacketed, agitated	3531
		Agitator	2700
		Filter	5000
		Dryer	3500
		conveyor	1000
		Mixing tank	100
		Total	53992
		Lang factor for Liquid system (ref: C&R)	4.7
		Total CAPEX	253762

2. *Intensified batch case*

Total material efficiency (kg material/kg product)	6.4	Raw materials	kg/year	kg material/kg prod	Weightage
Total material efficiency (kg product/kg material)	0.155384	Toluene	1340	0	6
		AC	2708	1	13
		DIPA	3290	1	15
		Water	4242	1	20
		HCl solution	1127	0	5
		NaCl solution	8183	2	38
		MgSO4	611	0	3
			21502	6	100

Total Energy Efficiency (kJ/kg prod)	149927	Energy	kJ/year	kJ/kg product	Weightage
		Agitation	82798807	24782	17
		Pump duties	5616000	1681	1
		Heating	412496703	123464	82
			500911509	149927	100

Waste index		Waste	kg/year	kg/kg prod	weightage
Total waste/total product	5.012852	Aqueous waste	16048	5	96
		solid waste	700.3155911	0	4
			16748.09965	5	100

Total OPEX per year (USD)	734682	Raw materials	USD/year	USD/kg prod	weightage
Total OPEX per year (USD/kg prod)	219.8966	Toluene	13712	4	2
Weightage		AC	426865	128	61
Waste treatment	1.894885	DIPA	221649	66	32
energy and utilities	2.414546	Water	4	0	0
raw materials	95.69057	HCl solution	3995	1	1
		NaCl solution	14021	4	2
		MgSO4	22775	7	3
			703021	210	100
		Energy and Utilities	USD/year	USD/kg prod	Weightage
		Electricity consumption	17309	5	98

		Chilled water consumption	430	0	2
			17739	5	100
		Waste treatment	USD/year	USD/kg prodt	Weightage
		Aqueous waste	11029	3	79
		Solid waste	492	0	4
		IBC	2400	1	17
			13921	4	100

Total CAPEX	210474	Equipment	USD
Reaction eqpt (%)	92	Pumps	16610
workup eqpt (%)	8	vacuum pump	10740
CAPEX per kg prodt (USD/kg prodt)	62.9968	Toluene storage tank (for 1 week)	513.6105105
		DIPA storage tank	262.11069
		AC storage tank	165.9574856
		Distillate receiver 1	87.87988262
		Distillate receiver 2	3.528957654
		Condenser	2000
		Reactor jacketed, agitated	1697
		Evaporator jacketed, agitated	1402
		Agitator	1800
		Filter	5000
		Dryer	3500
		conveyor	1000
		Total	44782
		Lang factor for Liquid system (ref: C&R)	4.7
		Total CAPEX	210474

3. Continuous reaction case

Total material efficiency (kg material/kg product)	15.0	Raw materials	kg/year	kg material/kg prodt	Weightage
Total material efficiency (kg product/kg material)	0.066813	Toluene	1340	0	3
		AC	2708	1	5
		DIPA	3290	1	7
		Water	32747	10	65

		HCl solution	1127	0	2
		NaCl solution	8183	2	16
		MgSO4	611	0	1
			50006	15	100

Total Energy Efficiency (kJ/kg prod)	167069	Energy	kJ/year	kJ/kg product	Weightage
		Agitation	47405703	14189	8
		Pump duties	98280000	29416	18
		Heating	412496703	123464	74
			558182405	167069	100

Waste index		Waste	kg/year	kg/kg prod	weightage
Total waste/total product	13.5444	Aqueous waste	44552	13	98
		solid waste	700.3155911	0	2
			45252.28468	14	100

Total OPEX per year (USD)	758695	Raw materials	USD/year	USD/kg prod	weightage
Total OPEX per year (USD/kg prod)	227.0839	Toluene	13712	4	2
Weightage		AC	426865	128	61
Waste treatment	4.982391	DIPA	221649	66	32
energy and utilities	2.352496	Water	28	0	0
raw materials	92.66511	HCl solution	3995	1	1
		NaCl solution	14021	4	2
		MgSO4	22775	7	3
			703045	210	100
		Energy and Utilities	USD/year	USD/kg prod	Weightage
		Electricity consumption	17344	5	97
		Chilled water consumption	505	0	3
			17848	5	100
		Waste treatment	USD/year	USD/kg prod	Weightage
		Aqueous waste	31159	9	82
		Solid waste	492	0	1
		IBC	6150	2	16
			37801	11	100

Total CAPEX	228581	Equipment	USD
Reaction eqpt (%)	89	Pumps	21140
workup eqpt (%)	7	vacuum pump	10740
CAPEX per kg prodt (USD/kg prodt)	68.41627	Toluene storage tank (for 1 week)	513.6105105
		DIPA storage tank	262.11069
		AC storage tank	165.9574856
		Distillate receiver 1	77.7300525
		Distillate receiver 2	3.121374944
		Condenser	2000
		Reactor jacketed, agitated	116
		Evaporator jacketed, agitated	1240
		Agitator	900
		Filter	5000
		Dryer	3500
		conveyor	1000
		DIPA mixing tank	136
		AC mixing tank	90
		static mixer	1581
		Decanter	168
		Total	48634
		Lang factor for Liquid system (ref: C&R)	4.7
		Total CAPEX	228581

4. Continuous process case

Total material efficiency (kg material/kg product)	14.7	Raw materials	kg/year	kg material/kg prodt	Weightage
Total material efficiency (kg product/kg material)	0.067946	Toluene	1340	0	3
		AC	2710	1	6
		DIPA	3290	1	7
		Water	32747	10	67
		HCl solution	1127	0	2

		NaCl solution	7348	2	15
		MgSO4	611	0	1
			49172	15	100

Total Energy Efficiency (kJ/kg prod)	420338	Energy	kJ/year	kJ/kg product	Weightage
		Agitation	918651079	274960	65
		Pump duties	56160000	16809	4
		Heating	371952000	111328	26
		Filtration	57600000	17240	4
			1404363079	420338	100

Waste index		Waste	kg/year	kg/kg prod	weightage
Total waste/total product	13.2944	Aqueous waste	43717	13	98
		solid waste	700	0	2
			44417.00664	13	100

Total OPEX per year (USD)	844738	Raw materials	USD/year	USD/kg prod	weightage
Total OPEX per year (USD/kg prod)	252.8374	Toluene	13712	4	2
Weightage		AC	427081	128	61
Waste treatment	4.407158	DIPA	221649	66	32
energy and utilities	12.51031	Water	28	0	0
raw materials	83.08254	HCl solution	3995	1	1
		NaCl solution	12590	4	2
		MgSO4	22775	7	3
			701830	210	100
		Energy and Utilities	USD/year	USD/kg prod	Weightage
		Electricity consumption	43636	13	41
		Chilled water consumption	62044	19	59
			105679	32	100
		Waste treatment	USD/year	USD/kg prod	Weightage
		Aqueous waste	30587	9	82
		Solid waste	492	0	1
		IBC	6150	2	17

			37229	11	100
--	--	--	-------	----	-----

Total CAPEX	485638	Equipment	USD
		Pumps	19630
		vacuum pump	7160
CAPEX per kg prodt (USD/kg prodt)	145.3556	Toluene storage tank (for 1 week)	539.0838901
		DIPA storage tank	275.1105118
		AC storage tank	174.1878951
		Distillate receiver 1	5490.751888
		Condenser	1000
		CSTR	242
		Wiped film dryer	19000
		Agitator	900
		Continuous filter	7250
		conveyor	500
		DIPA mixing tank (50 L)	193
		AC mixing tank (50 L)	193
		static mixer	1581
		Automatic screw feeder	9200
		CE	30000
		Total	103327
		Lang factor for Liquid system (ref: C&R)	4.7
		Total CAPEX	485638

Appendix B. Ortho-Lithiation Process – Part 1: Process Understanding

B.1 *In-situ IR monitoring of ortho-lithiation in STR*

Prior to the experiment, the 50 mL round bottom flask (RBF) was purged with nitrogen gas for 30 minutes. 0.21 g of amide 1 was dissolved in 20 mL of THF (0.044 M) and stirred at 500 rpm using the magnetic stirrer. The reactor was closed and cooled down to $-60\text{ }^{\circ}\text{C}$ which was the lowest attainable temperature for the setup.

The IR spectroscopy was carried out using Bruker Matrix-MR-ex, Mid IR ATR-FTIR with the IN350-T Fiber Probe and measures spectra range from 3500 to 720 cm^{-1} as shown in Table B-1. An exposure of 0.5 s with four acquisitions was employed for a single scan in this study. IR probe was submerged in the THF solution and the background spectra were taken using the initial reaction mixture as a reference.

Table B-1 Bond frequencies of major species present in the reaction.

Species	Band assignments	Frequency (cm^{-1})
Amide 1	C=O stretching of the amide	1585
Intermediate		1633
Aldehyde 1	Two C=O stretches	1700 and 1620
THF (solvent)		1633

The concentration of n-BuLi used was estimated to be 1.38 M. The reaction was started by dosing 0.2 mL (0.28 mmol, 0.3 amide 1 equivalents) of n-BuLi, after waiting for about 2 minutes, the second and third doses of 0.2 mL were added, each dose was followed by a 2 minutes wait. The fourth dose was 0.12 mL (0.17 mmol, 0.2 amide 1 equivalents)

Unfortunately, the solvent and intermediate peaks overlap at 1633 cm^{-1} , but they were able to resolve the intermediate peak through the use of BTEM curve resolution and multiple linear regression. In situ IR was used to investigate the rate of intermediate formation at 1633 cm^{-1} and starting material depletion at 1585 cm^{-1} .

Several studies has been done using in-situ IR (Godany et al., 2011; Newby et al., 2014) to monitor batch lithiation reactions but they were not extended to kinetic study. There is no existing published information on fundamental kinetic information on ortho-lithiation that is needed for the determination of the order of reaction for the reagents to date. Beak and Snieckus (1982) explained that the reaction mechanism for ortho-lithiation is very complex and specified which is dependent on the effects of many factors (e.g. aggregation, ion association, complexation and temperature, etc.) in order to speculate on the reaction mechanism. Initially, attempts were made to examine the possibility of tracking the reaction by offline GC and samples were taken in the shortest time possible (every 2 min). However, it was found that

sampling was a major challenge as it was impossible to maintain the reaction temperature during sampling. There was no meaningful result obtained from the GC samples.

In situ IR spectroscopy was successfully used to track the formation of the desired intermediate at $-60\text{ }^{\circ}\text{C}$. IR spectroscopy showed some overlapping peaks between THF and intermediate, but the overlapped peak could be deconstructed using band-target entropy minimization (BTEM) curve resolution algorithm (BTEM) successfully recovered the intermediate peak. The depleting starting material peaks and increasing intermediate peaks are illustrated in Figure B with their corresponding wavenumbers at 1580 and 1630 cm^{-1} . Their absolute concentrations were calculated from the relative area of the peaks.

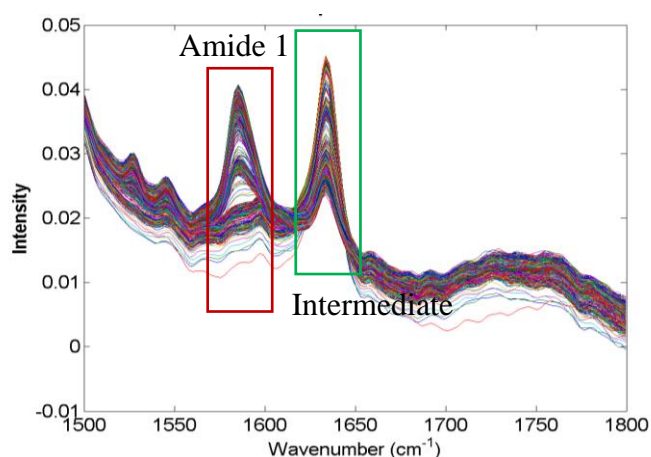


Figure B-1 IR spectrum of Step 1

In order to gain a better understanding of the relative rates of step 1 at different amide 1 concentrations, a series of “shot” of n-BuLi were added. The corresponding reaction condition is presented in Table B-2. As seen in Figure B-2, the first dose of n-BuLi only caused a slight dip in the amide 1 concentration; the reason could be the presence of traces of water in THF that consumed the n-BuLi. This resulted in overall conversion of only 80%. It is observed that the slopes of amide 1 and intermediate become gentler with decreasing concentrations of amide 1; this indicates a decreasing rate of lithiation. Although the general trend of intermediate formation mirrors the decreasing amide 1, it was not mass balanced. There was some side product formation (obtained from mass balance) as the overall yield, after addition of DMF, was only 67%. The formation of side products is only significant in the presence of n-BuLi, otherwise, the intermediate appears to be stable in the presence of excess amide 1 for at least 60 s. Insufficient mixing or ‘hotspot’ during n-BuLi addition might most likely trigger the side reactions.

Table B-2 IR step 1 reaction conditions

Step 1 reaction parameter	Condition
Temperature ($^{\circ}\text{C}$)	-60
Reaction volume (mL)	20

Initial amide 1 concentration (M)	0.044
Amount of 1 st n-BuLi dose	0.32 moleqv.
Amount of 2 nd n-BuLi dose	0.32 moleqv.
Amount of 3 rd n-BuLi dose	0.32 moleqv.
Amount of 4 th n-BuLi dose	0.1 moleqv.

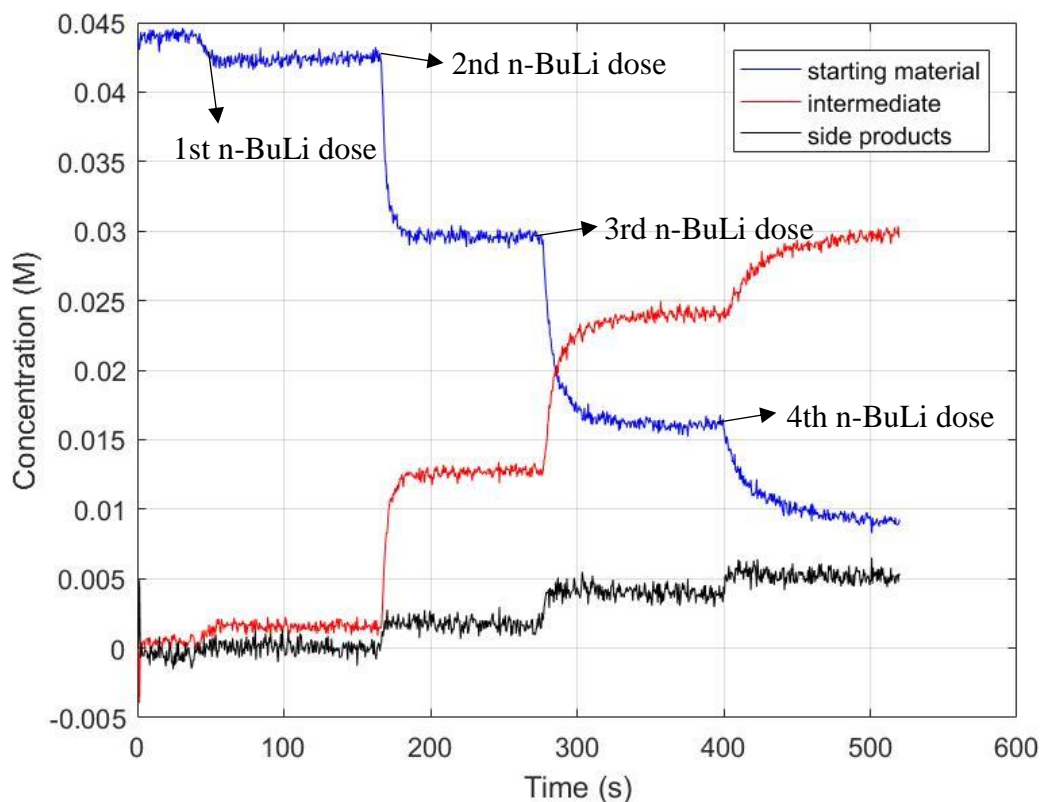


Figure B-2 In-situ IR monitoring of a series of n-BuLi shot-addition in step 1 at -60 °C.

The initial rates of the second, third and fourth doses were estimated based on initial gradients of amide 1 concentrations in Table B-3. Based on the initial rates shown in Figure B-2, the reaction appears to have an overall reaction order of two with first order with respect to amide 1 and n-BuLi.

Table B-3 Estimation of initial rate

No. of dose	Temperature (°C)	Initial amide 1 (M)	Initial n-BuLi (M)	Initial rate (mol/L/s)	Apparent rate constant, k (L/mols)
2 nd	-60	0.0423	0.0127	0.00226	6.5
3 rd	-60	0.0289	0.0127	0.00152	
4 th	-60	0.0143	0.0042	0.000223	

Rate equation is assumed as follows:

$$\frac{d[\text{Intermediate}]}{dt} = \frac{d[\text{Butane}]}{dt} = -\frac{d[\text{Amide 1}]}{dt} = -\frac{d[\text{nBuLi}]}{dt} = k[\text{Amide 1}][\text{nBuLi}]$$

Assumptions

1. First n-BuLi dose is not considered.

2. All amide 1 is converted to intermediate, no formation of side products.
3. Kinetic limited, not mixing limited.
4. Constant reaction temperature.

Figure B-3 shows the best fitting of the second order reaction with an overall rate constant of 6.5 L/mol.s to the IR data at -60 °C. Unfortunately, IR data at different temperatures were unattainable as the lowest reaction temperature achievable by the reactor setup was -60 °C. If higher temperatures were used, risk of formation of significant amount of side products would be greater and the measured rate of the desired reaction would be less accurate. Without activation energy, the measured rate constant of 6.5 L/mol.s is only applicable to reaction at -60 °C. Unfortunately, the spectral quality and reconstruction of step 2 was not satisfactory despite several attempts. The possible reason for this could be the change in compound concentration and solvent composition (addition of hexane) that might have caused the critical peaks to shift. Step 2 (electrophilic addition) is reported to be faster than step 1 (Newby *et al.*, 2014).

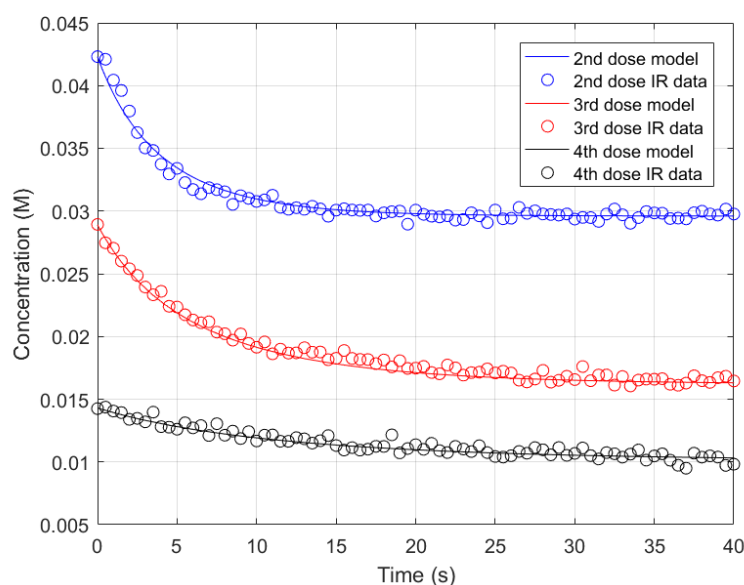


Figure B-3 Fitting of kinetic model to step 1 experimental data

Due to experimental constraints, the activation energy of the reaction was unable to be obtained from experiment. Assuming the activation energy of the reaction 94.6 kJ/mol (Sapse and Schleyer, 1995), the reaction time needed to obtain 99% amide 1 conversion to product is summarized in Table B-4. From the simulated results, the reaction time of step 1 is about 2.6×10^{-6} s at 20 °C and 0.4 M of initial amide 1 concentration. In general, the reaction time of Step 1 is shown to be extremely fast where it is highly likely to be mixing controlled reaction.

Table B-4 Determined Step 1 kinetic parameters from in-situ IR

Rate law	$r = k C_a C_b$
k, rate constant k at -60 °C (L/mol s)	6.5
E _a , activation energy (kJ/mol)	94.6 (Sapse and Schleyer, 1995)
k ₀ , frequency factor at 20 °C (s ⁻¹)	1.03 x 10 ²⁴
k, rate constant at 20 °C (L/mol s)	1.4 x 10 ⁷
Reaction time 99% conversion at 20 °C (s)	2.6 x 10 ⁻⁶

B.2 Analytical methods, n-BuLi titration, stability of aldehyde 1

GC analytical method and sample collection

Samples were collected at particular time intervals and analyzed using the internal standard method. The aldehyde 1 yield and reaction conversion were determined by Gas Chromatography (GC) using Agilent Technologies 6890N GC system with 7693 autosampler and a HP-5 column. Temperature ramp: 150 to 210 °C, 25 °C/min; run time: 15 min; post run: 280 (5 min); injection volume: 1 µl; detector temperature: 280 °C, control mode: constant pressure; pressure: 11.02 psi. Response factors of the aldehyde 1 and amide 1 were determined by calibration using n-hexadecane as the internal standard as seen in Figure B-4.

First, the samples were collected for a fixed time interval and weighed. About 1 mL of reaction mixture was taken and weighed separately, to which 1 mL of quench water was added. Followed by the addition of 50 mg of internal standard and mixed well. Lastly, 20 µL of the organic layer was drawn and diluted in 1 mL of ethyl acetate.

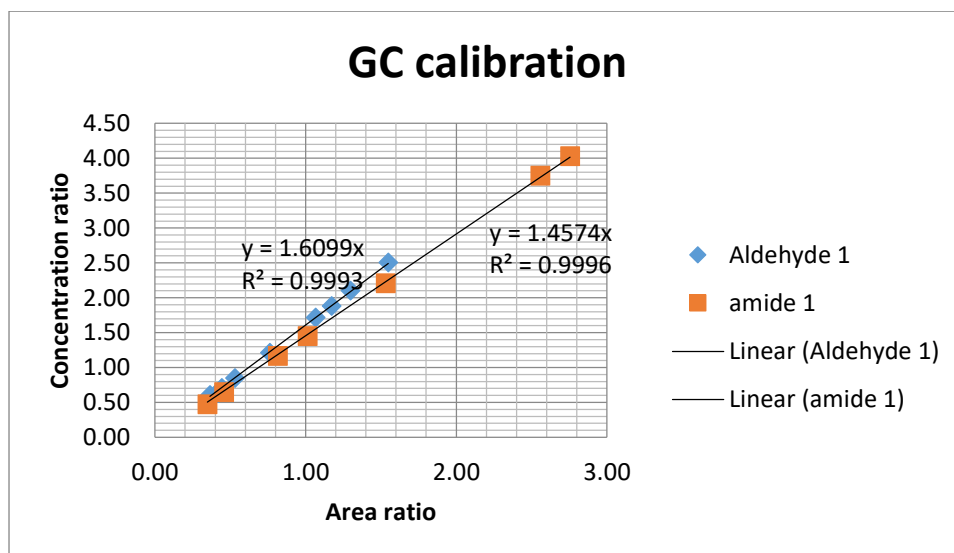


Figure B-4 Response factor for aldehyde 1 and amide 1 using internal standard method

LC-MS analytical method

LC-MS analysis was done at ambient temperature via reverse phase liquid chromatography with Tandem Mass Spectrometry (Waters Quattro Micro API™ LCMS/MS) with Restek Ultra C8 column (5 µm, 4.6 mm (i.d.), 150 mm (L)) an isocratic elution gradient of 50% acetonitrile/water was used. The samples were ionized by ESI and the ionized

components were analysed by a quadrupole analyzer. Retention time of amide 1 is 27 min; product 1 is 19 min; SP 1 is 15 min; SP 2 is 10 min.

n-BuLi Titration

The n-BuLi (~1.6 M solution in hexanes) was titrated once a week (Burchat et al., 1997). It is noted that the concentrations of the n-BuLi may vary (1.4-1.6 M). To account for the variation in n-BuLi concentration, the corresponding n-BuLi flow rates were adjusted.

100 mg of n-benzylbenzamide was dissolved in 10 mL of anhydrous THF. The solution was cooled to -40 °C and n-BuLi was added dropwise using a 1 mL microsyringe until the colourless solution turned blue. The volume of n-BuLi added was recorded. The titration was repeated for three times to get an average n-BuLi concentration.

Warning! BuLi solution are corrosive to human tissue, pyrophoric and explosive; therefore, they should be handled with care.

Stability of aldehyde 1 in organic solvents

The stability of aldehyde 1 in the final reaction mixture was investigated (Table B-5). Considerable loss of aldehyde 1 was observed after 1 and 2 days. This indicates that the isolation of aldehyde 1 should be done as soon as possible in a large scale batch production, storage of the reaction mixture for more than a day is undesirable.

Table B-5 Stability of aldehyde 1 in reaction mixture at ambient temperature

Storage time	Aldehyde 1 yield (%)	Overall conversion (%)	Impurity (%)
5 min	96	99	3
30 min	96	99	3
1 day	90	99	9
2 days	87	99	12

B.3 Differential scanning calorimetry (DSC): Amide 1 and Aldehyde 1

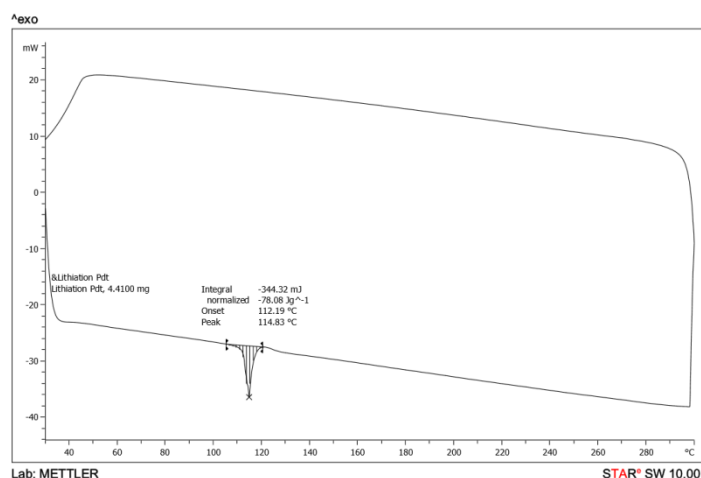


Figure B-5 DSC of Aldehyde 1 (20 °C to 300 °C)

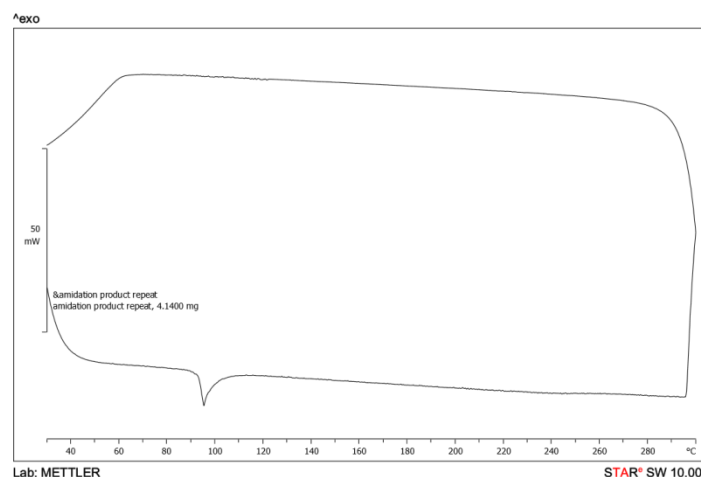
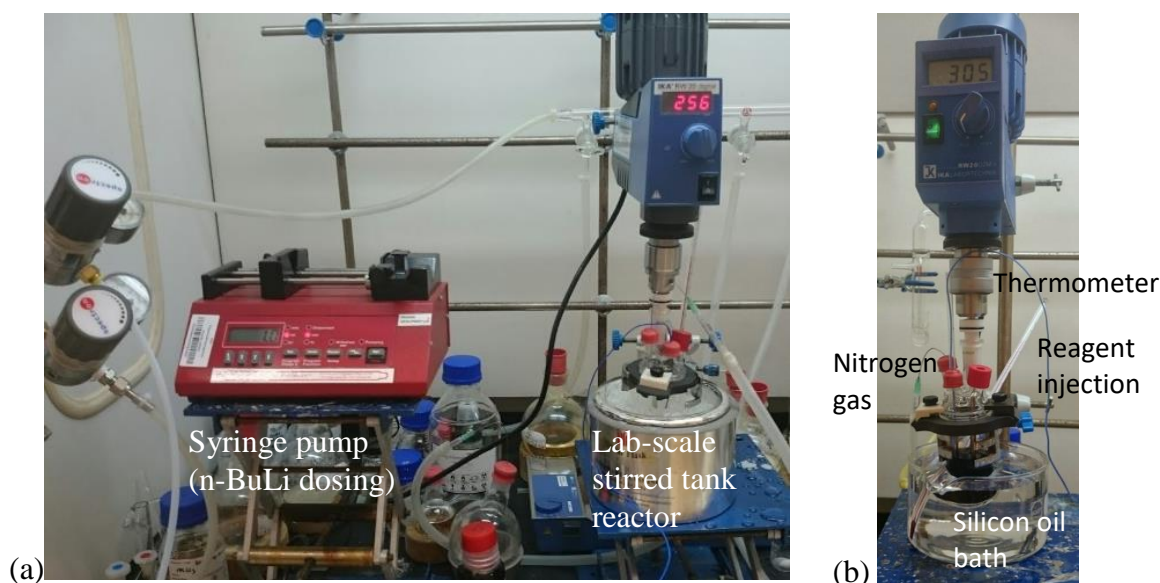


Figure B-6 Amide 1 (20 °C to 300 °C)

B.4 Stirred tank reactor (STR): Experiment procedure and results

For the batch stirred tank reactor (STR), a 50 mL Multi-max™ reactor (with standard overhead stirrer, 2 blade propeller impeller with diameter of 2.5 cm) was employed to conduct the ortho-lithiation reaction over a range of temperatures between -75 and 20 °C and impeller agitation speed between 50 to 400 rpm. A total of 2 g (8 mmol) of amide **1** was added into the reactor followed by 19 g of solvent, THF (anhydrous, 99.8%). The n-BuLi in hexanes (1.6 M, 1.2 mole equivalent) was added dropwise (0.4 mmol/min or 0.3 mL/min) via syringe pump (NE 1000) to the solution of starting material in THF in the reactor as seen in Figure B-. The reactor was submerged in an isopropyl alcohol (IPA) bath with constant addition of dry ice to maintain reactor internal temperature at about -70 °C monitored using a digital temperature sensor in contact with the reaction mixture. After which the reaction mixture was allowed to warm to about -50 °C when DMF (0.8 g, 11 mmol, 1.3 mole equivalent) was added at a rate of 10 mmol/min (0.8 mL/min) via syringe pump (NE 300). During the reaction, an inert reaction environment was maintained under nitrogen blanket.



Temperature was one of the most important process parameters for ortho-lithiation reaction in batch process. Attempts were made to perform the reaction at higher temperatures but side products were formed in large extent as shown in Table B-6, the drastic drop in yield. As expected, $-70\text{ }^{\circ}\text{C}$ was necessary for reaction in stirred tank reactor. In large scale batch production, the addition rate of n-BuLi should be adjusted to maintain the reaction temperature below $-70\text{ }^{\circ}\text{C}$.

Table B-6 Ortho-lithiation at different temperatures at constant agitation speed of 400 rpm in batch process.

Temperature ($^{\circ}\text{C}$)	Aldehyde 1 yield (%)	Overall conversion (%)	Impurity* (%)
20	3	93	90
0	26	99	73
-20	36	97	61
-70	96	99	3

(*) % impurity = % overall conversion - % aldehyde 1 yield

Mixing is also very important for ortho-lithiation which is a fast reaction. As seen in Table B-7, the results were very dependent on mixing which was measured by power input, determined by agitation speed. Poor mixing not only lead to increase in impurities but also lower overall conversion. The low agitation speed was expected to lead to a high n-BuLi localized concentration due to ineffective mixing which might encourage decomposition and/or attack on THF (Stanetty and Mihovilovic, 1997). The loss of n-BuLi was evident from the low consumption of amide 1 as seen in Table B-7 at agitation speeds of 50 and 100 rpm. For the

Multi-max™ reactor used, the maximum agitation speed achievable was 400 rpm. This corresponds to a power dissipation of 0.053 W/kg which was set as the minimum power dissipation for batch large scale production.

An example of STR power dissipation for 400 rpm (Paul et al., 2004)

$$\varepsilon = \frac{N_p N^3 D_i^5}{V}$$

Where N_p is the power number, D the impeller diameter (m), V the volume of liquid in the vessel (l),

N=400 rpm

D=0.025 m

V=0.028 L

$\rho = 920.6 \text{ g/L}$

Viscosity = 0.00186 Pa.s

Reaction mixture mass = 0.024 kg

$N_p=0.5$ (Paul et al., 2004)

$$\varepsilon = \frac{0.5 \times \left(\frac{400}{60}\right)^3 \times 0.025^5}{\frac{0.024}{920.6}} = 0.053 \text{ W/kg}$$

Table B-7 Ortho-lithiation at 0 °C under different agitation speeds where n-BuLi and DMF addition rates were kept constant at 0.4 and 2 mmol/min respectively.

Agitation (rpm)	Aldehyde 1 yield (%)	Overall conversion (%)	Power (W/kg)
400	26	99	0.053
200	25	99	0.007
150	22	98	0.003
100	7	42	0.0008
50	7	36	0.0001

To study the effect of mixing on step 2, two different DMF addition rates were used while keeping the agitation speed of the reactor constant at 400 rpm (Table B-8). The high charging rate of DMF might cause inhomogeneous mixing and hotspot formation that could lead to decomposition of the intermediates, where some of the lithiated intermediates might have been converted back to amide 1. This explained the lower overall conversion of amide 1 at fast DMF dosing rate.

Table B-8 Addition mode of DMF at -50 °C (Step 1 performed at -70 °C)

DMF addition rate	Aldehyde 1 yield (%)	Overall conversion (%)	Impurity* (%)	Agitation speed (rpm)
One shot (~10 mmol/s)	30	63	33	400
Usual dosing rate (2 mmol/min)	96	99	3	400

(*) % impurity = % overall conversion - % aldehyde 1 yield

Appendix C. Ortho-Lithiation Process – Part 2: Assessment of Sustainability Benefits for Reaction

C.1 Stirred tank reactor

Product produced (kg product/year)	3000
Number of batch per year	1818
Volume of reactor (L)	31.79
Throughput (kgprod/h)	0.38
Product yield (%)	96
Max inventory of processing at any point of time (L)	22
Max inventory of processing at any point of time (L/kgprod/h)	59
Volume efficiency	
Volume of reactor per kg product (L/kgprod/h)	85

Total material efficiency (kg material/kg product)	12	Raw materials	kg/year	kg material/kg prod	Weightage
		THF	24082	8	69
		DMF	1109	0	3
		n-BuLi (1.6M)	6679	2	19
		4-chloro-N,N-diisopropylbenzamide	2798	1	8
			34668	12	

Total Energy Efficiency (kJ/kg prod)	3956	Energy	kJ/year	kJ/kg product	Weightage
		Compressor duty	11329586	3777	95
		Agitation	15048	5	0
		Pump duties	522677	174	4
			11867311	3956	
Total OPEX per year (USD)	1369115	Raw materials	USD/year	USD/kg prod	weightage
		THF	105435	35	9

Weightage		DMF	7255	2	1
raw materials	88	n-BuLi (1.6M)	153060	51	13
energy and utilities	12	4-chloro-N,N-diisopropylbenzamide	940188	313	78
			1205938	402	100
		Energy and Utilities	USD/year	USD/kg prod	Weightage
		Electricity consumption	162211	54	99
		Chilled water consumption	209	0	0
		Argon	757	0	0
			163177	54	100

Total CAPEX	14343 7	Equipment	Volume (L)	Quantity	USD	Ref
	47.812 178	THF sanitary centrifugal pump		1	3300	https://www.coleparmer.com/i/sanitary-3a-centrifugal-pump-62-gpm-0-5hp-316-304ss-3600rpm-208-230-460-vac/7672000
		n-BuLi piston pump		1	4000	https://www.coleparmer.com/i/pw2003e-variable-speed-liquid-piston-pump-for-hazardous-duty-115-v-class-1-div-2/7930610
		DMF piston pump		1	2560	https://www.coleparmer.com/i/cole-parmer-piston-pump-system-w-drive-0-to-192-ml-min/0710884
		Product sanitary centrifugal pump		1	3300	https://www.coleparmer.com/i/sanitary-3a-centrifugal-pump-62-gpm-0-5hp-316-304ss-3600rpm-208-230-460-vac/7672000
		Chilled water centrifugal pump		1	194	https://www.coleparmer.com/i/md-6-220v-mag-drive-pp-centrifugal-pump-w-enclosed-motor-2-3-gpm-4-5-ft-220v/7201005
		R23 (kg)		29	441	https://www.alibaba.com/product-detail/Eco-friendly-R23-Refrigerant-Price_60481182470.html
		R32 (kg)		34	169	https://www.alibaba.com/product-detail/r32-refrigerant-price-R32_60484502044.html
		THF storage tank	1493	1	1247	https://www.alibaba.com/product-detail/1000-liter-wheeled-chemical-stainless-steel_60457310584.html
		DMF storage tank	65	1	222	https://www.alibaba.com/product-detail/1000-liter-wheeled-chemical-stainless-steel_60457310584.html
		Product storage tank	2149	1	1523	https://www.alibaba.com/product-detail/1000-liter-wheeled-chemical-stainless-steel_60457310584.html
		Cryogenic reactor vessel	32	1	7341	https://www.alibaba.com/product-detail/ss304-high-quality-stainless-steel-reactor_60560574880.html?s=p

		Agitator		1	900	https://wholesaler.alibaba.com/product-detail/The-strongest-design-SS304-Corrosion-resistant_60510700657.html
		Compressors		2	522	https://wholesaler.alibaba.com/product-detail/The-Copeland-Scroll-K5-Compressor-for_60552472035.html?spm=a2700.7724838.0.0.TrYNko
		Condenser (SS304 coils)		1	4800	https://www.alibaba.com/product-detail/High-Quality-SS304-Condenser-Coils-for_60508687907.html?s=p
		Total			30518	
		Lang factor for Liquid system (ref: C&R)			4.7	
		Total CAPEX			143437	

C.2 T-reactor

Product produced (kg product/year)	3040
Operation hours per year	8000
Volume of reactor (L)	18
Throughput (kgprod/h)	0.38
Product yield (%)	98.6
Max inventory of processing at any point of time (L)	0.002761
Max inventory of processing at any point of time (L/kgprod/h)	0.007266
Volume efficiency	
Volume of reactor per kg product (L/kgprod/h)	47

Total material efficiency (kg material/kg product)	11	Raw materials	kg/year	kg material/kg prod	Weightage
		THF	23573	8	69
		DMF	1684	1	5
		n-BuLi (1.6M)	5875	2	17
		4-chloro-N,N-diisopropylbenzamide	2798	1	8

			33930	11	
--	--	--	-------	----	--

Total Energy Efficiency (kJ/kg prod)	1321	Energy	kJ/year	kJ/kg product	Weightage
		Cooling	3870720	1273	96
		Agitation	83945	28	2
		Pump duties	61308	20	2
			4015974	1321	

Total OPEX per year (USD)	1234616	Raw materials	USD/year	USD/kg prod	weightage
Total OPEX per year (USD/kg prod)	406	THF	103207	34	9
Weightage		DMF	11017	4	1
raw materials	95	n-BuLi (1.6M)	134644	44	11
energy and utilities	5	4-chloro-N,N-diisopropylbenzamide	927997	305	79
			1176865	387	100
		Energy and Utilities	USD/year	USD/kg prod	Weightage
		Electricity consumption	57016	19	99
		Argon	734	0	1
			57750	19	100

Total CAPEX	93713	Equipment	Volume (L)	Quantity	USD	Ref
CAPEX (USD/kg prod)	30.82 463	THF sanitary centrifugal pump		1	33 00	https://www.coleparmer.com/i/sanitary-3a-centrifugal-pump-62-gpm-0-5hp-316-304ss-3600rpm-208-230-460-vac/7672000
		Amide 1 in THF piston pump		1	25 60	https://www.coleparmer.com/i/cole-parmer-piston-pump-system-w-drive-0-to-192-ml-min/0710884
		n-BuLi piston pump		1	26 10	https://www.coleparmer.com/i/cole-parmer-piston-pump-system-w-drive-0-to-30-ml-min/0710880
		DMF piston pump		1	26 10	https://www.coleparmer.com/i/cole-parmer-piston-pump-system-w-drive-0-to-30-ml-min/0710880
		Silicon HTF centrifugal pump		1	19 4	https://www.coleparmer.com/i/md-6-220v-mag-drive-pp-centrifugal-pump-w-enclosed-motor-2-3-gpm-4-5-ft-220v/7201005

	Mixing tank (8h supply)	41	2	17 3	346	https://www.alibaba.com/product-detail/Custom-made-chemical-storage-tank-on_60527019551.html?s=p
	Agitator		2	90 0	180 0	https://wholesaler.alibaba.com/product-detail/The-strongest-design-SS304-Corrosion-resistant_60510700657.html
	Product storage tank (1 weeks)	377	2	58 5	117 0	https://www.alibaba.com/product-detail/Custom-made-chemical-storage-tank-on_60527019551.html?s=p
	THF storage tank (1 weeks)	1024	1	69 2	692	https://www.alibaba.com/product-detail/Custom-made-chemical-storage-tank-on_60527019551.html?s=p
	DMF storage tank (2 weeks)	69	1	15 6	156	https://www.alibaba.com/product-detail/Custom-made-chemical-storage-tank-on_60527019551.html?s=p
	1/8" PTFE tube	50m	1	12 1	121	http://www.sigmaaldrich.com/catalog/product/supelco/58699?lang=en&region=SG
	P-713 Tee joint		2	10 0	200	https://us.vwr.com/store/product/9475346/upchurch-scientific-tees-multi-port-connectors-idx-health-science
	P300x Ferrule		8	20	156	http://www.cmscientific.com/proddetail.php?prod=P-300X
	P304 Nut		6	50	302	http://www.cmscientific.com/proddetail.php?prod=P-304
	P658 Luer lock adaptor		3	20	59	http://www.cmscientific.com/products.php?cat=Luer+Adapters
	P785 backpressure regulator		1	17 6	176	http://www.cmscientific.com/proddetail.php?prod=P-785
	Silicon HTF circulated bath (18L)		1	26 29	262 9	https://www.thomasci.com/Equipment/Circulators/_/Stirred-Thermostatic-Baths-and-Circulators?q=*
	Silicone oil (50cSt, 18L)		1	85 9	859	http://www.sigmaaldrich.com/catalog/product/aldrich/378356?lang=en&region=SG
	Total				199 39	
	Lang factor for Liquid system (ref: C&R)				4.7	
	Total CAPEX				937 13	

C.3 Spinning disc reactor

Product produced (kg product/year)	2281
Operation hours per year	8000
Volume of reactor (L)	17.25
Throughput (kgprod/h)	0.29

Product yield (%)	87.0
Max inventory of processing at any point of time (L)	0.016
Max inventory of processing at any point of time (L/kgprod/h)	0.055
Volume efficiency	
Volume of reactor per kg product (L/kgprod/h)	61

Total material efficiency (kg material/kg product)	15	Raw materials	kg/year	kg material/kg prod	Weightage
		THF	23588	10	69
		DMF	1684	1	5
		n-BuLi (1.6M)	5875	3	17
		4-chloro-N,N-diisopropylbenzamide	2798	1	8
			33945	15	

Total Energy Efficiency (kJ/kg prod)	2566	Energy	kJ/year	kJ/kg product	Weightage
		Cooling	3870720	1697	66
		Agitation	83926	37	1
		Pump duties	8553	4	0
		SDR	1888697	828	32
			5851896	2566	

Total OPEX per year (USD)	1253650	Raw materials	USD/year	USD/kg prod	weightage
Total OPEX per year (USD/kg prod)	550	THF	103273	45	9
Weightage		DMF	11017	5	1
raw materials	93	n-BuLi (1.6M)	134644	59	12
energy and utilities	7	4-chloro-N,N-diisopropylbenzamide	920898	404	79
			1169832	513	100
		Energy and Utilities	USD/year	USD/kg prod	Weightage

		Electricity consumption	83084	36	99
		Argon	734	0	1
			83818	37	100

Total CAPEX	1075 20	Equipment	Volume (L)	Quantity	USD		Ref
		THF sanitary centrifugal pump		1	3300	3300	https://www.coleparmer.com/i/sanitary-3a-centrifugal-pump-62-gpm-0-5hp-316-304ss-3600rpm-208-230-460-vac/7672000
		Amide 1 in THF piston pump		1	2560	2560	https://www.coleparmer.com/i/cole-parmer-piston-pump-system-w-drive-0-to-192-ml-min/0710884
		n-Buli piston pump		1	2610	2610	https://www.coleparmer.com/i/cole-parmer-piston-pump-system-w-drive-0-to-30-ml-min/0710880
		DMF piston pump		1	2610	2610	https://www.coleparmer.com/i/cole-parmer-piston-pump-system-w-drive-0-to-30-ml-min/0710880
		Silicon HTF centrifugal pump		1	194	194	https://www.coleparmer.com/i/md-6-220v-mag-drive-pp-centrifugal-pump-w-enclosed-motor-2-3-gpm-4-5-ft-220v/7201005
		Mixing tank (8h supply)	41	2	173	346	https://www.alibaba.com/product-detail/Custom-made-chemical-storage-tank-on_60527019551.html?s=p
		Agitator		2	900	1800	https://wholesaler.alibaba.com/product-detail/The-strongest-design-SS304-Corrosion-resistant_60510700657.html
		Product storage tank (1 weeks)	377	2	585	1170	https://www.alibaba.com/product-detail/Custom-made-chemical-storage-tank-on_60527019551.html?s=p
		THF storage tank (1 weeks)	1024	1	692	692	https://www.alibaba.com/product-detail/Custom-made-chemical-storage-tank-on_60527019551.html?s=p
		DMF storage tank (1 weeks)	69	1	156	156	https://www.alibaba.com/product-detail/Custom-made-chemical-storage-tank-on_60527019551.html?s=p
		1/8" PTFE tube	50m	1	121	121	http://www.sigmaaldrich.com/catalog/product/supelco/58699?lang=en&region=SG
		Silicone oil TCU (6L)	6L	1	500	500	https://www.alibaba.com/product-detail/Advanced-instruments-thermostatic-equipment-silicone-oil_60555478623.html
		316 stainless steel (m3)	10kg	1	1502	1502	http://sg.rs-online.com/web/p/stainless-steel-rods-bars/7703585/
		Electric motor		1	1111	1111	https://www.alibaba.com/product-detail/YE2-three-phase-electric-motor_60617245609.html?s=p
		Labour cost + frame		1	3919	3919	Assumption

		Silicone oil (50cSt, 6L)		1	28 6	286	http://www.sigmaaldrich.com/catalog/product/aldrich/378356?lang=en&region=SG
		Total				2287 7	
		Lang factor for Liquid system (ref: C&R)				4.7	
		Total CAPEX				1075 20	

Appendix D. Ortho-Lithiation to Reduction Process – Part 3: Assessment of Sustainability Benefits for Whole Process Featuring Consecutive Reaction from Ortho-Lithiation to Reduction

D.1 IR and GC calibration

The IR spectra show that the C=O bond stretching in the aldehyde 1 occurred at a frequency of between 1700 and 1620 cm^{-1} and gave a distinct peak as shown in Figure D-1.

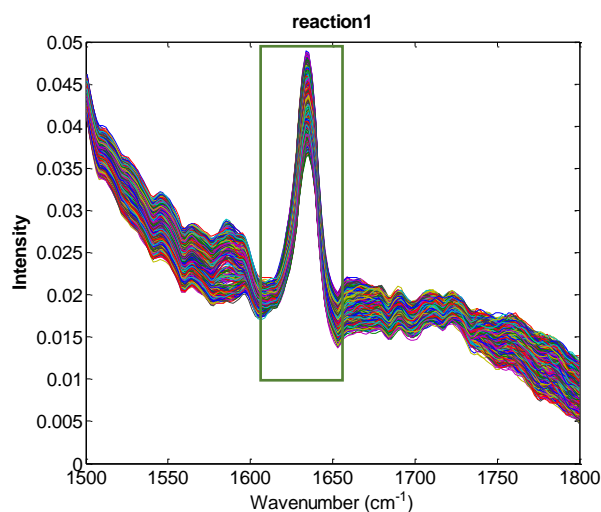


Figure D-1 IR spectra showing a gradual decrease in C=O peak area during reduction reaction

Calibrations based on the area of the peak corresponding to different starting aldehyde concentrations in the THF was obtained in Figure D-2.

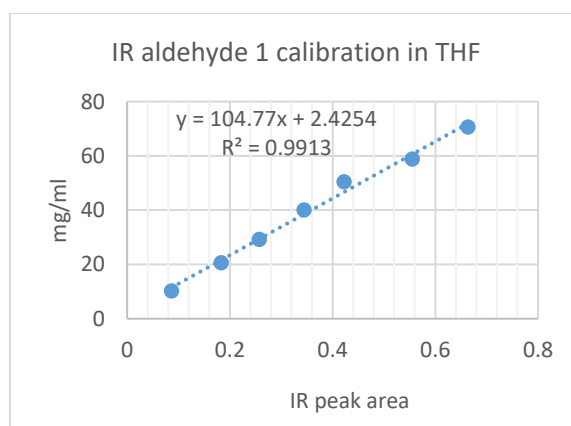


Figure D-2 IR calibration of aldehyde 1 in THF

The GC response factors of aldehyde 1 and alcohol 1 were determined by the following calibration graphs (Figure D-3 and Figure D-4).

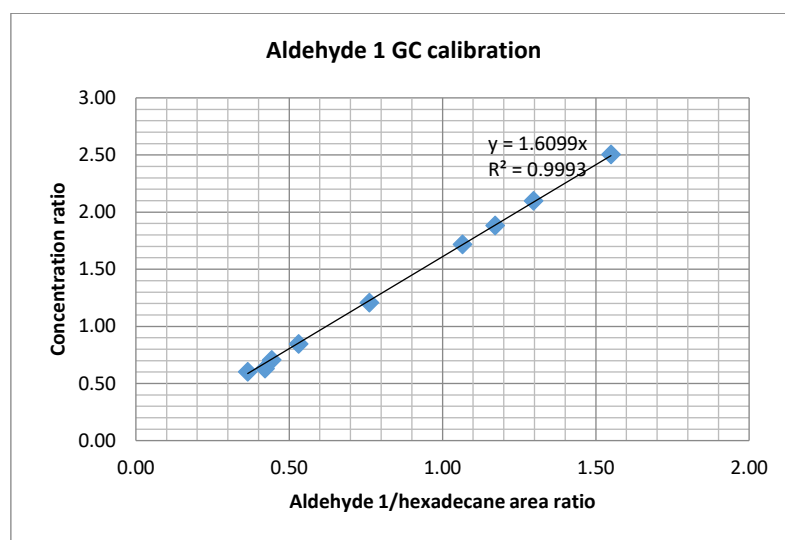


Figure D-3 Aldehyde 1 GC calibration

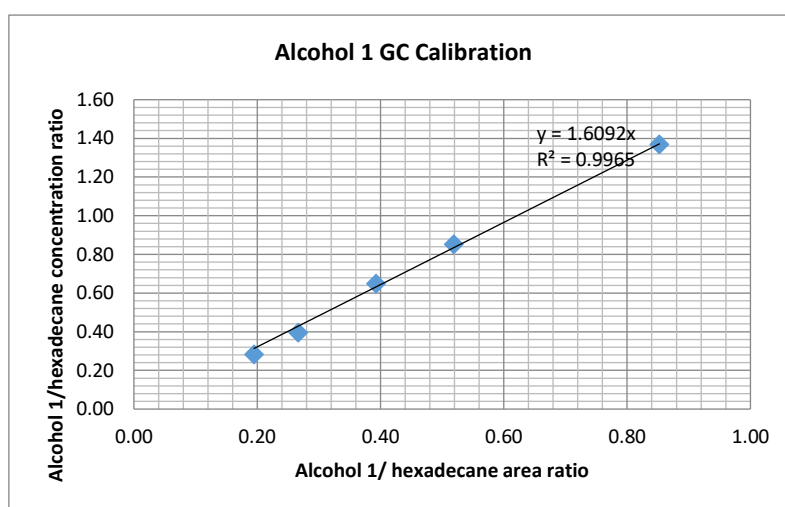


Figure D-4 Alcohol 1 GC calibration

D.2 *Ortho-lithiation workup results and discussion*

The mass and energy balances for the ortho-lithiation base case batch process are evaluated. The separation processes and purification steps has been fixed by Faigl *et al.* (2010) which is based on laboratory scale experiments. Additional experiments were performed to identify the issues that may arise and roughly estimate the amount of product loss at each step at large scale production. Figure D-5 shows the flow chart for the workup steps executed at laboratory scale. To ensure a safe and scalable base case, necessary modifications were made to the procedure reported by Faigl *et al.* (2010).

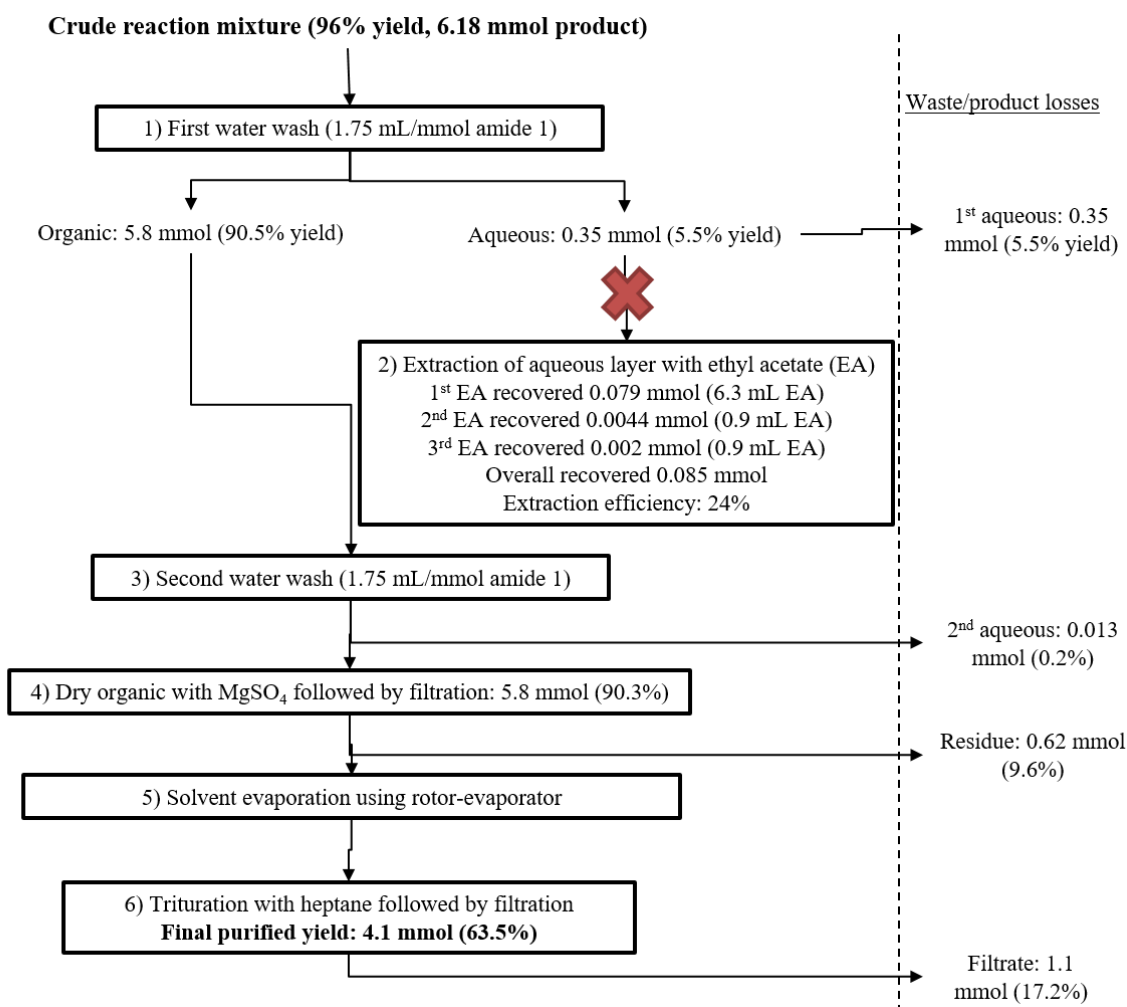


Figure D-5 Literature (Faigl *et al.*, 2010) workup procedure analysis

Step 1, the saturated ammonium chloride solution (2.24 mL/mmol amide 1) was replaced by water (1.75 mL/mmol amide 1) which was based on the solubility of lithium dimethylamine in water. Using lesser volume of water allowed the aqueous phase to be more concentrated in lithium dimethylamine which reduced the solubility of organic compounds in the aqueous layer. This might have minimized the amount of aldehyde 1 lost in the aqueous wash. It was assumed that this loss would exist regardless of the scale.

According to Faigl *et al.* (2010), the ethyl acetate was used to recover product from the first aqueous wash layer. However, it is found that the overall extraction efficiency of ethyl acetate (Step 2) was very low (24% of aldehyde 1 recovered) as the extraction efficiency of the extractions diminished after the first extraction. The low extraction efficiency is believed to be due to the low affinity of the product in ethyl acetate compared to water, so similar observation was likely to prevail at scale. The cost of ethyl acetate is calculated as 1/10 of a catalogue price (Laird, 2005), which is assumed as \$3.74/L. Table D-1 shows that just the price of ethyl acetate to recover 1 kg of product costs \$1337 which excludes energy cost for evaporation and waste treatment cost. Compared to the operating cost of batch reaction, the ethyl acetate

extraction operation was uneconomical as the amount recovered aldehyde 1 did not justify for the extraction. The decision was therefore to discard the aqueous phase and avoid the ethyl acetate extraction step to lower the operating cost.

Table D-1 Cost of ethyl acetate used in extraction of aldehyde 1

Volume of EA used in 3 extractions	8.1 mL
Mass of product recovered in extraction	0.023 g
Volume of EA/kg aldehyde 1 recovered	358 L
Cost of EA/kg product recovered (USD)	\$1337

The organic phase obtained after first water wash is washed again with water (Step 3) to ensure the removal of all water soluble by/side products and excess DMF. Brine instead of water is normally used (Faigl *et al.*, 2010); however in this study, brine is avoided as it tends to corrode the stainless steel reactor after prolonged exposure.

The organic phase was dried with anhydrous magnesium sulfate, followed by filtration (Step 4). This step is necessary to remove residual water in the organic layer which was, otherwise, challenging to evaporate using the rotor-evaporator. The experimental result showed that the 10% of aldehyde 1 was lost, which is expected to be minimized if it is performed at large scale where the equipment would be much more efficient than that in the lab-scale. No organics is assumed to remain on the residue as vacuum filtration is designed to be used.

D.3 Reaction mechanism for reduction reaction using aqueous base NaBH₄

The reduction of aldehyde 1 with sodium borohydride takes place in a heterogeneous aqueous base-organic solvent mixture, where aqueous phase contains dissolved sodium borohydride and organic phase contains aldehyde 1 dissolved in THF. The literature does not provide much detail about the mechanism of such biphasic borohydride reduction reaction. However, Yadav and co-workers presented a reaction mechanism for liquid-liquid Phase Transfer Catalysis (PTC) catalyzed borohydride reduction of carbonyl compounds (Yadav *et al.*, 2003; Yadav and Lande, 2006) where the rates of biphasic borohydride reductions can be intensified using PTC. The use of PTC is also applicable to the reaction system to enhance rate of reduction and could be investigated further in future work. Based on the understanding of Liquid-Liquid PTC, the reaction mechanism of biphasic reduction could be inferred as follows in Figure D-6:

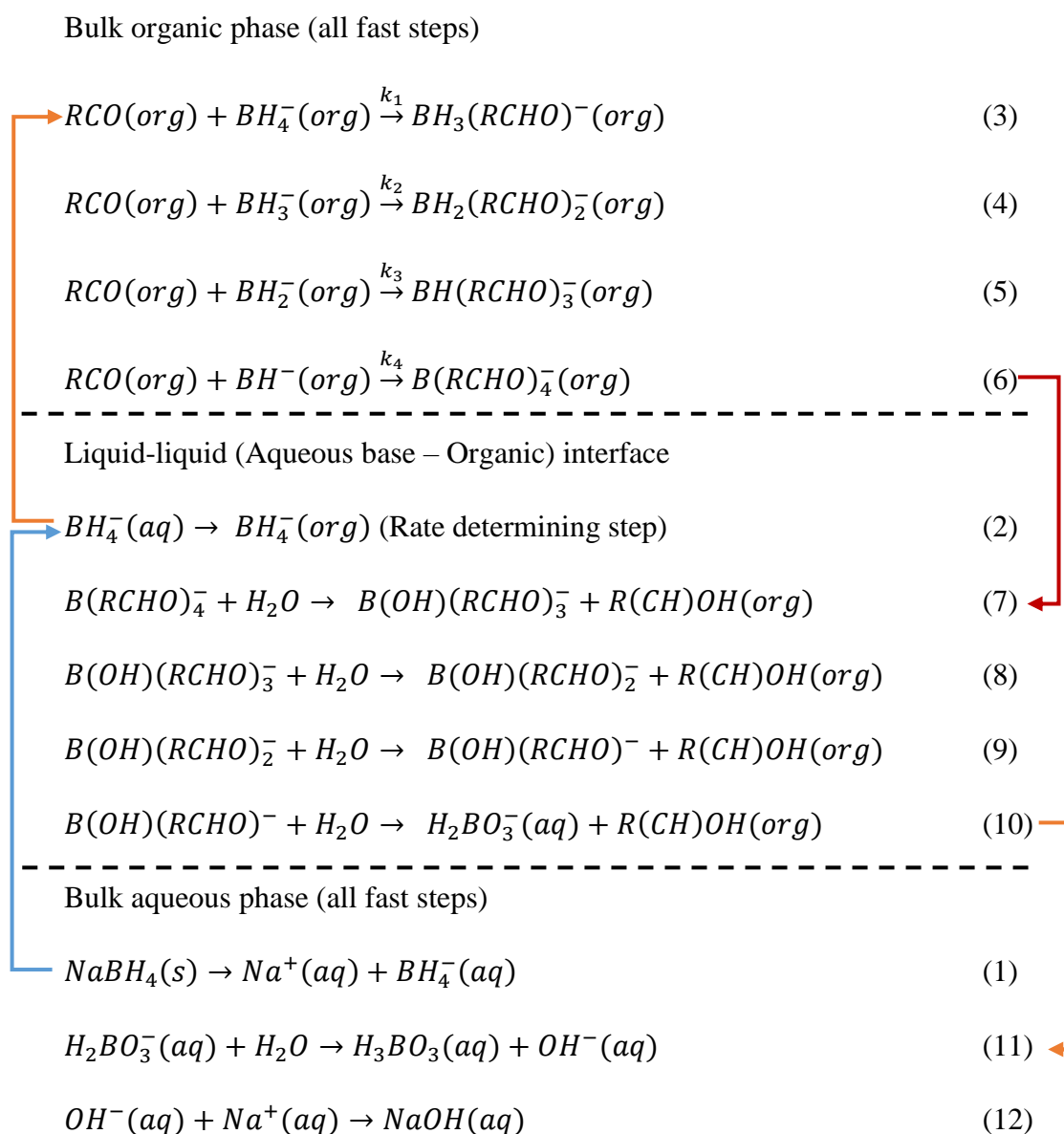


Figure D-6 Reaction mechanism for liquid-liquid borohydride reduction of aldehyde 1

If this was a Liquid-Liquid PTC reduction reaction (Zeynizadeh and Behyar, 2005; Yadav and Lande, 2006), step 3 would usually be the rate determining step as the presence of PTC would enhance the mass transfer of borohydride (BH_4^-) from aqueous to organic phase greatly, ensuring the reaction is kinetically controlled by step 3. However, in the absence of PTC in this biphasic reduction, step 2 is proposed to be the rate determining step and the rate of mass transfer of the borohydride species from aqueous to organic phase controls the overall rate of reaction. The subsequent reactions (steps 3-6) with borohydride complex in the organic phase are considered to be relatively faster than step 2. The fully complexed borohydride complex formed in step 6 is transferred from organic to aqueous phase across the interface where the complex is broken when in contact with water in aqueous phase. Alcohol 1 is released from the complex and transferred back to organic phase. Although the volume fraction of the

aqueous phase is quite small (1.5 v/v%), steps 7-10 are believed to be very fast and might get slower as the reaction proceeds with more water being consumed. The boric acid formed in step 11 is likely to be neutralized successively with NaOH in step 12.

D.4 Derivation of combined batch base case

Development of ortho-lithiation whole process

Based on the above process design, the performance metric of the whole process was evaluated in terms of volume, mass and energy efficiencies and estimated the expected operating (OPEX) and capital cost (CAPEX) respectively (Table D-2). Total production time of one batch was 9.6 h, based on 0.5 occupancy of the longest operation (drying, F-01), with 8000 h of operation per year. The performance metrics for ‘only reaction’ is obtained in Chapter 5 and it is shown alongside the whole process to demonstrate the difference due to separation process.

Maximum processing inventory at any point of time for whole process includes the stirred tank reactor volume (R-01), evaporator (R-02), filter dryer (F-01) and distillate collectors (T-07 and T-08).

Table D-2 Performance metric of ortho-lithiation base case at design scale of about 3 tons per year aldehyde 1

Performance metrics	Ortho-lithiation whole process
Total material efficiency (kg material/kg aldehyde 1)	37
Max inventory of processing at any point of time (L/kgprod/h)	456
E-factor (kg waste/kg aldehyde 1)	35
Material cost (USD/kg aldehyde 1)	634
Energy and utilities cost (USD/kg aldehyde 1)	111
Waste treatment cost (USD/kg aldehyde 1)	27
Total energy efficiency (kJ/kg aldehyde 1)	13,745
CAPEX (USD/kg aldehyde 1)	85
OPEX (USD/kg aldehyde 1)	771

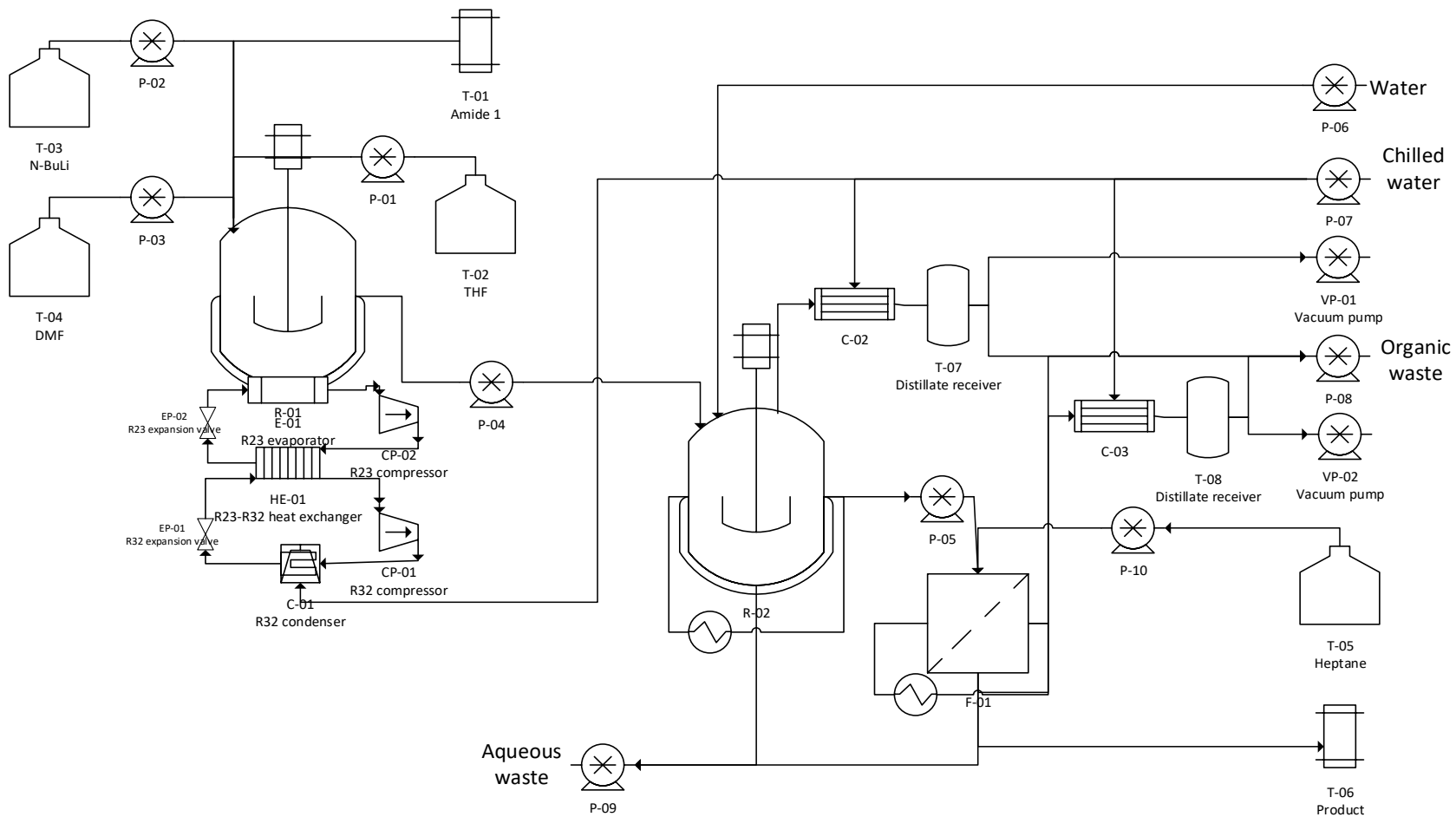


Figure D-7 Schematic process diagram for ortho-lithiation safe and scalable base case process.

Table D-3 shows a breakdown in terms of operation time and energy consumption for major equipment. As expected, the most energy consuming operation was R-02, evaporator. The filter dryer was most time consuming (4.6 h) and required energy intensive condition such as vacuum (100 mbar) and constant heating (jacket temperature at 50 °C). As expected, the major bottlenecks of the whole process lie in the separation process and these bottlenecks specifically include the following:

- The significant amount of aldehyde 1 loss in purification step decreased the overall process efficiency.
- The most time consuming operation was filter drying.
- The most energy intensive operation was evaporation of organic solvents.

Table D-3 Breakdown of operation time and energy consumption for ortho-lithiation whole process with a production target of 3 tons aldehyde 1 per year.

Equipment	Operation	Operation time (h)	Total volume (L)	Operation time fraction	Energy fraction
Reactor, R-01	Reaction	2.5	93	0.3	0.38
Vessel, R-02	1) First water wash Mixing Phase separation Discharge first aqueous layer	0.2	133	0.3	0.51
	2) Second water wash Mixing Phase separation Discharge second aqueous layer	0.2			
	3) Evaporation of organic solvents and addition of water	3.4			
Filter dryer, F-01	4) First filtration Discharge filtrate (water)	0.1	25	0.4	0.11
	5) Heptane wash Mixing	0.1			
	6) Second filtration Discharge filtrate (heptane)	0.1			
	7) Drying of residue	4.6			

Development of reduction whole process

Since major change in the solvent selection was made to the literature case, modifications had to be made to the separation steps. The objective of the laboratory scale workup experiment is to establish a safe and scalable separation process and identify major issues that can be encountered at scale.

The proposed batch separation process for reduction is summarised in Table D-4 where the alcohol 1 yields were obtained from laboratory scale experiments. In the first water wash, the phase separation between aqueous and organic (THF) is easy because of the high ionic strength of the salts and NaOH in aqueous phase. However, after the removal of the salts and NaOH, the second water-THF phase separation would be difficult as they have high solubility in each other and might result in high yield loss. Therefore, NaCl solution instead of water was used in the second wash to provide sufficient ionic strength in the aqueous phase to minimise loss of alcohol 1 in aqueous phase. Upon evaporation of THF in the rotor-evaporator, solid alcohol 1 was observed to stick strongly to the sides of the evaporating flask. Therefore, addition of water is necessary at scale to suspend alcohol 1 as precipitates after THF is fully evaporated.

Table D-4 Summary of reduction safe and scalable base case operations

Steps	Objectives	Alcohol 1 yield with respect to aldehyde 1 (%)
Reduction reaction	Reduction reaction	>99
1) Water wash	Quench the excess sodium borohydride. Remove salts, boric acid and sodium hydroxide in the aqueous phase.	96.2
2) 1 M NaCl wash	Remove any remaining by-products.	94.5
3) Evaporation of organic solvents and addition of water	Suspend product as precipitate in water phase for easy transfer out of the reactor.	94.5
4) Filtration	Remove water and obtain solid product as residue.	94.5
5) Drying	Dry product to a moisture content of 0.1%	94.5

The following process flow diagram in Figure D-8 summarised the key process steps. The long term stability of dissolved NaBH₄ is not excellent in dilute aqueous base of 1 M NaOH solution, so a mixing tank (M-01) was used to prepare aqueous NaBH₄ solutions before dosing into the reactor (R-01).

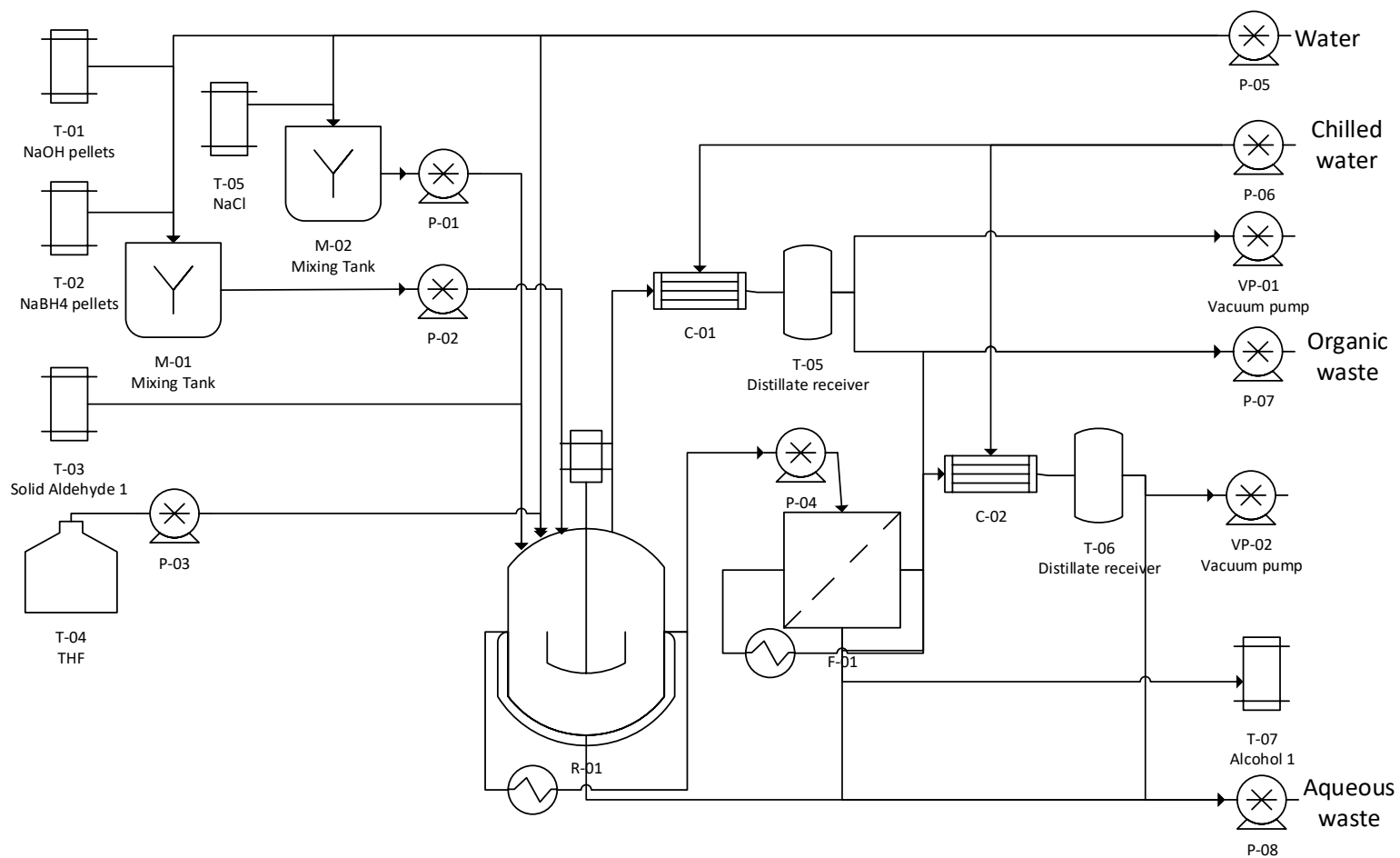


Figure D-8 Schematic process diagram for reduction safe and scalable base case process.

For reduction, it is noted that the material cost does not include the cost of aldehyde 1 as it was produced in-house (ortho-lithiation base case) and is not commercially available. This explains the relatively low reduction OPEX obtained as cost of raw material is one of the major process cost. The reduction material efficiency and E-factor were also relatively low because of the higher concentration of aldehyde 1 in THF was used (1 M instead of 0.4 M).

Table D-5 shows a breakdown in terms of operation time and energy consumption for two major equipment – reactor (R-01) and filter dryer (F-01). As expected, the most energy consuming operation is drying as it is very time consuming (15 h) and requires energy intensive condition such as vacuum (50 mbar) and constant heating (jacket temperature at 65 °C). In the reactor, majority of the energy consumed is for the evaporation of THF.

Table D-5 Breakdown of operation time and energy consumption for reduction whole process with a production target of 3 tons alcohol 1 per year.

Equipment	Operation	Operation time (h)	Total volume (L)	Operation time fraction	Energy fraction
Reactor, R-01	Reduction reaction	0.24	150	0.2	0.35
	1) Water wash Mixing Phase separation Discharge first aqueous layer	0.12			
	2) NaCl wash Mixing Phase separation Discharge second aqueous layer	0.05			
	3) Evaporation of THF and addition of water	0.59			
Filter dryer, F-01	4) First filtration Discharge filtrate (water)	0.02	25	0.8	0.65

D.5 Schematic of the continuous consecutive reaction process

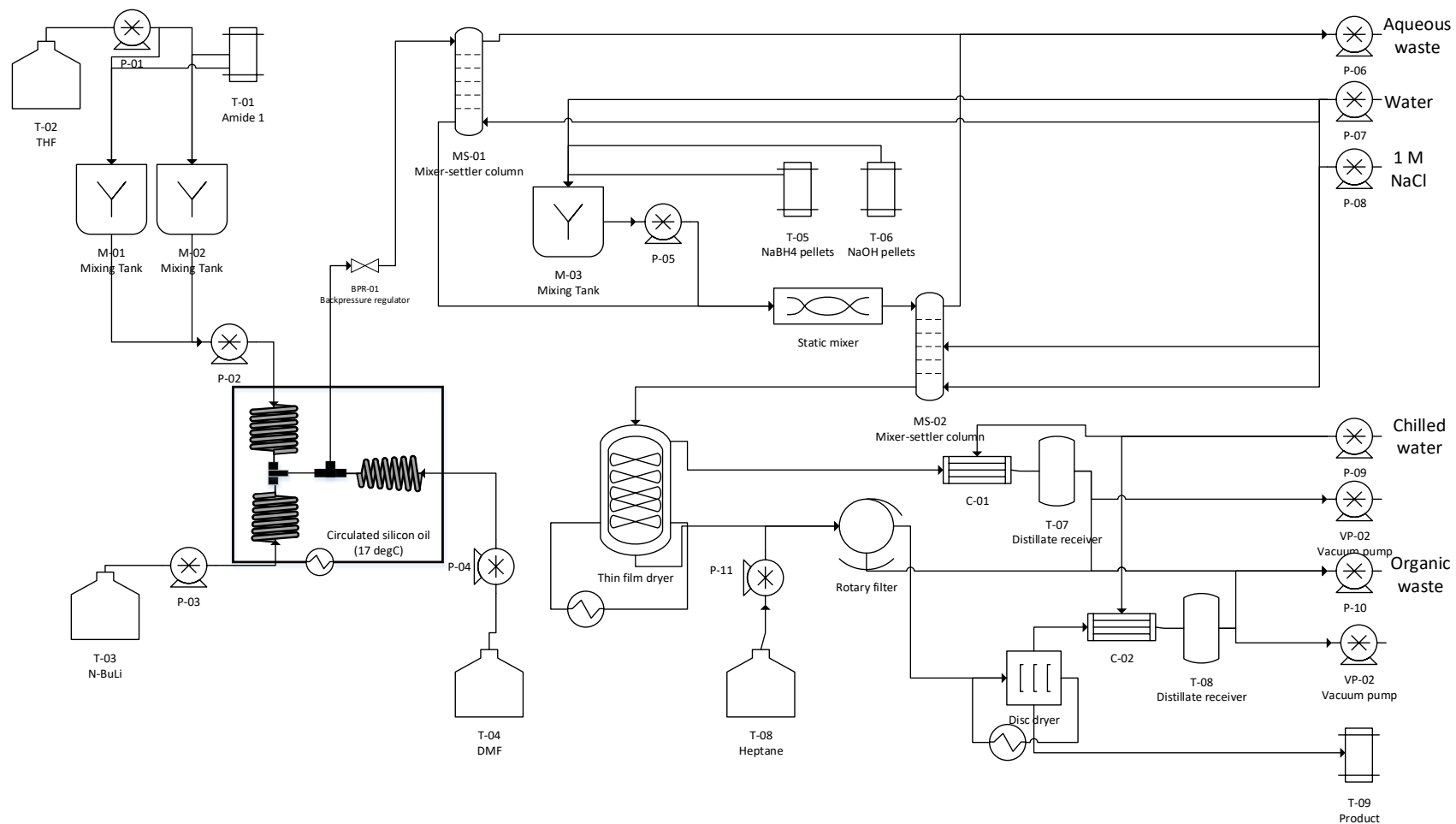


Figure D-9 Schematic process diagram for continuous consecutive ortho-lithiation and reduction reaction with final workup

E. Presentations and Publication

The results of the current research project have been presented in several international conferences and also published in form of journal article, as outlined below:

Presentations

1. Ruili Feng, Huancong Huang , Romain Frédéric Cadou, Sushil Rajan Ramchandani, Chuanzhao Li, Soo Khean Teoh, Kamelia Boodhoo, Paul Sharratt (2014). Poster on “Evaluation of Process Intensification in Early Development or Retrofitting Existing Processes for Green & Sustainability Benefits”, Process Intensification seminar, 24 Jul 2014, IPSP (Innovative Processing for Specialties & Pharma), Singapore
2. Ruili Feng, Sushil Rajan Ramchandani, Balamurugan Ramalingami, Song Wei Benjamin Tan, Romain Frédéric Cadou, Chuanzhao Li, Soo Khean Teoh, Kamelia Boodhoo & Paul Sharratt. Poster on “Intensification of ortho-lithiation reaction using continuous flow microreactor, T-joint reactor and spinning disc reactor”, ECCE10 + ECAB3 +EPIC5 conference, Nice, France, 2015.
3. Ruili Feng, Sushil Rajan Ramchandani, Balamurugan Ramalingami, Song Wei Benjamin Tan, Chuanzhao Li, Soo Khean Teoh, Kamelia Boodhoo & Paul Sharratt. Oral presentation on “Continuous flow intensification of ortho-lithiation at ambient conditions”, 5th International Congress on Green Process Engineering, Quebec, Canada, 2016

Journal publication

Feng, R., Ramchandani, S., Ramalingam, B., Tan, S. W. B., Li, C., Teoh, S. K., Boodhoo, KVK. & Sharratt, P. Intensification of Continuous Ortho-Lithiation at Ambient Conditions- Process Understanding and Assessment of Sustainability Benefits. *Organic Process Research & Development* 2017, 21(9), pp 1259-1271.